

**FUNCTIONAL STUDIES ON SULPHATION STATUS OF
HEPARAN SULPHATE IN BREAST NON-TUMOURIGENIC
EPITHELIAL AND CANCER CELLS**

GUO CHUNHUA

**NATIONAL UNIVERSITY OF SINGAPORE
2008**

**FUNCTIONAL STUDIES ON SULPHATION STATUS OF
HEPARAN SULPHATE IN BREAST NON-TUMOURIGENIC
EPITHELIAL AND CANCER CELLS**

GUO CHUNHUA
(B.Med., M.Med.)



A THESIS SUBMITTED

FOR THE DEGREE OF DOCTOR OF PHILOSOPHY

DEPARTMENT OF ANATOMY

FACULTY OF MEDICINE

NATIONAL UNIVERSITY OF SINGAPORE

2008

ACKNOWLEDGEMENTS

I would like to express my deepest gratitude and indebtedness to **Assistant Professor Yip Wai Cheong, George**, Department of Anatomy, Yong Loo Lin School of Medicine, National University of Singapore (NUS), for his invaluable guidance, advice and instruction, without which this work would not have been possible. He has guided me throughout the study with his original ideas, critical comments, as well as continuous encouragement and patience. Apart from it, I have learned a lot from him regarding the attitude and philosophy to research, and life as well.

I deeply appreciate my co-supervisor, **Professor Bay Boon Huat**, Department of Anatomy, Yong Loo Lin School of Medicine, National University of Singapore (NUS), for his open-mindedness, expert advice and pivotal suggestions, which have enlightened me and inspired my independent thinking. His consistent encouragement and support have been essential for the completion of this study.

It was a great honor to be supervised by them. The precious experience of working with them will benefit me in my future career.

My sincere appreciation is given to **Professor Ling Eng Ang**, the Head of Department of Anatomy, Yong Loo Lin School of Medicine, National University of Singapore (NUS), for the opportunity to pursue my Ph D candidature in the Department of Anatomy. His positive and energetic attitude helped me throughout the ups and downs of the whole research. He has impressed and influenced me with his amiability and gentlemanly manner.

I wish to express my heartfelt thanks to my former supervisor **Assistant Professor Valerie Lin Chun-Ling**, School of Biological Sciences, Nanyang Technological University. She has not only introduced me to an entirely new basic

Acknowledgements

research field but also has been a role model for hardworking and commitment to research. Her deep and sustained interest, immense patience and stimulating discussions have been most invaluable later in my Ph.D study.

My sincere appreciations are to **Ms. Chan Yee Gek**, and **Ms. Wu Ya Jun** who have assisted me in the learning of confocal and electron microscopy as well as immunohistological techniques. I must also acknowledge my gratitude to **Mrs Ng Geok Lan** and **Mrs Yong Eng Siang** for their excellent technical assistance; I am very grateful to **Mr Yick Tuck Yong** for his constant assistance in computer work, **Mr Lim Beng Hock** for looking after the experimental animals, **Mdm Ang Lye Gek Carlyne**, **Mdm Teo Li Ching Violet**, and **Mdm Singh** for their secretarial assistance.

I am also grateful to fellow students who have spent time in our research group. In particular, I am grateful to **Ms. Koo Chuay Yeng**, **Ms. Yvonne Teng**, **Ms. Choo Siew Hua**, **Dr. Zou Xiaohui**. They are always so patient and like to discuss all of the problems during the research.

I would also like to express my earnest gratitude to all the staff members of the Department of Anatomy, Yong Loo Lin School of Medicine, National University of Singapore (NUS) for their generous help and friendship. I continue to thank the academic and technical staff of the BFIG lab (Clinical Research Center, Faculty of Medicine) for their support in my Affymetrix GeneChip analysis project.

It has indeed been my good fortune to work with Mr. Li Wenbo, Mr. Xia Wenhao, Mr. Guo Kun, Ms. Wu Chun, Ms. Yin Jing. The friendly atmosphere they created has been unforgettable. Their support helped me a lot during the writing of my thesis.

Acknowledgements

I would also like to thank my former colleagues Ms.Woon Chow Thai, Dr.Zheng Ze Yi, Dr. Cao Sheng Lan and Mrs. Joyce Leo Ching Li for their generous help and friendship.

I greatly acknowledge the National University of Singapore for giving me the Research Scholarship, without which I can not finish my Ph.D. study.

I am also deeply indebted to my parents, brother and sister-in-law for their unfailing love, concern and support in my past years.

TABLE OF CONTENTS

ACKNOWLEDGEMENTS	i
TABLE OF CONTENTS	iv
SUMMARY	ix
LIST OF TABLES.....	xii
LIST OF FIGURES	xiv
LIST OF ABBREVIATIONS	xvii
LIST OF PUBLICATIONS.....	xx
CHAPTER 1 INTRODUCTION.....	1
1.1 Introduction of breast cancer.....	2
1.1.1 Epidemiology of breast cancer	3
1.1.2 Risks of breast cancer	4
1.1.3 Classification of breast cancer	6
1.1.4 Diagnostics of breast cancer.....	7
1.1.5 Treatment of breast cancer.....	9
1.1.5.1 Locoregional therapy.....	8
1.1.5.2 Systemic therapy	9
1.2 Proteoglycan and glycosaminoglycans (GAGs).....	13
1.3 Heparan Sulphate Protoglycan (HSPG)	18
1.3.1 Introduction of HSPG	18
1.3.2 Synthesis of HS.....	19
1.3.3 Function of HS	23
1.3.3.1 HS and cell proliferation / growth	25
1.3.3.2 HS and cell adhesion	27
1.3.3.3 HS and cell migration.....	29
1.3.3.4 HS and cell invasion	30
1.3.3.5 HS and angiogenesis.....	31
1.3.4 3-O sulphation in HS	33
1.4 RNAi technology	36
1.4.1 Introduction of RNAi.....	36
1.4.2 Mechanism of RNAi.....	36

1.4.4 RNAi and cancer.....	37
1.4.4 RNAi and proteoglycans.....	39
1.5 Genomic microarray.....	42
1.5.1 What is microarray?.....	42
1.5.2 Microarray applications.....	44
1.5.3 Microarray data analysis.....	44
1.5.3.1 Differential gene expression.....	44
1.5.3.2 Exploratory data analysis.....	46
1.5.3.3 Functional analysis.....	46
1.5.3.4 Pathway analysis.....	46
1.6 Scope of study.....	48
CHAPTER 2 MATERIALS AND METHODS.....	49
2.1 Materials and reagents.....	50
2.2 Cell culture.....	51
2.3 siRNA transfection.....	52
2.4 Blyscan assay for glycosaminoglycan level analysis.....	52
2.5 Measurement of cellular DNA content with propidium iodide (PI) by flow cytometry.....	54
2.6 Confocal laser scanning microscopy.....	54
2.6.1 Antibody staining in culture cells.....	54
2.6.2 Evaluation of apoptotic nuclear morphology.....	56
2.7 <i>In situ</i> hybridization of <i>HS3ST3A1</i> on breast cancer patients.....	56
2.7.1 Patients and tumours.....	56
2.7.2 <i>HS3ST3A1 in situ</i> RNA probes preparation.....	57
2.7.3 <i>In situ</i> hybridization of <i>HS3ST3A1</i> on breast cancer patients.....	58
2.7.4 Analysis of <i>in situ</i> hybridization of <i>HS3ST3A1</i>	59
2.8 Western Blot.....	59
2.8.1 Extraction of protein.....	59
2.8.2 Preparation of separating gel.....	61
2.8.3 Preparation of stacking gel.....	61
2.8.4 Separating protein in the SDS-PAGE gel.....	62
2.8.5 Transfer of protein to PVDF membrane.....	62
2.8.6 Incubation with primary and secondary antibody.....	62

2.8.7 Band development by Enhanced Chemiluminescence (ECL).....	63
2.8.8 Densitometric analysis of the band intensity	63
2.9 Quantitative real time polymerase chain reaction (qPCR).....	64
2.9.1 Extraction of total RNA.....	64
2.9.2 Synthesis of first strand cDNA	65
2.9.3 Quantitative real time polymerase chain reaction (qPCR)	65
2.9.4 Agarose gel electrophoresis for the qPCR product.....	67
2.9.5 Gene expression analysis of qPCR data	68
2.10 Proliferation assay	68
2.11 Adhesion assay	70
2.12 Migration assay	70
2.13 Invasion Assay	71
2.14 Gene expression profiling using GeneChip™ Microarray	72
2.14.1 RNA preparations.....	72
2.14.2 Preparation of Labeled cRNA and Array Hybridization	73
2.14.2.2 Second Strand Synthesis.....	73
2.14.2.3 Clean Up of Double Stranded cDNA.....	74
2.14.2.4 Synthesis of Biotin-Labeled cRNA (cRNA in-vitro transcription, IVT).....	75
2.14.2.5 Cleanup and Quantification of Biotin-Labeled cRNA	75
2.14.2.6 Quantification and fragmentation of cRNA	76
2.14.2.7 Fragmentation of cRNA	78
2.14.2.8 Hybridization to Affymetrix GeneChip U133 plus 2.0	78
2.14.2.9 Washing and staining procedure	79
2.14.2.10 Image scanning.....	81
2.14.3 Gene expression data analysis	81
2.14.3.1 MAS5 analysis:	82
2.14.3.2 GeneSpring analysis	84
2.14.3.3 dChip analysis.....	85
2.14.3.4 RMA analysis.....	86
2.14.4 Functional categorization of target genes	87
2.14.5 Pathway analysis.....	87
2.15 Statistical analysis	87

CHAPTER 3	88
Studies on the effects of undersulphation of HS and differentially sulphated HS on breast carcinoma cellular behaviour	89
3.1 Sodium chlorate inhibited sulphation of HS in MCF-7 breast cancer cells.....	89
3.2 Sulphate group in heparan sulphate was involved in regulating breast cancer cell proliferation.....	93
3.3 Effect of undersulphation of heparan sulphate on cell cycle changes in MCF-7 and MDA-MB-231 breast cancer cells.....	98
3.4 Sodium chlorate did not induce apoptotic nuclear morphology in MCF-7 and MDA-MB-231 breast cancer cells.....	101
3.5 Sulphate group in heparan sulphate was involved in regulating breast cancer cell adhesion.....	103
3.6 Comparative effects of differentially sulphated heparan sulphate species on cancer cell adhesion.....	105
3.7 Cell adhesion increase induced by sodium chlorate was associated with FAK and paxillin recruitment.....	111
3.8 Contrasting effects of different heparan sulphate species on migration of breast cancer cell.....	116
3.9 Undersulphation of GAGs inhibited invasion of breast cancer cell <i>in vitro</i>	120
Discussion.....	123
HSPG and breast cancer growth.....	123
HSPG and adhesion, migration and invasion in breast cancer cells.....	127
 CHAPTER 4	 132
Studies on phenotypic alterations in MCF-12A cells after silencing 3-O-HS sulphotransferase 3A1 (<i>HS3ST3A1</i>) gene	133
4.1 Quantitative real-time PCR analysis of <i>HS3ST3A1</i> and <i>HS3ST3B1</i> mRNA expression levels in breast epithelial and breast cancer cell lines.....	133
4.2 <i>In situ</i> hybridization analysis of <i>HS3ST3A1</i> expression in breast cancers.....	134
4.3 Optimization of the transfection parameters for knocking down of <i>HS3ST3A1</i> mRNA expression by siRNA.....	137
4.4 Knockdown of <i>HS3ST3A1</i> mRNA expression by siRNA was gene-specific and dose-dependent.....	137
4.5 Silencing the expression of <i>HS3ST3A1</i> impaired the synthesis of HSPG in	

MCF-12A cells.	146
4.6 Reduction of <i>HS3ST3A1</i> expression by siRNA in the MCF-12A cells inhibited cell proliferation.	146
4.7 Reduction of <i>HS3ST3A1</i> expression by siRNA in the MCF-12A cells inhibited cell cycle S/G ₂ transition.	148
4.8 Knockdown of <i>HS3ST3A1</i> expression in MCF-12A cells inhibited cell adhesion to fibronectin and collagen I.....	150
4.9 Suppression of <i>HS3ST3A1</i> expression in MCF-12A cells promoted cell migration <i>in vitro</i>	150
4.10 Suppression of <i>HS3ST3A1</i> expression increased MCF-12A cell invasive capacity through Matrigel <i>in vitro</i>	151
Discussion.....	154
CHAPTER 5.....	161
Gene expression profiling by Affymetrix GeneChips in MCF-12A cells after silencing <i>HS3ST3A1</i> gene.....	162
5.1. Assessment of yield, quality and integrity of total RNA obtained from MCF-12A cells.	163
5.2. Assessment of yield and quality / integrity of total cRNA and fragmented cRNA	165
5.3 Analysis of microarray data.....	168
5.4 Validation of microarray expression data by real-time PCR	172
5.5 Principal component analysis (PCA) of microarray expression data	184
5.6 Hierarchical clustering of microarray expression data	188
5.7 Functional categorization of target genes	188
5.8 Possible pathway analysis.....	190
Discussion.....	193
CHAPTER 6 CONCLUSIONS and FUTURE STUDIES.....	210
REFERENCES.....	214
APPENDIX	

SUMMARY

Breast cancer is the most common cancer in women worldwide. The development and clinical progression of breast cancer are well defined with invasion and metastasis as the main causes of death. Substantial evidence have demonstrated that heparan sulphate and its sulphation status are involved in many biological processes of breast cell malignant transformation and cancer progression, such as cell proliferation, adhesion, migration, invasion and metastasis. Nevertheless, depending on the tumour microenvironment, heparan sulphate may act as a promoter or inhibitor in tumour growth and progression. Targeting heparan sulphate in breast cancer treatment therefore is still one of the challenges in breast cancer research. A better understanding of the effects of differentially sulphated heparan sulphate on cancer cell behaviours is important for the development of these molecules as therapeutic targets for breast cancer.

The present study examined the effects of sulphation status of heparan sulphate on modulating the biological behaviours such as cell proliferation, adhesion, migration and invasion in breast epithelial and cancer cells. Diverse regulatory functions of differentially sulphated heparan sulphate in breast cancer *in vitro* biological processes were also explored.

Reduction in heparan sulphation in breast cancer cells was demonstrated to inhibit breast cancer cell proliferation. The inhibitory effect could be rescued by addition of porcine intestine mucosa-derived heparan sulphate (HS-PM), but not of highly sulphated bovine kidney derived heparan sulphate (HS-BK). Undersulphation also disturbed cell cycle progression in breast cancer cells. Reduction in heparan sulphation in breast cancer cells was shown to increase cancer cell adhesion and

formation of focal adhesion complex with upregulation of FAK and paxillin at both gene transcript and protein levels. The increment in adhesion could be completely blocked by exogenous HS-BK and partially blocked by HS-PM. Results also showed that inhibition of heparan sulphation as well as the presence of HS-BK, both led to a significant reduction in cell migration. In contrast, HS-PM was able to block inhibitory effect on migration. Reduction in HS sulphation also inhibited breast cancer invasion *in vitro*.

The present study also showed loss of function of *HS3ST3A1* by siRNA silencing in MCF-12A cells impaired heparan sulphation. Evaluation of *in vitro* cell proliferation, adhesion, migration and invasion after silencing *HS3ST3A1* in MCF-12A cells indicated phenotypic changes in the cells with a low proliferation rate and low adhesiveness, but higher mobility and invasiveness.

In order to elucidate the molecular networks following silencing of *HS3ST3A1*, genomic gene expression profiles after silencing *HS3ST3A1* in MCF-12A cells were analyzed by Affymetrix GeneChip. Differentially expressed probe sets (186 genes) were identified. Among these genes, of particular interest were cell-cycle related genes and cell-ECM communication genes. Most of the cell cycle related genes were down-regulated and the cell-ECM communication genes were dysregulated. This gene expression profile was in accordance with the phenotypic changes observed in MCF-12A cells after silencing *HS3ST3A1*.

The study increased the knowledge of the function of undersulphation in heparan sulphate in human breast cancer and epithelial cells regarding cell growth and progression. The study also broadened understanding of the function of structure-specific heparan sulphation by *HS3ST3A1* in cell phenotypic changes. Furthermore, the gene expression profiling analysis revealed gene expression pattern

or “gene fingerprint” after silencing *HS3ST3A1* in the regulation of the phenotypic changes in breast epithelial cell by 3-O-sulphation HS, which could serve as the basis for assessing different gene functions in breast cancer progression in the future.

LIST OF TABLES**CHAPTER 1**

Table 1.1 Structure of disaccharide: heparan sulphate, chondroitin sulphate, dermatan sulphate, keratan sulphate and hyaluronic acid.....	15
Table 1.2 Classification of proteoglycans on the basis of their localization and type of core protein	16
Table 1.3 Studies in knockdown of expression of proteoglycan-related genes in different species and systems.....	39

CHAPTER 2

Table 2.1 Formula of separating and stacking gel for Western blot.....	62
Table 2.2 Primers for quantitative real-time PCR.....	67
Table 2.3 SAPE stain solution	80
Table 2.4 Antibody Solution	80
Table 2.5 Washing Protocol	81

CHAPTER 3

Table 3.1 Flowcytometer analysis of cell cycle in MCF-7 breast cancer cells.....	99
Table 3.2 Flowcytometer analysis of cell cycle in MDA-MB-231 breast cancer cells.	100

CHAPTER 4

Table 4.1. Quantitative real-time PCR analysis of the mRNA expression of <i>HS3ST3A1</i> and <i>HS3ST3B1</i> in normal breast cell line MCF-12A and four breast cancer cell lines.	134
Table 4.2. Correlations between <i>HS3ST3A1</i> expression and various clinicpathologic factors in patients with invasive breast carcinoma.....	136
Table 4.3 Reduction of <i>HS3ST3A1</i> mRNA expression inhibited MCF-12A cell cycle progression.....	149

CHAPTER 5

Table 5.1	cRNA quality verification on Test Chips	168
Table 5.2	63 genes significantly up-regulated by HS3ST3A1 silencing in MCF-12A cells (threshold 2 fold change) with functional categories.	174
Table 5.3	123 genes significantly down-regulated by HS3ST3A1 silencing in MCF-12A cells (threshold 2 fold change) with functional categories....	176
Table 5.4	Primers for 80 genes selected for validation by real-time PCR	179
Table 5.5	Validation for the expression of 57 genes selected from differentially expressed gene list.	181
Table 5.6	Validation for the expression of 23 genes selected randomly from the microarray data.	183

LIST OF FIGURES

CHAPTER 1

Fig. 1.1. Structure of the GAG linkage to protein in proteoglycans 12

CHAPTER 3

Fig. 3.1. Sodium chlorate disrupted GAG sulphation in MCF-7 cell surface HSPG...91

Fig. 3.2. Measurement of sulphation in GAGs and heparan sulphate in MCF-7 cells.92

Fig. 3.3 Growth inhibition of breast cancer cells through undersulphation by 30 mM sodium chlorate..... 94

Fig. 3.4. HS-PM blocked the inhibitory effects of sodium chlorate on MCF-7 breast cancer cell proliferation. 96

Fig.3.5. HS-BK did not block the inhibitory effects of sodium chlorate on MCF-7 breast cancer cell proliferation..... 96

Fig. 3.6 HS-PM blocked the inhibitory effects of sodium chlorate on MDA-MB-231 breast cancer cell proliferation..... 97

Fig. 3.7 HS-BK did not block the inhibitory effects of sodium chlorate on MDA-MB-231 breast cancer cell proliferation. 97

Fig. 3.8. Effect of undersulphation of GAGs on cell cycle changes in MCF-7 cells...99

Fig. 3.9 Effect of undersulphation of heparan sulphate on cell cycle changes in MDA-MB-231 breast cancer cells..... 100

Fig.3.10. Sodium chlorate did not induce apoptosis in MCF-7 and MDA-MB-231 breast cancer cells. 102

Fig. 3.11. Sodium chlorate did not induce Caspase-3 activity in MDA-MB-231 breast cancer cells..... 102

Fig. 3.12. Sodium chlorate increased MCF-7 and MDA-MB-231 cell adhesion. 104

Fig. 3.13. HS-BK blocked the enhancing effects of sodium chlorate on MCF-7 breast cancer cell adhesion. 106

Fig. 3.14. HS-PM blocked the enhancing effects of sodium chlorate on MCF-7 breast cancer cell adhesion. 107

Fig. 3.15. HS-BK blocked the enhancing effects of sodium chlorate on MDA-MB-231 breast cancer cell adhesion. 109

Fig. 3.16. HS-PM did not block the enhancing effects of sodium chlorate on MDA-MB-231 breast cancer cell adhesion.	110
Fig. 3.17. Effect of sodium chlorate on the distribution of FAK, Paxillin and F-actin in MCF-7 cells.	113
Fig. 3.18. Effects of reduced glycosaminoglycan sulphation on ITGB1, FAK and paxillin expression in MCF-7 cells.	114
Fig. 3.19. Sodium chlorate enhances MCF-7 cell focal adhesion formation on fibronectin.	115
Fig. 3.20. Sodium chlorate inhibited MCF-7 cells migration.	117
Fig. 3.21. Sodium chlorate inhibited MDA-MB-231 cells migration.	118
Fig. 3.22. HS-PM, but not HS-BK rescued the inhibitory effect of sodium chlorate on the MCF-7 cells migration.	119
Fig. 3.23. Sodium chlorate inhibited MDA-MB-231 cell invasion through Matrigel <i>in vitro</i>	121
Fig. 3.24 Sodium chlorate inhibited MCF-7 cell invasion through Matrigel <i>in vitro</i>	122
 CHAPTER 4	
Fig. 4.1. In situ hybridization analysis of HS3ST3A mRNA expression in normal breast tissue and breast cancers.	135
Fig. 4.2. Average IPS score of in situ hybridization analysis of HS3ST3A mRNA expression in normal breast tissue and breast cancers.	136
Fig. 4.3. Transfection efficiency was determined by Cy3-labelled control siRNA in the MCF-12A cells.	138
Fig. 4.4. Cell morphology after transfection.	139
Fig. 4.5. Silencing effect of positive siRNA targeting GAPDH mRNA in MCF-12A cells.	140
Fig. 4.6. Knockdown effect of three different siRNA sequences targeting <i>HS3ST3A1</i> mRNA in MCF-12A cells.	141
Fig. 4.7. Time-dependent knockdown effect of <i>HS3ST3A1</i> siRNA on the mRNA expression of <i>HS3ST3A1</i> and <i>HS3ST3B1</i> in MCF-12A cells.	143
Fig. 4.8. Real-time PCR melting curve and agarose gel electrophoresis analysis of <i>HS3ST3A1</i> (A) and <i>HS3ST3B1</i> (B) amplification.	144

Fig. 4.9. Silencing effect of concentration titration of <i>HS3ST3A1</i> siRNA on the mRNA expression of HS3STA1 and <i>HS3ST3B1</i> in MCF-12A cells.....	145
Fig. 4.10. Immunohistochemical localization of heparan sulphate proteoglycan in MCF-12A cells using 10E4 mAb	147
Fig. 4.11. Reduction of <i>HS3ST3A1</i> mRNA expression inhibited MCF-12A cell proliferation.....	148
Fig. 4.12. Representative histograms of MCF-12A cell cycle analyzed by ModFit software.....	149
Fig. 4.13. Suppression <i>HS3ST3A1</i> mRNA expression decreased MCF-12A cell adhesion to fibronectin and collagen I.....	152
Fig. 4.14. Suppression of <i>HS3ST3A1</i> mRNA expression in MCF-12A cells promoted cell migration <i>in vitro</i>	153
Fig. 4.15. Suppression <i>HS3ST3A1</i> expression increased MCF-12A cell invasion <i>in vitro</i>	145

CHAPTER 5

Fig. 5.1. Analysis of total RNA of MCF-12A cells after silencing HS3ST3A1 expression by using RNA 6000 LabChip kit.....	164
Fig. 5.2. Analysis of unfragmented cRNA quality and size distribution.....	166
Fig. 5.3. Analysis of fragmented cRNA quality and size.....	167
Fig. 5.4. Representative two-dimensional scatter-plot of microarray hybridization data.....	170
Fig. 5.5. Experimental design and comparison of the overlapped probesets among four analysis softwares.....	171
Fig. 5.6. Validation of mRNA expression of selected 14 gene examples by quantitative real-time PCR for microarray data.....	173
Fig. 5.7. Validation for the expression of F11R protein.....	186
Fig. 5.8. Principle component analysis (PCA) of microarray data.....	187
Fig. 5.9. Hierarchical clustering of differentially expressed genes in the control group as compared with those in the siRNA groups.....	189
Fig. 5.10 Interactive pathway analysis in PathwayStudio 4.0 from the list of differentially expressed genes.....	191

LIST OF ABBREVIATIONS

Ab	Antibody
ANOVA	Analysis of variance
ATCC	American Type Culture Collection
β 4GalT	β 1,4-galactosyltransferase;
BM	Basement membrane
bp	Base pair
BRCA1	Breast cancer 1 gene
BRCA2	Breast cancer 2 gene
BSA	Bovine serum albumin
cDNA	Complementary DNA
Col	Collagen
CS	Chondroitin sulphate;
DEPC	Diethylpyrocarbonate
DMEM	Dulbecco's modified Eagle's medium
DMSO	Dimethyl sulfoxide
DNA	Deoxyribonucleic acid
DS	Dermatan sulphate;
dsRNA	Double-stranded RNA
ECL	Enhanced chemiluminescence
ECM	Extracellular matrix
EDTA	Ethylenediaminetetraacetic acid
EGF	Epidermal growth factor
EGFR	Epidermal growth factor receptor
ERK1/2	Extracellular signal-regulated kinase-1 or -2
EXT	Hereditary multiple exostoses gene
EXTL	EXT-like gene
FACS	Fluorescence activated cell sorter
FAK	Focal adhesion kinase
FBS	Foetal bovine serum
FGF	Fibroblast growth factor
FGFR	Fibroblast growth factor receptor
FITC	Fluorescein isothiocyanate
FN	Fibronectin
GAGs	Glycosaminoglycans
Gal	Galactose
GalNAc	N-acetylgalactosamine
GalT	Galactosyltransferase
GAPDH	Glyceraldehyde-3-phosphate dehydrogenase
GAPDH	Glyceraldehyde-3-phosphate
Glc	Glucose

GlcA	D-glucuronic acid
GlcAT	Glucuronyltransferase
GlcNAC	N-acetyl-D-glucosaminoglycan
GlcNS	N-sulphoglucosamine
GPI	Glycosylphosphatidylinositol
HA	Hyaluronic acid
HER-2/neu	Human epidermal growth factor receptor-2
HME	Hereditary multiple exostoses
HRP	Horse radish peroxidase
HS	Heparan sulphate;
HS2ST	Heparan sulphate 2- <i>O</i> -sulphotransferase
HS3ST	Heparan sulphate 3- <i>O</i> -sulphotransferase
HS6ST	Heparan sulphate 6- <i>O</i> -sulphotransferase
HSPG	Heparan sulphate proteoglycan
IdoA	L-Iduronic acid
Ig	Immunoglobulin
IgG	Immunoglobulin G
IgM	Immunoglobulin M
IL	Interlukine
ITGB1	β 1-Integrin
kDa	Kilodalton
KS	Keratan sulphate;
LM	Laminin
mAb	Monoclonal antibody
MAPK	Mitogen-activated protein kinase
MRI	Magnetic resonance imaging
mRNA	Messenger RNA
NDST	N-deacetylase/N-sulphotransferase
PAPS	3'-phosphoadenosine 5'-phosphosulphate
PBS	Phosphate buffered saline
PCR	Polymerase chain reaction
PE	Phytoerythrin
PET	Positron emission tomography
PG	Proteoglycan
PI	Propidium iodide
PI3K	phosphoinositide 3-kinase
PKC	protein kinase C
PMSF	Phenyl methyl sulphonyl flouride
PVDF	Polyvinylidene diluoride
RNA	Ribonucleic acid
RNAi	RNA interference
RT	Room temperature
RT-PCR	Reverse transcription polymerase chain reaction

SDS-PAGE	Sodium dodecyl sulphate polyacrylamide gel electrophoresis
siRNA	Small interfering RNA
TEMED	N,N,N',N'-tetramethylethylene diamine
TGF- β	Transforming growth factor beta
Tris	2-amino-2-(hydroxymethyl)-1,3-propanediol
VEGF	Vascular endothelial growth factor
VEGFR	VEGF receptor
WB	Western blotting
Xyl	Xylose

LIST OF PUBLICATIONS

Articles

1. **Guo C.H.**, Koo C.Y., Bay, B.H., Tan, P.H., and Yip, G.W.C. (2007). Comparison of the effects of differentially sulphated bovine kidney- and porcine intestine-derived heparan sulphate on breast carcinoma cellular behaviour. *Int J Oncol.* 31(6):1415-1423.
2. **Guo C.H.**, Bay, B.H., and Yip, G.W.C. Functional study and gene expression profiling in MCF-12A breast epithelial cells after silencing heparan sulphate 3-O sulphotransferase 3A1. Manuscript in preparation, 2007.
3. **Guo C.H.**, Bay, B.H., and Yip, G.W.C. Competitive inhibition of proteoglycan synthesis disturbs key biological processes of breast cancer cells in vitro. Manuscript in preparation, 2007.

Meeting Proceedings

1. **Guo, C.H.**, Bay, B.H., and Yip, G.W.C.. Competitive inhibition of proteoglycan synthesis disturbs key biological processes of breast cancer cells in vitro. In Proceedings of the AACR 97th Annual Meeting. (2007). 14-18 April, 2007, Los Angeles, California, USA.
2. **Guo, C.H.**, Bay, B.H., and Yip, G.W.C.. Disruption of heparan sulphation affects adhesion and motility of breast cancer cells. In Proceedings of the 16th International Microscopy Congress(IMC16, 2006). 3-8 September, 2006, Sapporo, Japan.
3. Yip, G.W.C., **Guo, C.**, Tan, P.H. and Bay, B.H.. Heparan sulphation regulates behaviour of malignant MDA-MB-231 human breast cancer cells.

- European Journal of Cell Biology, 84 25. (2005). 28th Annual Meeting of the German Society for Cell Biology, 16-19 March, 2005, Heidelberg, Germany.
4. Yip, G.W.C., **Guo, C.**, Aw, M.Y., Bay, B.H. and Tan, P.H.. Regulatory roles of sulphated glycosaminoglycans in breast cancer. In Proceedings of the 22nd New Zealand Conference on Microscopy. (2005). 6-9 February, 2005, University of Otago, Dunedin, New Zealand.3.
 5. **Guo, C.**, Bay, B.H., Tan, P.H., and Yip, G.W.C.. Disrupting glycosaminoglycan sulphation affects cell proliferation and DNA synthesis of breast cancer in vitro. In Proceedings of the International Biomedical Science Conference (2004). 3-7 December, 2004, Kunming, China.
 6. **Guo, C.**, Bay, B.H., Tan, P.H., and Yip, G.W.C.. Competitive inhibition of glycosaminoglycan sulphation inhibits cell invasiveness and migration in vitro. In Proceedings of the International Biomedical Science Conference (2004). 3-7 December, 2004, Kunming, China.
 7. Yip, G.W.C., **Guo, C.**, Aw, M.Y., Tan, P.H. and Bay, B.H.. Analysis of heparan sulphate proteoglycans in breast cancer. International Journal of Molecular Medicine, 14 S41 (2004). 9th World Congress on Advances in Oncology and 7th International Symposium on Molecular Medicine, 14-16 October 2004, Hersonissos / Crete, Greece).
 8. Yip, G.W.C., **Guo, C.**, Aw, M.Y., Tan, P.H. and Bay, B.H.. Evaluation of heparan sulphation in breast cancer. In Proceedings of the 8th NUS-NUH Annual Scientific Meeting (2004). 7-8 October 2004, Singapore, Singapore.

Awards:

1. Laureate of IMC16/IFSM (International Federation of Societies for Microscopy).
Scholarships for Young Scientists, KAZATO Foundation. The 16th International
Microscopy Congress (IMC16), Japan, Sapporo (2006.09).
2. Laureate of Travel Scholarship, Microscopy Society (Singapore) for the 16th
International Microscopy Congress (IMC16), Japan, Sapporo (2006.09).
3. Laureate of Travel Scholarship, Microscopy Society (Singapore) for the
International Biomedical Science Conference, Kunming, China (2004.12).

CHAPTER 1

INTRODUCTION

1.1 Introduction of breast cancer

Breast cancer is a malignant tumour that arises from epithelial cells lining the ducts and lobules of breast. It occurs in both men and women, although male breast cancer is rare as the male breast is a rudimentary structure.

The mammary gland is a structurally dynamic organ, varying with age, menstrual cycle and reproductive status. Structurally it contains a branched tubuloalveolar system. The mammary gland has about 12 to 20 breast lobes. Fibrous suspensory ligaments radiating out from the nipple separate these lobes by collagenous connective tissue. Each lobe drains into separate lactiferous ducts and from there into lactiferous sinuses that narrow and converge on the nipple. Within the lobes are varying amounts of adipose tissue. Each lactiferous duct is lined by a two-cell layered cuboidal-low columnar or epithelium with a sparse discontinuous outer layer of myoepithelial cells and a basal lamina. In the non-pregnant state, the mammary gland consists of lactiferous ducts, each ending in a group of blind saccular evaginations, named alveoles.

At puberty, circulating estrogen (in the presence of prolactin) stimulates the development of the lactiferous ducts and the enlargement of the surrounding fat tissue. Progesterone stimulates the formation of new alveolar buds, replacing old, regressing buds, which eventually disappear at the end of ovarian cycle. These cyclic changes are repeated during the menstrual cycles.

During pregnancy, the mammary gland comes under the influence of oestrogen and progesterone. Prolactin and placental lactogen, in the presence of estrogen,

progesterone and growth factors, stimulate the development of lactiferous ducts and secretory alveoli at the ends of the branched ducts. During lactation, the lactiferous duct system and the lobular alveolar tissue are fully developed and functional. Prolactin stimulates secretion by alveolar cells. These hormones cause a further branching of the ductal system which ends in clusters of saccules, named alveoli. In humans, approximately 200 alveoli are surrounded by a connective tissue to form a lobule. The lobule is the basic functional unit for milk production. About 25 lobules are packaged to form a lobe. Luminal epithelial cells of ducts and alveoli are precursors of myoepithelial cells, which migrate to the basal region of the lining epithelium. The epithelial-myoepithelial conversion also occurs in the mature mammary gland. This understanding of breast anatomy is important because breast lumps including cancer develop mostly within the ducts and glands. Malignant transformation of breast epithelial cells from noncancerous to precancerous and cancerous stages is a multistep disease process with progressive genetic and phenotypic alterations. Numerous factors have been reported to contribute to breast malignant transformation, including chemical carcinogens, genetic susceptibility, dysregulation of oncogenes and dietary habits.

1.1.1 Epidemiology of breast cancer

According to the NCI SEER Cancer Statistics Review, the age-adjusted incidence rate of breast cancer is 127.8 per 100,000 women per year in USA. These rates are based on cases diagnosed in 2000-2004 from 17 SEER geographic areas. It is estimated that 178,480 women will be diagnosed with breast cancer and 40,460

women in USA will die of the disease in 2007 (Ries *et al.*, 2007). The American Cancer Society (ACS) has a higher estimation with 240,510 new cases of breast cancer expected to be diagnosed among women in the United States: 178,480 invasive breast cancers and 62,030 cases of in situ breast cancer (Fritz *et al.*, 2000; American Cancer Society, 2007).

Though breast cancer incidence rates have been reported to be different between Asian and Caucasian populations (Leung *et al.*, 2002; Chia *et al.*, 2005; Shen *et al.*, 2005) there is a rapid rise in female breast cancer incidence in rapidly developing Asian countries including Singapore. The current age-adjusted breast cancer incidence rate in Singapore is 54.9 per 100,000 women per year during the 5-year period of 1998–2002, from just 20 per 100 000 women in 1968–1972, increasing by approximately 3 folds from year 1968 (Seow *et al.*, 2004). Many researchers believe that adoption of a "Westernised" lifestyle in Singapore which includes a combination of decreased parity, delayed childbearing, diet rich in saturated fats, early menarche and a sedentary lifestyle pattern has been associated with increased incidence of breast cancer (Ng *et al.*, 1997; Gago-Dominguez *et al.*, 2003; Chia *et al.*, 2005; Chew *et al.*, 2006; Ursin *et al.*, 2006; Sim *et al.*, 2006).

1.1.2 Risks of breast cancer

Breast cancer is the most common cancer among women in Singapore, affecting about 1000-1100 women annually. However there is no single underlying cause of breast cancer. Research has revealed a complex interplay of factors such as hormonal,

reproductive, genetic, environmental, dietary and other factors can cause breast cancer.

Some of the known risk factors include:

- 1) Early menarche, late menopause and long duration of menstruation (Kato *et al.*, 1988);
- 2) Nulliparity or delayed first childbirth (e.g. >30 years at first child birth) (Menes *et al.*, 2007); Additional child birth is positively related to breast cancer. Having one child was not associated with a decrease in breast cancer risk. But each additional birth was found to reduce breast cancer risk by 14% in women who were 40 and older (Andrieu *et al.*, 2006)
- 3) Genetic susceptibility. Since the discovery of the BRCA1 and BRCA2 genes, much attention has been focused on characterizing the genetic risk of breast cancer. It is typically estimated that mutations in BRCA1 and BRCA2 account for 15%–25% of the familial breast cancers (Easton *et al.*, 1993; Ford *et al.*, 1995; Yang and Lippman, 1999; Balmain *et al.*, 2003). Other genetic association with breast cancer have also been reported (Walsh *et al.*, 2006; Walsh and King, 2007);
- 4) Hormone Use of hormone replacement therapy (Tavani *et al.*, 1997; Coombs *et al.*, 2005). Studies of breast cancer have consistently found an increased risk associated with elevated blood levels of endogenous estrogen, clinical indicators of persistently elevated blood estrogen levels, and exposure to exogenous estrogen plus progestin through hormone-replacement therapy and the use of oral contraceptives. In

experimental animals, estrogen treatment leads to the development of mammary tumors (Clemons and Goss, 2001; Fournier et al., 2005);

- 5) Family history of breast cancer, especially the first degree females (Collaborative Group on Hormonal Factors in Breast Cancer., 2001);
- 6) History of atypical epithelial hyperplasia on breast biopsy (Dupont and Page, 1985; Hartmann *et al.*, 2005);
- 7) Obesity (Kuhl, 2005; Carmichael, 2006);
- 8) Cigarette smoking (Couch *et al.*, 2001; Terry and Rohan, 2002);

1.1.3 Classification of breast cancer

Clinically, TNM (primary tumour, regional lymph nodes, distant metastasis) classification system is recommended by American Joint Committee on Cancer (AJCC) (Singletary and Connolly, 2006) to assess a breast cancer patient's prognosis and help doctors to make treatment decisions.

Stage 0: Carcinoma in situ (non-invasive cancer).

Stage I: Tumour is small (≤ 2 cm), and cancer has not spread to the lymph nodes.

Stage II: Tumour is small, but cancer has spread to the lymph nodes; OR tumour is moderate in size (2 to 5 cm), with or without lymph node involvement; OR tumour is large (over 5 cm), but cancer has not spread to the lymph nodes.

Stage III: Tumour is large, and cancer has spread to the lymph nodes; OR tumour is of any size, but lymph node involvement is substantial; OR tumour is of any size, but cancer has spread to chest wall or skin.

Stage IV: Cancer has metastasized beyond the axillary lymph nodes to other parts of the body.

1.1.4 Diagnosis of breast cancer

Diagnosis of breast cancer is made through a process called triple assessment, which includes clinical examination, imaging procedures (e.g., mammography, breast ultrasonography, magnetic resonance imaging [MRI scan]), and biopsy of a mass detected by physical examination or mammography (Berg *et al.*, 2004). Systematic screening by means of clinical examination and mammography results in early diagnosis of breast cancer and a 25 to 30 percent decrease in mortality (Kerlikowske *et al.*, 1995; Karesen *et al.*, 2002; Dillon *et al.*, 2005).

1.1.4.1 Clinical breast examination

Research on clinical breast examination plus mammography found that clinical breast examination contributed to breast cancer detection independent of mammography (Barton *et al.*, 1999).

1.1.4.2 Mammography

Mammography now is the most popular examination method. It is non-invasive and easy to perform. The benefit value of mammography is higher in women with a family history of breast cancer (Kerlikowske *et al.*, 1993).

1.1.4.3 Ultrasonography

Ultrasonography has been widely used in the screening of those with a palpable breast lesion, and ultrasonography now is also used for guiding fine needle aspiration. Recent research found that the combination of ultrasonography and mammography is significantly better than either modality used alone, together resulting in 9% more breast cancers detected (Benson *et al.*, 2004).

Ultrasonography has also been considered as a screening tool for younger women who are at high risk for breast cancer because their breast tissues are more dense compared with their older cohort.

1.1.4.4 Magnetic Resonance Imaging (MRI)

MRI as a screening test for breast cancer was first reported in the 1980s. Studies using MRI in high-risk women report that MRI is significantly more sensitive than mammography. In a recent study of high-risk women, MRI was found to be better at ruling out breast cancer but more likely to produce false-positive results. The American Cancer Society recently recommended that women at high risk of breast cancer undergo annual MRI screening as an adjunct to mammography beginning at age 30 (Saslow *et al.*, 2007).

1.1.4.5 Positron-emission tomography

Positron-emission tomography (PET) scanning is an imaging method based on increased glucose utilization by malignant cells. It provides a quantitative evaluation of *in vivo* biodistribution of a radioactive tracer, such as the glucose analog fluorine-18–labeled 2-fluoro-2-deoxy-D-glucose (FDG) (Wahl *et al.*, 1991). In the

evaluation of suspicious breast lesions, PET scanning has been found to be remarkably sensitive and specific for breast cancer detection (Wahl *et al.*, 2004).

1.1.4.6 Biopsy

Biopsy and cytopathological examination are also widely accepted diagnostic methods and most of the time are deemed as the “gold standard” in the diagnosis of breast cancer based on the histopathologic or cytologic features. Today, fine-needle aspiration or core needle biopsy is still the standard step in “triple assessment” (Chaiwun and Thorner, 2007). Ultrasound-guided core needle biopsy and stereotactic directed biopsy have become important diagnostic tools, especially for women with suspicious but non-palpable breast masses.

1.1.4.7 Biomarkers

Apart from the above methods, detections for specific tumour markers such as CEA and CA153 tissue polypeptide antigen (TPA) are also the common examination methods for breast cancer screening (Soletormos *et al.*, 1996; Meisel *et al.*, 1998; Duffy, 1999; Soletormos *et al.*, 2004).

1.1.5 Treatment of breast cancer

1.1.5.1 Locoregional therapy

Locoregional therapy is mainly surgery and surgery is still the primary treatment for breast cancer. Depending on the tumour size, part or all of the breast may be removed. However removal of the whole breast, called radical mastectomy, is rarely performed today due to its severe physiologic and psychological disadvantages. Modified radical mastectomy is more widely accepted as the “standard” surgery

procedure today (Punglia *et al.*, 2007). Lumpectomy is also performed if the breast cancer is only a “non-invasive ductal carcinoma” or “ductal carcinoma in situ”.

Locoregional radiation therapy is an integral part of breast-conserving treatment. It is also adopted in those who can not receive surgery. This radiation therapy is more often used in the prophylactic prevention of recurrence of breast cancer after the surgery. Clinical investigations have shown that post-mastectomy radiotherapy reduces the incidence local and regional recurrences by 50 to 75 percent (The Early Breast Cancer Trialists' Collaborative Group, 1995; Whelan and Levine, 2005; Gebiski *et al.*, 2006).

1.1.5.2 Systemic therapy

Systemic therapy uses medications to treat cancer cells throughout the body. Systemic treatments include chemotherapy, hormonal therapy and biological therapy.

1.1.5.2.1 Chemotherapy

Chemotherapy is usually administered after surgery in women with operable breast cancer to reduce the risk of recurrence (Goldhirsch *et al.*, 2005). However, for women with large tumours, preoperative chemotherapy now called neoadjuvant chemotherapy is also performed to shrink the size of the tumour. Research finding has shown that the efficacy of adjuvant and neoadjuvant chemotherapy is the same.

Several different chemotherapy regimens may be used. However, the use of anthracyclines and taxanes in adjuvant chemotherapy is now increasingly becoming standard clinical practice in many countries (Singletary, 2003; Trudeau *et al.*, 2005), in view of the superior efficacy of sequential epirubicin followed by

cyclophosphamide, methotrexate, and 5-fluorouracil (CMF) (Goldhirsch *et al.*, 2006; Verma and Clemons, 2007).

1.1.5.2.2 Hormonal treatment

Hormonal therapy has a well-established role in treatment of oestrogen receptor-positive invasive breast cancer (Early Breast Cancer Trialists' Collaborative Group, 1998). Until recently tamoxifen was the most commonly used agent in the hormonal therapy in premenopausal and postmenopausal women (Carlson *et al.*, 2006). Recent evidence showed that aromatase (oestrogen synthetase) inhibitors are superior to tamoxifen as anti-oestrogen therapy (Carlson *et al.*, 2006). These clinical studies include both second line trials after disease progression on tamoxifen and first-line trials where aromatase inhibitors were compared directly to tamoxifen (Eiermann *et al.*, 2001; Poole and Paridaens, 2007).

1.1.5.2.3 Biological therapy

An increased understanding of the biology of breast cancer has led to the identification of novel therapeutic targets such as the HER-2/neu protein (human epithelial growth factor receptor 2, also known as c-erbB-2,). Amplification and/or overexpression of the HER2/neu gene are in ~30% breast cancers and is associated with a poor prognosis (Tuma, 2006; Ferretti *et al.*, 2007). Herceptin (also known as trastuzumab) is a monoclonal antibody against the HER-2/neu oncogene protein, which was first found to inhibit the proliferation of tumour cells in which HER-2 was overexpressed. Published results from three large clinical trials suggest that patients with early-stage disease benefit significantly from Herceptin (Piccart-Gebhart *et al.*,

2005; Romond *et al.*, 2005; Tuma, 2006; Ferretti *et al.*, 2007).

Although significant advances have been achieved in breast cancer early detection, diagnosis and medical treatment, the death rate is still high. The vast majority of breast cancer related mortality is due to metastasis to distant organs, such as bone, lung and liver with bone being the most preferential distant metastasitic site.

Metastasis is a complicated multiple-step process which includes uncontrolled cell proliferation and detachment from the primary tumour mass, invasion of cancerous cells through the basement membrane, intravasation into the blood vessels, survival in the blood circulation by escaping immuno-surveillance, re-attachment to and extravasation out of the blood vessel wall, colonization to the target organ and continuation of uncontrolled cell growth and neovascularization (Chambers *et al.*, 2002; Klein, 2003). Hence metastasis requires a cascade of sequential steps containing proper coordination of cell adhesion, motility and growth (Minn *et al.*, 2005; Gupta and Massague, 2006).

Over the past few decades, advances in molecular and cell biology have elucidated the molecular steps in cancer metastasis. The metastatic cascade requires sequential interactions between cell-cell and cell-extracellular matrix (ECM). The central components of these extracellular interactions are proteoglycans, which are present at the cell-ECM interface or in the ECM of virtually all kinds of cells. Proteoglycans have been widely shown to have crucial regulatory roles in normal physiological processes, such as embryogenesis, as well as in pathophysiological conditions such as tumourigenesis and progression.

1.2 Proteoglycan and glycosaminoglycans (GAGs)

Proteoglycans are very large macromolecules, consisting of a core protein covalently linked with complex glycosaminoglycans (GAGs). The structural morphology of proteoglycan is like “a decorated Christmas tree”.

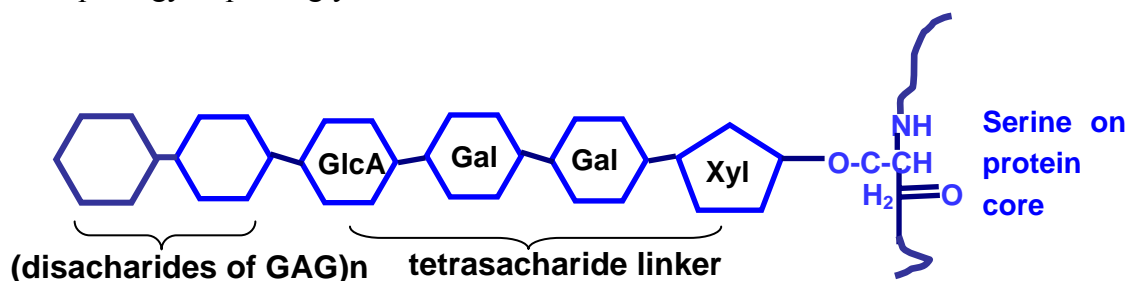


Fig. 1.1 Structure of the GAG linkage to protein in proteoglycans

Glycosaminoglycans are unbranched, highly sulphated polysaccharides containing repeating disaccharides (typically repeating 40-100 times), containing hexosamine and hexuronic acid (GlcA or IdoA). They are modified by epimerization and sulphation during synthesis in the Golgi apparatus. Thus GAG is a finely structured chain with distinct sulphation patterns which have specific binding affinities to different proteins and growth factors as well as cytokines.

There are four classes of GAGs based on the differences in GAG disaccharide composition, epimerization and sulphation pattern, namely, heparan sulphate (HS)/heparin, chondroitin sulphate (CS)/dermatan sulphate (DS), keratan sulphate (KS) and hyaluronic acid (HA, also called Hyaluronan) (Kjellen and Lindahl, 1991; Esko and Selleck, 2002, see **Table. 1**).

HS/Heparin is synthesized as a polymer of repeating disaccharide of hexuronic acid and glucosamine with different sulphation at various positions (see detailed

below). The difference between HS and heparin is that heparin is more highly sulphated than heparan sulphate (Coombe and Kett, 2005).

CS and DS share the same biosynthetic precursor. CS chains always contain glucuronic acid while DS can have iduronic acid whose presence actually is sufficient to define the GAG as a DS more than a CS. CS is usually categorized on the basis of the position of sulphation of the hexosamine such as C-4S, C-6S and C-4, 6 S.

KS is relatively distinct from all of the other GAGs. It is shorter and possesses galactose instead of an uronic acid in the repeating disaccharide. It can contain branching fucose residues and may be end-capped by various sugars, such as sialic acids (Funderburgh, 2000).

HA is unique in that it is synthesized at the plasma membrane and is not attached covalently to a core protein. It is also a very large polymer with molecular weights up to 100kDa -10,000kDa (Fraser *et al.*, 1997; Weigel *et al.*, 1997).

Apart from HA, synthesis of all GAGs including the HS/Heparin and CS/DS occur in the Golgi apparatus and is initiated by formation of the tetrasaccharide linker, Xylose-galactose-galactose-glucuronic acid with the xylose covalently linked to a serine residue on the core protein. The repeating disaccharide of CS/DS is glucuronic acid and N-acetylgalactosamine whereas in HS/Heparin, is glucuronic acid and N-acetyl glucosamine. Thus the backbone of HS/Heparin is a linear polysaccharide of the disaccharide glucuronic acid- β 1-4 N-acetyl glucosamine whereas the corresponding product of CS/DS is a linear polysaccharide of the disaccharide glucuronic acid- β 1-3 N-acetylgalactosamine.

The newly synthesized backbone chain is then subjected to a series of modification by different enzymes. These modifications generate along the GAG chains specific structures which render the GAGs diverse functions. These modifications are most clearly known in the synthesis of HS/Heparin (see detail Section 1.3 below).

Proteoglycans are also classified according to the localization of their core proteins (Waddington and Embery, 2001; Delehedde *et al.*, 2001, **see Table 1.2**).

Table 1.1 Structure of disaccharide: heparan sulphate, chondroitin sulphate, dermatan sulphate, keratan sulphate and hyaluronic acid (Adapted from Kjellen and Lindahl, 1991; Esko and Selleck, 2002)

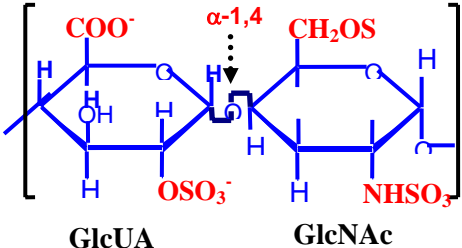
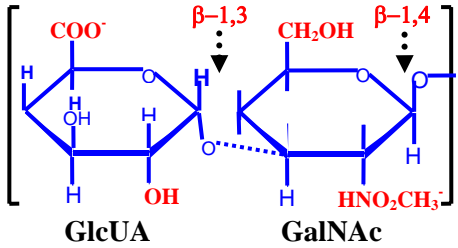
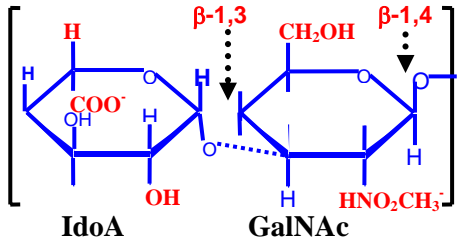
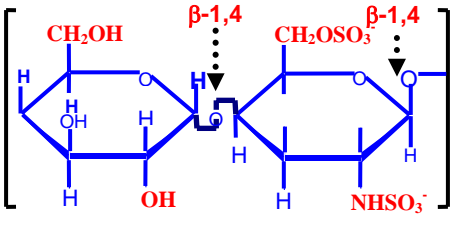
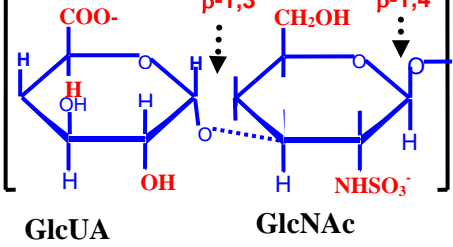
<p>Heparin/Heparan sulphate</p> <p>GlcN and GlcUA or IdUA</p> <p>N and O sulphation (C2,3,6)</p> <p>α-1,4 glycosidic linkage</p>	 <p style="text-align: center;">GlcUA GlcNAc</p>
<p>Chondroitin sulphate:</p> <p>GlcUA-Gal-Gal-Xyl-O-Ser</p> <p>Link sulphate at 4 or 6 C of GalNAc</p> <p>β-1,3 glycosidic linkage</p>	 <p style="text-align: center;">GlcUA GalNAc</p>
<p>Dermatan sulphate:</p> <p>IdoA with some GlcUA</p> <p>Sulphation at 4 or 6 C of GalNAc</p> <p>β-1,3 glycosidic linkage</p>	 <p style="text-align: center;">IdoA GalNAc</p>
<p>Keratan Sulphate:</p> <p>Type I: GlcNAc and Gal (no UA)</p> <p>Sulphation on C6 of Gal or HexN</p> <p>β-1,4 glycosidic linkage</p> <p>Type II: GalNAc-O-Ser or Thr</p>	 <p style="text-align: center;">Gal GlcNAc</p>
<p>Hyaluronan (unsulphated):</p> <p>No core protein</p> <p>No sulphate</p> <p>β-1,3 glycosidic linkage</p>	 <p style="text-align: center;">GlcUA GlcNAc</p>

Table 1.2 Classification of proteoglycans on the basis of their localization and type of core protein. (Based on Waddington and Embery, 2001; Delehedde *et al.*, 2001)

Localization	GAG-chain	Mr of the core protein (kD)	Principal members
ECM	HA, CS, KS	225-250	aggrecan, versican
Collagen-associated	CS, DS, KS	40	decorin, biglycan, fibromodulin
Basement membrane	HS	120	perlecan
Cell-surface	HS, CS	33-60-92	syndecans, glypican, betaglycan, CD44E, cerebroglycan
Intracellular granules	heparin, CS	17-19	serglycin

(CS, chondroitin sulphate; DS, dermatan sulphate; KS, keratan sulphate; HA, hyaluronic acid; HS, heparan sulphate)

1.3 Heparan Sulphate Protoglycan (HSPG)

1.3.1 Introduction of HSPG

Heparan sulphate proteoglycans (HSPGs) are highly sulphated proteoglycans with the basic structure consisting of a core protein covalently linked with heparan sulphate glycosaminoglycan (HS-GAG) chains (Esko and Selleck, 2002; Whitelock and Iozzo, 2005; Sasisekharan *et al.*, 2006). They are expressed virtually in all kind of mammalian cells and ubiquitously distributed on the surface of mammalian cells and in the extracellular matrix (ECM).

Based on its core protein, HSPGs can be classified into several types. The major family of HSPGs is syndecan which is anchored to the cell surface via a transmembrane domain. Glypican, another family of HSPGs, is GPI-anchored to cell surface. The third group of HSPGs is perlecan, agrin and the hybrid HSPG/collagen type XVIII, which are secreted into the ECM (Iozzo, 2005). Studies have revealed that, due to different core proteins, syndecans have four isoforms (syndecan 1, 2, 3, and 4) and glypicans have six isoforms (glypican 1, 2, 3, 4, 5, and 6) (Esko and Selleck, 2002; Whitelock and Iozzo, 2005; Sasisekharan *et al.*, 2006).

Heparan sulphate glycosaminoglycans (HS-GAG) are unbranched and highly acidic chains of polysaccharide. They consist of repeating β 1-4 linked disaccharide units, D-glucosamine and glucuronic/idouronic acid (Esko and Selleck, 2002; Whitelock and Iozzo, 2005; Sasisekharan *et al.*, 2006). These disaccharide units are substituted with acetyl and/or sulphate groups at various positions of the sugar circle (Aikawa *et al.*, 2001; Shriver *et al.*, 2002; Nakato and Kimata, 2002; Grobe *et al.*,

2002; Liu and Pedersen, 2006; Mulloy and Rider, 2006). Such substitutions along the HS-GAG chains render a defined acetylation and sulphation pattern and make HS-GAGs a heterogeneous mixture at the whole level. Through the long unbranched and heterogeneous structure of HS-GAG chains, HSPGs can interact with a variety of proteins such as extracellular matrix proteins, enzymes, growth factors, and cytokines as well as their receptors (Esko and Selleck, 2002). Thus HSPGs can exert a critical role in modulating cell functions such as cell proliferation, adhesion, migration, invasion and angiogenesis (Jiang and Couchman, 2003; Segev *et al.*, 2004; Sanderson *et al.*, 2004; Farach-Carson *et al.*, 2005; Hacker *et al.*, 2005; Iozzo, 2005; Coombe and Kett, 2005; Cool and Nurcombe, 2006; Jenniskens *et al.*, 2006; Van *et al.*, 2006; Vives *et al.*, 2006). To better understand the relationship between the function of HS and its complicated structure, it is necessary to understand the biosynthesis of HS.

1.3.2 Synthesis of HS

HS synthesis is a non-template driven process and involves multi-steps that occur in a specific and sequential manner. These steps involve many different enzymes in the endoplasmic reticulum (ER) and Golgi apparatus in the cells (Esko and Selleck, 2002; Whitelock and Iozzo, 2005; Sasisekharan *et al.*, 2006).

Cells begin HS synthesis by building up blocks with monosaccharide and sulphate through specialized transporter in the plasma membrane. Sugars are activated by nucleotide consumption in the cytosol to form UDP-sugars. At the same time, sulphate is also activated and transported to the ER and Golgi by recruiting free sulphate groups into 3'-phosphoadenosine 5'-phosphosulphate (PAPS) (Esko and

Selleck, 2002; Whitelock and Iozzo, 2005; Sasisekharan *et al.*, 2006). PAPS is the universal donor of sulphate to all sulphotransferases, both in the Golgi apparatus and the cytosol.

The HS chain is initiated at a tetrasaccharide linker [GlcA β 1,3 –Gal β 1,3 –Gal β 1, 4 -Xyl- β 1-O-(Ser)] which is covalently linked with the core protein at the Ser residue via the Xylose residue. The core proteins have a consensus peptide sequence of Ser-Gly/Ala-X-Gly (where X stands for any amino acid) at the GAG-protein attachment site. The tetrasaccharide linkage is formed by stepwise addition of each UDP-sugar residue to the serine residue of the core protein by respective glycosyltransferases: xylosyltransferase (XyT-I), galactosyltransferase I (GalT-I), galactosyltransferase II (GalT-II), and glucuronyltransferase I (GlcAT-I) (Esko and Selleck, 2002; Whitelock and Iozzo, 2005; Sasisekharan *et al.*, 2006).

After completion of the synthesis of the tetrasaccharide, the addition of the fifth monosaccharide determines if the GAG chain becomes HS/heparin or CS/DS. In HS/Heparin, the fifth sugar is a N-acetylated glucosamine (α -GlcNAc) added by the key enzyme α -N-acetylglucosaminyltransferase I (GlcNAcT-I) (Fritz *et al.*, 1994), whereas in CS/DS, it is GalNAc which is added by β -N-acetylgalactosaminyltransferase I (GalNAcT-I) (Rohrman *et al.*, 1985; Naganaka *et al.*, 1999). HS elongation then proceeds by the action of glycosyltransferases (GlcNAc-TII and GlcA-TII), which add 1,4-GlcA and 1,4-GlcNAc units in alternating sequence to the nonreducing end of the growing polymer. These unbranched chains contain typically 40-100 times repeating

disaccharides [GlcA-GlcNAc]_n (Esko and Selleck, 2002). The exostosin (EXT) family of genes encodes this α -glycosyltransferase involved in heparan sulphate biosynthesis. Five members of this family have been cloned to date in human: EXT1 (Ahn *et al.*, 1995), EXT2 (Le Merrer *et al.*, 1994), EXTL1 (Wise *et al.*, 1997), EXTL2 (Wuyts *et al.*, 1997), and EXTL3 (Van *et al.*, 1998). After that, the nascent HS polymer is subjected to consecutive modification by substrate-specific enzymes. These modifications include N-deacetylation and N-sulphation of GlcNAc, C5 epimerization of GlcA to form iduronic acid (IdoA), 2-O-sulphation of IdoA and GlcA residues, as well as 6-O-sulphation and 3-O-sulphation of glucosamine (Lindahl *et al.*, 1998; Aikawa *et al.*, 2001; Shriver *et al.*, 2002; Grobe *et al.*, 2002; Nakato and Kimata, 2002; Liu and Pedersen, 2006; Mulloy and Rider, 2006). N-deacetylation and N-sulphation of GlcNAc are catalyzed by the dual functional enzyme N-deacetylase and N-sulphotransferase (NDST). C5- epimerization is exerted by the C5- uronyl transferase (C5 epimerase) and O- sulphation is catalyzed by different O-sulphotransferases at the specific positions of the disaccharide. These sulphotransferases are named according to the sugar residue position they sulphate. HS2ST sulphates the 2-O position of uronic acid, whereas HS3ST and HS6ST enzymes sulphate the 3-O or 6-O positions of glucosamine, respectively (Lindahl *et al.*, 1998). The first modification is the N-deacetylation and N-sulphation of GlcNAc which is catalyzed by the bifunctional N-deacetylase/N-sulphotransferase (NDST). N-sulphation is important in that it is a signal for other modification. Thus 6-O-sulphation occurs preferentially on N-sulphated glucosamine or on N-acetylated

glucosamines that are immediate neighbors of an N-sulphated glucosamine (Habuchi, 2000). Similarly C5 epimerization of glucuronic acid to iduronic acid only occurs in the uronic acid linked to an adjacent N-sulphated glucosamine (Habuchi, 2000). Iduronic acid may be 2-O-sulphated as long as it is flanked on both sides by N-sulphates. The 3-O sulphation of glucosamine residues of HS-GAG chain is a rare but important modification in HS synthesis such as for the anticoagulant activity of HS/Heparin (Dementiev *et al.*, 2004; Petitou and van Boeckel, 2004). The difference between HS and heparin widely used clinically is that in heparin over 85% of glucosamine are N-sulphated, while in HS N-sulphation is only 40-50%.

Due to the fine structure of the HS chain, all of the enzymes, except C5 epimerase and 2-O- sulphotransferase (Habuchi, 2000; Forsberg and Kjellen, 2001; Kusche-Gullberg and Kjellen, 2003; Habuchi *et al.*, 2004), have distinct isoforms for unique substrate preference with selective expression level in different kinds of cells. Nowadays almost every isoform of the sulphation enzymes has been cloned and isolated (Pikas *et al.*, 1998; Kusche-Gullberg and Kjellen, 2003; Habuchi *et al.*, 2004). There are four isoforms of NDSTs, three isoforms of 6-O- sulphotransferases and seven isoforms of 3- O- sulphotransferase (Habuchi, 2000; Kusche-Gullberg and Kjellen, 2003).

The synthesis of heparan sulphate is such a highly coordinated process that cells with loss of any such enzyme would result in impaired heparan sulphate synthesis (Forsberg and Kjellen, 2001). Many researches have demonstrated that cells lacking full capacity to transport sulphate have diminished sulphation (Esko *et al.*,

1986). Cells lacking of a specific glycosyltransferase (Bai *et al.*, 1999), with deficiency of an enzyme for transportation or formation a particular substrate, such as EXT (Stickens *et al.*, 2005), UDP-Gal (Nakamura *et al.*, 2002) or PAPS (Dejima *et al.*, 2006), C5-epimerase (Li *et al.*, 2003; Feyerabend *et al.*, 2006), or specific sulphotransferase, such as 2-O sulphation (Bai and Esko, 1996; Merry *et al.*, 2001), N-sulphation (Bame and Esko, 1989; Humphries *et al.*, 1999), 6-O sulphation (Pratt *et al.*, 2006), have been found to possess a limited capability to synthesize or to sulphate HS glycosaminoglycans.

1.3.3 Function of HS

From the synthetic processes of heparan sulphate proteoglycan, biological functions of HSPGs are dictated largely by the specific structure of heparan sulphate chains, their pattern of sulphation and their core proteins as well as cooperation with cytokines, extracellular matrix proteins, enzymes, protease inhibitors, growth factors and other molecules (Bernfield *et al.*, 1999; Lander and Selleck, 2000; Iozzo, 2001; Esko and Selleck, 2002; Nakato and Kimata, 2002).

Sulphation modifications occur non-uniformly throughout the heparan sulphate chain, thus forming peculiar sulphation patterns with the concomitant presence of highly sulphated domains (S-domain) and under-/ non-sulphated domains. These sulphation patterns create binding specificity for different substrates. One of the best studied examples is the interaction between FGF-2 and heparan sulphate. This interaction requires at least some degree of 2-O sulphation, and a chain length of at least octasaccharide of heparan sulphate. For FGF-2 binding to its receptor FGFR,

there must also be 6-O sulphation. Both 2-O-sulphate and 6-O-sulphate groups of heparan sulphate are essential for the ternary formation of HS-FGF2-FGFR (Aviezer *et al.*, 1994; Pye *et al.*, 1998; Jemth *et al.*, 2002; Harmer, 2006) and FGF2 signaling. Modifications of sulphation at specific position of HS are important modulating steps in physiological as well as pathophysiological conditions in cells. For example, heparan sulphate 6-O-endosulphatase (Sulf) is exosulphatase which remove 6-O-sulphate groups from the non-reducing-end glucosamine residues within heparan sulphate (Dhoot *et al.*, 2001) (Lai *et al.*, 2003). Research has showed that Sulf functions as a negative regulator of FGF signaling and FGF2-dependent angiogenesis by disrupting the FGF2-FGFR1-heparan sulphate ternary complex formation (Wang *et al.*, 2004) which inhibited both tumour growth and tumour angiogenesis in xenografts in mice induced by Sulf-1 over-expressing MDA-MB-468 breast cancer cells (Narita *et al.*, 2006).

Degradation is an additional functional variation of HS GAGs, since variable stability and turnover of GAGs may depend upon their susceptibility to enzymatic degradation. Heparan sulphate cleavage is by the β -D-endoglucuronidase, heparanase (HPSE), which acts via a hydrolytic mechanism to cleave glycosidic bonds in heparan sulphate. Degradation of the ECM such as the heparan sulphate (Eccles, 1999) is a key aspect of tumour cell migration, invasion and metastasis (Edovitsky *et al.*, 2004).

Core proteins in HS proteoglycans also exert functions through interactions with other molecules, especially when these HS proteoglycans are involved in the formation of extracellular matrix. Cell surface proteoglycans, syndecans and

glypicans generally function by the interaction with extracellular matrix as receptors or facilitators for cell adhesion (Woods *et al.*, 1998). Syndecan-4 is a peculiar transmembrane heparan sulphate proteoglycan present together with β 1-integrins in focal adhesion on different substrates (fibronectin, laminin, vitronectin, or type I collagen) (Saoncella *et al.*, 1999a; Woods and Couchman, 2001).

Thus, the detailed positions and degree of sulphation and stability of HS GAGs as well as the core proteins provide a variety of specificities for functions, including cell proliferation, adhesion, migration and invasion as well as other biological processes, such as angiogenesis.

1.3.3.1 HS and cell proliferation / growth

HSPG in cell proliferation has been well established. Interaction of HSPG and FGF-2 in cell proliferation has been well studied. As mentioned above, FGF-2 exerts its effect through the binding of its receptor and HS glycosaminoglycan with both 2-O and 6-O sulphation. FGF-2 is an important growth factor in regulating cell proliferation (Spivak-Kroizman *et al.*, 1994). FGFs mediate their cellular responses by binding to FGF receptors and activating a family of four receptor tyrosine kinases (RTKs) (Jaye *et al.*, 1992) which eventually leads to stimulation of intracellular downstream signaling pathways such as activation of the Ras/MAP kinase signaling pathway that cause cell proliferation, cell differentiation, cell migration, cell survival and cell shape (Spivak-Kroizman *et al.*, 1994; Kouhara *et al.*, 1997). It has been shown that FGF-2 is a mitogen for breast cancer T47D, MCF-7 and BT-20 cells

(Karey and Sirbasku, 1988; Peyrat *et al.*, 1991). The stimulation effect of FGF-2 on MCF-7 cell proliferation was completely abolished after heparinase treatment which degraded HSPG or was significantly inhibited by chlorate treatment which removed the sulphate group in the HS chains (Delehedde *et al.*, 1996). These results have demonstrated that HSPG plays a crucial role in modulating FGF-2 induced proliferation in breast cancer cells. Removal of the 6-O sulphation in pancreatic cancer cells by over-expression of Sulf resulted in reduced anchorage-dependent and -independent cell growth as well as invasion by blocking FGF-2 signaling pathway (Li *et al.*, 2005). Previous studies have elucidated that addition of exogenous highly sulphated HS-GAGs such as heparin (Majack and Clowes, 1984) as well as lower sulphated HS-GAGs (Forsten *et al.*, 1997) inhibited FGF-2 mediated proliferation of smooth muscle cells. Exogenous heparin has also been reported to inhibit FGF-2 induced proliferation in endothelial cells (Giroux *et al.*, 1998). Recently, studies also showed that inhibition of HS-GAGs synthesis abrogated FGF-2-induced mitogenic response in bovine aortic endothelial cells (Fujiwara and Kaji, 1999).

In addition to FGF, HSPGs have also been reported to participate in regulation of other growth factors. Sulf over-expression in head and neck squamous cell carcinoma cell lines inhibited the signaling activities of HS-dependent epidermal growth factor, resulting in repression of tumour growth and cell migration (Lai *et al.*, 2003; Lai *et al.*, 2004). It has been reported that syndecan-4 regulates protein levels of the endothelial growth factor receptors (erb-B2 and -B3) in a colon cancer cell line (Isabel *et al.*, 2001). Moreover, syndecan-2 can bind and regulate the signaling of

tumour growth factor- β (Chen *et al.*, 2004). Syndecan-1 is also implicated in hepatocyte growth factor signaling. Binding of hepatocyte growth factor to syndecan-1 induced activation of PI3-kinase and mitogen-activated protein kinase pathways (Seidel *et al.*, 2000; Derksen *et al.*, 2002).

The significance of glypicans (GPC) in tumour growth was identified in breast cancer and pancreatic cancer. GPC-3 functioned predominantly as growth inhibitor and modulator of cell survival and inducer of apoptosis (Filmus and Selleck, 2001), while GPC-1 was a promoter of cell growth (Filmus, 2001). GPC-1 was found over expressed in breast cancer and modulated mitogenic effect of growth factors in breast cancers (Matsuda *et al.*, 2001). It was also found GPC-1 was over-expressed in pancreatic cancer both by the cancer cells and the stroma cells (Kleeff *et al.*, 1998). Silencing its expression by anti-sense treatment reduced the response of pancreatic cell to growth factors such as FGF-2 and EGF (Kleeff *et al.*, 1999). On the contrary, GPC-3 expression was silenced in breast cancer due to its promoter hypermethylation (Xiang *et al.*, 2001). Over-expression GPC-3 in breast cancer induced apoptosis (Gonzalez *et al.*, 1998). It has been established that GPC-1 is a key tumour-promoting HSPG while GPC-3 acts as a tumour suppressor.

1.3.3.2 HS and cell adhesion

HSPGs are expressed on almost every cell surface and in the extracellular matrix. Many researches have demonstrated that HSPG are involved in cell cytoskeletal remodeling, adhesion and focal adhesion. Over-expression of syndecan-1 has been shown to promote cell spreading in *in vitro* and *in vivo* models of breast cancer, which suggested that syndecan-1 promoted tumorigenesis by regulating tumour cell spreading and adhesion (Beauvais and Rapraeger, 2003; Burbach *et al.*, 2004) as well as proliferation, and angiogenesis. Syndecan-2 has also been shown to be involved in cell adhesion. Fibroblasts overexpressing syndecan-2 form filopodia-like membrane protrusions, and a role for syndecan-2 in cell motility has also been shown (Fears *et al.*, 2006). Addition of exogenous soluble recombinant syndecan-2 ectodomain to brain microvascular endothelial cells increased cell–cell interactions on matrigel (Fears and Woods, 2006). However, when syndecan-2 was overexpressed in colorectal cancer-derived cells, the cells showed a flattened appearance with loss of cell–cell contacts, lamellipodial or filopodial membrane protrusions, and increased migration across the transwell membrane (Contreras *et al.*, 2001).

The best evidence for a specific role of syndecans in cell adhesion comes from studies of Syndecan-4 in focal adhesion formation. Syndecan-4 is a transmembrane heparan sulphate proteoglycan present together with integrins in focal adhesions on different substrates (fibronectin, laminin, vitronectin, or type I collagen) (Woods and

Couchman, 1994). Specific stimulation with antibodies against the ectodomain of mouse syndecan-4 promoted focal adhesion assembly (Saoncella *et al.*, 1999). Woods *et al.* (2000) found when glycosaminoglycan chains of syndecan-4 binds to recombinant heparin binding fragment of fibronectin, syndecan-4 redistributes into forming focal adhesions. Mahalingam *et al.* (2007) found that cellular adhesion responses to the heparin-binding (HepII) domain of fibronectin require N- sulphated glucosamine in the HS. In the more complex response of focal adhesion formation through syndecan-4, both N-sulphation and glucosamine 6-O-sulphation were required. Moreover, interactions with the HepII domain of fibronectin required for activation and stability of FAK and to maintain fibroblast cell survival (Wilcox-Adelman *et al.*, 2002). Evidence has also shown that the sulphation pattern influenced cell adhesion to different substrate. For example, Keller *et al.* (1989) reported sodium chlorate inhibited the binding of 3T3 cell to fibronectin. Undersulphation by sodium chlorate inhibited C6 glioma cell adhesion to fibronectin, laminin and collagen IV (de Aguiar *et al.*, 2002).

1.3.3.3 HS and cell migration

HS is known to play a role in cell migration. Research findings have strongly suggested that function of HS in cell migration depends on specific cell type and HS structural motifs in the sequence. Intact HSPGs have been reported to promote stable focal adhesion that may retard cell migration in endothelial cells (Moon *et al.*, 2005). Nurcombe *et al.* (2000) showed that HS preparations that were known to be specific

for FGF-1 (HS-GAG A)) or FGF-2 (HS-GAG-B) have different function in cell migration in MCF-7 and MDA-MB-231 breast cancer cells. Combination of FGF-1/HS-GAG-A induced greatest migration in MDA-MB-231 cells and MCF-7 cells. Although increases in motility were seen on HS-GAG-A or FGF-1 alone, the effects of their combination were synergistic and led to significant greater migratory speeds. In contrast, the motility was only slightly increased when adding the combination of FGF-2 and HS-GAG-B.

HS core protein is also involved in cell migration. Overexpressing full-length core protein of syndecan-4 in CHO-K1 cells results in increased focal adhesion formation and decreased cell motility (Longley *et al.*, 1999).

Disturbance in HS sulphation has also been demonstrated to influence cell migration. Lacking of 2-O sulphation in 2-O-sulphotransferase mutant *Caenorhabditis elegans* caused specific cell-migration defects of the gonad leader cells and of hermaphrodite-specific neurons (Kinnunen *et al.*, 2005). Sodium chlorate treatment of brain endothelium cells or monocytes significantly reduced transendothelial migration. In addition, enzymatic removal of heparan sulphate chains also inhibited monocyte transendothelial migration (Floris *et al.*, 2003). On the other hand increasing 6-O-sulphation by overexpressing a dominant positive Sulf significantly increased invasion through Matrigel and migration of vascular smooth muscle cell compared to control cells (Sala-Newby *et al.*, 2005).

1.3.3.4 HS and cell invasion

Metastasis of tumour cells is a multistep cascade. A tumour cell invades into

tissues by first degrading extracellular matrix constituents including fibronectin, collagens, laminins and HSPGs. Highly sulphated heparin and heparan sulphate have been demonstrated significantly enhanced melanoma cell invasion *in vitro* into Matrigel (Brunner *et al.*, 1998). The enhancement of tumour cell invasion was due to a stimulation of plasminogen activation by the sulphated glycosaminoglycans.

Results from the *ex vivo* experiment using MCF-7 cells transfected with heparanase cDNA have also demonstrated that HS is associated with tumour invasion. When the transfected MCF-7 cells were injected into the mammary pad of nude mice, it showed enhanced tumour growth and invasion compared with tumours produced by mock-transfected cells (Cohen *et al.*, 2006). Further more, when heparanase was silenced by using either ribozymes or siRNA, both human breast carcinoma (MDA-MB-435) and mouse melanoma (B16-BL6) tumour cells were found reduced invasion and adhesion *in vitro* and were less metastatic *in vivo* (Edovitsky *et al.*, 2004). These findings were recently confirmed independently by a Chinese group in MDA-MB-435 breast cancer cells (Zhang *et al.*, 2007c). These findings suggested that heparanase may facilitate tumour invasion by degrading HSPG in the cell extracellular matrix and basement membrane.

Transfection of mouse mammary tumour cells with anti-sense mRNA for syndecan-1 resulted in an epithelial to mesenchymal transformation and increased invasion (Leppa *et al.*, 1991; Leppa *et al.*, 1992). Overexpression of syndecan-1 in syndecan-deficient myeloma cells remarkably inhibited cell invasion (Liu *et al.*, 1998). These results indicate syndecan may be a tumour suppressor.

1.3.3.5 HS and angiogenesis

Angiogenesis is a coordinated multicellular process for the formation of new blood vessels from the existing vasculature and is necessary for tumour growth. HSPGs have long been implicated in these processes. HS sequester, stabilize and protect growth factors such as VEGF from inactivation and thus promote angiogenesis in tumours. VEGF is a specific mitogen for vascular endothelial cells *in vitro* and angiogenic factor *in vivo* (Ferrara, 1996; Ferrara and Gerber, 2001). The optimal binding of VEGF to heparin/heparan requires 6-O-sulphation of glucosamine (Ono *et al.*, 1999) although 2-O-, 6-O-, and N-sulphation of HS contributed to the strength of the VEGF165 interaction (Robinson *et al.*, 2006). Removal of 6-O-sulphate group from HS resulted in the significant loss of binding to VEGF165. However, knock-down of the expression of Sulf in normal endothelial cells by siRNA reduced VEGF165 (one short type of VEGF) mediated angiogenic response (Narita *et al.*, 2006).

Syndecans have also been shown to be involved in tumour angiogenesis. In an *in vivo* model of breast cancer in which breast cancer cells were co-injected with syndecan-1-expressing fibroblasts into the mouse flank, enhanced tumour growth and increased tumour vascularization was observed (Maeda *et al.*, 2004; Maeda *et al.*, 2006). Syndecan-2 was highly expressed in the microvasculature of mouse gliomas. When its expression was down-regulated in mouse brain microvascular endothelial cells, formation of capillary tube-like structures *in vitro* was reduced (Fears *et al.*, 2006). Heparanase has also been found to facilitate angiogenesis as it degrades HSPG

in the basement membrane, liberating endothelial cell to invade and migrate toward angiogenic factors (Elkin *et al.*, 2001).

1.3.4 3-O sulphation in HS

Many research findings have verified that HS functions are dependent on specific sulphation as HS binds to a variety of growth factors, cytokines, signaling molecules and ECM proteins (Sasisekharan *et al.*, 2006; Mulloy and Rider, 2006). Here gives a brief literature review on 3-O sulphation in HS.

3-O sulphation of glucosamine residues of HS-GAG chain is a rare but important modification of HS synthesis. Until today, at least seven isoforms of 3-O-sulphotransferases (3-O-STs) have been identified and partially characterized (Liu *et al.*, 1996; Liu *et al.*, 1999; Shworak *et al.*, 1999; Xia *et al.*, 2002; Lin, 2004). They are 3-O-ST-1 (HS3ST1), 3-O-ST-2 (HS3ST2), 3-O-ST-3A (HS3STA), 3-O-ST-3B (HS3STB), 3-O-ST-4 (HS3ST4), 3-O-ST-5 (HS3ST5) and 3-O-ST-6 (HS3ST6). The success in cloning and characterization of HS 3-O-sulphation enzymes increased the understanding for the mechanisms of generating HS with defined sequences and the sequence-specific function.

One of the most studied enzymes, 3-O-sulphotransferase (3-O-ST, now known as 3-O-ST-1, HS3ST1) converts non-anticoagulant heparan sulphate into anticoagulant heparan sulphate, which is widely used in clinic and well known as heparin (Dementiev *et al.*, 2004; Petitou and van Boeckel, 2004). Blood coagulation is a cascade involving a series of reactions which results in the activation of factor Xa

that is the key player in formation of a blood clot. The anticoagulant heparin sulphate, by interacting with antithrombin, which undergoes conformational change in its structure, inhibits activation of factor Xa as well as other proteases in the blood coagulation cascade (Olson and Bjork, 1994). Thus as an anticoagulant, heparan sulphate can stop blood coagulation.

Modification of 3-O-sulphation in anticoagulant heparan sulphate by 3-O-ST-1 determines the formation of specific HS binding sequences for ligands such as antithrombin and thus influences HS function. The preference of substrate and production of antithrombin-binding motif by 3-O-ST-1 suggest the possibility that other heparan sulphate 3-O-sulphation enzymes may function in a similar way. By controlling production of other important HS fine motifs, these enzymes may also play important roles in HS functions. For example, 3-O-ST-5 has been found to synthesize antithrombin-binding motif along HS chain which exhibits anticoagulant activity (Xia *et al.*, 2002). But this AT-bind structure is different from what is produced by 3-O-ST-1. Research findings have demonstrated that 3-O-ST-5 has a broader substrate specificity compared with that of 3-O-ST-1 (Mochizuki *et al.*, 2003; Chen *et al.*, 2003; Duncan *et al.*, 2004; Chen and Liu, 2005). 3-O-ST-5 sulphates glucosamine units that are linked to a glucuronic acid (or iduronic acid) as well as 2-O-sulphated iduronic acid units, thus the HS motif also has the function of promoting herpes simplex virus 1 into target cells (Chen *et al.*, 2003; Duncan *et al.*, 2004; Chen and Liu, 2005).

Research has also revealed that 3-O-ST-2 (Chen and Liu, 2005), 3-O-ST-3A (Moon *et al.*, 2004b), 3-O-ST-3B (Moon *et al.*, 2004a), 3-O-ST-4 (Chen and Liu, 2005), and 3-O-ST-6 (Xu *et al.*, 2005) can generate herpes simplex virus 1(HSV-1) gP-binding motif which serves as an entry receptor for the virus (Shukla *et al.*, 1999; Xu *et al.*, 2005) but none of these 3-O-sulphation enzymes can produce anticoagulant HS motif. These biochemical studies have greatly contributed to our knowledge of the function of HS3STs based on their respective substrate preferences and the resultant HS structures, but their biological functions, including those of 3-OST-3A is still unknown.

In summary, HSPGs have multifaceted functions in the regulation of cell growth, adhesion, migration, tumourigenesis and progression. As mentioned above, in some instances, HSPGs can sequester growth factors away from their cell surface receptors, hindering signaling. Whereas in other cases, HSPGs can participate in a ternary complex with the growth factors, promote growth factor binding with its receptor resulting in enhanced signaling. The discrepancy among the different studies reiterates the notion that whether HSPG and its sulphation are pro-or anti- factors in cell growth and tumour progression is dependent on the microenvironment of cell HSPG and its specific binding ligands such as growth factors. Targeting heparan sulphate in breast cancer treatment therefore is still one of the challenges in breast cancer research. A better understanding of the effects of differentially sulphated heparan sulphate on breast cancer cell behaviour is important for the development of these molecules into potential therapeutic targets for breast cancer.

1.4 RNAi technology

1.4.1 Introduction of RNAi

RNA interference (RNAi) is a general term given to a gene-silencing regulation process that is induced by double-stranded RNA (dsRNA) in sequence-specific degradation of complementary mRNA or by inhibiting translation (Fire *et al.*, 1998).

Double-stranded RNA-mediated interference has recently emerged as a powerful tool to silence gene expression in human cells. Over the past 2 decades since RNAi was first discovered (Napoli *et al.*, 1990), the possibility of RNA interference is one of the most exciting new technologies in functional genomics. RNA interference has been not only proven to be an invaluable research tool in basic science, allowing much more rapid characterization of the function for known genes, but more importantly, this new technology accelerates the discovery of novel genes involved in disease processes and it gives promising clinical results that may lead to novel therapies in the future.

1.4.2 Mechanism of RNAi

The mechanism of RNAi has been investigated by both biochemical and genetic approaches. RNA interference is mediated by small interfering RNAs (siRNAs) which are intracellularly generated from long endogenous microRNA (miRNA) or exogenous double-stranded RNA molecules (dsRNAs). RNAi relies on a multi-step intracellular pathway which can be roughly divided into two phases, the initiation phase and the effector phase.

In the first phase, the long, double-stranded RNA (dsRNA) is recognized and cleaved by Dicer, a ribonuclease (RNase) III enzyme, to form short 21–23 nt duplexes (small interfering RNA, siRNA) with a symmetric 2 nt overhang at the 3'-end and a 5'-phosphate and 3'-hydroxy group (Zamore *et al.*, 2000; Elbashir *et al.*, 2001; Bernstein *et al.*, 2001).

In the second phase, the produced siRNAs are incorporated into the multiprotein complex, RNA-induced silencing complex (RISC). A helicase in RISC unwinds the duplex siRNA by peeling of the sense strand of the siRNA and this complex becomes activated with the single-stranded siRNA. The antisense strand of the siRNA is then hybridized perfectly to its complementary mRNA in the cells. The RISC complex cleaves the target mRNA, 10 nucleotides from the 5' end of the incorporated siRNA–target mRNA duplex. Due to the generation of unprotected RNA ends, the target gene mRNA rapidly degrades. Hence, expression of the targeting gene was decreased.

1.4.4 RNAi and cancer

Cancer is viewed as a multi-step disease. According to the established model of oncogenesis, to become a cancer cell, normal cell must undergo several essential alterations in cellular physiology which includes uncontrolled proliferation, resistance to apoptosis, angiogenesis, invasion and metastasis (Hanahan and Weinberg, 2000). Currently, cancer research are using different technologies to understand biological mechanisms implicated in the transformation of normal cells to malignant phenotypes.

Traditionally, gene function in cancer has been studied using animal knockout models. RNA interference offers a number of advantages over the traditional systems, including ease of use, high specificity and efficacy in nearly any biological system, and the ability to perform large-scale screening for gene functions. Since RNAi mechanism has high specificity and efficiency in down-regulating gene expression, this methodology has been widely used in recent years in studying the function of genes in cancer, as loss of function indicates a specific effect exerted by the gene (Gartel and Kandel, 2006; Gaither and Iourgenko, 2007; Fuchs and Borkhardt, 2007).

So far, various genes have been knocked-down using RNAi technique in different tumour cell lines *in vitro* as well as *in vivo* mouse models. By such an easy and convenient way, scientists have been able to study the profound biological consequences following the knockdown of their expression. These genes include oncogenes/suppressors, anti-apoptosis or pro-apoptotic genes, telomerase, growth factors and their receptors, signaling molecules and as well as a panel of other genes (Devi, 2006; Gartel and Kandel, 2006; Chang, 2007). Our understanding of function of genes and their interactions has changed dramatically with the development of RNAi systems.

1.4.4 RNAi and proteoglycans

RNAi has also been used to investigate the functions of those genes involved in the synthesis of proteoglycans. Using siRNA to silence the genes involved in the synthesis of proteoglycans has been studied in various species. **Table 1.3** summarizes the currently known studies targeting different proteoglycan related genes in different species and systems.

Unfortunately, our current knowledge about the roles of one specific gene in cancer development is insufficient to describe the behaviours of tumours and predict the outcome of potential therapeutic effects. Therefore, the process of multiple genes especially that exert their functions synergistically in the same pathway in cancer models will improve the understanding of their function in cancers. Since their advent in the mid-1990s, DNA microarrays have been the choice for genome-wide expression analysis (see below, Genomic Microarray introduction part). The synergistic effect from the combined usage of RNA interference and the whole genomic expression profiling by microarray analysis is providing researchers with vast amounts of information. When comprehensively analyzed, the outcomes from the combination of these two new methodologies will provide a unique opportunity to annotate the unknown genes as well as the “known” genes together with their interactions in pathways occurring in cancer cells (Laflamme and Robichaud, 2007). As a result, it is much easier to understand the function of any given gene that interacts with a number of different partners within specific pathways in cancer progression (Williams *et al.*, 2003; Jazag *et al.*, 2005; Sachse *et al.*, 2005).

Table 1.3 Studies in knockdown of expression of proteoglycan related genes in different species and systems.

Target	Cell type	Results	Reference
Glypican-1	Lymphoblastoid cells	Enhanced BMP signaling	(O'connell <i>et al.</i> , 2007)
	Turkey myogenic satellite cells	Decreased myogenic satellite cell proliferation	(Zhang <i>et al.</i> , 2007a)
Syndecan-1	T lymphocytes mainly of the CD4+ cells	Reduced CyPB-induced p44/p42 MAPK activation and consequent migration and adhesion,	(Pakula <i>et al.</i> , 2007)
	Mouse embryonic fibroblasts	Ras-ERK signaling pathway	(Li <i>et al.</i> , 2006)
	Breast cancer MDA-MB-231 cells	Disrupted alpha(v)beta(3)-dependent cell spreading and migration	(Beauvais <i>et al.</i> , 2004)
	Keratinocytes	Decreased cell adhesion	(Ogawa <i>et al.</i> , 2007)
	Breast cancer T47D cells	Inhibited carcinoma cell mitogenesis	(Su <i>et al.</i> , 2007)
	B82L mouse fibroblasts	Inhibited cell attachment and spreading on vitronectin	(McQuade <i>et al.</i> , 2006)
Syndecan-2	Human embryonic kidney cells	Inhibited filopodia and spine formation	(Lin <i>et al.</i> , 2007)
	Human osteosarcoma cells	Inhibited chemotherapy-induced apoptosis.	(Orosco <i>et al.</i> , 2007)
Syndecan-4	Dendritic cell	Decreased dendritic cell motility	(Averbeck <i>et al.</i> , 2007)
	HeLa cells	Syndecan-4 behaves as CXCL12 receptor in p44/p42 pathways	(Charnaux <i>et al.</i> , 2005)
	Lymphoblastoid cells	Decreased BMP signaling in LCLs	(O'connell <i>et al.</i> , 2007)
	Vascular smooth muscle cells VSMC	Reduced DNA synthesis and ERK pathway	(Rauch <i>et al.</i> , 2005)
Glypicans (Dally)	Drosophlia	Inhibited Hedgehog signal transduction	(Desbordes and Sanson, 2003)
Perlecan	Prostate LNCaP cells	Decreased SHH signaling	(Datta <i>et al.</i> , 2006; Marker, 2007)
	Murine malignant melanoma B16-F10 cells	Blocks tumour growth and angiogenesis	(Adatia <i>et al.</i> , 1997)
	Human colon carcinoma cells	Inhibition of tumour growth and neovascularization	(Sharma <i>et al.</i> , 1998)
	prostate cancer C4-2B cells	Reduces cell adhesion <i>in vitro</i> and tumour growth <i>in vivo</i>	(Savore <i>et al.</i> , 2005)

Table 1.3 Studies in knockdown of expression of proteoglycan related genes in different species and systems (Cont'd)

Target	Cell type	Results	Reference
beta4GalT7	Drosophila	Inhibited the development of wing and leg	(Nakamura <i>et al.</i> , 2002)
6-OST(dHS6ST)	Drosophila	Caused embryonic lethality and disruption of the primary branching of the tracheal system	(Kamimura <i>et al.</i> , 2001)
3-OST	Drosophila	Inhibited Notch signaling	(Kamimura <i>et al.</i> , 2004)
2-OST	<i>C. elegans</i>	Inhibited cell migration	(Kinnunen <i>et al.</i> , 2005)
3-OST-3B	Peripheral blood T lymphocytes and Jurkat T cells	Inhibited of ERK pathway and migration and integrin-mediated adhesion	(Vanpouille <i>et al.</i> , 2007)
Sulf-1	Human umbilical vein endothelial cells HUVEC	Increased proliferation and enhanced downstream signaling	(Narita <i>et al.</i> , 2006)
	Breast cancer cell MDA-MB-468 cells	Increased autocrine activation of ERK	(Narita <i>et al.</i> , 2007)
	Ovarian cancer	Enhanced cisplatin-induced cytotoxicity	(Staub <i>et al.</i> , 2007)
HPSE	B16 mouse melanoma cells	Decreased in VEGF and p38 phosphorylation	(Zetser <i>et al.</i> , 2006)
	Hepatocellular carcinoma	Inhibited the invasion, angiogenesis and metastasis of human hepatocellular carcinoma	(Zhang <i>et al.</i> , 2007b)
	Breast carcinoma cells	Reduced invasion and adhesion <i>in vitro</i>	(Zhang <i>et al.</i> , 2007c)
	Breast cancer MDA-MB-231 cells	Reduced invasion and adhesion <i>in vitro</i>	(Edovitsky <i>et al.</i> , 2004)
	Breast cancer MDA-MB-231 cells Myeloma cell lines	Inhibited tumour metastasis and angiogenesis Decreased syndecan-1 gene expression	(Ilan <i>et al.</i> , 2006) (Mahtouk <i>et al.</i> , 2007)

1.5 Genomic microarray

The Human Genome Project (HGP) completely sequenced the human genome (Venter *et al.*, 2001; Lander *et al.*, 2001; Collins *et al.*, 2003). This advent job has provided a tremendous list of genes in human. However, deciphering the functions of all these genes has proven to be another even more difficult job compared with the HGP itself. Fortunately, the availability of microarray, which was first introduced in 1995 (Schena *et al.*, 1995), has proven to be an indispensable tool for biologists who are trying to identify the functions of all of these genes.

1.5.1 What is microarray?

A microarray is typically defined as a collection of microscopic spots which are referred to as probes containing a single species of a nucleic acid and representing the genes of interest, immobilised on a solid support (normally nylon, glass, silicon) in a highly parallel manner forming an array, hence the term. This technology is based on the hybridization between labeled targets derived from a biological sample and the probes (Southern *et al.*, 1999). The targets, normally mRNA, extracted from biological samples and labelled with a detectable molecule or dye such as a fluorophore, Cy3 or Cy5, are hybridized to the microarray probes. The hybridization signal emitted by the labeling dye represents the relative mRNA expression level of the corresponding gene in the sample. The signals are detected, acquired, quantified, integrated and digitalized with dedicated software, creating a “gene expression profile” or “molecular portrait” for all of the genes in the samples (Duggan *et al.*, 1999). The resultant digital data are then further deep-mined by sophisticated

softwares to obtain useful information such as differential gene expression and pathways.

The most widely used microarrays are Affymetrix GeneChips (<http://www.affymetrix.com>). Affymetrix GeneChips are high density oligonucleotide microarrays. The probe is fabricated by in situ light-directed chemical synthesis from phosphoramidite nucleotide monomers directly on a quartz wafers , which combines solid-phase chemical synthesis with photolithographic fabrication techniques, also known as photolithography, widely employed in the semiconductor industry (Fodor *et al.*, 1991; Fodor *et al.*, 1993; Lockhart *et al.*, 1996; Lipshutz *et al.*, 1999).

The group of probes corresponding to a given gene is known as the probe set. Affymetrix GeneChip microarrays utilize approximately 11-20 such probe pairs to interrogate a single transcript sequence. For each probe, there is also a mismatch sequence for each probe wherein the mismatch has a single nucleotide mutation compared with its corresponding probe. These are designated Perfect Match (PM) and Mismatch (MM) probes, respectively. The mismatch probes serve as a control for non-specific hybridization and increase the signal-to-noise ratios.

Affymetrix GeneChip Human Genome U133 Plus 2.0 Array (HG-U133 Plus 2.0) comprises 1,300,000 unique oligonucleotide features covering over 47,000 transcripts and variants.

1.5.2 Microarray applications

The applications of microarrays in breast cancer researches have increased dramatically since the introduction of microarray. The main applications of microarrays in breast cancer studies are to:

- 1) Identify genes that are differentially expressed between breast tumour and normal breast tissues or cells as well as the drug-treated or stimulated and non-intervened samples.
- 2) Identify and categorize new subtypes of breast cancer (molecular tumour classification) on the basis of gene expression pattern--- gene signature, or gene portrait,
- 3) Develop a classifier on the basis of gene signature, allowing the better evaluation of prognosis and more accurate prediction of patient response to a particular treatment and eventually tailoring treatment for the individual patient, known as “personalized medicine”.

1.5.3 Microarray data analysis

1.5.3.1 Differential gene expression

With thousands of genes explored simultaneously, microarray profiling generates vast amounts of biological data. These enormous amounts of data require computational analysis and visualization for biological function interpretation. A plethora of automated data mining softwares are now available to evaluate microarray data ranging from the simple fold-change for identifying differentially expressed

genes, to complex computational algorithms for tumour classification. The most commonly used software packages are Affymetrix's own Microarray Analysis Suite or GeneChip Operating Software (MAS 5.0 or GCOS) (Affymetrix, 2001; Affymetrix Inc, 2002), DNA-Chip Analyzer (dChip) (Li and Wong, 2001a; Li and Wong, 2001b), and the so-called Robust Multichip Analysis(RMA, Irizarry *et al.*, 2003a; Irizarry *et al.*, 2003b), with other deep data mining tools like GeneSpring (Silicon Genetics, Redwood City, CA, USA) (Chu *et al.*, 2001) which can be linked to public databases.

1.5.3.2 Exploratory data analysis

It is more valuable to use clustering techniques such as hierarchical clustering, Principal Component Analysis (PCA) in conjunction with pathway analysis software for understanding the biological function of gene expression.

Hierarchical Clustering is an analytic algorithm to reduce the complexity of data sets by classifying genes into categories with similar expression manners. All genes start as an individual cluster, then the clusters with nearest distance are merged into a new cluster, such calculation repeated till a clustering tree structure is set up. Hierarchical cluster analysis is usually used near the end of microarray data analysis to identify genes that are co-regulated. D-chip and GeneSpring have hierarchical clustering function built in the softwares (Sorlie *et al.*, 2003; Sotiriou and Piccart, 2007).

Principal components analysis (PCA) is a statistical technique for determining the key variables in a multidimensional data set by reducing the dimensionality into three most significant variances, known as principal components, that must be considered in the microarray analysis. PCA can be used not only in classifying samples with a similar expression pattern, e.g. related to a specific treatment or phenotype. It can also be used in identifying the interested genes that are most important for the differences between the groups (Yeung and Ruzzo, 2001). GeneSpring has the Principal Component Analysis function.

1.5.3.3 Functional analysis

Gene Ontology (GO) is widely accepted for gene function analysis. It consists of three categories, biological process, molecular function, and cellular component. The classification for the differentially expressed genes based on the GO Ontology category will list co-regulated genes and thus provides a tool that is able to highlight some pathways hidden in the data. GO analysis tools are collected by the Gene Ontology Consortium. One can also get access to NetAffx GO Mining Tool (Cheng *et al.*, 2004) in Affymetrix website.

1.5.3.4 Pathway analysis

Genes are working together in a cascade of networks. As a result, analyzing the microarray data in a pathway perspective could lead to a higher level of understanding of gene functions. PathwayStudio (Nikitin *et al.*, 2003) is a network exploring bioinformatics software which comes with ResNet Core, a database of more than

50,000 validated facts and 1000+ reconstructed pathways, which can be extended to over 800,000 facts available in the ResNet™ 4.0 database. It includes a pathway simulation module to explore the dynamic behavior of pathways and new tools for building relevance networks and connectivity maps from the microarray expression data, and Ariadne's MedScan Reader™ biomedical literature browser. MedScan Reader enables the viewing and automated extraction of scientific facts from biomedical literature, including MEDLINE abstracts, journal articles and other source references.

In summary, microarray technology is a versatile technology that allows global analysis of gene expression patterns simultaneously. Many tools are being developed to assist with the analysis of such high throughput data. This technology can identify novel gene-gene interactions and gene pathways. Combination with the recently emerged siRNA gene silencing technology, microarray technology will have an increasingly important role in the post-genomic era.

1.6 Scope of study

The transformation from breast normal epithelial cell to malignant cell phenotype and breast cancer progression involves multiple steps including uncontrolled cell proliferation, detachment from the primary tumour mass, invasion of cancerous cells through the basement membrane, intravasation into and extravasation out of the blood vessels and colonization to the target organ, and continuation of uncontrolled cell growth and neovascularization (Couldrey and Green, 2000; Hanahan and Weinberg, 2000; Lu and Kang, 2007). These processes require sequential interactions between cell-cell and cell-extracellular matrix (ECM). The central components of these interactions are proteoglycans, which are present at the cell-ECM interface and in the ECM. Heparan sulphate is one kind of GAGs. Any change in heparan sulphate will influence these processes in the malignant transformation and cancer progression.

Hypothesis: The main hypothesis is that HS sulphation status is involved in the regulation of breast cancer behaviours. To support this hypothesis: (a) Inhibition of HS or addition of exogenous differentially sulphated HS should affect biological activities of breast cancer cells. (b) Alteration in expression of sulphation transferase *HS3ST3A1* should have some effect on cellular behaviours of breast epithelial and cancer cells.

The objectives of the present study are to:

- 1) Examine the effects of undersulphation in GAG induced by sodium chlorate in breast cancer cell lines *in vitro*.
- 2) Investigate the effects of differentially sulphated exogenous heparan sulphate on the biological activities of breast cancer cell lines *in vitro*.
- 3) Evaluate the expression level of *HS3ST3A1* in breast cancer cells and normal breast epithelial cells *in vitro* and in breast benign and cancer tissues *in vivo*.
- 4) Study the function of *HS3ST3A1* in breast epithelial cells with regard to:
 - (a) Changes of cell phenotype such as cell proliferation, adhesion, migration and invasion after specifically knockdown of this gene by using siRNA.
 - (b) Differentially expressed genes after silencing *HS3ST3A1* expression by using microarray analysis.
 - (c) Possible mechanic pathways involved in phenotypic alterations after silencing *HS3ST3A1* expression in MCF-12A cells.

CHAPTER 2

MATERIALS AND METHODS

2.1 Materials and reagents

Cell culture flasks and 6 well plates were bought from Nalge Nunc (Nalge Nunc International, Rochester, NY, USA). Petri dishes, 96-well plates and migration transwells were purchased from Corning (Costar, Corning, NY, USA). Bovine serum albumin (BSA), epidermal growth factor (EGF), cholera toxin, insulin, hydrocortisone, sodium chlorate and crystal violet were purchased from Sigma-Aldrich (Sigma, St.Louis, Mo, USA). Foetal bovine serum (FBS) was purchased from Hyclone (Hyclone, Logan, UT, USA). OPTI-MEM I medium was purchased from Invitrogen (Invitrogen, Carlsbad, CA, USA). Extracellular proteins fibronectin and collagen type I were purchased from BD Bioscience (Becton Dickinson & Company, Bedford, MA, USA). BioCoat Cell Environments, MatrigelTM invasion chamber were also bought from BD Bioscience.

Heparan sulphate from porcine intestinal mucosal (HS-PM) and heparan sulphate from bovine kidney (HS-BK) were all purchased from Sigma-Aldrich Chemicals (Sigma Chemical Co., St.Louis, MO, USA).

The anti-heparan sulphate chain antibody (clone F58-10E4, mouse immunoglobulin M [IgM]) was purchased from Seikagaku (Seikagaku Corp., Tokyo, Japan).

FAK rabbit polyclonal antibody C-20 was from Santa Cruz Biotechnology (Santa Cruz, CA, USA). The anti-FAK C-20 polyclonal antibodies were raised against peptides corresponding to amino acids 1033–1052 mapping at the C terminus of human FAK. Mouse monoclonal anti-paxillin, anti-FAK and anti-F11R were obtained from

BD Bioscience. Fluorescein isothiocyanate (FITC)-phalloidin and all fluorescence-conjugated secondary antibodies were purchased from Molecular Probe (Molecular Probe, Inc., Eugene, OR, USA).

Sodium chlorate was prepared as a stock concentration of 3 M in double distilled water and stored at -20°C. The chemical was further diluted in FBS-free culture medium immediately before use.

Ambion's Silencer™ siRNA Transfection Kit was brought from Ambion. The kit contains siPORT transfection agents, siPORT™ Amine Transfection Agent and siPORT™ Lipid Transfection Agent. The kit also includes GAPDH synthetic siRNA and its corresponding scrambled control siRNA (siRNA Transfection II Kit. Catalog #: 1631, Ambion, Inc., Ambion, Austin, TX, USA).

2.2 Cell culture

MCF-12A (ATCC: CRL-10782), MCF-7 (ATCC: HTB-22), MDA-MB-231 (ATCC: HTB 26), T47D (ATCC: HTB-133) and ZR-75-1 (ATCC: CRL 1500) cell lines were obtained from American Tissue Culture Collection (ATCC, Manassas, VA, USA). The MCF-12A cell line is a spontaneously immortalized and non-tumorigenic mammary epithelial cell line. It was derived from the mortal cell line MCF-12M which was established from the tissue taken at reduction mammoplasty from a nulliparous patient with fibrocystic breast disease that contained focal areas of intraductal hyperplasia (Paine *et al.*, 1992). The characteristics of MCF-12A breast epithelial cell line and culture condition are well established. MCF-12A cells were cultured in a 1:1 mixture of Dulbecco's modified Eagle's medium and F12 medium (DMEM-F12,

Invitrogen, Carlsbad, CA, USA) supplemented with 5% FBS, hydrocortisone (0.5 µg/ml), insulin (10 µg/ml), epidermal growth factor (20 ng/ml), cholera toxin (100 ng/ml), and 40 µg/ml gentamicin (Invitrogen, Carlsbad, CA, USA). MDA-MB-231 and MCF-7 breast cancer cells were routinely maintained in DMEM with phenol-red and supplemented with 7.5% FBS, 2 mM glutamine, and 40 µg/ml gentamicin. T47D and ZR-75-1 breast cancer cells were routinely maintained in RPMI 1640 medium with phenol-red and supplemented with 7.5% FBS, 2 mM glutamine, and 40 µg/ml gentamicin.

2.3 siRNA transfection

For siRNA transfection, MCF-12A cells were cultured in the maintaining medium with antibiotics. The transfection was carried out using reverse transfection method as recommended by Ambion (Ambion, Inc., Ambion, Austin, TX, USA). Briefly, MCF-12A cells transfected with siRNA and siPort Amine mixture while the cells were still in suspension (i.e. after trypsinization and prior to plating). Transfection parameters include MCF-12A cell number, amount of transfection agent siPort Amine, exposure time of transfection agent to MCF-12A cells, and siRNA quality. Several experiments were designed to optimize these transfection parameters. Optimization of transfection was performed using Ambion's Silencer™ siRNA Transfection Kit.

2.4 Blyscan assay for glycosaminoglycan level analysis

MCF-7 cells were cultured with or without 30 mM sodium chlorate for 48 hrs. The culture medium was collected. The cells were collected by directly scratching with a cell scraper in 500 µl cold PBS. The cell lysates were then sonicated for 20 s. Twenty

μl of the medium and the sonicated cell lysates were removed and kept at $-80\text{ }^{\circ}\text{C}$ for protein analysis.

The crude glycosaminoglycans were precipitated by adding 1.3% potassium acetate in 95% ethanol at -20°C overnight after boiling for 10 min. The pellet was digested with 2 mg pronase at 55°C for 16 hrs. After inactivating the pronase by boiling for 10 min, the supernatant was collected by centrifugation at $14,000 \times g$ for 15 min. These supernatant was again precipitated overnight at $-20\text{ }^{\circ}\text{C}$ with 1.3% potassium acetate in 95% ethanol before the total glycosaminoglycans were collected by centrifugation at $14,000 \times g$ for 15 min. Sulphated glycosaminoglycan content was determined with the Blyscan TM kit (Sulphated Glycosaminoglycan Assay, Biodye science, Newtownabbey, Northern Ireland, UK) according to the manufacturer's instructions. The Blyscan assay is a quantitative dye-binding method for the measurement of sulphated proteoglycans and GAGs. The assay is based on the specific binding of the cationic dye, 1, 9-dimethyl methylene blue to sulphated GAGs. Briefly, $100\text{ }\mu\text{l}$ of medium supernatant or re-suspended GAGs solution was mixed with 1 ml Blyscan dye and incubated for 30 min at room temperature with gentle shaking to allow a precipitable complex to form. The proteoglycan–dye complex was precipitated by centrifugation for 10 min at $13\ 000\text{ rpm}$ and the supernatant was removed. The bound dye was dissolved in 1 ml dissociation reagent for 20 min and the absorbance was measured at 562 nm . A standard curve using standard GAG samples was made during each quantitation. The coefficient of the linear regression for the standard curve was

0.98 or greater. All samples were run in duplicates. The final results were calculated as μg sulphated GAG per μg protein.

2.5 Measurement of cellular DNA content with propidium iodide (PI) by flow cytometry

1.5×10^5 cells were grown in 6-well plates for 24 hrs and serum-starved for overnight using 2% FBS-containing DMEM before being treated with 30 mM sodium chlorate serum-containing media. At various time points after treatment, the cells were harvested and stained with propidium iodide (PI) in Vindelov's cocktail [10 mM Tris HCl (pH 8), 10 mM NaCl, 50 mg PI/litre, 10 mg/litre ribonuclease A, and 0.1% Nonidet P-40] for 1 h at 4°C in the dark. The stained cells were analyzed and the fluorescence was collected in a linear scale using the FACS Calibur flow cytometer (Becton Dickinson, Lincoln Park, NJ, USA) running the CellQuest software with excitation wavelength of 488 nm. At least 10000 events were collected for each sample. The DNA distribution in cell cycles (FL2-A parameter) was analyzed by the ModFit software (Beckton Dickson, Mountain View, CA, USA).

2.6 Confocal laser scanning microscopy

2.6.1 Antibody staining in culture cells

Cells were grown on acid-etched coverslips for 24 hrs before treatment with and without 30 mM sodium chlorate. For staining HSPG, cells were fixed using Sainte-Marie's fixative as this gives better preservation of glycosaminoglycans (Tuckett and Morriss-Kay, 1988). Cells were blocked for 1 h at room temperature in blocking solution (PBS containing 10% FBS) and then stained with anti-HSPG

monoclonal antibody 10E4 (1:100 dilution). The cells then were washed with PBS and incubated with Alexa-488 conjugated secondary goat anti-mouse IgM antibody (1:400 dilution)

For staining paxillin and focal adhesion kinase (FAK) and F-actin, the cells were fixed with 4% paraformaldehyde in PBS for 10 min and permeabilized for 10 min with 0.2% Triton X-100 in PBS. Cells were blocked for 1 hr at room temperature in blocking solution (PBS containing 10% FBS). The cells were then incubated with anti-paxillin monoclonal antibody or anti-FAK polyclonal antibody in PBS containing 2% FBS at 4°C overnight, washed, and further incubated at room temperature for 1 hr with Alexa-568 conjugated secondary goat anti-mouse or goat anti-rabbit IgG antibody (1:200 dilution) and with fluorescein isothiocyanate (FITC)-conjugated phalloidin (for F-actin, 1:50 dilution) for 1 h at room temperature.

For staining cells on the fibronectin-coated coverslips, the coverslips were first coated with 20 µg/ml fibronectin at 4°C overnight and blocked with 1% BSA at room temperature for 1 hr. The coverslips were air-dried in the culture hood. MCF-7 cells were treated with 30 mM sodium chlorate for 48 hrs and re-plated onto the fibronectin-coated coverslips for 2 hrs with or without (control) sodium chlorate. The cells were then processed as above.

All coverslips were mounted on slides with Vectashield fluorescent mounting medium containing 4, 6-diamidino-2-phenylindole (DAPI) nuclear stain (Vector Laboratories, Burlingame, CA, USA). Stained cells were viewed and examined by

using an Olympus FluoView FV1000 Laser Scanning Confocal Microscope (Olympus, Melville, NY, USA).

2.6.2 Evaluation of apoptotic nuclear morphology

Briefly, cells were treated with 30 mM sodium chlorate for 48 hrs. Cells were then washed with phosphate-buffered saline (PBS). Cells were then fixed with 4% paraformaldehyde for 15 min. After washing, cells were incubated in DAPI at a final concentration of 10 µg/ml at room temperature for 15 min. Nuclear morphology was then examined with a Zeiss LSM510 confocal microscope (Carl Zeiss, Göttingen, Germany).

The apoptotic cells were recognized on the basis of nuclear condensation and DNA fragmentation including chromatin condensation, segmentation of nuclear chromatin of irregular size in DAPI stained cells under confocal microscope. The apoptotic index was expressed in percentage as positive cells per 100 cancer cells assessed in 10 high power fields, where apoptotic index (AI) = Number of apoptotic cells counted / Total number of nuclei × 100%.

2.7 *In situ* hybridization of *HS3ST3A1* on breast cancer patients

2.71 Patients and tumors

Formalin-fixed, paraffin embedded tissue sections from matched normal and invasive ductal breast cancer tissues of 22 patients were obtained from Department of Pathology, Singapore General Hospital (SGH). Clinicopathological information collected included patient age, tumor size, ER, PR and cerB2 status, and lymph node metastasis.

2.7.2 *HS3ST3A1 in situ* RNA probes preparation

Conventional PCR was run for amplification of *HS3ST3A1* gene using the following primers: Forward, 5'-ttgggcgagtctaagacgat-3' (Accession No.NM_006042, 524-543), Reverse, 5'-aggccaggggactcttcttc-3' (NM_006042, 1138-1157). The PCR product was cloned into a pDrive cloning vector (Qiagen, Hilden, Germany). The cDNA template was sequenced to confirm insert identity and orientation. The probe was then generated and digoxigenin-labelled using DIG RNA labelling kit (Roche Applied Science, Mannheim, Germany) according to the manufacturer's instructions. Briefly, equivalent of 1 µg of insert DNA was digested to linearize the template. SP6 or T7 RNA polymerase was used to produce antisense or sense probes respectively. To synthesize riboprobes, in a total volume 20 µl reaction, the following were added:

- 1 µg linearized plasmid DNA
- 2 µl 10 x DIG RNA labeling mix,
- 2 µl 10 x Transcription buffer,
- 2 µl 20 U/µl RNA polymerase (SP6 or T7)
- Add sterile RNase free double distilled water

The reaction was allowed for 2 hrs at 37° C before RNase-free, DNase I was add to remove template DNA for 15 min at 37° C. The reaction was stopped by adding 2 µl 0.2 M EDTA (pH 8.0). The probes were purified by ethanol precipitation to remove unincorporated nucleotides. The probes were diluted in hybridization buffer and stored at ~80 °C till usage.

2.7.3 *In situ* hybridization of *HS3ST3A1* on breast cancer patients

In situ hybridization was carried out in RNase-free procedures. Section slides were de-paraffinized and de-waxed by immersing in fresh xylene for 5 min with two changes and re-hydrated in graded series of ethanol of 100% ethanol, followed by one change of 90%, 70% and 50% respectively (each change lasting for 60 s). After fixation with 4% paraformaldehyde in PBS for 10 min and permeabilization with 20 µg/ml proteinase K for 20 min at room temperature, the slides were post-fixed for 5 min at room temperature with 4% paraformaldehyde in PBS. The slides were then washed with PBS containing 0.1% Tween-20 and acetylated for 10 min using 0.25 % acetic anhydride in 0.1M Triethanolamine-HCl pH 8.0. After wash again, the slides were incubated in pre-hybridization solution at 70°C for at least 2 hrs to block non-specific binding sites. The slide then incubated with hybridization buffer containing digoxigenin-labeled *HS3ST3A1* RNA probe (1 µl probe per 100 µl hybridization solution) at 70°C overnight in a humid chamber. After that the slides were washed with 1 x SSC containing 50% formamide for 30 min at 65 °C and then with NTE buffer (500 mM NaCl, 10 mM Tris, 1 mM EDTA, pH 7.5) for 10 min at 37°C. The slides were added 20 µg/ml RNase A to digest any single-stranded (unbound) RNA probe for 30 min at 37°C in NTE buffer. The slides were washed once with NTE for 10 min at 37°C and then with 2 x SSC for 20 min and with 0.2x SSC for 20 min at 65°C twice before blocked in 20% HISS/MABT solution (20% heat inactivated sheep serum in 100 mM Maleic acid, 150 mM NaCl, 0.1% Tween-20, ph 7.5) for 1 hr. The slides were then incubated with sheep anti-DIG-alkaline phosphatase (1: 2500, Roche Applied Science,

Mannheim, Germany) overnight in a humid chamber. After washing, the substrate NBT/BCIP solution (Roche) was added. The reaction was carried out in a humid chamber for 48-72 hrs in the dark until the color development was optimal and then the color reaction was stopped by washing out the NBT/BCIP solution and slides were fixed in 4% formaldehyde. Coverslips were mounted on the slides with mounting media (Vector Laboratories, Burlingame, CA, USA). No counter-staining was carried out and negative controls were performed by using sense probes.

2.7.4 Analysis of *in situ* hybridization of *HS3ST3A1*

To analyse the staining intensities, a semi-quantitative method was used as described in (Koo *et al.*, 2006). The scoring was represented by the percentage of positive cells x staining intensity (IPS). The intensity of staining is classified from a range of 0 = no expression, 1+ = weak expression, 2 + = moderate expression, 3+ = strong expression. The maximum IPS will be 300.

2.8 Western Blot

2.8.1 Extraction of protein

For Western blotting analysis of integrin, FAK and paxillin, MCF-7 cells were cultured with or without 30 mM sodium chlorate for 48 hrs. The cells were re-seeded onto fibronectin-coated (20 µg/ml) flask for 2 hrs. The cells were washed three times with ice-cold PBS, then lysed in cold lysis buffer (50 mM HEPES, 150 mM NaCl, 1% Triton X-100, 5 µg/ml pepstatin A, 5 µg/ml leupeptin, 2 µg/ml aprotinin, 1 mM PMSF, 100 mM sodium fluoride and 1 mM sodium vanadate, pH 7.5) and left standing on ice for 20 min. For analysis of F11R in MCF-12A cells, the cells were lysed in RIPA

buffer (50 mM Tris-HCl, pH 7.4, 150 mM NaCl, 1% NP40, 0.25% Na-deoxycholate, 5 µg/ml pepstatin A, 5 µg/ml leupeptin, 2 µg/ml aprotinin, 1 mM PMSF, 100 mM sodium fluoride and 1 mM sodium vanadate, pH 7.5). After removal of cell debris by centrifugation at 13,000 rpm for 20 min, the protein supernatant were collected and aliquoted and stored at -80°C until use.

The concentration of the protein was determined by using bicinchoninic acid (BCA) protein assay kit (Pierce, Rockford, IL, USA). Briefly, 25 µl of serial diluted standards and 25 µl of unknown sample (normally 5 times dilution, 5 µl of collected protein diluted in 20 µl lysis buffer) was pipetted into 96-well plate. Subsequently, 200 µl of the BCA reagent mixture solution (50 units of Bicinchoninic Acid Solution with 1 unit of 4% (w/v) $\text{CuSO}_4 \cdot 5\text{H}_2\text{O}$ Solution) was added to each well and mixed well. The plate was incubated at 37°C for 30 min and the absorbance was read at 562 nm. The concentration of protein in each sample was quantified by normalizing to the standard curve. The mechanism of BCA kit is that under alkaline pH conditions, the cysteine, cystine, tryptophan, tyrosine, and the peptide bond in the protein could reduce the Cu^{2+} to Cu^{1+} in the Cu^{2+} -protein complex. The reduction is proportional to the amount of the protein in the sample. The Bicinchoninic acid forms a purple-blue complex with Cu^{1+} in alkaline conditions, which has a maximum absorbance at 562 nm. BCA assay has several advantages over other protein quantitation assays such as Biuret, Lowry and Bradford assay. These advantages include a more stable color complex, tolerance of higher concentration of detergents and a broad range of protein concentrations.

2.8.2 Preparation of separating gel

Spacers and glass were washed and wiped with 70% ethanol. Separating gel (10%) was prepared with N, N, N', N'-Tetramethylethylenediamin (TEMED) and ammonium persulfate (APS) (Bio-Rad, Hercules, CA, USA) added in the final step (Refer to Table 2.7.1). The gel mixture was then quickly added into the space between the spacer and glass without causing any air bubble. Double distilled water was slowly overlaid on the gel to make an even surface of the gel. The gel was allowed to polymerize for at least half an hour.

2.8.3 Preparation of stacking gel

Waiting until the separating gel was completely polymerized, poured off the over-layer water. The mixture of stacking gel (4%) was added onto top of the separating gel. The teflon comb was carefully inserted into the stacking gel to make sure that no air bubbles were trapped under the comb. Waiting for another half an hour to allow the stacking gel to polymerize before gently pulled out the comb. Distilled water was squirted into the wells to wash out the remaining unpolymerized acrylamide.

Table 2.1 Formula of separating and stacking gel for Western blot

	Separating gel		Stacking gel	
	solutions	10%	solutions	4%
1.0 mm spacer	dd H ₂ O	2.785 ml	dd H ₂ O	2.165 ml
	1 M Tris pH8.5	3.75 ml	1 M Tris pH 6.8	375 µl
	30% Acrylamide	3.3 ml	30% Acrylamide	400 µl
	10% SDS	100 µl	10% SDS	30 µl
	10% APS	50 µl	10% APS	20 µl
	TEMED	15 µl	TEMED	10 µl
	Total volume	10 ml	Total volume	3 ml

2.8.4 Separating protein in the SDS-PAGE gel

The protein lysate was mixed with 5x sample buffer containing 5% β -mercaptoethanol (β -ME) and heated at 100°C for 10 min for reducing gel. For non-reducing gel, the protein lysate was mixed with 5x sample buffer without the β -ME and was not heated. Precision Protein Standards marker (Bio-Rad, Hercules, CA, USA) was added into a lane to indicate the molecular weight of protein. Twenty μ g of the samples were loaded into the well of the stacking and run until the bromophenol blue in sample buffer reached the bottom of the separating gel.

2.8.5 Transfer of protein to PVDF membrane

A “gel-sandwich” was made on a semi-dry transfer cassette. From the bottom of the cassette to the top, lay a Whatman’s paper, PVDF membrane (Amersham Biosciences, Freiburg, Germany) which was soaked in methanol for 10 s and equilibrated in transfer buffer for 10 min, SDS-PAGE gel, another piece of Whatman’s paper sequentially. Each layer of the “gel-sandwich” was rolled over by a glass band to remove any air bubbles that may be trapped. The process of protein transfer was run for 50 min at 15 v voltage.

2.8.6 Incubation with primary and secondary antibody

After the transferring, the membrane was gently rinsed 2 times in TBST buffer (10 mM Tris-HCl, pH 7.5, 150 mM NaCl, 1% Tween-20). Then the membrane was incubated with 5% non-fat milk for 1 hr at room temperature to block the non-specific binding sites. The membrane was incubated with different primary antibodies diluted in the 5% non-fat milk at room temperature for 1 hr or at 4°C overnight. The

membrane was washed 3 times in TBST buffer, each for 10 min, before re-probed with horseradish peroxidase (HRP) conjugated secondary antibodies (1:1000 to 1:10000, diluted in the 5% non-fat milk) for 1 hr at room temperature. The membrane was again washed with TBST for 2 times before adding of the ECL. For β -actin blotting, membrane was stripped with stripping buffer containing 62.5 mM Tris- HCl (pH 6.7), 2% SDS and 100 mM β -mercaptoethanol at 55 °C for 30 min and re-probed with monoclonal mouse anti-actin antibody for normalization of protein loading.

2.8.7 Band development by Enhanced Chemiluminescence (ECL)

Enhanced Chemiluminescence substrates (ECL Western Blotting Detection Kit, Amersham Pharmacia, Germany) was mixed in a 1:1 ratio according to the product insertion and added onto the membrane which was placed on a backbone film. The membrane together with the backbone was wrapped with cling wrap film carefully. The whole package was then placed in a film cassette. One piece of film was exposed to the membrane for 1-5 min to obtain optimal results.

2.8.8 Densitometric analysis of the band intensity

The bands on the film indicating the protein size and the expression level were scanned with a densitometer (Imaging Densitometer, Model GS-710, Bio-Rad, CA, USA). The intensity of the bands were measured with the Quantity-one Image Analysis software (Bio-Rad, version 4.62). The ratio of the intensity of the bands relative to β -actin was then calculated and used to quantify the expression level of the protein.

2.9 Quantitative real time polymerase chain reaction (qPCR)

2.9.1 Extraction of total RNA

Total RNA was extracted from monolayer cells grown in the 6-well plate with a commercially available RNeasy mini kit (Qiagen, Hilden, Germany). All the principal reagents were provided in the kit. The extraction process was following the protocol provided in the user manual of the kit. Briefly, cells growing in monolayer in the 6-well plates were first washed completely with cold 1 x PBS to remove any remaining medium. The cells were then lysed by adding of 350 μ l buffer RLT containing 1% β -ME. The cell lysates were collected by a cell scraper and further homogenized by passing through a 27# gauge for 5 times. Subsequently, the cell lysates were mixed well with 1 volume of 70% RNase-free methanol and transferred into a RNeasy MiniElute spin column in a 2 ml collection tube. The column was then centrifuged for 15 s at maximum. After discarded the flow through, 350 μ l Buffer RW1 was added to the column to wash the membrane by centrifugation. RNA was then treated with 10 μ l ribonuclease (RNase)-free deoxyribonuclease I (DNaseI, 2.7 Kunitz units/ μ l, Qiagen, Hilden, Germany) diluted in 70 μ l buffer on the column at room temperature for 15 min to remove all trace of genomic DNA. The column was further washed by 500 μ l Buffer RPE by centrifugation for 2 times. Finally, 32 μ l RNase-free water was pipetted directly onto the center of the silica-gel membrane in the MiniElute column and allowed to soak the membrane for 1 min before eluting the RNA by centrifugation for 1 min at maximum speed. Concentration and purity of RNA were measured by a spectrophotometer (Biophotometer, Eppendorf, Hamburg,

Germany) in a 1-cm path-length quartz cuvette. All RNA preparation had an OD₂₆₀:OD₂₈₀ ratio between 1.8 and 2.1.

2.9.2 Synthesis of first strand cDNA

Complementary DNA (cDNA) was synthesized from 2 µg DNA-free total RNA with random hexamer primer and SuperScript III reverse transcriptase (Invitrogen Life Technologies, Carlsbad, CA, USA). Briefly, 2 µg RNA was mixed with 1 µl random hexamer primer (50 ng/µl) and 1 µl of dNTP (10 mM stock), topped up with DEPC-treated H₂O to 13 µl, followed by centrifugation and heating at 65°C for 5 min. The mixture was immediately put on ice for at least 3 min. Subsequently, 4 µl of 5 x first strand reaction buffer, 1 µl of Rnase inhibitor, 1 µl SuperScript III reverse transcriptase and 1 µl DEPC-treated H₂O were added to make up the total reaction volume of 20 µl. The content was mixed thoroughly before allowed to react at 50 °C for 1 hr. Immediately after the reaction, the mixture was heated at 70 °C for 15 min to inactivate the SuperScript III, and the resultant cDNA was then diluted 1:10 with DEPC-treated H₂O and aliquoted and stored at -20°C until use.

2.9.3 Quantitative real time polymerase chain reaction (qPCR)

Real time PCR was performed with the Light Cycler System (Roche, ID, USA), using the QuantiTect SYBR Green PCR kit (Qiagen, Hilden, Germany). Primers were designed using the PRIMER3 software (<http://www.genome.wi.mit.edu>) and the BLASTn version 2.2.16 (<http://www.ncbi.nlm.nih.gov/blast>) was used to compare the obtained sequence against the non-redundant nucleotide database to make sure the

primer was specific. Then the primers were sent out for commercial synthesis (synthesized by First Base, Singapore) as following:

Table 2.2 Primers for quantitative real-time PCR

Gene	Gene accession No.	Primers (5'-3')	Span range	Amplicon length (bp)
HS3ST3A1	NM_006042	F:5'-cagtgcctctccacctc-3' R:5'- gccaggcagtagaagacgtaa-3'	(819-836) (906-926)	108
HS3ST3B1	NM_006041	F: 5'- ctggcttcaggcaaggagat-3' R: 5'- gaccactgaaaaagctgga-3'	(622-641) (706-725)	104
ITGB1	NM_002211	F: 5'- ctgcgagtgtggtgtctgtaa-3' R: 5'- gaacattcctgtgtgcatgtg -3'	(1962-1982) (2103-2123)	162
FAK	NM_005607	F: 5'- tggacgatgtattggagaagg-3' R: 5'- atgaggatggtcaaactgacg-3'	(1491-1511) (1645-1645)	175
PXN	NM_002859	F: 5'- ccacacataccaggagattgc-3' R: 5'- gggttggagacactggaagt-3'	(185-205) (353-373)	189
β -actin	NM_001101	F: 5'- ggcattgggtcagaaggatt-3' R:5'- aggtgtggtgccagatttc-3'	(209-227) (322-341)	133
36B4	NM_001002	F: 5'- ctgttgcacagtacccatt-3' R: 5'- gccttgacctttcagcaag-3'	(875-895) (958-977)	103

The total volume of real time PCR reaction was 10 μ l containing 1 μ l of the diluted cDNA , 0.5 μ l forward primer, 0.5 μ l reverse primer (each of 10 μ M stock) and 5 μ l QuantiTect SYBR Green Master solution and 3 μ l DEPC-treated H₂O. According to the manufacturer's instructions of the QuantiTect SYBR Green Master solution kit, the cycle parameters of the real time PCR consisted of four programs:

Program 1: Denaturation of the template cDNA and activation of the polymerase. The mixture was preincubated at 95 °C for 15 min for 1 cycle to activate the recombinant Taq DNA polymerase.

Program 2: Amplification of the target gene. Cycle parameters were set as following: denaturation at 94 °C for 15 s, annealing for 25 s (annealing temperature depending on primers, but the primer design in such a way that the annealing

temperature normally is 60°C), extension at 72 °C for 12 s, 35 - 45 cycles.. Fluorescence was detected at the end of the annealing step of each cycle to monitor the progress of amplification.

Program 3: Melting curve analysis. To examine if there was primer-dimer or non-specific amplification, melting-curve analysis was performed immediately after the amplification. The melting curve analysis parameters were set as the following: denaturation at 95 °C for 0 s by a temperature transition rate of 20 °C /s, incubation at 65 °C for 15 s, and heating up to 95°C with transition rate of 0.1 °C/s. Melting-curve was plotted as the first negative derivative of the fluorescence versus temperature $[-d(F)/dT]$ by the LightCycler data analysis software. A single, narrow and sharp peak normally means a specific amplification.

Program 4: Cooling the rotor and thermal chamber: Temperature was decreased to 40 °C for 30 s to cool the system.

2.9.4 Agarose gel electrophoresis for the qPCR product

The qPCR product was also checked by agarose gel electrophoresis to exclude the possibility of non-specific amplification. After the qPCR amplification, the amplified products were acquired by a short spin with capillaries inverted into eppendorf tubes. 5 µl of the qPCR product was mixed with 1µl of loading dye (Blue/Orange 6x loading dye containing 15% Ficoll 400, 0.03% bromophenol blue, 0.03% xylene cyanol FF, 0.4% orange G, 10 mM Tris-HCL pH 7.5 and 50 mM EDTA) and electrophoresed on 1% agarose gel in the presence of ethidium bromide in TAE buffer (40 mM Tris-acetate, 1 mM EDTA, pH 8.1-8.3) or TBE buffer (89 mM

Tris-Boric acid, 2 mM EDTA, pH 8.1-8.3) to further verify the product specificity. The band was viewed by Gel Documentation Image Analysis System V6.03 (ChemiGenius SynGene, Cambridge, UK).

2.9.5 Gene expression analysis of qPCR data

The $2^{-\Delta\Delta C_t}$ method was used to calculate fold changes in the expression levels of the genes (Livak and Schmittgen, 2001). Threshold cycle (C_t) was determined as the cycle number at which the SYBR fluorescence signal in the sample first exceeds the level of background noise and becomes exponential which reflects the amplification copies of interested gene, using the second-derivative maximum method of the LightCycler software.

ΔC_t is equal to the difference in threshold cycle for target gene and reference gene ($C_{t, \text{target}} - C_{t, \text{reference}}$) in one group. Subsequently, the $\Delta\Delta C_t$ values were calculated by subtracting the ΔC_t value of untreated control from that of the treated group at same time point: $\Delta\Delta C_t = (C_{t, \text{target}} - C_{t, \text{reference}})_{\text{treated}} - (C_{t, \text{target}} - C_{t, \text{reference}})_{\text{control}}$.

Relative quantification of the fold changes in gene expression were calculated by using the formula: fold change = $2^{-\Delta\Delta C_t}$

2.10 Proliferation assay

Proliferation assay was done by MTS method or crystal violet method. For crystal violet method, in 96-well plates, 4×10^3 MCF-7 cells or 2×10^3 MDA-MB-231 cells per well in 200 μ l volume were seeded in serum-containing media in the presence or absence of 30 mM sodium chlorate and incubated for 24, 48, 72, 120 and 168 hrs. Medium was changed every 48 hrs. For the study of the effect of different exogenous

HS species on MCF-7 cell growth and MDA-MB-231 cell growth, 6×10^3 MCF-7 cells or MDA-MB-231 cells per well in 200 μ l volume were seeded in serum-containing media in the presence or absence of 30 mM sodium chlorate with or without the exogenous HS and incubated for 72 hrs. Cell number was determined using crystal violet assay. Briefly, at each experimental time point, cells were washed with phosphate-buffered saline (PBS), fixed in 4% formaldehyde for 15 min and stained with 0.25% crystal violet in 20% methanol in PBS for 30 min. After washing again, crystal violet was released with 1% sodium dodecyl sulfate (SDS) for 1 hr. Absorbance was read at 595 nm using a plate reader. Growth was measured as compared to a standard curve of cells grown in serum-containing media.

For MTS assay, after 72 hrs post-transfection of *HS3ST3A1* siRNA in MCF-12A cells, MTS method was used to determine the cell number. MTS assay was performed using the CellTiter 96 Aqueous non-radioactive proliferation assay (MTS, Promega Corp., Madison, WI, USA) which is a colorimetric method for determining the number of viable cells in proliferation assays. The main components in the assay are the tetrazolium compound 3-(4,5-dimethylthiazol-2-yl)-5-(3-carboxymethoxyphenyl)-2-(4-sulfophenyl)-2H-tetra-zolium (MTS) and phenazine methosulfate. MTS is bio-reduced due to the mitochondrial activity in the cells into a soluble formazan which can be measured directly at 490 nm. The quantity of formazan is directly proportional to the number of living cells in culture.

2.11 Adhesion assay

96-well cell culture plates were coated with fibronectin (20 µg/ml) and collagen I (20 µg/ml) in 100 µl volume in PBS at 4°C overnight. Wells were then washed with PBS and the unbound sites were blocked with 100 µl 1% BSA for 1 hr at 25°C. Wells were then washed twice with PBS again and air-dried in the hood and stored in 4°C for later use. Cells are harvested with 0.02% EDTA and 0.25% trypsin. Cells were re-suspended in cell growth medium without FBS and re-seeded at a concentration of 1×10^5 MCF-7 cells and MDA-MB-231 cells per well in 96-cell plates or 8×10^4 MCF-12A cells per well in 100 µl volume in 96-cell plates and allowed to attach for 30 min at 37°C in a humidified incubator containing 5% CO₂. The cell number was determined as in Section 2.10 (Proliferation assay).

2.12 Migration assay

Migration assay was performed by two methods. One is using wound scratching model. The other is using a commercially available transwell. For the “wound scratching” model, MCF-7 cells or MDA-MB-231 cells were seeded in 6-well plates and grown to confluence in the presence or absence of 30 mM sodium chlorate with or without different HS species. The number of seeded cells was selected so that the culture will become confluent 48 hrs after seeding. The scratch wound in the confluent cell monolayer was made using a sterile 200 µl-yellow plastic pipette tip. And the cells were continued to culture with medium containing 2% FBS in the presence or absence of 30 mM sodium chlorate. Wound closure was monitored every 4 hrs and photographed using Nikon Digital Sight DS-L1 camera (Nikon, Melville, NY, USA).

The distance between the wound edges was measured. These experiments were repeated at least three times. The distance migrated was given by the difference between the initial wound width and the wound width at each of the monitored time points.

For migration assays performed by Costar transwell insert (8- μ m pore size). MCF-12A cells are harvested with 0.02% EDTA and 0.25% trypsin after 72 hrs post-transfection of *HS3ST3A1* siRNA in MCF-12A cells. Cells were re-suspended in DMEM/F12 medium containing 0.1% BSA (Sigma-Aldrich) without FBS. Cells were seeded at a concentration of 5×10^4 /well in 100 μ l volume in the upper chamber of the transwell. The lower chamber was filled with 600 μ l MCF-12A cell full growth medium containing 15% FBS as chemoattractant. Cells were allowed to migrate for 16 hrs at 37°C in a humidified atmosphere containing 5% CO₂. Non-migrated cells on the upper side of the membrane were removed with a cotton swab. Migrated cells attached to the lower side of the membrane were fixed and stained with 0.5% crystal violet in 20% methanol in PBS for 30 min. The cells were counted using a light microscope at 100x magnification (Nikon, Melville, NY, USA). Each data point represents the mean of five independent microscopic fields in three independent experiments (15 fields). All migration assays were performed on three separate experiments, run on duplicates.

2.13 Invasion Assay

Cell invasion assay was carried out using BD BioCoat Cell Environments, Matrigel™ invasion chamber. MCF-7 cells and MDA-MB-231 cells were harvested after 48 hrs culture in the presence or absence of 30 mM sodium chlorate in

serum-containing media. MCF-12A cells are harvested with 0.02% EDTA and 0.25% trypsin after 72 hrs post-transfection of *HS3ST3A1* siRNA. Cells were re-suspended in each growth medium containing 0.1% BSA (Sigma-Aldrich) without FBS. Cells were seeded at a concentration of 1×10^5 /well in 100 μ l volume in the upper well of the invasion chamber. The lower chamber were filled with 600 μ l full growth medium containing 15% FBS as chemoattractant. Cells were allowed to invade for 24 hrs at 37°C in a humidified atmosphere containing 5% CO₂. The matrigel and the non-invaded cells in the upper well were removed with a cotton swab. Invaded cells attached to the lower side of the membrane were fixed and stained with 0.5% crystal violet in 20% methanol in PBS for 30 min. The cells were counted using a light microscope at 100x magnification (Nikon). Each data point represents the mean of five independent microscopic fields in three independent experiments (15 fields). The invasion assays were performed in duplicates on three separate occasions.

2.14 Gene expression profiling using GeneChip™ Microarray

2.14.1 RNA preparations

For RNA preparations, MCF-12A cells were transfected with *HS3ST3A1* siRNA for 48 hrs. Total RNA was extracted with RNeasy Mini kit (Qiagen, Hilden, Germany) as in Section. RNA was also treated with ribonuclease (RNase)-free deoxyribonuclease I (DNaseI) to remove all trace of genomic DNA.

2.14.2 Preparation of Labeled cRNA and Array Hybridization

All procedures were performed according to the instructions from Affymetrix (Santa Clara, CA).

2.14.2.1 First Strand Synthesis

Total RNA (2.5 µg) was converted into first-stranded cDNA by using SuperScript II reverse transcriptase (Invitrogen Life Technologies, Carlsbad, CA, USA) and an T7-(dT)24 primer. T7-(dT)24 primer sequence: 5'-GCCAGTGAATTGTAATACGACTCACTATAGGGAGGCGG-(dT)24 - 3'

The steps taken were:

1. Primer hybridization:
 - 2.5 µg Total RNA
 - (Variable) Nuclease free H₂O (to complete 1st strand final reaction volume of 11 µl)
 - 1 µl T7-(dT)24 primer (50 ng/µl)
 2. Incubation at 70°C for 10 min
 3. Sample was quickly spun down and put on ice to avoid the re-naturing the RNA
 4. Addition of
 - 4 µl 5X First strand cDNA buffer
 - 2 µl 0.1 M DTT
 - 1 µl 10 mM dNTP mix
 - 1 µl RNAsin (RNase inhibitor)
- And the mixture was spun down and incubated at 42°C for 2 min
5. And Addition of 1 µl Superscript II
 6. Mixed well and incubated at 42°C for 1 hr
 7. Centrifuged briefly and placed on ice

2.14.2.2 Second Strand Synthesis

To synthesize second strand, the following steps were taken:

Addition of the following in an Eppendorf tube:

- 91 μ l DEPC treated H₂O
- 30 μ l 5 x Second strand buffer
- 3 μ l 10 mM dNTP mix
- 1 μ l E.Coli DNA Polymerase I (10 U/ μ l)
- 1 μ l E.Coli DNA Ligase (10 U/ μ l)
- 1 μ l RNase H (2 U/ μ l)

1. Final Volume: 150 μ l
2. Gently tapped the tube to mix the content and, briefly centrifuged down
3. Incubated at 16°C for 2 hrs
4. Addition of 2 μ l (10 U) T4 DNA Polymerase
5. Incubated for 5 min at 16°C
6. Reaction was stopped with 10 μ l of 0.5 M EDTA

2.14.2.3 Clean Up of Double Stranded cDNA

To remove the unbound dNTP and enzymes, the yield double stranded cDNA was cleaned up by the following steps:

1. Addition of 600 μ l cDNA binding buffer
2. Mixed by vortexing for 3 s
3. Application of 500 μ l of the solution to cDNA Clean Spin Column
4. Centrifuged at 13,000 rpm for 1 min
5. Reloaded the remaining mixture and repeated the centrifugation
6. Transferred the column into a new 2 ml Collection tube
7. Addition of 750 μ l cDNA Wash buffer
8. Centrifuged for another 1 min at 13,000 rpm
9. Discarded the flow-through
10. Opened the column cap and re-centrifuged for 5min at 13,000 rpm to dry the membrane
11. Transferred the column into a new 1.5 ml Collection tube
12. Addition of 14 μ l Elution buffer and centrifuged for 1 min at 13,000 rpm to elute the “clean-up” double stranded cDNA

13. Retaining the elution.

2.14.2.4 Synthesis of Biotin-Labeled cRNA (cRNA in-vitro transcription, IVT)

The double stranded cDNA was used as template to generate biotin-labeled cRNA in vitro with the EnZo BioArray High Yield Transcript Labling Kit (Enzo Diagnostics, Inc. Farmingdale, USA).

To make IVT Master Mix , the following steps were taken at room tempature:

1. Addition of the following

- 12 μ l double stand cDNA
- Variable Nuclease free H₂O (final reaction volume of 40 μ l)
- 4 μ l 10x IVT Labeling Buffer
- 12 μ l IVT Labeling NTP Mix
- 4 μ l IVT Labeling Enzyme Mix
- Total Volume 40 μ l

2. Incubated at 37°C for 16 hours

3. Proceeded to Cleanup and Quantification of Biotin-Labeled cRNA or cRNA was kept at -20°C until use.

2.14.2.5 Cleanup and Quantification of Biotin-Labeled cRNA

To remove the unbound Labeling NTP and enzymes, the following steps were taken and the yield cRNA was cleaned up.

1. Addition of 60 μ l RNase-free H₂O to the IVT reaction tube and mixed.
2. Addition 350 μ l IVT cRNA Binding Buffer and mixed.
3. Addition 250 μ l 100% ethanol to the mixture, and mixed by pipetting.
4. Applied the sample (about 700 μ l) to the IVT cRNA Cleanup Spin Column
5. Centrifuged at 13,000 rpm for 15 s
6. Pipetted 500 μ l of IVT cRNA Wash Buffer onto the spin column and centrifuged at 13,000 rpm for 15 s to wash the column membrane
7. Discarded the flow-through
8. Opened the column cap and centrifuged for 5 min at 13,000 rpm to dry the membrane

9. Transferred the column into a new 1.5 ml Collection tube
10. Addition 11 μ l Elution buffer to the centre of the membrane and allow the buffer to soak the membrane for 1 min
11. Centrifuged the column at 13,000 rpm for 1min
12. Re-added 10 μ l Elution buffer to the centre of the membrane and centrifuged at 13,000 rpm for 1min
13. The “cleaned-up” cRNA was be kept at -20°C until use after the quantification step (see below)

2.14.2.6 Quantification and fragmentation of cRNA

Before hybridize the cRNA to the GeneChip microarray, the cRNA must be quantified in order to use the same amount cRNA as the start material in hybridization.

Quantification of cRNA

According to the GeneChip analysis technique manual, because total RNA was used as starting material in this experiment, (Gene expression profiling in MCF-12A cells after knock-down the *HS3ST3A1* by siRNA), so the final cRNA yield was adjusted to excluded the carryover amount of the unlabelled total RNA.

Adjustment formula was as following by using an estimation of 100% carryover.

$$\text{Adjusted cRNA yield} = \text{cRNA}_{\text{total}} - (\text{starting total RNA}) \times (y)$$

where: $\text{cRNA}_{\text{total}}$ = amount of cRNA measured after IVT (μg)

starting total RNA = starting amount of total RNA (μg)

y = fraction of double stranded cDNA reaction used in IVT

In this experiment, 2.5 μg total RNA was the starting amount and 100% of the double stranded cDNA product was added to the IVT.

So adjusted cRNA yield = measurement amount of the total cRNA- (2.5 µg total RNA) x (100% fraction)

The quantity, quality, and purity of the RNA and cRNA were checked first by using an Eppendorf spectrophotometer (Biophotometer, Eppendorf, Hamburg, Germany) and a 1-cm path-length cuvette. The absorbance was measured at the wavelength of 260 nm and 280 nm and the A260:A280 ratios were calculated. Then the quantity, quality, and purity of the RNA and cRNA were assessed by detecting 28S/18S ribosomal RNA peak using the RNA 6000 Nano LabChip[®] kit on the Agilent 2100 Bioanalyzer (Agilent Technologies, Palo Alto, CA, USA) according to the manufacturer's instructions as described in the RNA 6000 Nano Assay reagent kit guide (Agilent Part number: G2941-90126). Briefly, the chip was primed with gel-dye mix made of 1 µl of RNA 6000 Nano dye and 65 µl of filtered gel and the conditioning was done using 9 µl of RNA 6000 Nano gel-dye solution. Five µl of RNA 6000 Nano Marker was added to each of the sample wells and the well for the RNA ladder. One µl of heat denatured RNA ladder (diluted 150-fold) was added to the RNA ladder well and 1 µl of sample was added to each of the sample wells. The chip was vortexed in the IKA vortex station at 2400 rpm for 1 min and was then inserted into the Agilent 2100 BioAnalyzer. Only samples that reached the anticipated purity and integrity parameters (RIN \geq 9.5; A260:A280 \geq 1.9) were introduced within the microarray pipeline process.

The RIN (RNA Integrity Number) is an algorithm developed by Agilent (Agilent Technologies, Palo Alto, CA, USA). The algorithm assigns integrity values to RNA by

selecting and calculating several features of the RNA integrity. This is a user-independent and automated process that makes the RNA integrity measurements standardized across all the samples. The Agilent 2100 Bioanalyzer can be used to measure the quantity, integrity and purity of small amount of RNA. A valuable advantage of the Agilent 2100 Bioanalyzer is that it combines and automates rapid sample handling, sensitive separation and accurate analysis through the micro-channels in a Lab-on-a-Chip at the same time.

2.14.2.7 Fragmentation of cRNA

Twenty ug of the labeled cRNA was fragmented.

Addition of :

- 20 μg adjusted cRNA
- 8 μl 5 x Fragmentation buffer
- ~12 μl Rnase-free H₂O to top up to 40 μl final reaction volume

1. Incubated at 94°C for 35 min.
2. Put on ice and 1 μl of the fragmented cRNA was used for analysis on the Bioanalyzer 2100. The standard fragmentation procedure produced a distribution of RNA fragment sizes from approximately 35 to 200 bases

2.14.2.8 Hybridization to Affymetrix GeneChip U133 plus 2.0

The final hybridization mixture was prepared as following:

Addition of

- 15 μg Fragmented cRNA (about 3/4 reaction volume of the above fragmented cRNA)
- 5 μl Control oligonucleotide B2
- 15 μl 20x Eukaryotic Hybridization Controls (bioB, bioC, bioD, Cre)
- 3 μl Herring Sperm DNA (10 mg/ml)
- 3 μl BSA (50 mg/ml)
- ~84 μl Nuclease free water
- 150 μl 2x Hybridization Buffer

Total volume: 300 μl

1. Denaturation of the hybridization cocktail at 99 °C for 5 min
2. Transferred the hybridization cocktail to a 45°C heat block for 5 minutes.
3. Hybridization cocktail(s) was spun at maximum speed in a microcentrifuge for 5 min to remove any insoluble material from the hybridization cocktail
4. Addition of the cocktail to the Affymetrix Test 3 array to check the quality of the hybridization cocktail according to manufacturer's criteria and if the Test chip gave a satisfactory hybridization results, the "real" hybridization was run.

The criteria of a satisfactory hybridization included:

- 3'/5' ratios of housekeeping genes, β -actin and GAPDH were ≤ 3 and very close to 1.0
 - Signal background was below 100
 - Relative ratios of scaling factors among all the chips were ≤ 3
 - Spike-in controls of bioC, BioD and cre must be present
 - Spike-in control of bioB must be present in at least 50% of arrays
5. The cocktail was then added to Affymetrix GeneChip U133 plus 2.0 and allowed to hybridize for 16 hrs at 45°C with rotation at 60 rpm in the Hybridization Oven 640 (Affymetrix Inc., Santa Clara, CA, USA)

2.14.2.9 Washing and staining procedure

After 16 hrs hybridization, the hybridization cocktail was removed from the GeneChip U133 plus 2.0 array and stored at -80°C. The Chips were filled completely with Non-Stringent Wash Buffer to remove any remaining air bubbles. Then the U133 plus 2.0 arrays were washed and stained with streptavidin-phycoerythrin conjugate (Molecular Probes, Eugene, OR, USA). The washing and staining procedure were

performed in the Fluidics Station 400 (Affymetrix) by using the appropriate fluidics protocols, following the manufacturer's instructions.

During the washing and staining processes, the GeneChip was stained with a streptavidin-phycoerythrin (SAPE) that binds to biotin which was conjugated to cRNA on the Chips. This streptavidin-biotin interaction was a signal amplification step that resembles the mechanism of the ABC kit as in Section 2.4 Immunohistochemistry. On the day of washing and staining, prepare the following SAPE stain solution and antibody solution as in Table 2.3 and Table 2.4. The Affymetrix Fluidics Station was set up to perform the protocol as in Table 2.5.

Table 2.3 SAPE stain solution

Components	Volume	Final Concentration
2x MES Stain Buffer	600.0 μ l	1x
50 mg/mL acetylated BSA	48.0 μ l	2 mg/ml
1 mg/mL Streptavidin-Phycoerythrin (SAPE)	12.0 μ l	10 μ g/ml
Water	540.0 μ l	
Total	1200 μl	

Table 2.4 Antibody Solution

Components	Volume	Final Concentration
2x MES Stain Buffer	300.0 μ l	1x
50 mg/mL acetylated BSA	24.0 μ l	2 mg/ml
10 mg/mL Normal Goat IgG	6.0 μ l	0.1 mg/ml
0.5 mg/mL biotinylated antibody	3.6 μ l	3 μ g/ml
Water	266.4 μ l	
Total	600 μl	

Table 2.5 Washing protocol

Post Hybridization Wash 1	10 cycles of 2 mixes/cycle Wash Buffer A at 25°C
Post Hybridization Wash 2	4 cycles of 15 mixes/cycle Wash Buffer B at 50°C
Stain	Stain probe array for 30 minutes SAPE Solution at 24°C
Final Wash	10 cycles of 4 mixes/cycle Wash Buffer A at 25°C

2.14.2.10 Image scanning

After washing and staining, the GeneChips were again filled completely with Non-Stringent Wash Buffer to remove any remaining air bubbles. The microarrays were then scanned by Affymetrix GeneChip Scanner 3000 according the Affymetrix protocol. Scanned output image files (.Dat file) were analyzed with Affymetrix Microarray Suit V5.0 (MAS5) to create .CEL Files and .CHIP Files.

2.14.3 Gene expression data analysis

The scanned images was read and pre-processed by Affymetrix Microarray Suite 5.0 (Affymetrix, Santa Clara, CA, USA). All microarrays were pre-processed and scaled to a standard target intensity of 500 by using the MAS 5.0 software. Then the .CEL files were processed and normalized using different analysis softwares

For every probeset, background subtraction, normalization and expression summaries were calculated by three commonly used methods. First the MAS5 method was used to obtain probeset summaries. The MAS 5.0 algorithm uses a scale normalization technique taking into account perfect match (PM) and mismatch (MM) probe pairs to correct for non-specific hybridization A detailed description of this algorithm has been widely published (Affymetrix, 2001; Affymetrix Inc, 2002). Next,

dCHIP software (Li and Wong, 2001a; Li and Wong, 2001b) was used. This software incorporates the model-based expression indexes (MBEI) which by using of a multiplicative model to take account for probe affinity effects in calculating probeset expression. Finally, the robust multiarray average (RMA) method (Irizarry *et al.*, 2003a; Irizarry *et al.*, 2003b) was used; this method first uses a model-based background noise correction which ignores MM values and then performs a quantile normalization, and finally runs an iterative median polish to remove probe affinity effects when calculating probe set expression.

2.14.3.1 MAS5 analysis:

For **single array analysis**, MAS 5.0 first calculates the value for each probe pair by subtracting the MM (non-specific) signal from the PM (total) signal, then MAS5 calculates statistical significance for the average difference between probe pairs and generates the detection calls Absent (A), Marginal (M), or Present (P) for each probe set which indicates whether a gene transcript is reliably detected or not. A value of $p > 0.06$ indicates that the gene is not detected at a level significantly different from background and is thus designated as Absent; a p value between 0.06 and 0.04 results in a Marginal call; and a $p < 0.04$ indicates Present. The average of the differences represents the final "signal" and is reflective of the level of expression of the gene. During this single array analysis, each array was checked by looking into the hybridization control spikes which were used to address the array hybridization sensitivity and efficiency. Quality control for spike controls BioB and BioC were present in all 6 arrays. Internal controls GAPDH and β -actin were inspected by

calculating the 3'/5' ratio. In all our experiment, these ratios in all 6 samples were near 1 (not more than 3 according to Affymetrix protocol).

The comparison analysis: MAS 5.0 estimates the magnitude and direction of changes (Signal Log Ratio) of a gene transcript in two conditions by comparing each other (for example, experiment versus control). In our present study, comparison files were generated from .CEL files by MAS5 for each array of the two group samples, using control array as a baseline and the siRNA group array as an experiment, thus generating 9 comparisons. The scale used for Signal Log Ratio) was base 2, making it easy to calculate fold change as a Change of 1 in Signal Log Ratio indicates 2 fold change of the expression level.

The Change algorithm generated “Change p- value” and an associated a change call of Increase (I), Marginal Increase (MI), No Change (NC), Marginal Decrease (MD), or Decrease (D). Change p-values range in scale from 0.0 to 1.0 with those close to 0.0, indicating likelihood for an increase in gene transcript expression. This strategy removes differences (variability) due to different probe binding efficient and cancels out much of the proportional relationship between random error and signal intensity, it is therefore a more accurate estimate of differential expression than comparisons made from single-array analyses where the probe pairs are first averaged so that only a single pair of values is used for comparison. Finally the MAS 5.0 program creates the user's file (so-called .CHP file), which can be two forms: single array file or comparison file.

Filter criteria for gene selection in MAS5

The following criteria were used for determining the selection for those differentially expressed genes in MAS5.

First filter: Detection calls, P call was at least 50% present in 6 arrays

Second filter: Change algorithm calls, the same Change directions were at least 5 out of the 9 comparisons, for example 5 Is out 9 comparisons, or 4 Ds plus 1 MD out of 9 comparisons.

Third filter: Fold Change, the absolute fold-change value was at least 2 fold between the average of the control group and the siRNA groups.

2.14.3.2 GeneSpring analysis

The data set was then loaded into a data mining program, GeneSpring 7.0 (Silicon Genetics, Redwood City, CA, USA). Expression values for each gene were calculated using the Affymetrix Microarray suite (MAS5.0) software as above. In each array, the expression files were normalized to the median (50th percentile) intensity of the same array. The expression value were normalized across the arrays by scaling the average of the intensities of all the probesits to a constant target intensity and compare the expression change in DATA Mining Tool 3.0 (Affymetrix, Santa Clara, CA, USA). The resultant file containing signals, p-values, and detection calls were imported to GeneSpring V7.0 (Silicon Genetics, Redwood City, CA) software for subsequent analysis. Differentially expressed genes were analyzed by One-Way ANOVA with P level of 0.05 taken as statistically significant. Agglomerative average-linkage hierarchical clustering of the 6 arrays of two experimental groups was obtained for

selected genes with GeneSpring (Chu *et al.*, 2001) software using standard correlation as similarity matrix.

Filter criteria for gene selection in GeneSpring

The following criteria were used for determining the selection for those differentially expressed genes analyzed by GeneSpring.

First filter: Detection calls, P call was at least 50% present in 6 arrays and if the Present calls were just 50%, then they must be in all of the 3 control groups or in all of the siRNA experimental groups. **Second filter:** Fold Change, the absolute fold-change value was at least 2 fold between the average of the control group and the siRNA groups. **Third filter:** Statistically significance, analyzed by One-Way ANOVA with P level of 0.05 taken as statistically significant.

2.14.3.3 dChip analysis

DNA-Chip Analyzer 2007 (dChip; <http://www.dchip.org/>) software was used to normalize the raw microarray intensity by read in the .CELfiles and then calculate the model-based expression indexes (MBEI) using the PM-MM-only model with outlier detection. dCHIP software (Li and Wong, 2001a; Li and Wong, 2001b) incorporates the model-based expression indexes (MBEI) that applies an invariant probe set normalization method to summarize gene-level intensity. The “invariant probe set” chooses a subset of PM-only probes with small within-subset rank difference in the two microarrays to serve as the basis for fitting a normalization curve with one array as a reference array and keeps the expression ratio values between two datasets under consideration unchanged by forcing the selected non-differentially expressed genes to

have equal values. The outlier detection algorithm of the dChip software allowed further quality assessment of microarray data by cross-referencing one array with other arrays through a modeling approach to identify problematic arrays (Li and Wong, 2001a).

Filter criteria for gene selection in dChip

The following criteria were used for determining the selection for those differentially expressed genes analyzed by dChip.

First filter: Detection calls, P call was at least 50% present in 6 arrays and if the

Present calls were just 50%, then they must be in all of the 3 control groups or in all of the siRNA experimental groups. For example, control 1, P, control 2, P, control 3, P and siRNA1, A, siRNA2, A, siRNA3, A. or control 1, A, control 2, A, control 3, A and siRNA1, P, siRNA2, P, siRNA3, P.

Second filter: Fold Change, the absolute fold-change value was at least 2 fold

between the average of the control group and the siRNA groups.

2.14.3.4 Robust Multi-array Analysis (RMA) analysis

Robust multi-array analysis, RMA (Irizarry *et al.*, 2003b) software was used to normalize the raw microarray intensity by read in the .CEL files. RMA performs the following operations: first, probe-specific background correction was used to remove nonspecific binding using PM distribution rather than PM-MM method to summarize probe intensities into a gene expression value; Secondly, RMA estimates a common mean non-specific hybridization background (for an entire chip) from PM using a

convolution model and subtracts this background from PM to generate the PMrma; Thirdly, probe-level multichip quantile normalization was applied to unify PM distributions across all microarrays; Finally the robust probe-set summary of the log-normalized probe-level data by median polishing was performed to determine genes with a greater than 2-fold difference.

Filter criteria for gene selection in RMA was those genes with a greater than 2-fold difference after the normalization and summaries.

2.14.4 Functional categorization of target genes

Gene functions were curated based on Gene Ontology available in PubMed (<http://www.ncbi.nlm.nih.gov/>) and the Affymetrix NetAffx database (Cheng *et al.*, 2004). Based on the above mentioned gene selection criteria, differentially expressed genes were extracted and categorized according to their biological function.

2.14.5 Pathway analysis

The differentially expressed genes were imported into PathwayStudio 4.0 PathwayStudio® 4.0 (Nikitin *et al.*, 2003) Ariadne Genomics, Inc pathway analysis software to find possible pathways that account for the phenotype changes in MCF-12A after silencing the *HS3ST3A1* expression.

2.15 Statistical analysis

The GraphPad Prism statistical package version 4.03 (GraphPad Prism, San Diego, CA, USA) was used for statistical analysis. Student's *t*-test or ANOVA followed by post-hoc Tukey or Bonferroni test was performed to compare the means between groups. $p < 0.05$ was considered statistical significant.

CHAPTER 3

CHAPTER 3 Studies on the effects of undersulphation of HS and differentially sulphated HS on breast carcinoma cellular behaviours

Substantial evidence demonstrated that HSPG is involved in many biological processes of the malignant cells including cell proliferation, adhesion, migration and invasion (Esko and Selleck, 2002; Whitelock and Iozzo, 2005; Sasisekharan *et al.*, 2006). These biological effects are influenced by the sulphate group of the heparan sulphate (HS) chains. Sulphate groups modulate the ability of heparan sulphate to bind and interact with different growth and signaling factors. Researchers have shown that the MCF-7 and MDA-MB-231 breast cancer cells produce high levels of sulphated proteoglycans. MCF-7 cells are known to release HSPG as the main proteoglycan component into the culture medium (Delehedde *et al.*, 1997). The aim of this study was to investigate the effects of undersulphation of HS and differentially sulphated HS on breast carcinoma cellular behaviours.

3.1 Sodium chlorate inhibited sulphation of HS in MCF-7 breast cancer cells

To determine the effect of disrupting sulphation of glycosaminoglycans by sodium chlorate on MCF-7 cells, MCF-7 breast cancer cells were cultured in the presence of 30 mM sodium chlorate. Sodium chlorate is a widely used and well-known competitive inhibitor of glycosaminoglycan sulphation. It acts as a sulphate analogue in the cellular synthesis of the sulphate donor 3'-phosphoadenosine

5'-phosphosulphate, which is required for glycosaminoglycan sulphation (Humphries and Silbert, 1988; Keller *et al.*, 1989; Delehedde *et al.*, 1996; Yip *et al.*, 2002).

Many studies involving breast cancer cell cultures and other biological systems have shown that sodium chlorate disrupted sulphation of glycosaminoglycans while having no significant effects on glycosaminoglycan chain or protein synthesis when chlorate was used at concentrations of up to 30 mM (Greve *et al.*, 1988; Humphries and Silbert, 1988; Keller *et al.*, 1989; Delehedde *et al.*, 1996). Thus it is a useful tool to investigate the role of sulphate moieties in HSPG.

To define the distribution of HSPG on MCF-7 cell surface after sodium chlorate treatment, HSPG specific monoclonal antibody 10E4 was used. 10E4 anti-HSPG monoclonal antibody recognizes N-sulphated glucosamine-containing domains in the HSPGs. The binding specificity was demonstrated by David *et al.* (1992). Immunostaining results showed that prominent staining of HSPG on the MCF-7 cells was observed in the control cells (**Fig. 3.1, a**). In contrast, markedly diminished staining of HSPG on the cells was observed in the sodium chlorate treated MCF-7 cells (**Fig. 3.1, c**), which indicated that 30 mM sodium chlorate could successfully inhibit the sulphation of HSPG in MCF-7 cells.

To further verify the de-sulphation of glycosaminoglycans by sodium chlorate on the MCF-7 proteoglycans, sulphation of total glycosaminoglycans and heparan sulphate were measured using the Blyscan glycosaminoglycan assay (Biocolor Ltd, Belfast, Ireland). Blyscan glycosaminoglycan assay is based on the specific binding of the cationic dye, 1, 9-dimethylmethylene blue (Farndale *et al.*, 1986). Sulphated

glycosaminoglycans (GAG) were purified from cell monolayers and culture medium with or without sodium chlorate treatment. **Fig.3.2A** shows that compared with the total sulphation of GAG measured in control cells, sodium chlorate significantly inhibited sulphation of total GAG as the GAG/protein ratio was reduced to 60.8%. The sulphation inhibition in heparan sulphate was also confirmed because the GAG/protein ratio was reduced to 54.5% as shown in **Fig. 3.2B**. These data therefore collectively confirmed that sulphation of heparan sulphate in MCF-7 cells was strongly inhibited by sodium chlorate.

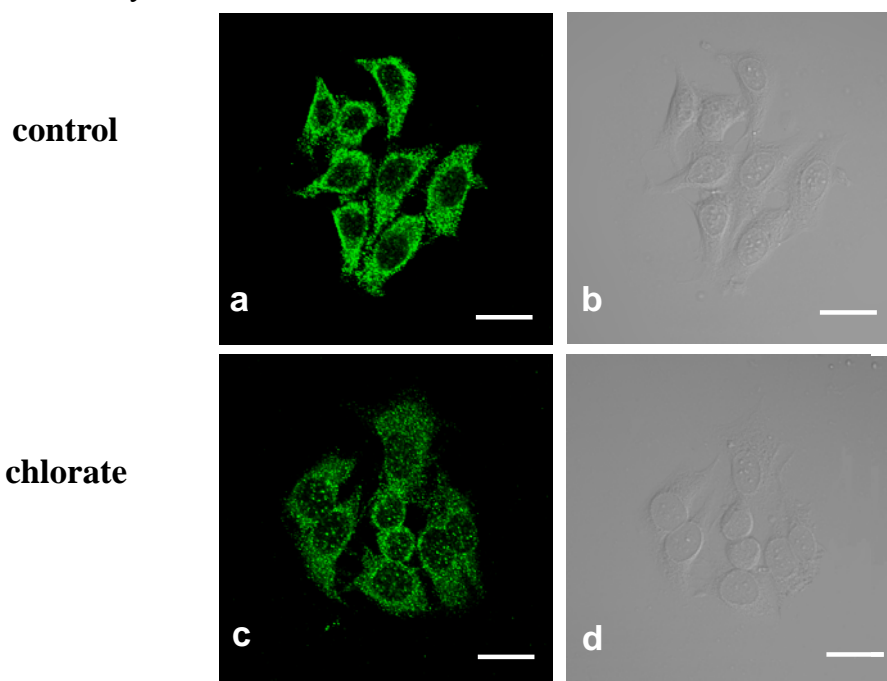


Fig. 3.1. Sodium chlorate disrupted GAG sulphation in MCF-7 cell surface HSPG. MCF-7 cells were cultured for 24 hrs before the 30 mM sodium chlorate added for treatment for 48 hrs. Cells were fixed using Sainte-Marie's fixative and blocked by 5% FBS in PBS for 1 hr at room temperature. The cells were then incubated for anti-HSPG antibody 10E4 mAb (1:100 dilution in PBS containing 2% FBS) (Seikagaku Corp, Japan). Cells were then washed 3 times with PBS, incubated with Alexa Fluor 488 labeled goat anti-mouse IgM antibody (1:400 dilution) (Molecular Probes, Eugene, OR) for 1 hr at room temperature, washed with PBS and mounted with Vectashield mounting medium. The cells were viewed by fluorescence confocal microscope. a: control, b: transmitted light image of control, c: sodium chlorate treated MCF-7 cells, d: transmitted light image of sodium chlorate treated MCF-7 cells. Scale bar = 20 μ m.

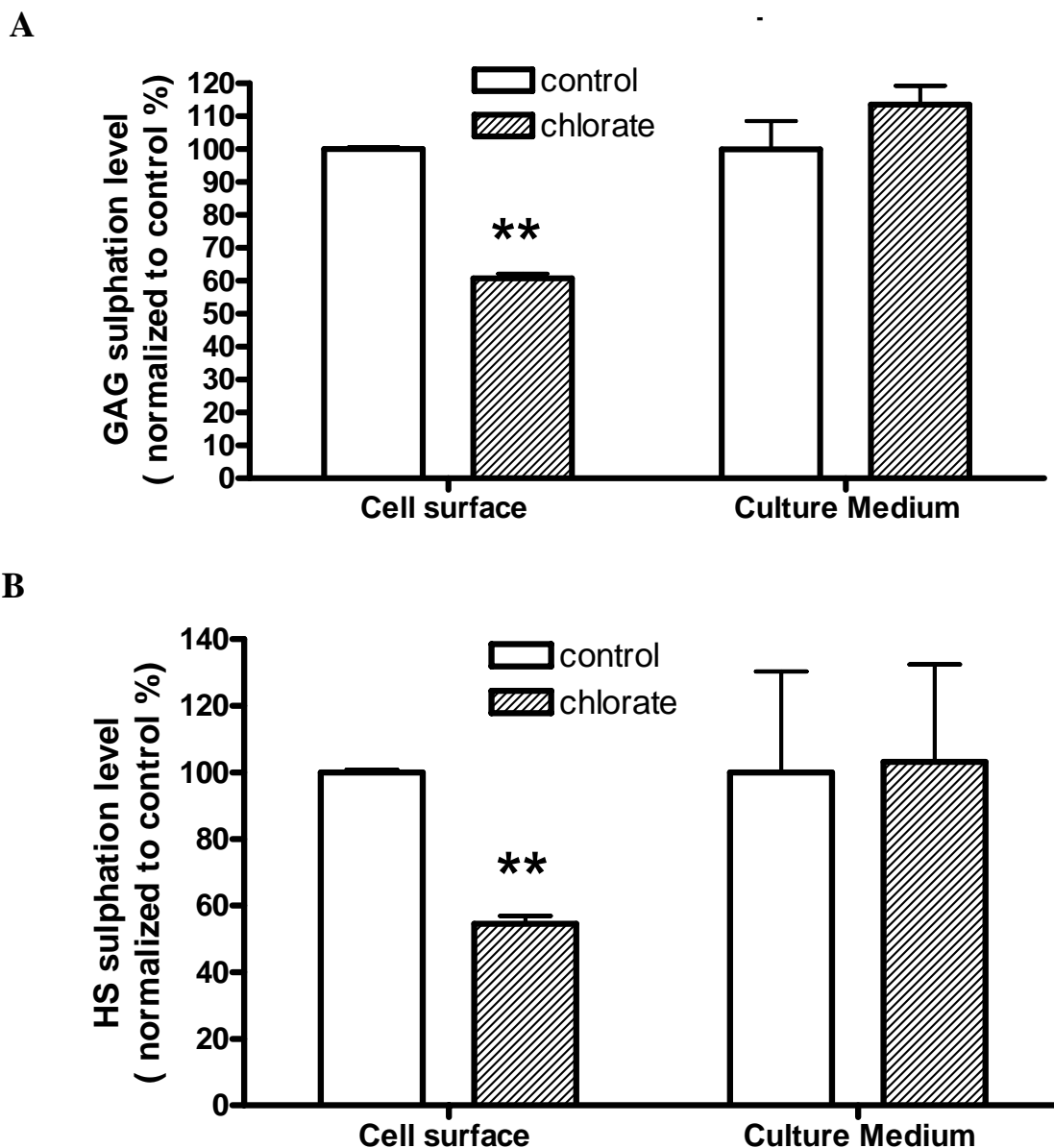


Fig. 3.2. Measurement of sulphation in GAGs and heparan sulphate in MCF-7 cells. **A.** MCF-7 cells were cultured with or without 30 mM sodium chlorate for 48 hrs. The culture medium were collected. The cell were collected by directly scratch with a cell scraper. The total GAG were extracted and measured with Blyscan kit as described in *Materials and Methods*. Data were expressed as mean \pm SD. $n = 3$, ** $p < 0.01$. Student's t -test. **B.** MCF-7 cells were cultured with or without 30 mM sodium chlorate for 48 hrs. The culture medium were collected. Cells were collected by directly scratch with a cell scraper. The total GAG were extracted and treated with nitrous acid to remove the heparan sulphation. The total and remaining GAG sulphation was measured with Blyscan kit as described in *Materials and Methods*. Heparan sulphation was calculated by subtracting the remaining sulphation from the total sulphation. Data were expressed as mean \pm SD. $n = 3$, ** $p < 0.01$. Student's t -test.

3.2 Sulphate group in heparan sulphate was involved in regulating breast cancer cell proliferation

To examine whether sulphation of heparan sulphate is involved in regulating the proliferation of breast cancer cells, the effect of undersulphation of GAG on MCF-7 and MDA-MB-231 cell growth was first studied.

MCF-7 and MDA-MB-231 cells were cultured in medium with or without 30 mM sodium chlorate for 7 days. Cell growth curve results showed that sodium chlorate significantly inhibited MCF-7 cell proliferation over a seven-day treatment period as revealed by crystal violet assay (**Fig. 3.3A**). Similar inhibition results were obtained from MDA-MB-231 cells cultured with 30 mM sodium chlorate (**Fig. 3.3B**). These results show that presence of sulphation group in the glycosaminoglycan of breast cancer cells is important for breast cancer cell proliferation.

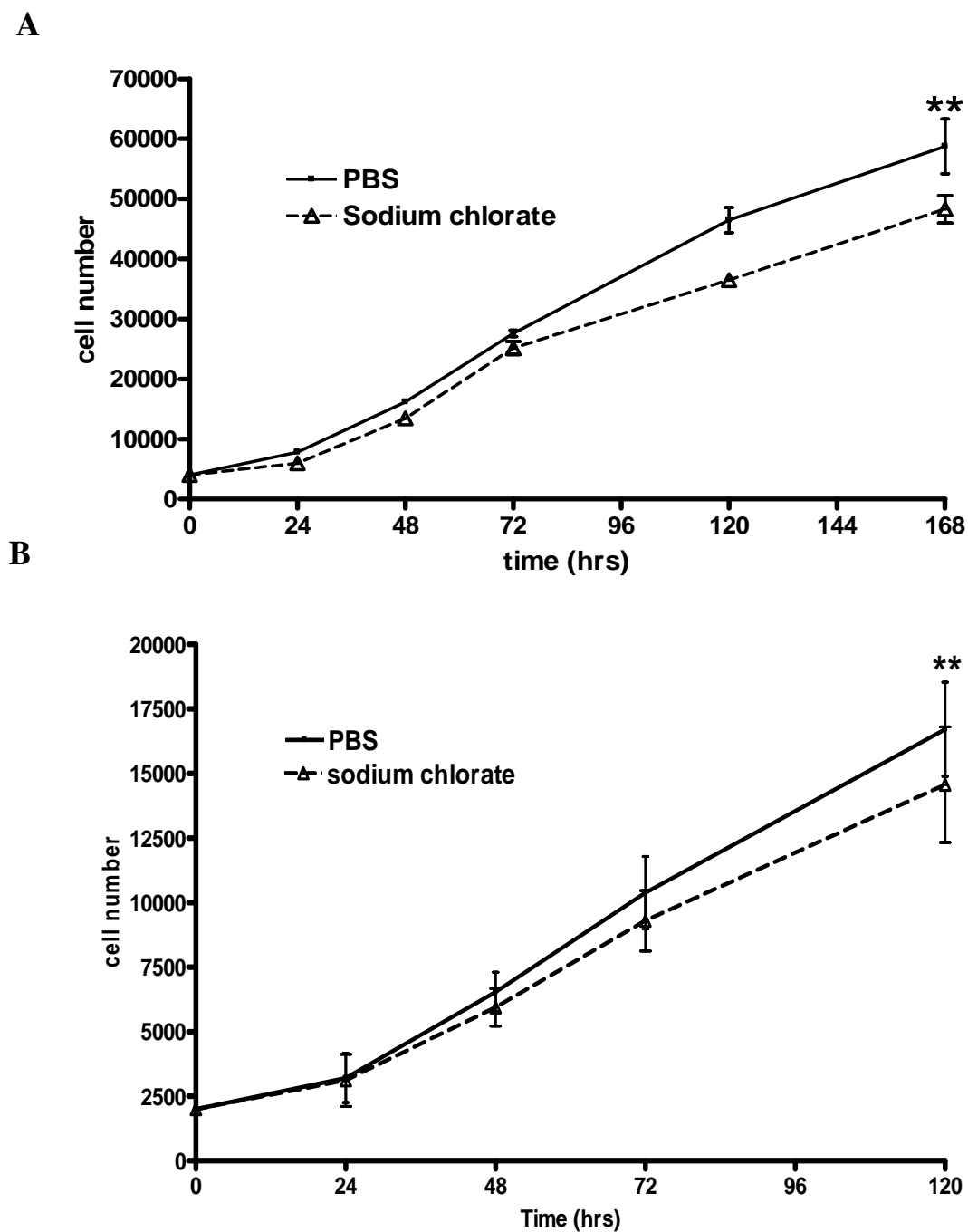


Fig. 3.3. Growth inhibition of breast cancer cells through undersulphation of HS. 4×10^3 MCF-7 cells (A) and 2×10^3 MDA-MB-231 cells (B) were seeded in 96-well plates, and treated with PBS (control) or 30 mM sodium chlorate (to inhibit glycosaminoglycan sulphation) for 7 days (A) or 5 days (B). The cell number was determined by crystal violet assay. Data were expressed as mean \pm SD. $n = 8$, $**p < 0.01$.

To examine if differentially sulphated heparan sulphate species would rescue the inhibitory effect of sodium chlorate on breast cancer cell proliferation, two types of exogenous heparan sulphates were used, heparan sulphate from porcine intestinal mucosal (HS-PM) and from bovine kidney (HS-BK). MCF-7 and MDA-MB-231 cells were cultured in medium with 100 ng/ml HS-BK or HS-PM in the presence or absence of 30 mM sodium chlorate for 72 hrs.

As shown in **Fig. 3.4** and **Fig. 3.5**, HS-PM, but not HS-BK significantly reduced the growth inhibitory action of sodium chlorate on the growth of breast cancer MCF-7 cells. A small rescue effect was seen in MDA-MB-231 cells cultured in medium containing 100 ng/ml HS-PM and 30 mM sodium chlorate (**Fig. 3.6**), but no such effect was found with HS-BK (**Fig. 3.7**). These data further verified that sulphation group in heparan sulphate glycosaminoglycan was indeed involved in the cell proliferation of breast cancer.

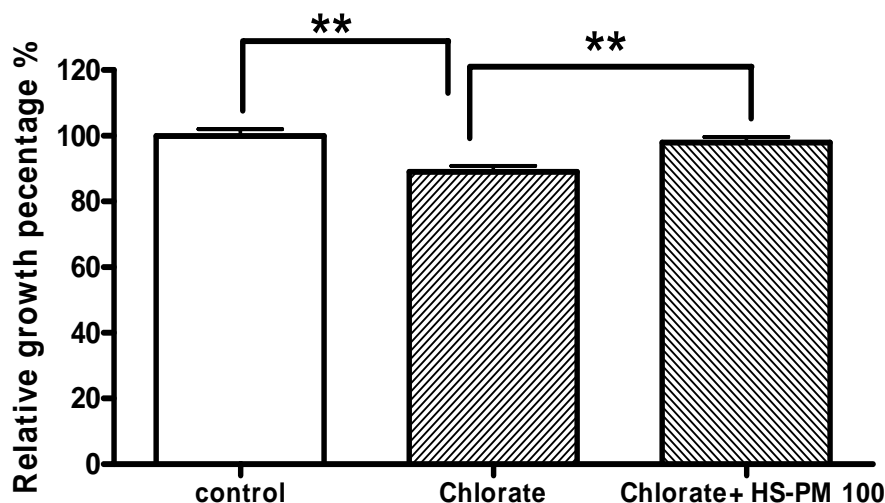


Fig. 3.4. HS-PM blocked the inhibitory effects of sodium chlorate on MCF-7 breast cancer cell proliferation. MCF-7 cells were cultured in medium containing 100 ng/ml HS-PM as described in *Materials and Methods*. Cell proliferation was assessed by crystal violet assay at 72 hrs. Data were expressed as percentage of control. Data represent means \pm SE of 8 determinations from 3 separate experiments. One-way ANOVA, ** $p < 0.01$, Tukey post hoc analysis, sodium chlorate group vs. sodium chlorate plus HS-PM group, ** $p < 0.01$.

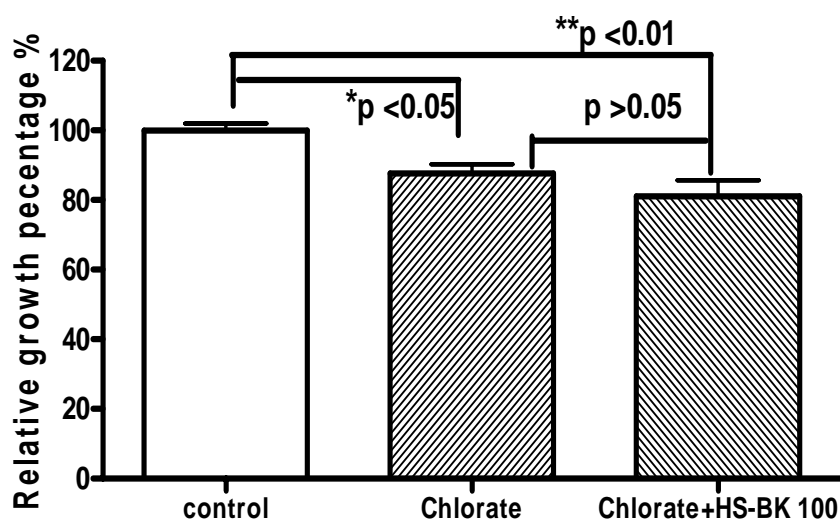


Fig.3.5. HS-BK did not block the inhibitory effects of sodium chlorate on MCF-7 breast cancer cell proliferation. MCF-7 cells were cultured in medium containing 100ng/ml HS-BK as described in *Materials and Methods*. Cell proliferation was assessed by crystal violet assay at 72 hrs. Data were expressed as percentage of the control. Data represent means \pm SE of 8 determinations from 3 separate experiments. One-way ANOVA, ** $p < 0.01$, Tukey post hoc analysis, sodium chlorate group vs. sodium chlorate plus HS-BK group, $p > 0.05$.

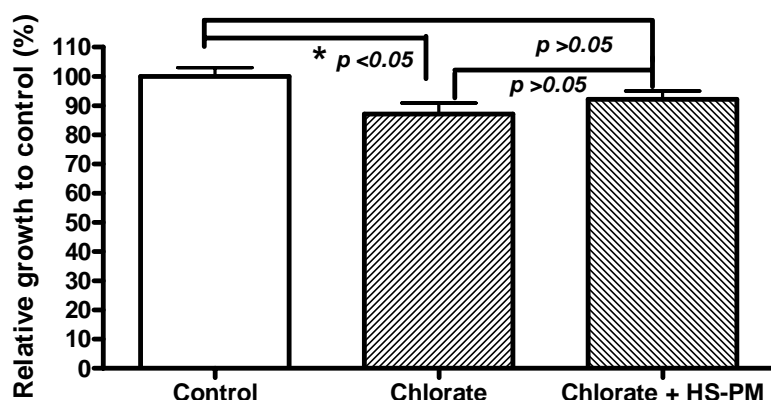


Fig. 3.6. HS-PM blocked the inhibitory effects of sodium chlorate on MDA-MB-231 breast cancer cell proliferation. MDA-MB-231 cells were cultured in medium containing 100 ng/ml HS-PM as described in *Materials and Methods*. Cell proliferation was assessed by crystal violet assay at 72 hrs. Data were expressed as percentage of control. Data represent means \pm SE of 8 determinations from 3 separate experiments. One-way ANOVA, $p = 0.0329$, Tukey post hoc analysis, control group vs. sodium chlorate group, $*p < 0.05$, control group vs. sodium chlorate plus HS-PM group, $p > 0.05$

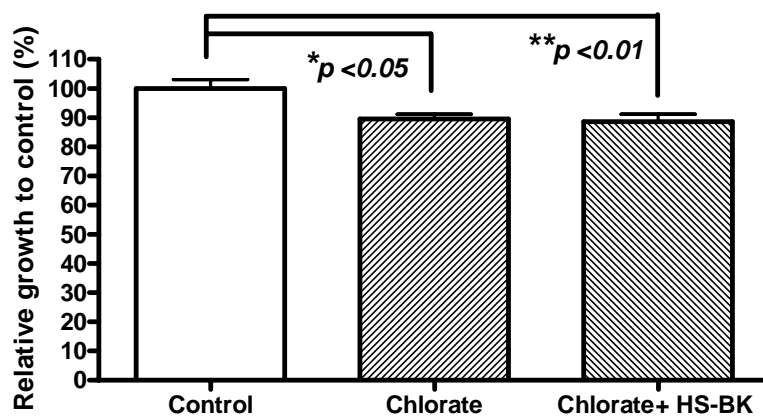


Fig. 3.7. HS-BK did not block the inhibitory effects of sodium chlorate on MDA-MB-231 breast cancer cell proliferation. MDA-MB-231 cells were cultured in medium containing 100 ng/ml HS-BK as described in *Materials and Methods*. Cell proliferation was assessed by crystal violet assay at 72 hrs. Data were expressed as percentage of the control. Data represent means \pm SE of 8 determinations from 3 separate experiments. One-way ANOVA, $p = 0.0057$, Tukey post hoc analysis, control group vs. sodium chlorate group, $*p < 0.05$, control group vs. sodium chlorate plus HS-PM group, $**p < 0.01$, sodium chlorate group vs. sodium chlorate plus HS-BK group, $p > 0.05$.

3.3 Effect of undersulphation of heparan sulphate on cell cycle changes in MCF-7 and MDA-MB-231 breast cancer cells.

Cell cycles progression reflects cell proliferation. To test if undersulphation of heparan sulphate by sodium chlorate influence cell cycle, MCF-7 cells were treated with 30 mM sodium chlorate for 12 hrs, 24 hrs and 36 hrs. After 24 hrs, the S-phase fraction of cells treated with sodium chlorate was ~18.0% whereas the S-phase of control cells was ~22.7%. This indicated that cells in S phase after 24 hrs treatment were reduced by 22.0%. This was accompanied by an increase in cells of similar magnitude in the G₀-G₁ phase of the cell cycle (**Fig. 3.8** and **Table 3.1**). The cell cycle analysis results suggested that sodium chlorate inhibited the G₀/S phase transition at 24 hrs treatment as the cells in G₂-M phase were almost the same between the control and sodium chlorate-treated cells. An important note was that there was no sub-G₁ peak before the G₁ peak either in the control or the sodium chlorate treated cells which suggested there were no obvious apoptosis (**Fig. 3.8**). These results are consistent with previous report that 30 mM sodium chlorate was sufficient to suppress heparan sulphation without inducing cytotoxic effect. This inhibition in G₁ /S transition was also seen in MDA-MB-231 cells treated with 30 mM sodium chlorate (**Fig. 3.9** and **Table 3.2**).

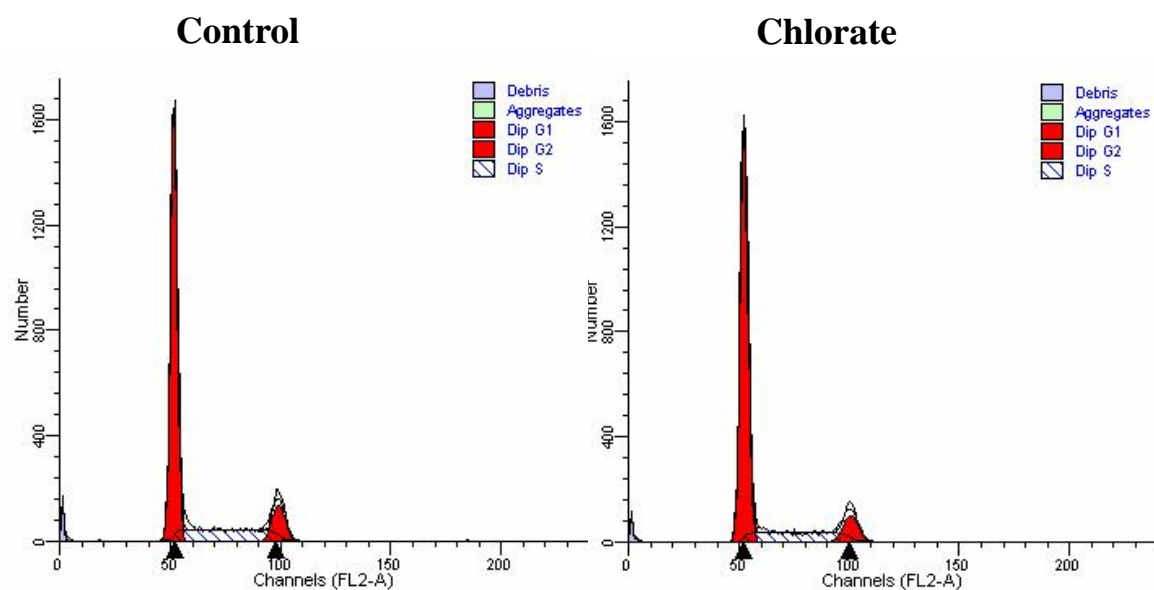


Fig. 3.8. Effect of undersulphation of GAGs on cell cycle changes in MCF-7 breast cancer cells. MCF-7 cells were seeded at a density of 1.5×10^5 cells per well in 6-well plates, and treated with PBS (control) or 30 mM sodium chlorate for 12, 24 or 36 hrs. MCF-7 cells were processed as described in *Material and Methods* and analyzed by flow cytometry. **Fig.** shows a representative histogram of the cell cycle analyzed by ModFit software.

		G1	S phase	G2
control		66.43 ± 0.06	23.01 ± 0.35	10.56 ± 0.40
chlorate	12 hrs	$69.45 \pm 0.18^*$	$19.32 \pm 0.32^*$	11.24 ± 0.46
control		66.79 ± 0.39	22.72 ± 0.50	10.49 ± 0.11
chlorate	24 hrs	$72.81 \pm 0.11^{**}$	$17.96 \pm 0.29^{**}$	9.23 ± 0.22
control		66.25 ± 0.03	23.24 ± 0.44	10.50 ± 0.42
chlorate	36 hrs	$68.32 \pm 0.46^*$	$20.72 \pm 0.73^*$	10.96 ± 0.30

Table 3.1. Flowcytometer analysis of cell cycle in MCF-7 breast cancer cells. Data were expressed as mean \pm SE. n = 3. Student's *t*-test, * $p < 0.05$, ** $p < 0.01$.

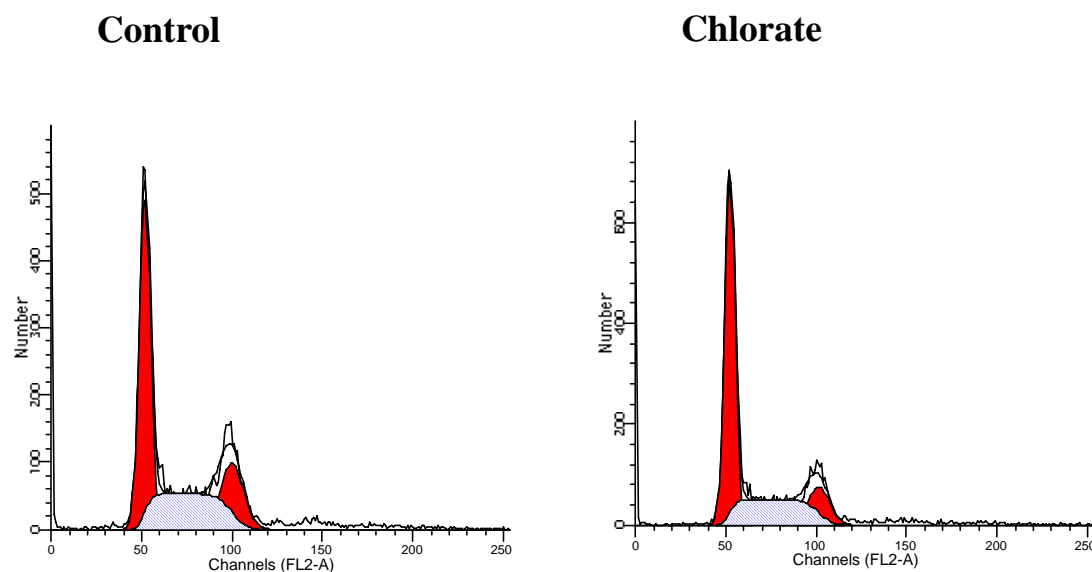


Fig. 3.9. Effect of undersulphation of GAGs on cell cycle changes in MDA-MB-231 breast cancer cells. MDA-MB-231 cells were seeded at a density of 1.5×10^5 cells per well in 6-well plates, and treated with PBS (control) or 30 mM sodium chlorate for 12, 24 and 36 hrs. MDA-MB-231 cells were processed as described in *Material and Methods* and analyzed by flow cytometry. **Fig.** shows representative histograms of the cell cycle analyzed by ModFit software.

		G1	S phase	G2
control		59.73 ± 1.07	27.80 ± 1.30	12.47 ± 0.19
chlorate	12 hrs	62.13 ± 1.56	25.41 ± 1.47	12.46 ± 0.19
control		52.41 ± 0.82	32.10 ± 0.97	15.50 ± 0.99
chlorate	24 hrs	$62.43 \pm 0.80^{**}$	$26.52 \pm 1.70^{**}$	11.05 ± 0.93
control		60.43 ± 1.27	28.56 ± 0.33	11.01 ± 0.94
chlorate	36 hrs	$62.58 \pm 0.85^*$	$22.82 \pm 1.37^{**}$	14.60 ± 0.56

Table 3.2 Flowcytometer analysis of cell cycle in MDA-MB-231 breast cancer cells. Data were expressed as mean \pm SE. n = 3. Student's *t*-test, * $p < 0.05$, ** $p < 0.01$.

3.4 Sodium chlorate did not induce apoptotic nuclear morphology in MCF-7 and MDA-MB-231 breast cancer cells.

To further exclude the possibility that the inhibitory effect on proliferation by 30 mM sodium chlorate was due to its toxicity, apoptotic cell death was estimated by analyzing its effect on nuclear morphology of the cells using DAPI staining. The apoptotic cells were recognized on the basis of nuclear condensation and DNA fragmentation of DAPI stained cells under confocal microscope. It was found that after 48 hrs treatment with 30 mM sodium chlorate, there were no obvious apoptotic cells in MCF-7 and MDA-MB-231 cells under fluorescence microscope as no cells exhibited characteristics of apoptotic nuclear morphological changes, including chromatin condensation, segmentation of nuclear chromatin of irregular size (**Fig. 3.10**).

In MDA-MB-231 cells, Caspase-3 activity was examined after 24 and 48 hrs treatment with 30 mM sodium chlorate. MDA-MB-231 cells were treated with sodium chlorate (30 mM) in the presence or absence of caspase-3 inhibitor z-VAD-fmk (50 $\mu\text{mol/L}$) for 24 and 48 hrs. Cells were then harvested and the total protein was collected. The activation of caspase-3 in the cytosolic fraction was detected by the CaspACE™ Colorimetric Assay System (Promega, Cat.# G7220, G7351). Results showed the caspase-3 activity was not changed between the sodium chlorate treated cells with the caspase-3 inhibitor treated cells (**Fig. 3.11**). These results together with those in the cell cycle analysis strongly suggested that the anti-proliferative effect of 30 mM sodium chlorate was not due to its cell toxicity.

These findings collectively showed that 30 mM sodium chlorate effectively induced undersulphation of HSPG in breast cancer which inhibited the proliferation of MCF-7 and MDA-MB-231 cells through inhibition of cell G_1/S transition without any apoptotic effect.

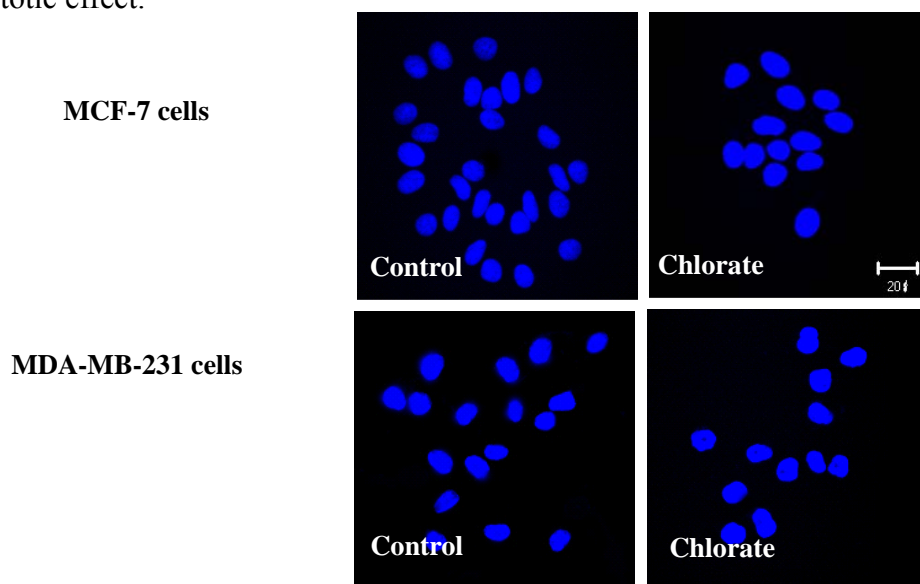


Fig.3.10. Sodium chlorate did not induce apoptosis in MCF-7 and MDA-MB-231 breast cancer cells. Cells were seeded on the coverslip for 24 hrs and cultured with PBS (control) or 30 mM sodium chlorate for 48 hrs. The cells were then stained with DAPI before were fixed and mounted with Vectashield mounting medium. The cells were viewed by fluorescence confocal microscope. Scale bar = 20 μ m

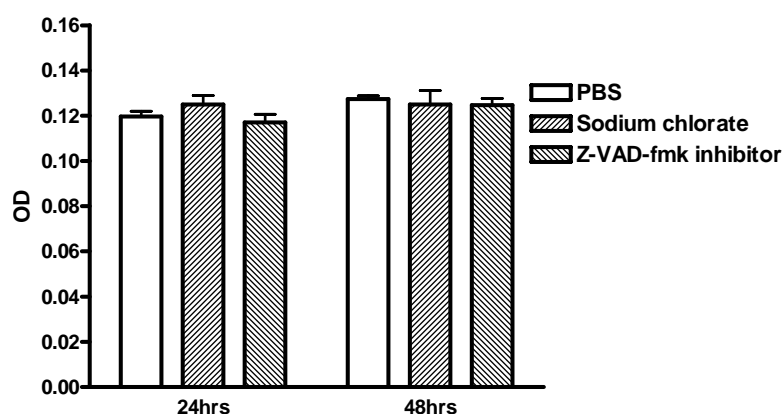


Fig. 3.11. Sodium chlorate did not induce Caspase-3 activity in MDA-MB-231 breast cancer cells. MDA-MB-231 cells were treated with sodium chlorate (30 mM) in the presence or absence of caspase-3 inhibitor z-VAD-fmk (50 μ M) for 48 hrs. Cells were then harvested and the total protein was collected. The activation of caspase-3 in the cytosolic fraction was detected by the CaspACE™ Colorimetric Assay System (Promega, Cat.# G7220, G7351)

3.5 Sulphate group in heparan sulphate was involved in regulating breast cancer cell adhesion

Research has been exploring the role of cell surface expressed HSPG in cell adhesion to ECM components such as fibronectin, collagen I, collagen IV, laminin and selectin.

To determine if sulphate group of heparan sulphate affects breast cancer cell adhesion, MCF-7 and MDA-MB-231 cells were cultured in medium in the presence of 30 mM sodium chlorate for 48 hrs before re-seeding them onto fibronectin and collagen I-coated surface. **Fig. 3.12A** shows that undersulphation of GAGs of MCF-7 cells by incubation the cells with 30 mM sodium chlorate for 48 hrs resulted in significantly increased adherence to fibronectin by approximately 18% and to collagen I by approximately 37% ($p = 0.0331$ and $p = 0.0114$, Student's *t*-test, control vs chlorate). A similar increase was also seen when MDA-MB-231 human breast cancer cells were cultured in medium containing 30 mM chlorate. There were an ~25% increase in adhesion to fibronectin and an ~37% increase in adhesion to collagen I ($p < 0.001$ and $p < 0.001$, Student's *t*-test, control vs chlorate) (**Fig. 3.12B**). These results suggested competitive inhibition of glycosaminoglycan sulphation in breast cancer cells increased cell adhesion.

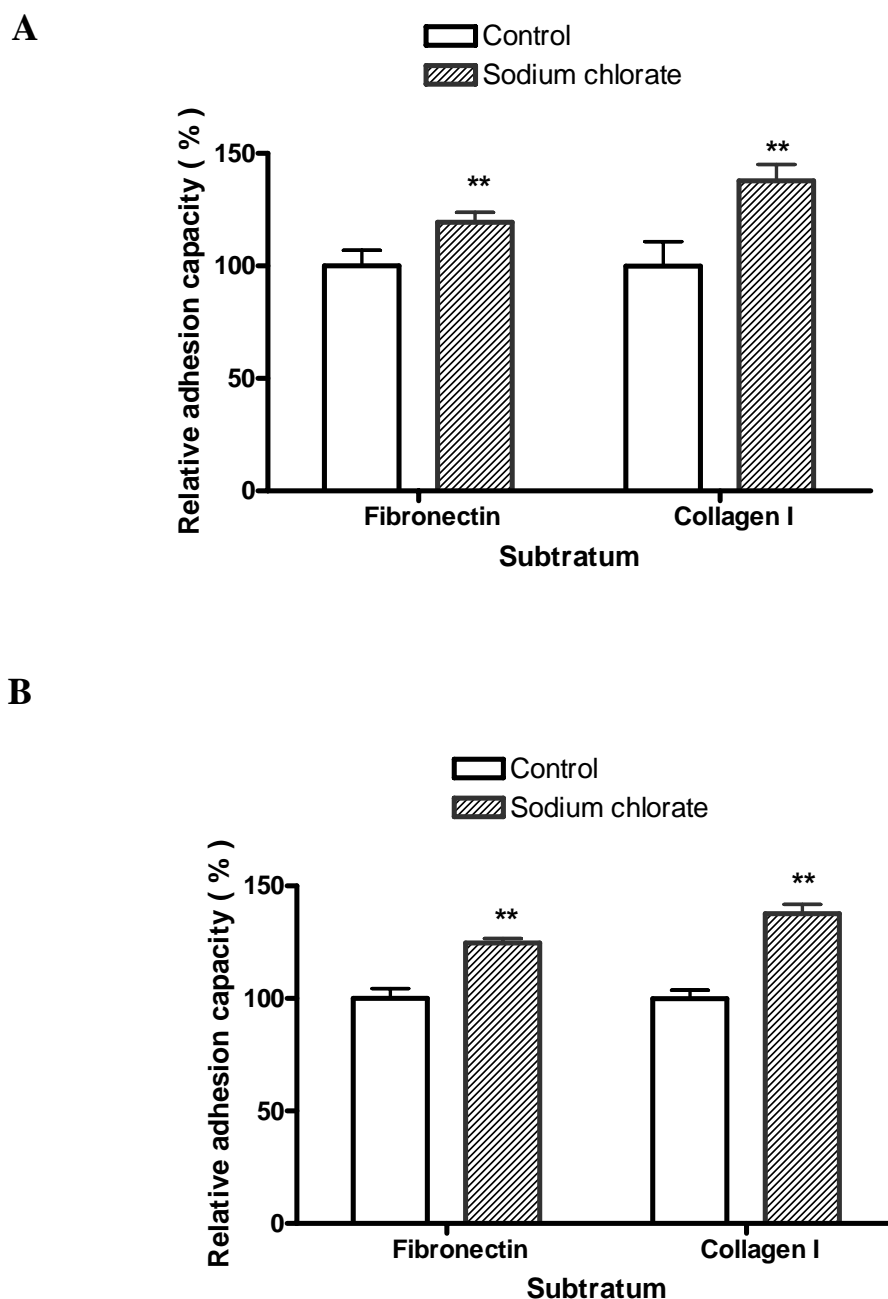


Fig. 3.12. Sodium chlorate increased MCF-7 and MDA-MB-231 cell adhesion. Cells were pre-treated with PBS (control) or 30 mM sodium chlorate for 48 hrs. Cells were trypsinized and resuspended in DMEM with 0.1% BSA containing either 30 mM sodium chlorate or equal volume PBS. 1×10^5 cells in 100 μ l volume were seeded in each well of 96-well fibronectin or collagen I coated-plate for 30 min. The attached cell number was determined by the crystal violet assay. Data were calculated as percentage of control and expressed as mean \pm SE. $n = 8$, Student's t -test, ** $p < 0.01$. A: MCF-7 cells, B: MDA-MB-231 cells.

3.6 Comparative effects of differentially sulphated heparan sulphate species on cancer cell adhesion.

Sodium chlorate inhibits sulphation of all glycosaminoglycans and does not act specifically on heparan sulphate. Thus, to determine if the sodium chlorate-induced increase in cancer cell adhesion was due to a reduction in sulphation of heparan sulphate molecules, bovine kidney-derived heparan sulphate (HS-BK) was added to MCF-7 cells grown in chlorate-containing medium. As shown in **Fig. 3.13A and B**, supplementation of the culture medium with adequately sulphated HS-BK abolished the effect of chlorate on MCF-7 cell adhesion to fibronectin completely and drastically blocked the increment of adhesion to collagen I (**Fig. 3.13B**) suggesting that the sulphation status of heparan sulphate is important in regulating cancer cell adhesion.

To investigate this further, repeated experiment was performed by adding porcine intestine mucosa derived heparan sulphate (HS-PM) to the chlorate-containing culture medium instead of the bovine kidney-derived species. Addition of HS-PM resulted in only a partial, instead of complete, block of the sodium chlorate-induced increase in cell adhesion to fibronectin (**Fig. 3.14A**). However it showed a complete blockage of the adhesion enhancement to collagen I induced by sodium chlorate (**Fig. 3.14B**). As heparan sulphate from porcine intestines mucosa possesses a higher degree of sulphation compared to that obtained from bovine kidney (Tsuda *et al.*, 1996; Toida *et al.*, 1997), it might be that HS-PM and HS-BK are differentially effective in blocking the effect of sodium chlorate on cell adhesion to fibronectin and collagen I.

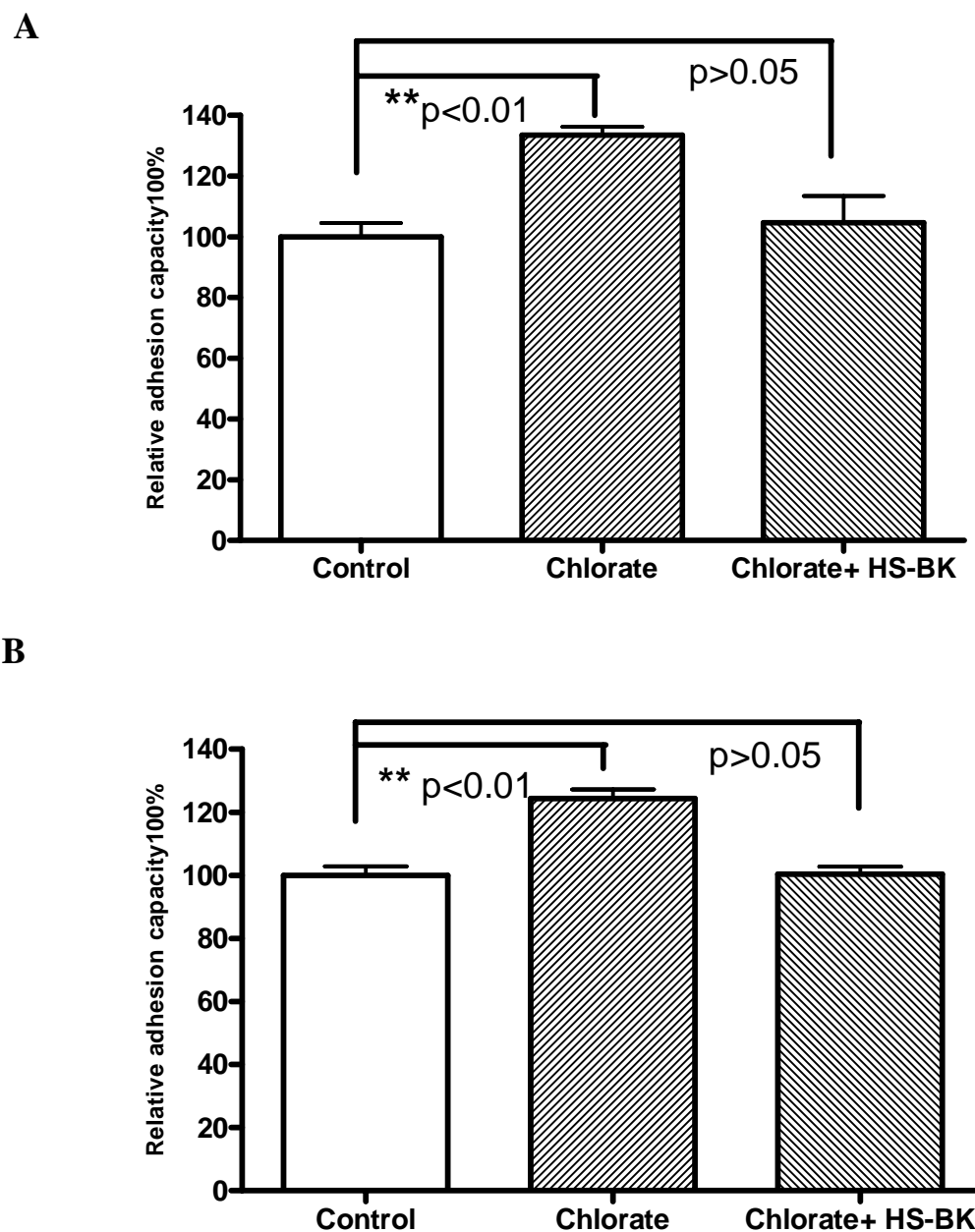
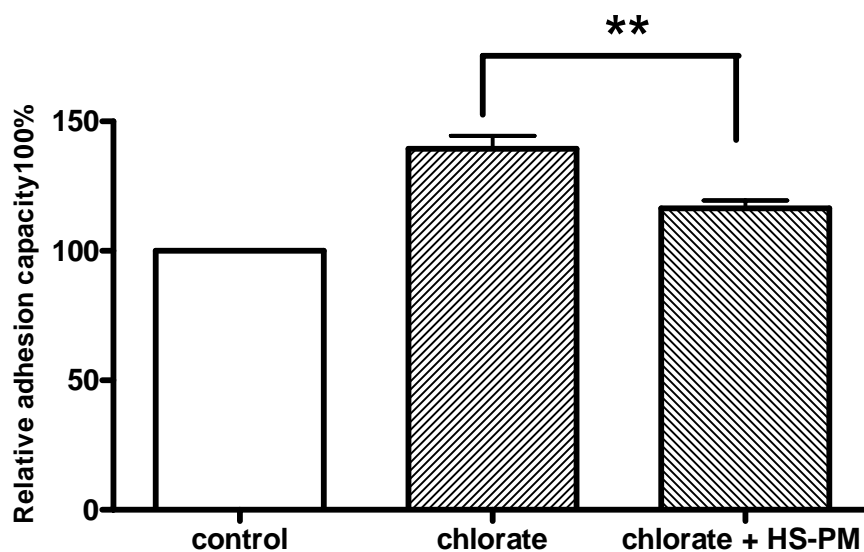


Fig. 3.13. HS-BK blocked the enhancing effects of sodium chlorate on MCF-7 breast cancer cell adhesion. MCF-7 cells were cultured in medium containing 100 ng/ml of HS-BK with or without sodium chlorate as described in *Materials and Methods*. The cells were trypsinized and resuspended in DMEM with 0.1% BSA containing the same concentration of HS-BK and /or 30 mM sodium chlorate or equal volume PBS. 1×10^5 cells in 100 μ l volume were seeded in each well of 96-well Fibronectin (**A**) or Collagen I (**B**) coated-plate for 30 min. The attached cell number was determined by the crystal violet assay. Data were calculated as percentage of control and expressed as mean \pm SE. $n = 8$, One-way ANOVA, $p < 0.001$, Tukey post hoc analysis, sodium chlorate group vs. sodium chlorate plus HS-BK group,, ** $p < 0.01$.

A



B

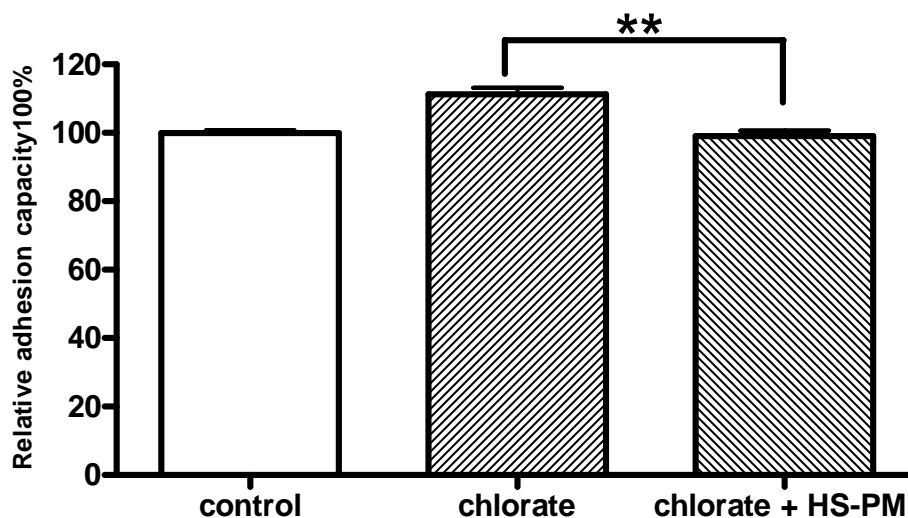


Fig. 3.14. HS-PM blocked the enhancing effects of sodium chlorate on MCF-7 breast cancer cell adhesion. MCF-7 cells were cultured in medium containing 100 ng/ml of HS-PM with or without sodium chlorate as described in *Materials and Methods*. The cells were trypsinized and resuspended in DMEM with 0.1% BSA containing the same concentration of HS-PM and /or 30 mM sodium chlorate or equal volume PBS. 1×10^5 cells in 100 μ l volume were seeded in each well of 96-well Fibronectin (**A**) or Collagen I (**B**) coated-plate for 30 min. The attached cell number was determined by the crystal violet assay. Data were calculated as percentage of control and expressed as mean \pm SE. $n = 8$, One-way ANOVA, $p < 0.001$, Tukey post hoc analysis, sodium chlorate group vs. sodium chlorate plus HS-PM group, * $p < 0.05$, ** $p < 0.01$.

Indeed, as shown in **Fig. 3.15A and B** , **Fig. 3.16A and B**, different effects were also seen between these two kinds of heparan sulphate in the blockage of the adhesion enhancement to fibronectin and collagen I induced by sodium chlorate in MDA-MB-231 breast cancer cells. Addition of HS-BK completely blocked the adhesion increase of MDA-MB-231 cell to both fibronectin (**Fig. 3.15A**) and collagen I (**Fig. 3.15B**) while HS-PM did not block the increasing effect of MDA-MB-231 cell either to fibronectin (**Fig. 3.16A**) and collagen I (**Fig. 3.16B**).

Taken together, these results suggested the sulphation of endogenous HSPG as well as the difference in sulphation of exogenous heparan sulphation must be of importance in the mediating the interactions between MCF-7 and MDA-MB-231 breast cancer cells and extracellular matrix such as fibronectin and collagen I.

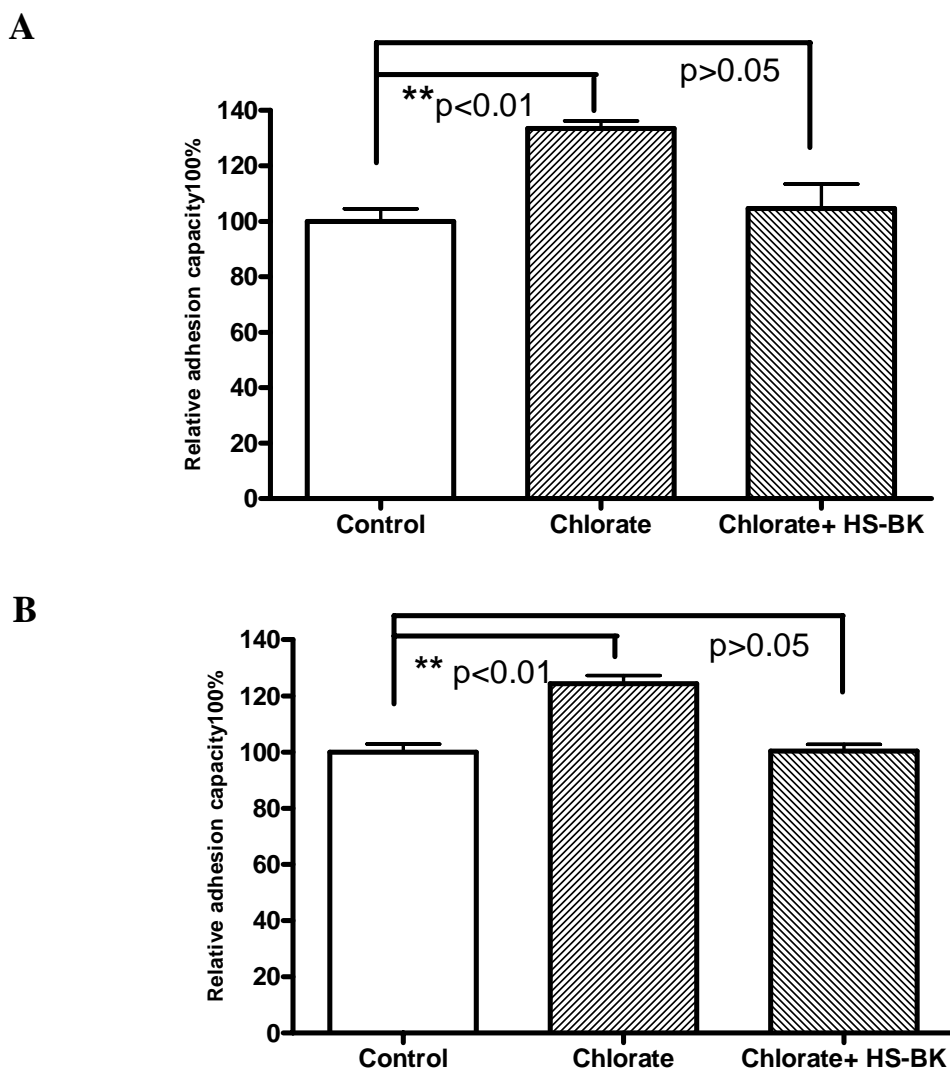


Fig. 3.15. HS-BK blocked the enhancing effects of sodium chlorate on MDA-MB-231 breast cancer cell adhesion. MDA-MB-231 cells were cultured in medium containing 100 ng/ml of HS-BK with or without sodium chlorate as described in *Materials and Methods*. The cells were trypsinized and resuspended in DMEM with 0.1% BSA containing the same concentration of HS-BK and /or 30 mM sodium chlorate or equal volume PBS. 1×10^5 cells in 100 μ l volume were seeded in each well of 96-well fibronectin (**A**) and collagen I (**B**) coated-plate for 30 min. The attached cell number was determined by the crystal violet assay. Data were calculated as percentage of control and expressed as mean \pm SE. $n = 8$. In **Fig. 3.15A**, One-way ANOVA, $p < 0.01$, Tukey post hoc analysis, control group vs. sodium chlorate group, $**p < 0.01$, control group vs. sodium chlorate plus HS-PM group, $p > 0.05$, sodium chlorate group vs. sodium chlorate plus HS-BK group, $**p < 0.01$. In **Fig. 3.15B**, One-way ANOVA, $p < 0.0001$, Tukey post hoc analysis, control group vs. sodium chlorate group, $**p < 0.001$, control group vs. sodium chlorate plus HS-PM group, $p > 0.05$, sodium chlorate group vs. sodium chlorate plus HS-BK group, $**p < 0.001$.

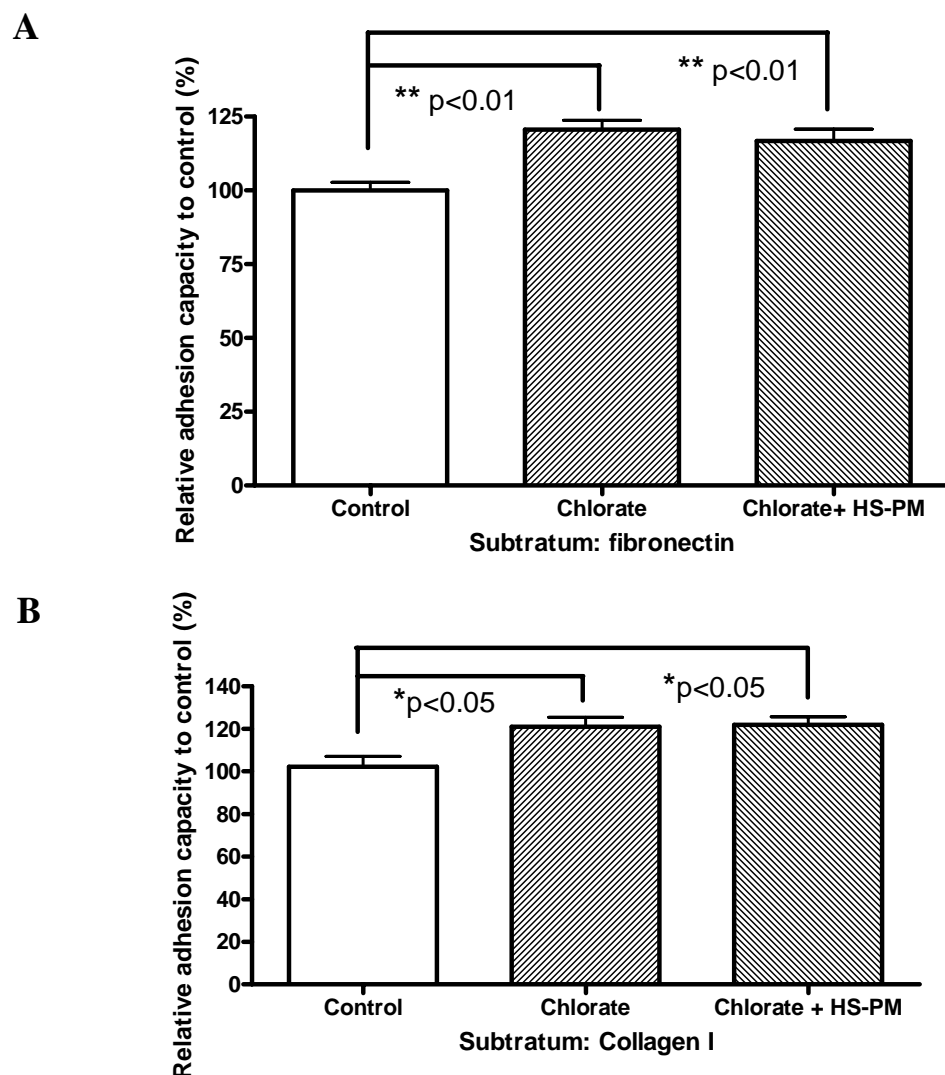


Fig. 3.16. HS-PM did not block the enhancing effects of sodium chlorate on MDA-MB-231 breast cancer cell adhesion. MDA-MB-231 cells were cultured in medium containing 100 ng/ml of HS-BM with or without sodium chlorate as described in *Materials and Methods*. The cells were trypsinized and resuspended in DMEM with 0.1% BSA containing the same concentration of HS-PM and /or 30 mM sodium chlorate or equal volume PBS. 1×10^5 cells in 100 μ l volume were seeded in each well of 96-well to fibronectin (**A**) and collagen I (**B**) coated-plate for 30 min. The attached cell number was determined by the crystal violet assay. Data were calculated as percentage of control and expressed as mean \pm SE. $n = 8$. In **Fig. 3.16A**, One-way ANOVA, $p = 0.0006$, Tukey post hoc analysis, control group vs. sodium chlorate group, $**p < 0.001$, control group vs. sodium chlorate plus HS-PM group, $**p < 0.01$, sodium chlorate group vs. sodium chlorate plus HS-PM group, $p > 0.05$. In **Fig. 3.16B**, One-way ANOVA, $p = 0.0069$, Tukey post hoc analysis, control group vs. sodium chlorate group, $**p < 0.05$, control group vs. sodium chlorate plus HS-PM group, $*p < 0.05$, sodium chlorate group vs. sodium chlorate plus HS-PM group, $p > 0.05$.

3.7 Cell adhesion increase induced by sodium chlorate was associated with FAK and paxillin recruitment

Focal adhesion kinase (FAK) and paxillin, both members of the focal adhesion, are key regulatory components in controlling cell adhesion and cell movement (Turner, 1998; Cary and Guan, 1999; Turner, 2000; Hanks *et al.*, 2003; Schaller, 2004). To explore if augment of adhesion caused by sodium chlorate would change the expression levels of focal adhesion molecules like FAK and paxillin, focal adhesion formation in the MCF-7 cells treated with or without 30 mM sodium chlorate was studied by fluorescence immunostaining. MCF-7 cells were cultured on coverslip in the medium containing 30 mM sodium chlorate for 48 hrs and stained with anti-FAK and anti-paxillin antibody. Confocal microscopy observation showed that after treatment with sodium chlorate for 48 hrs, focal adhesion formation was increased as demonstrated by the recruitment of the FAK or paxillin (red) to the end of F-actin (green). While in the control cells, FAK (**Fig. 3.17A, red**) or paxillin (**Fig. 3.17B, red**) exhibited a low degree of colocalization at the end of F-actin (green), as revealed by the few yellow spots representing focal adhesion complex (**Fig. 3.17** inserts and arrows).

To further verify the changes in the focal adhesion molecules in the adhesion increase induced by sodium chlorate, MCF-7 cells were treated with or without 30 mM sodium chlorate and re-seeded them into fibronectin-coated dishes or coverslips for 2 hrs. The total mRNA and protein were collected.

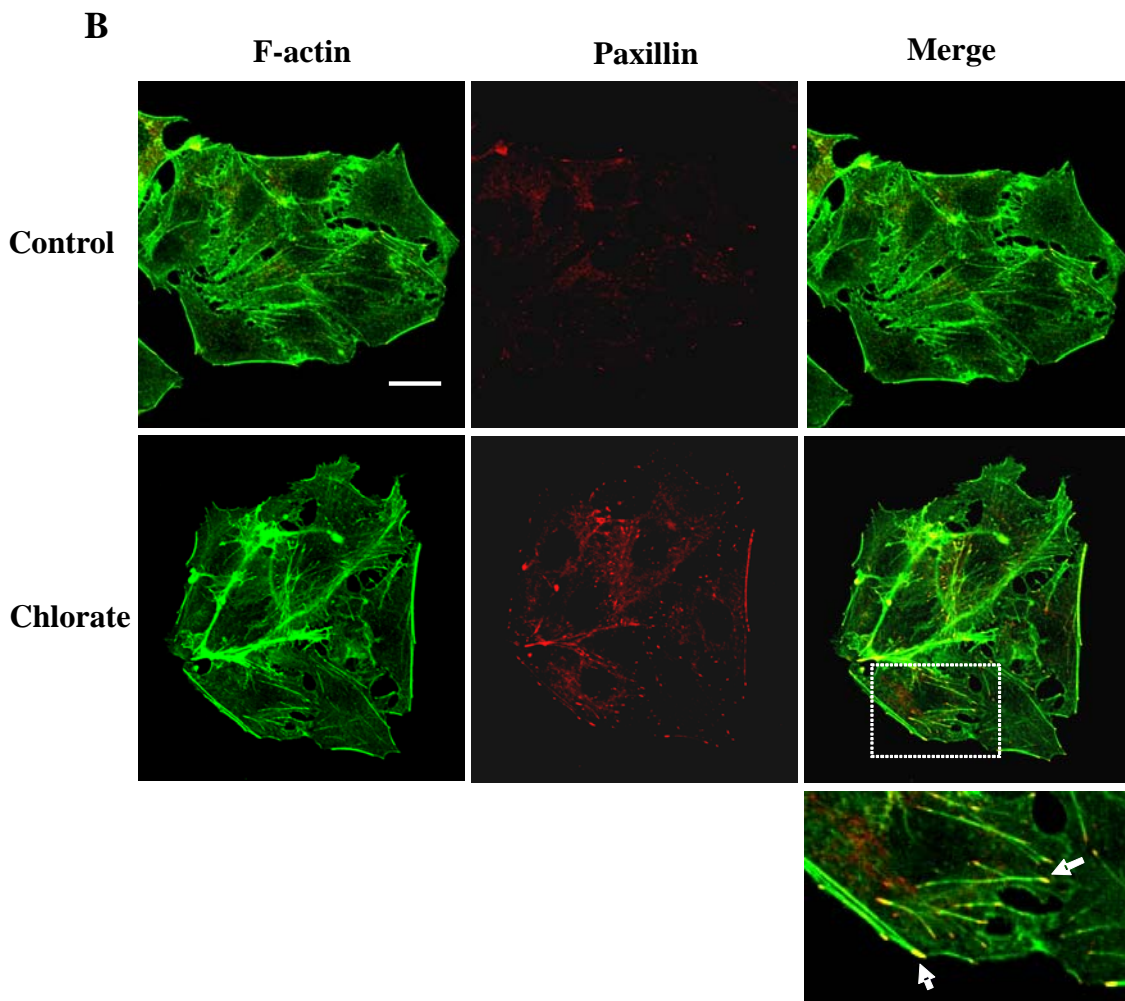
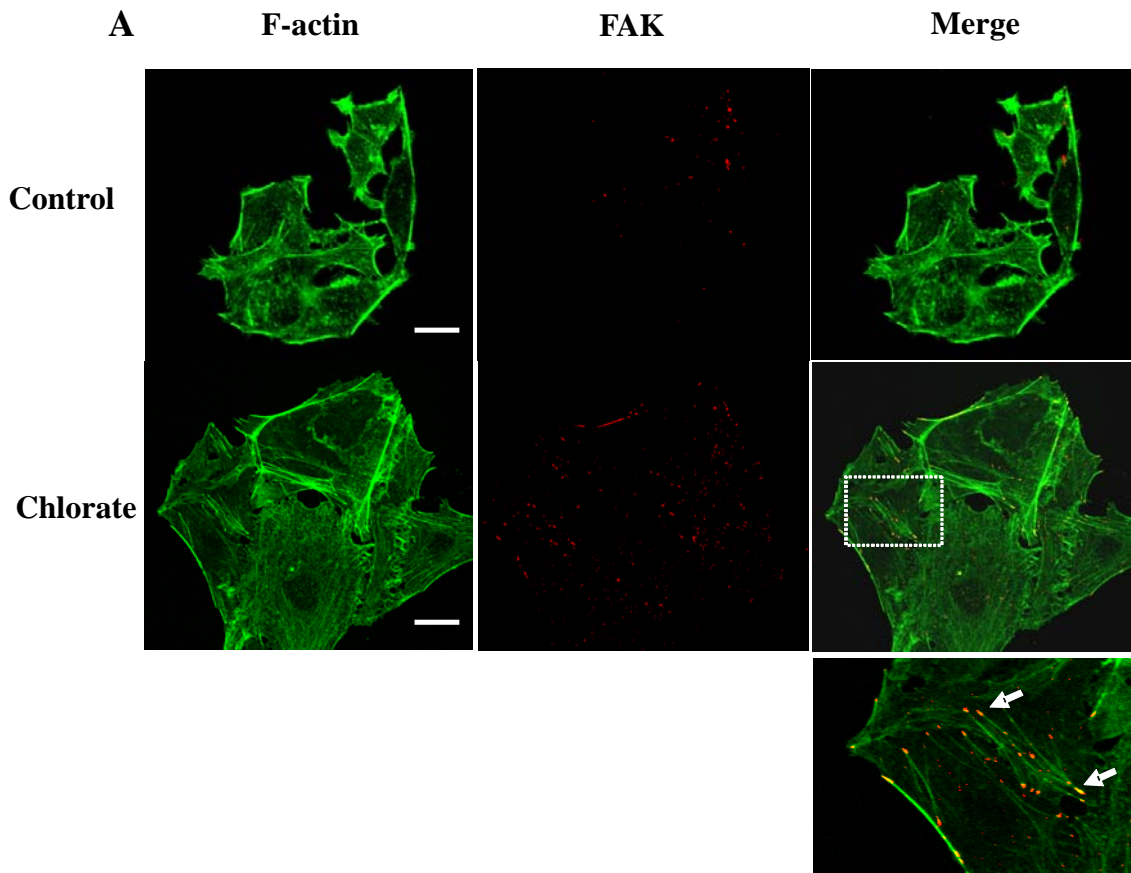
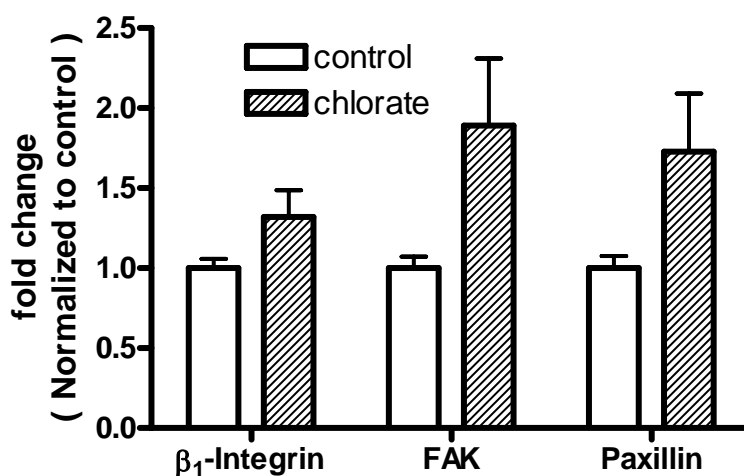


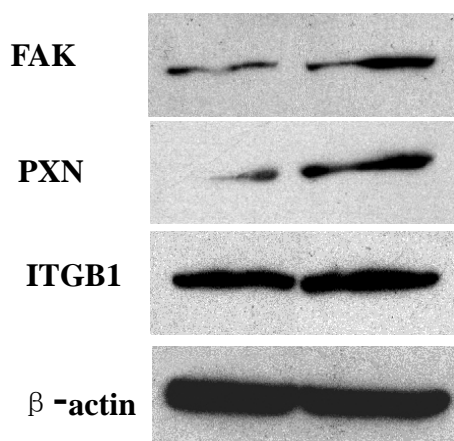
Fig. 3.17. Effect of sodium chlorate on the distribution of FAK, Paxillin and F-actin in MCF-7 cells. MCF-7 cells were processed as described in *Material and Methods*. Stress fiber F-actin was probed with fluorescein isothiocyanate (FITC)-conjugated phalloidin (green), FAK and Paxillin were detected with anti-FAK polyclonal antibody or anti-paxillin monoclonal antibody, followed by Alexa-568-labeled second Antibody (red). The arrows indicate the areas of F-actin and FAK (**Fig. 3.17A**) or F-actin and Paxillin (**Fig. 3.17B**) colocalization in the focal adhesion formation sites (yellow). Insertion is the high magnification of the focal adhesion complex in the sodium chlorate-treated cells. Scale bar = 20 μm

Previously β_1 -integrin (ITGB1) has been shown to influence the activity of FAK and paxillin, with resultant effects on breast cancer cell adhesion and spreading (Lin *et al.*, 2000). Using real-time RT-PCR, reduction in glycosaminoglycan sulphation was shown to significantly increase the expression of FAK and Paxillin by 1.9- and 1.7-fold respectively (**Fig. 3.18A**). The expression of β_1 -integrin (ITGB1) was also upregulated, although this did not reach statistical significance. The changes in gene transcript levels were accompanied by similar upregulation in protein levels, as determined by Western blotting (**Fig. 3.18B and C**). Expressions of ITGB1, FAK and PXN proteins in sodium chlorate-treated cells were increased by 1.3-, 3.1- and 1.6-fold respectively. Using fluorescence immunocytochemistry, cells in the treatment group were found to possess a more obvious increase in focal adhesion formation together with stronger staining intensities for PXN and FAK proteins compared against those in the control group (**Fig. 3.19A and B, arrows**).

A



B



C

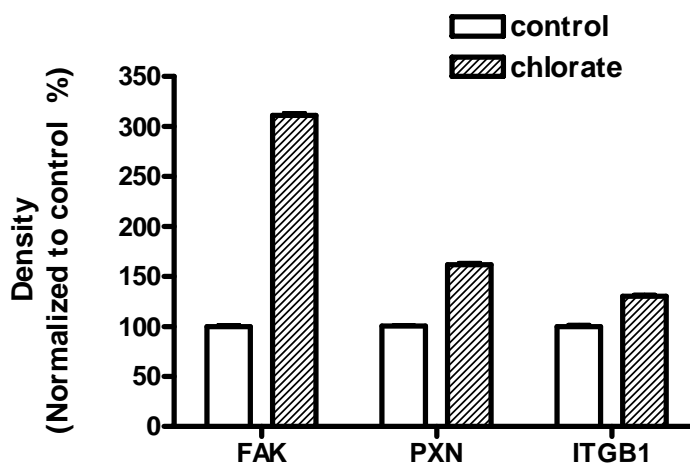


Fig. 3.18. Effects of reduced glycosaminoglycan sulphation on ITGB1, FAK and paxillin expression in MCF-7 cells. MCF-7 cells were cultured for 48 h in medium supplemented with PBS (control group) or 30 mM chlorate and re-seeded on fibronectin-coated coverslips for 2 hrs. Total mRNA and protein was collected. mRNA was used for real time PCR analysis and total protein was analyzed by Western blot (A) Gene transcript levels of ITGB1, FAK and PXN were measured using real-time RT-PCR. Chlorate treatment significantly upregulated the expression of FAK ($p = 0.0375$) and PXN ($p = 0.0440$). (B) Representative Western blot of three independent experiments. (C) Analysis by densitometry measurements showed increased levels of ITGB1 ($p = 0.0016$), FAK ($p = 0.0002$) and PXN ($p = 0.0003$). Values represent mean \pm SEM of three replicates.

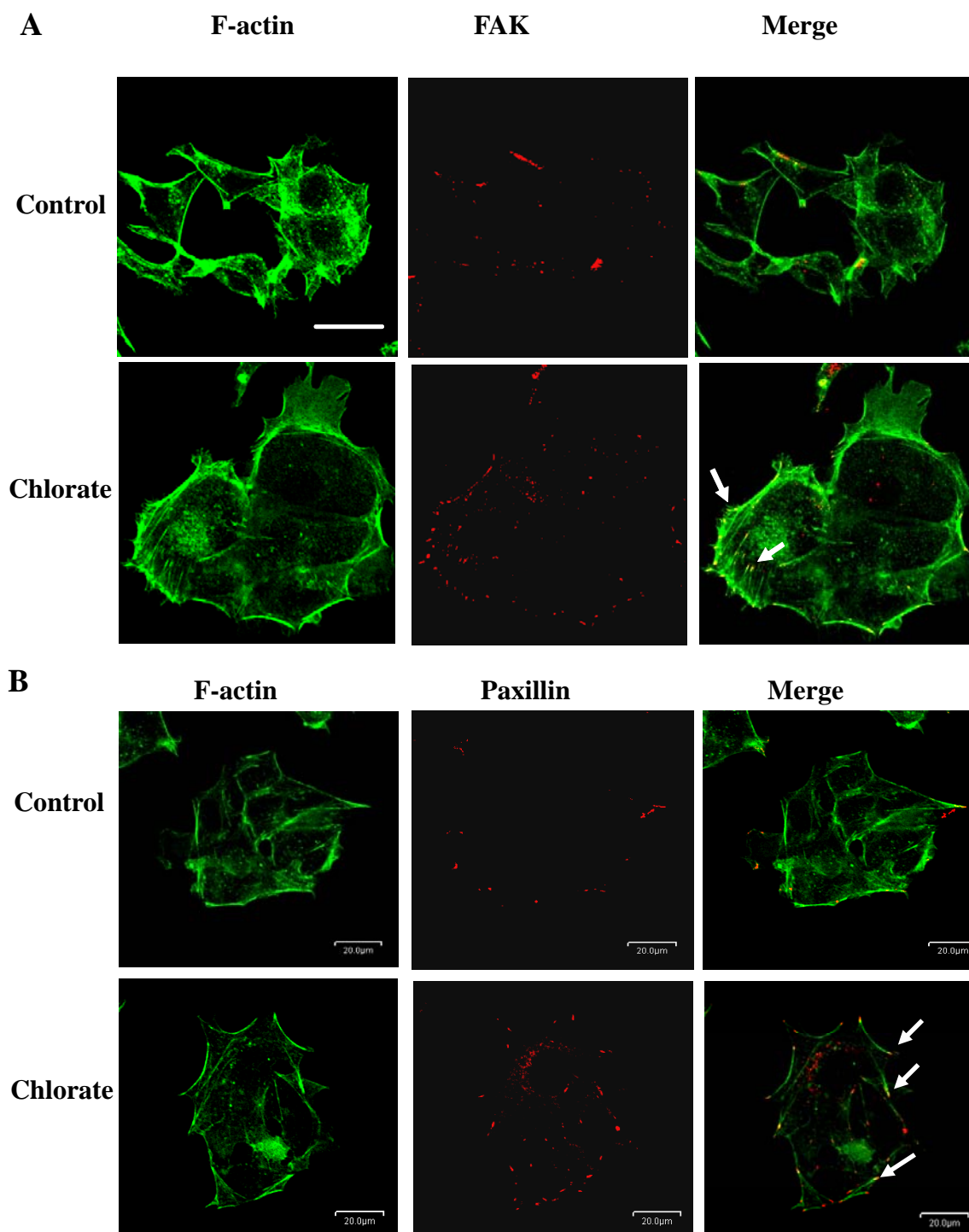


Fig. 3.19. Sodium chlorate enhanced MCF-7 cell focal adhesion formation on fibronectin. Coverslips were coated with 20 $\mu\text{g/ml}$ fibronectin at 4°C overnight and blocked with 1% BSA at room temperature for 1 hr. MCF-7 cells were treated with 30 mM sodium chlorate for 48 hrs and re-plated onto the fibronectin-coated coverslip for 2 hrs.. FAK (A) or Paxillin (B) were detected with anti-FAK polyclonal antibody or anti-paxillin monoclonal antibody, followed by Alexa-568-labeled second Ab (red), F-actin was probed with FITC-phalloidin (green). Panels are representative of triplicate experiments. The arrows indicate the areas of F-actin and FAK or F-actin and Paxillin colocalization in the focal adhesion formation sites. Scale bar = 20 μm .

3.8 Contrasting effects of different heparan sulphate species on migration of breast cancer cell.

To determine if the increment in cell adhesion due to reduced glycosaminoglycan sulphation would affect cancer cell migration, wound scratch assay was used to evaluate migration capacity *in vitro*. MCF-7 cells (**Fig. 3.20A**) and MDA-MB-231 cells (**Fig. 3.21A**) were cultured in the presence of sodium chlorate with medium containing only 2% FBS, and measured the distance migrated by the cells across a wound gap. Two percent FBS was much lower than normal culture condition (7.5% FBS) so that the cell proliferation was remarkably inhibited and the proliferation rate would not be a cofounder in the migration assay. Results showed that inhibition of glycosaminoglycan sulphation resulted in a significant decrease in cell migration of MCF-7 cells (**Fig. 3.20A and B**, Two-way ANOVA, $p < 0.01$) and MDA-MB-231 cells (**Fig. 3.21A and B**) (Two-way ANOVA, $p < 0.01$)

This sodium chlorate-induced reduction in cell migration could be completely abolished by supplementation of the culture medium with porcine intestine mucosa-derived heparan sulphate (HS-PM, **Fig. 3.22A**). However, in contrast to what was observed in the cell adhesion experiments (**Fig. 3.13**), addition of bovine kidney-derived heparan sulphate (HS-BK) to the sodium chlorate-containing culture medium led to a significant further decrease in cell migration instead of blocking the effect of chlorate (**Fig. 3.22B**). This suggests that differentially sulphated heparan sulphate species have diametrically opposite effects on breast cancer cell migration.

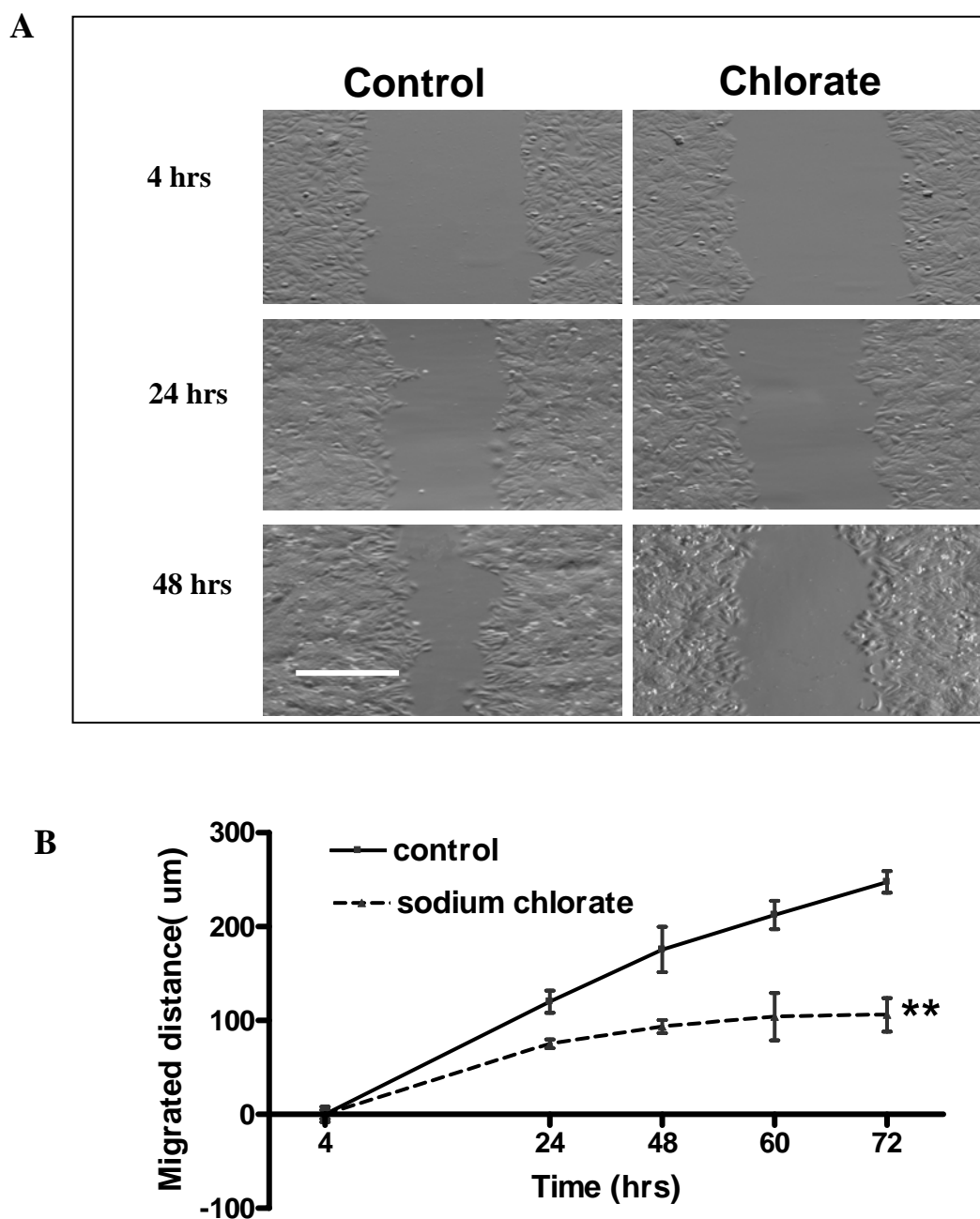
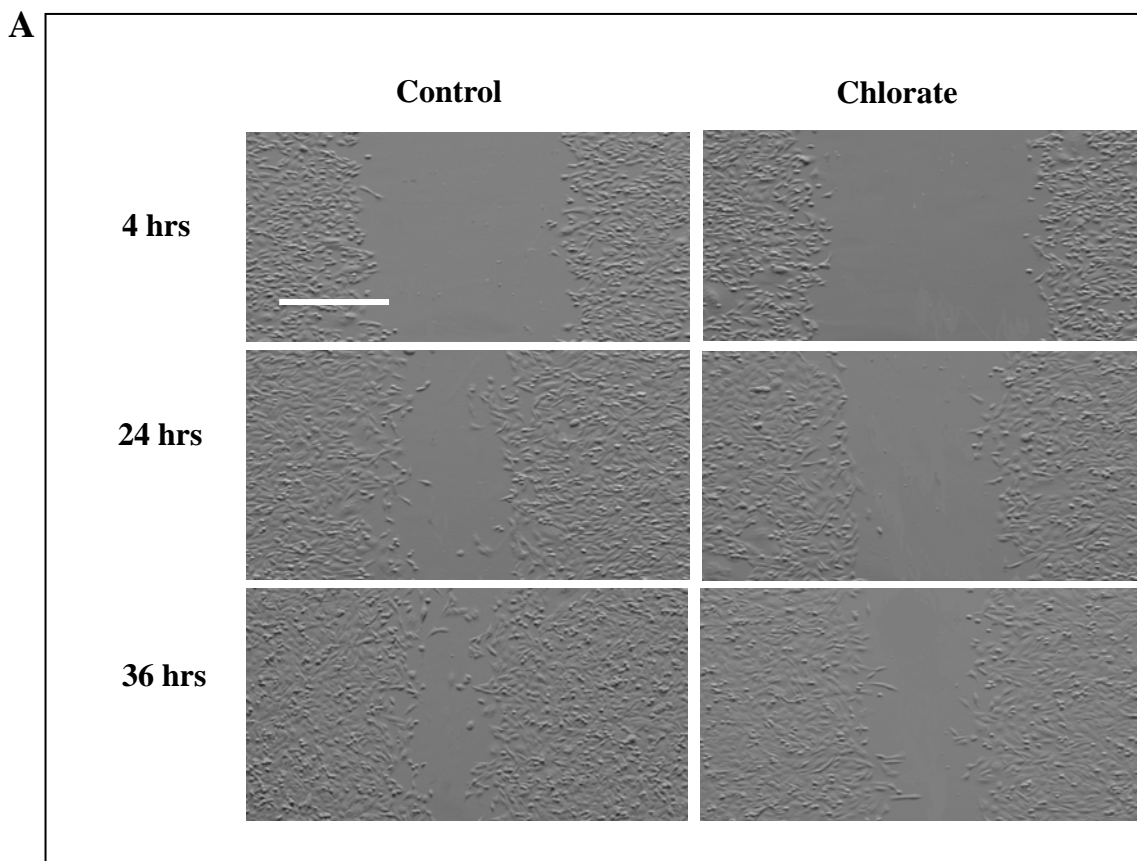


Fig. 3.20. Sodium chlorate inhibited MCF-7 cells migration. MCF-7 cells were seeded in 6-well plate and grew with or without 30 mM sodium chlorate till confluent. The cell monolayer was scratched with a 200 μ l pipette tip (T= 4hr as baseline) and the culture continued with or without sodium chlorate (A). The distances of the wound gap were measured using the image analysis software at 5 randomly-selected sites. The migrated distance was calculated as the distance at the baseline time point minus the distance at the indicated time point (B). Distance data were expressed as mean \pm SE. n = 5, ** $p < 0.01$.



B

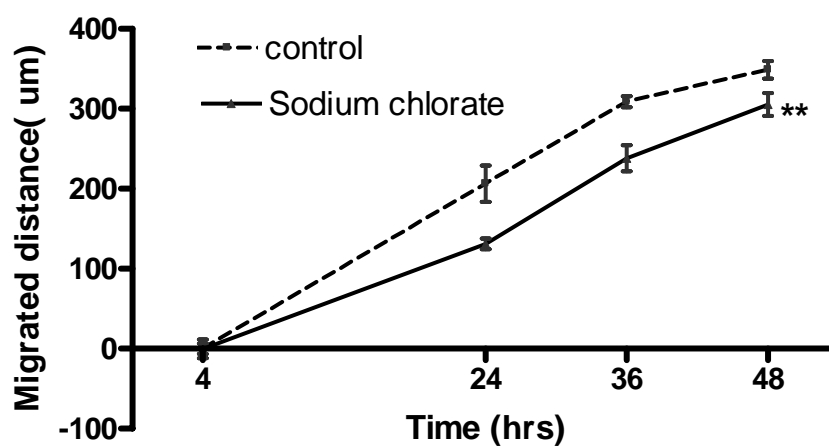
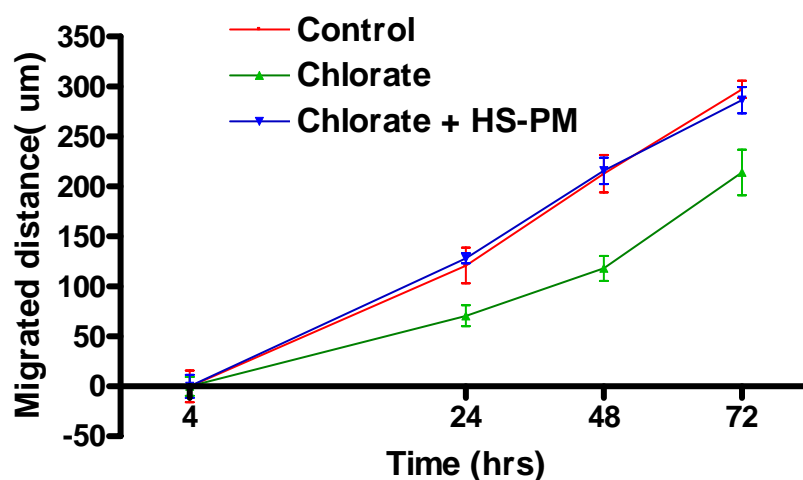


Fig. 3.21. Sodium chlorate inhibited MDA-MB-231 cells migration. MDA-MB-231 cells were seeded in 6-well plate and grew with or without sodium chlorate till confluent. The cell monolayer was scratched with a 200 μ l pipette tip (T = 4hr as baseline) and the culture continued with or without sodium chlorate. (A) The distances of the wound gap were measured using the image analysis software at 5 randomly-selected sites. (B) The migrated distance was calculated as the distance at the baseline time point minus the distance at the indicated time point. Distance data were expressed as mean \pm SE. n = 5, ** $p < 0.01$.

A



B

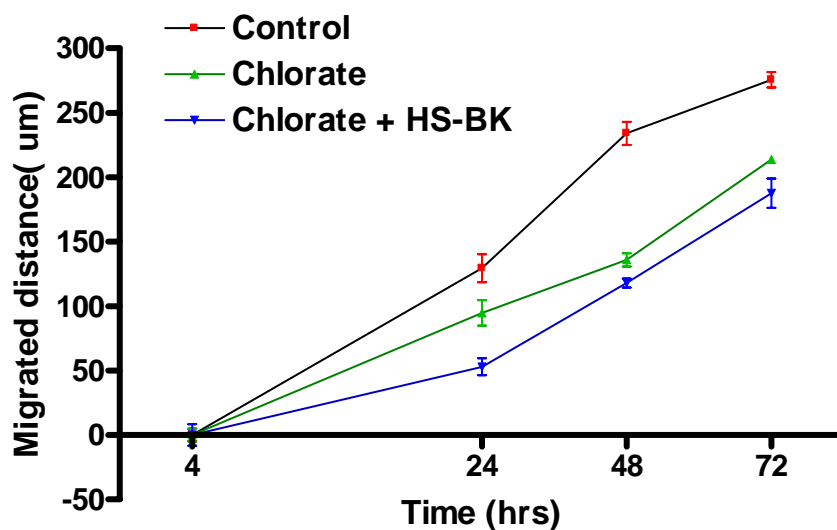
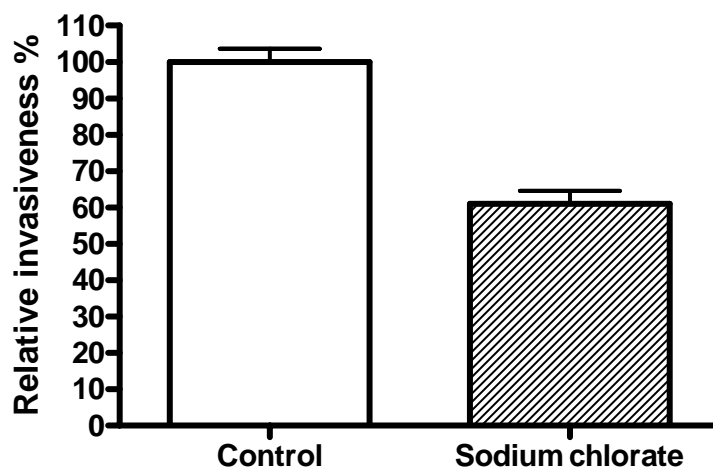


Fig. 3.22. HS-PM, but not HS-BK rescued the inhibitory effect of sodium chlorate on the MCF-7 cells migration. MCF-7 cells were seeded in 6-well plate and grew with or without HS-PM (A) or HS-BK (B) in the presence or absence of sodium chlorate till confluent. The cell monolayer was scratched with a 200 μ l pipette tip (T = 4 hr as baseline) and the culture continued with or without HS-BK or HS-PM in the presence or absence of sodium chlorate. The distances of the wound gap were measured using the image analysis software at 5 randomly-selected sites. The migrated distance was calculated as the distance at the baseline time point minus the distance at the indicated time point. Distance data were expressed as mean \pm SE. n = 5, Chlorate vs Chlorate+ HS-PM, * $p < 0.05$, Chlorate vs Chlorate+ HS-BK, $p > 0.05$

3.9 Undersulphation of GAGs inhibited invasion of breast cancer cell *in vitro*.

Cancer cell penetrating through the ECM and basement membrane is an indispensable step for tumour cells to invade and metastasize. To examine the significance of undersulphation of GAGs in affecting the MCF-7 and MDA-MB-231 breast cancer cell invasion *in vitro*, Matrigel invasion chamber was used. MDA-MB-231 cells exhibited relative high capabilities to penetrate through Matrigel-coated filters whereas after the sodium chlorate treatment, the invasion capacity was reduced 39% compared with the control MDA-MB-231 cells (**Fig. 3.23A and B**). A similar decrease (~43%) in cell invasion was also found in the MCF-7 cells cultured in the presence of sodium chlorate (**Fig. 3.24A and B**). These studies indicated that under sulphation in HSPG decreased the capacity of breast cancer cells to penetrate through the basement membrane, reflecting their impaired ability to invade.

A



B

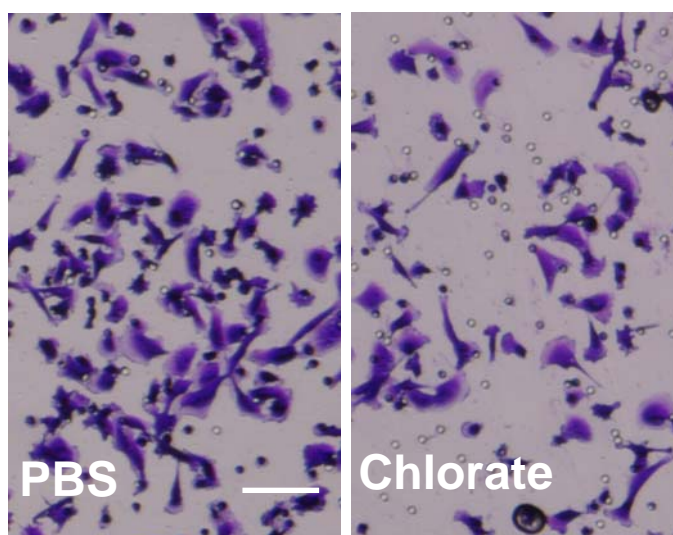
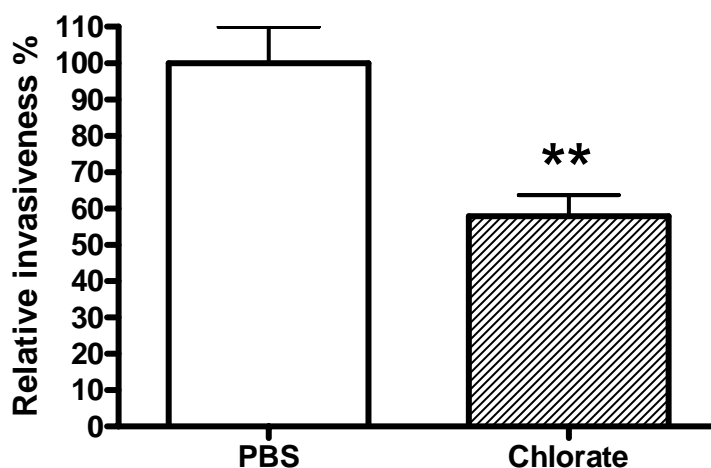


Fig. 3.23. Sodium chlorate inhibited MDA-MB-231 cell invasion through Matrigel *in vitro*. Matrigel Invasin chambers (24-well, 8 μm pore size) were used for invasion assay. **A:** MDA-MB-231 cells pretreated with sodium chlorate (30 mM) or PBS (control) for 48 hrs were harvested and seeded at a density of 5.0×10^4 cells per well. Cells were allowed to invade for 24 hrs. The number of cells that had invaded through the insert membrane pores was manually counted per high power field ($100\times$ magnification) using a microscope. Cell number at the bottom of the chamber was normalized against the control which was set at 100%. **B:** Images show representative fields of crystal violet stained MDA-MB-231 cells on the bottom of a Matrigel invasion chamber as captured from a Nikon microscope at $100\times$ magnifications. Scale bar = 100 μm .

A



B

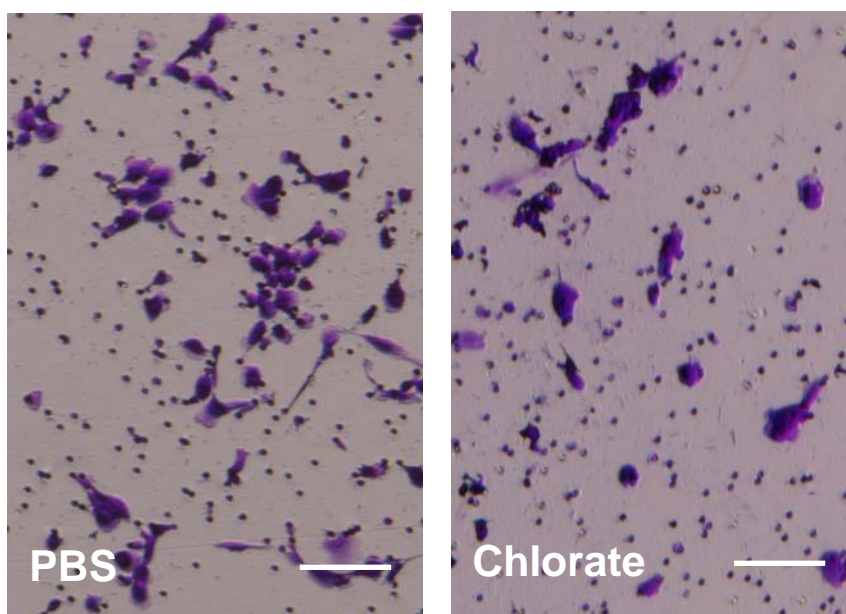


Fig. 3.24 Sodium chlorate inhibited MCF-7 cell invasion through Matrigel *in vitro*. Matrigel Invasin chamber (24-well, 8 μm pore size) was used for invasion assay. (A) MCF-7 cells pretreated with sodium chlorate (30 mM) or PBS (control) for 48 hrs were harvested and seeded at a density of 1.0×10^5 cells per well. Cells were allowed to invade for 24 hrs. The number of cells that had invaded through the insert membrane pores was manually counted per high power field (100 \times magnification) using a microscope. Cell number at the bottom of the chamber was normalized against the control which was set at 100%. (B) Images show representative fields of crystal violet stained MCF-7 cells on the bottom of a Matrigel invasion chamber as captured from a Nikon microscope at 100 \times magnifications. Scale bar = 100 μm .

Discussion

The main findings in the current study were 1) undersulphation in endogenous heparan sulphate in the breast cancer cells altered the biological processes in cancer progression such as proliferation, adhesion, migration and invasion; 2) differentially sulphated heparan sulphate derived from different species had different function in these processes.

HSPG and breast cancer growth

Research findings have demonstrated that HSPG is involved in many biological behaviors of malignant cells including cell proliferation, adhesion, migration and invasion. These biological effects are influenced by the highly sulphated groups of heparan sulphate (HS) chains.

Recently, expression of heparan sulphate glycosaminoglycan chain was shown to be correlated with tumour grade and cell proliferation in phyllodes tumours, one type of breast cancers (Koo *et al.*, 2006). This year in our paper (Guo *et al.*, 2007), Koo CY examined the expression of the 10E4 epitope of HSPG in both epithelial and stromal compartments of 32 samples of breast invasive ductal carcinoma and paired non-cancerous mammary tissues from corresponding patients. The study revealed that expression of the sulphated 10E4 epitope was up-regulated in both the epithelial and stromal compartments of breast cancers compared with normal mammary tissues. More importantly, the average immunoreactivity score of 10E4 in the cancer samples was 2.8 times higher than that of normal breast tissues, suggesting that heparan

sulphate would be a useful biomarker for breast invasive ductal carcinoma.

One of the major features of metastatic cells is the re-organization of specific cytoskeleton components (e.g. F-actin, proteoglycans) and activation of specific degrading enzymes (e.g. heparanase, MMPs) which degrade the proteoglycan surrounding the cells and allow cell to penetrate the extracellular matrix (Bogenrieder and Herlyn, 2003; Elkin *et al.*, 2003; Edovitsky *et al.*, 2004; Reiland *et al.*, 2004; Boyd and Nakajima, 2004; Gingis-Velitski *et al.*, 2004b; Yip *et al.*, 2006; Gotte and Yip, 2006). Indeed, studies on heparanase, an endoglucuronidase that hydrolyses heparan sulphate, suggest that degradation of heparan sulphate leads to enhanced breast cancer growth and invasion (Vlodavsky *et al.*, 1999). Cohen *et al.* (2006) also reported that using MCF-7 cells transfected with heparanase cDNA that were injected into the mammary pad of nude mice, they found enhanced tumour growth and invasion compared with tumours produced by mock-transfected cells. Up-regulated expression of heparanase, with a consequential reduction in heparan sulphate level, has been reported in breast cancers. Maxhimer *et al.* (2002) demonstrated that immunohistochemical staining of heparanase expression in breast cancer was positively associated with a larger tumour size and the presence of tumour metastases, together with a lack of heparan sulphate deposition. One recent study revealed that heparanase was more frequently expressed in invasive breast cancers than in *in situ* ductal carcinomas of the breast (Imada *et al.*, 2006). These studies suggest that heparan sulphate glycosaminoglycan chains are involved in breast carcinogenesis.

However, recent studies have shown that not all heparan sulphate chains are bad, and that the sulphation status of different heparan sulphate species is an important determinant of the biological effects of molecules on cancer cells so that tumour cell surface heparan sulphate can be either promoters or inhibitors of tumour growth and metastasis. Liu *et al.* (2002) reported that heparan sulphate fragments released by Hep I treatment from the surface of the tumour cell were able to promote primary tumour growth. In contrast heparan sulphate fragments released by Hep III inhibited both primary tumour growth and tumour metastasis. The latter inhibition in tumour growth was related to the inhibition in proliferation and induction of apoptosis. Further studies confirmed that the Hep III treatment derived HS fragments had more of tri- and di-sulphated disaccharides, whereas the Hep I-treated HS fragments had more mono- and un-sulphated disaccharides

This has been highlighted in the past few years in reports on the Sulf-1 gene, which codes for the enzyme sulphatase-1 that removes 6-O-sulphate groups from heparan sulphate (Dhoot *et al.*, 2001; Ohto *et al.*, 2002; Morimoto-Tomita *et al.*, 2002). Loss of 6-O-sulphate groups by Sulf-1 was shown to be a negative regulator of FGF signaling and FGF-FGFR binding. Disrupting FGF2-FGFR1-heparan sulphate ternary complex formation (Wang *et al.*, 2004) inhibited both tumour growth and tumour angiogenesis in xenografts in mice of Sulf-1 over-expressing MDA-MB-468 breast cancer cells (Narita *et al.*, 2006). Previously results showed that sodium chlorate preferentially reduce 6-O-sulphation of heparan sulphate (Safaiyan *et al.*, 1998; Safaiyan *et al.*, 1999).

Experiments with sodium chlorate, which competitively inhibits glycosaminoglycan sulphation and thus mimics overexpression of sulphatase-1 in the loss of 6-O-sulphate groups, showed a reduction in cell proliferation. This phenomenon could be blocked by addition of adequately sulphated heparan sulphate to the culture medium, with porcine intestine mucosa-derived heparan sulphate (HS-PM, Fig. 3.4). Porcine intestine mucosa-derived heparan sulphate has a high degree of sulphation compared with bovine kidney HS, especially GlcN 6-O-sulphate and IdoA 2-O-sulphate groups (Coltrini *et al.*, 1994; Maccarana *et al.*, 1996; Bianchini *et al.*, 1997; Warda *et al.*, 2003). In a previous work, Delehedde *et al.* (1996) reported that sodium chlorate treatment reduced sulphation of proteoglycans in MCF-7 cells which totally inhibited FGF-2-mediated proliferation. Many studies have confirmed that FGF-2 binds FGFR1 through HS which must contain N-sulphated glucosamine (GlcNS) residues and at least one 2-O-sulphated IdoA as well as to a sequence rich in GlcNS, 6-O-sulphated glucosamine residues (Maccarana *et al.*, 1993; Ishihara *et al.*, 1995; Wu *et al.*, 2003; Ibrahim *et al.*, 2004). Altering 2-O sulphation or 6-O sulphation diminishes FGF-2 binding and signaling (Guimond *et al.*, 1993; Zhang *et al.*, 2001).

Thus these results suggested that the partial rescue action in the proliferation by exogenous HS-PM supplementation, but not HS-BK, may act via selectively transferring sulphate group from the exogenous HS-PM to the endogenous HS or HS-PM has a higher capacity of protection FGF-2 from proteolytic cleavage, thus HS-PM partially blocked the inhibitory effect of sodium chlorate on breast cancer cell proliferation.

HSPG and adhesion, migration and invasion in breast cancer cells

Interestingly, heparan sulphate regulation of breast cancer cell migration appears to be affected not only by the number of sulphate groups present but also by the position of the sulphate groups. Thus, inhibition of heparan sulphation, as well as the presence of highly sulphated bovine kidney derived heparan sulphate, both led to a significant reduction in cell migration (Fig. 3.22). In contrast, optimally sulphated porcine intestine mucosa-derived heparan sulphate was able to block the effect of sodium chlorate treatment (Fig.3.22).

Heparan sulphate has been shown to be a key player in a number of signaling pathways in cell migration. It has been reported to modulate transendothelial migration of monocytes by regulating G-protein-dependent signaling (Floris *et al.*, 2003). Study also revealed addition of the 65-kDa latent heparanase to endothelial cells stimulated phosphatidylinositol 3-kinase- (PI3K) dependent endothelial cell migration and invasion (Gingis-Velitski *et al.*, 2004a). HT1080 fibrosarcoma cells that overexpressed the heparan sulphate proteoglycan syndecan-2 showed activation of the small GTPase Rac and increased cell migration (Park *et al.*, 2005). Furthermore, in addition to acting as a co-receptor in FGF signalling, heparan sulphate may act as a direct receptor in the FGF-2 activation of ERK1/2, which is required for bronchial epithelial and corneal epithelial cell migration (Chua *et al.*, 2004). Kaneider *et al.* (2004) found that cleavage of heparan sulphate from proteoglycans on the leukocyte surface completely inhibited chemotactic migration. Chemotactic migration was also abolished by pretreating the cells with heparinase, sodium chlorate, or anti-syndecan-4 antibodies. This study

clearly indicated that heparan sulphate, especially syndecan-4 and the sulphation of HS were involved in cell migration.

One of the important roles of HSPG is interaction with ECM molecules such as fibronectin, collagen and laminin, thus modulating cell adhesion and migration (Lark *et al.*, 1985a; Saunders and Bernfield, 1988; Lundmark *et al.*, 2001; Mendes de Aguiar *et al.*, 2002). HSPG have been associated with newly formed adhesion of adherent cell. Together with integrin it is also involved in cell motility by promoting cell adhesion and spreading at the leading edge of a moving cell (Lark *et al.*, 1985b).

The primary receptor for adhesion to fibronectin commonly involves the RGD motif through integrins (Pytela *et al.*, 1985). Integrin-mediated cell adhesion leads to recruitment of the cytoplasmic protein tyrosine kinase FAK to focal adhesion sites, and the phosphorylation of both FAK and paxillin (LaFlamme and Auer, 1996; Mostafavi-Pour *et al.*, 2003). FAK is a prominent constituent of these focal adhesions complexes (Cary and Guan, 1999; Hanks *et al.*, 2003; Mitra *et al.*, 2005). Paxillin is a cytoskeletal focal adhesion docking protein that localizes at adhesion sites by binding to the carboxyl terminus of FAK (Anfosso *et al.*, 1998; Turner, 1998; Turner, 2000). But this integrin mediated interaction is only sufficient for cell attachment and spreading.

Additional signaling through the cell surface proteoglycan syndecan-4 is required for focal adhesion formation and rearrangement of the actin cytoskeleton into bundled stress fibers (Woods *et al.*, 1998; Longley *et al.*, 1999; Woods and Couchman, 2001). Syndecan-4 is a ubiquitous vertebrate transmembrane heparan sulphate proteoglycan

(HSPG), which localizes to focal adhesion complex and acts as a co-receptor with $\alpha_5\beta_1$ -integrin (Woods, 2001; Mostafavi-Pour *et al.*, 2003). Syndecan-4 interacts with the Hep II domain of fibronectin through its heparan sulphate chains (Woods *et al.*, 2000) and with PKC-alpha through its cytoplasmic domain (Murakami *et al.*, 2002; Lim *et al.*, 2003; Keum *et al.*, 2004). Expression of syndecan-4 in Chinese hamster ovary (CHO) cells resulted in increased numbers of focal adhesion complexes (Longley *et al.*, 1999). On the other hand, CHO cell mutants deficient in glycosaminoglycans showed reduced focal adhesion formation when cultured on a fibronectin substrate (LeBaron *et al.*, 1988).

In the present study, reduction in heparan sulphation in MCF-7 breast cancer cells was shown to increase cancer cell adhesion and upregulate FAK and paxillin at both gene transcript and protein levels, and the increment in adhesion could be completely blocked by exogenous heparan sulphate HS-BK and partially blocked by HS-PM.

The results in the present study that undersulphation in endogenous heparan sulphate increased the adhesion of breast cancer cells and retarded their migration as well as the differentially regulatory function of exogenous heparan sulphate derived from different species in these processes are in agreement with the recently proposed concept of a 'heparanome', in which differentially sulphated sugar sequences regulate the biological activities of different heparan sulphate species (Turnbull *et al.*, 2001; Lamanna *et al.*, 2007). Heparan sulphate has been shown to affect cancer cellular behaviour through several mechanisms (Bernfield *et al.*, 1999; Timar *et al.*, 2002; Liu *et al.*, 2002). It is able to bind to and interact with a multitude of growth factors and

signaling proteins, resulting in stimulation of growth and metastasis of cancer cells (Turnbull *et al.*, 2001; Mulloy and Rider, 2006; Kreuger *et al.*, 2006). Heparan sulphate in the extracellular matrix also acts as a reservoir for aggregation of growth and angiogenic factors. Furthermore, binding of heparan sulphate to these molecules could protect them from degradation and thus prolong their effects on cancer cells. On the other hand, degradation of heparan sulphate may release fragments that antagonize these growth factors and signaling molecules, leading to the inhibition of tumour growth and metastasis (Timar *et al.*, 2002). Thus by modulating the composition or “sulphation signature” of heparan sulphate at cell surface and in the ECM, cell provide itself a systemic mechanism for fine control of the final function of heparan sulphate proteoglycan, determining whether it is a promoter or an inhibitor of tumour growth and metastasis.

In conclusion, in the present study, it has been demonstrated heparan sulphate is involved in regulating cancer cell proliferation, adhesion, focal adhesion complex formation, migration and invasion through different sulphation patterns on its sugar residues. Uncontrolled proliferation, loosening adhesive contacts with the extracellular matrix, increasing migration and invasiveness are characteristics of breast cancer growth and metastasis, contributing significantly to patient morbidity and mortality. The challenge to targeting heparan sulphate in breast cancer treatment therefore depend on selective inhibition of tumour promoting mediators, or identification and blockage of causative factors contributing to their unfavourable phenotypic alteration. A better understanding of the effects of differentially sulphated heparan sulphate species on

cancer cell behaviors is important for the development of these molecules into therapeutic targets for breast cancer.

CHAPTER 4

CHAPTER 4 Studies on phenotypic alterations in MCF-12A cells after silencing 3-O-HS sulphotransferase 3A1 (*HS3ST3A1*) gene

Many research findings have verified that heparan sulphate (HS) functions are dependent on specific sulphation motifs. 3-O sulphation of glucosamine residues of HS-GAG chain is a rare but important modification of HS synthesis. The success in cloning and characterization of HS 3-O-sulphation enzymes increased the understanding for the mechanisms of generating HS with defined motif and the sequence-specific function. One good example, 3-O-sulphotransferase (3-O-ST, now known as 3-O-ST-1, *HS3ST1*) converts non-anticoagulant heparan sulphate into anticoagulant heparan sulphate, which is widely used in clinic and well known as heparin (Dementiev *et al.*, 2004; Petitou and van Boeckel, 2004). *HS3ST3* has been cloned and partially characterized (Shukla *et al.*, 1999; Shworak *et al.*, 1999; Liu *et al.*, 1999b). Biochemical studies have revealed the enzymatic function of *HS3ST3s* based on their respective substrate preferences and the resultant HS structures, but their biological functions in mammalian cells are still at large.

4.1 Quantitative real-time PCR analysis of *HS3ST3A1* and *HS3ST3B1* mRNA expression levels in breast epithelial and breast cancer cell lines.

In this study the expression of *HS3ST3A1* in breast epithelial MCF-12A cells and breast cancer cell lines was first investigated by quantitative real-time PCR. As shown in **Table 4.1**, compared with that in MCF-12A, the expression level was

down-regulated about 230-fold in MCF-7 cells, 33-fold in ZR-75-1 cells and was undetectable in MDA-MB-231 cells and T47D cells. These results suggest that *HS3ST3A1* may play an important role in breast tumourigenesis and progression.

	MCF-12A	MCF-7	MDA-MB-231	T47D	ZR-75-1
<i>HS3ST3A1</i>	1.00 ± 0.84	↓230.72 ± 1.72	undetectable	undetectable	↓32.90 ± 1.75
<i>HS3ST3B1</i>	1.00 ± 0.73	↓6.96 ± 1.22	2.91 ± 1.05	↓3.70 ± 1.12	↓3.56 ± 1.15

Table 4.1. Quantitative real-time PCR analysis of the mRNA expression of *HS3ST3A1* and *HS3ST3B1* in normal breast cell line MCF-12A and four breast cancer cell lines. The expression levels are shown normalized to the expression of the reference gene β -actin. Data are expressed as average fold change of at least 3 experiments, mean \pm SD. Fold change was calculated as $2^{-(\Delta\Delta Ct)}$. “↓” symbols down-regulation.

4.2 *In situ* hybridization analysis of *HS3ST3A1* expression in breast cancers. (Courtesy of Koo Chuayyeng)

To further assess the expression of *HS3ST3A1* in normal breast tissues and breast cancers, *in situ* hybridization was performed on corresponding breast normal and cancer tissues from 22 patients. Strong expression of *HS3ST3A1* was detected in the epithelial cells of ducts in normal tissues but not in the tumour cells of the cancers in all of the 22 patients examined as shown in **Fig. 4.1**. The epithelial cells of the ducts in the normal tissues (**Fig.4.1, A**) were intensely stained as compared to the tumour cells (**Fig.4.1, B and C**). Low signal intensity was observed in Fig. 4.1d as this section was hybridized with the sense probe. To evaluate *HS3ST3A1* expression semi-quantitatively, average IPS (Koo *et al.*, 2006) was calculated from the epithelial

cells of ducts in the normal tissues and the tumour cells. There was a significant difference in the average IPS between the normal breast tissues and breast cancers (Fig 4.2., $p < 0.001$), which was consistent with the results obtained from the breast cancer cell lines (Table 4.1)

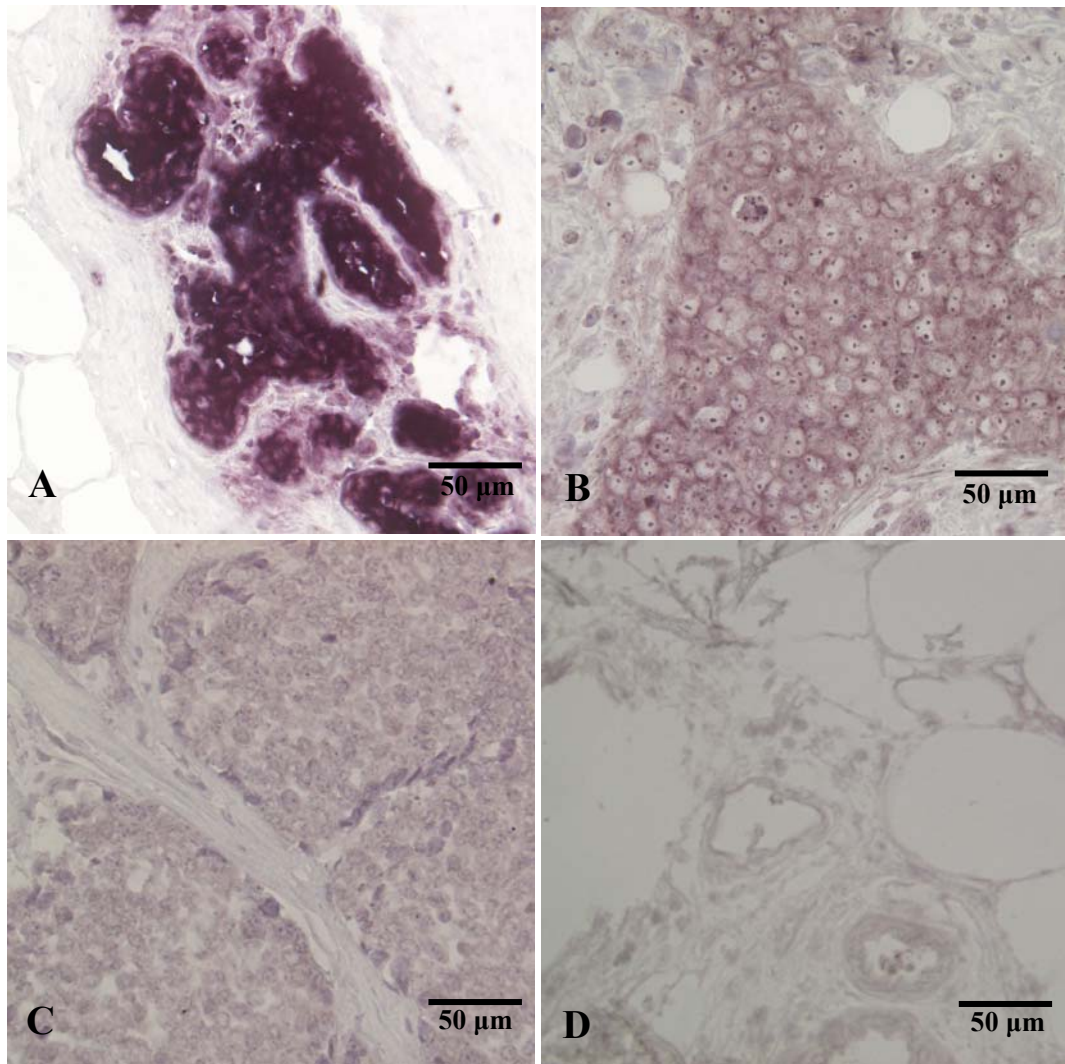


Fig. 4.1. *In situ* hybridization analysis of *HS3ST3A* mRNA expression in normal breast tissue and breast cancers. A: normal tissue, B: infiltrating ductal carcinoma, C: invasive ductal carcinoma, D: negative control (sense probe).

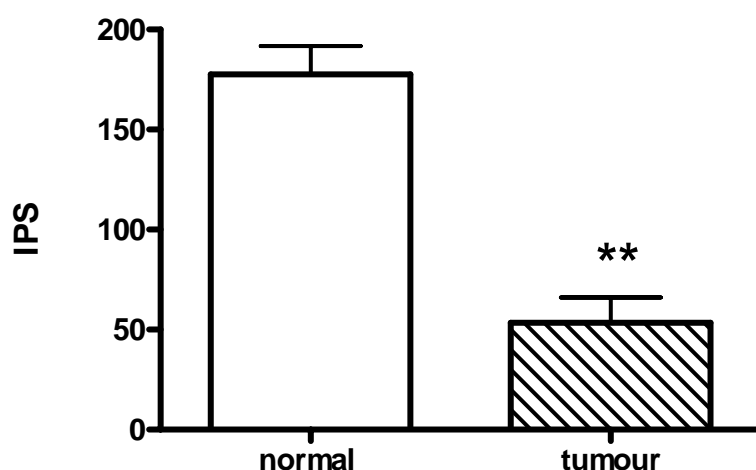


Fig. 4.2. Average IPS score of *in situ* hybridization analysis of *HS3ST3A* mRNA expression in normal breast tissue and breast cancers. Normal versus tumour cells ($p < 0.0001$).

Characteristic	<i>HS3ST3A1</i> negative (IPS ≤ 40)	<i>HS3ST3A1</i> positive (IPS > 40)	Significance (P value)
Tumour size ≤ 40 mm	6	4	1
Tumour size > 40 mm	5	7	
ER -	5	0	0.0315*
ER +	6	11	
PR -	9	0	0.0002*
PR +	2	11	
cerB 2 -	3	3	1
cerB 2 +	8	8	
Lymph Node Stage 1-2	6	7	1
Lymph Node Stage 3	5	4	

Table 4.2. Correlations between *HS3ST3A1* expression and various clinicopathologic factors in patients with invasive breast carcinoma.

4.3 Optimization of the transfection parameters for knocking down of *HS3ST3A1* mRNA expression by siRNA.

Based on the above results, silencing *HS3ST3A1* expression in MCF-12A cells using chemically synthesized siRNA was performed. In order to obtain good silencing effect, optimization experiments were first conducted by using Cyanine (Cy3)-conjugated scrambled siRNA that has no targeting gene. The optimization for transfection efficiency include transfection reagent amount, cell density and incubation time. As shown in **Fig. 4.3**, the transfection efficiency was about 97.1% at 24 hrs and the transfection parameters were: final siRNA concentration, 30 nM; transfection time, 8 hrs and cell density, 3.5×10^5 cells per well in 6-well plate (approximately 50% cell confluent at the time of transfection). There was no significant morphology change between cells in the control siRNA transfected group and the *HS3S3A1* siRNA transfected cells at 48 hrs or 72 hrs as shown in **Fig. 4.4**. These results indicate that the transfection efficiency is quite satisfactory. Using these parameters, the positive control of *GAPDH* siRNA (Ambion, Inc. Cat No. AM4605) achieved a 97.6% knockdown effect with least cell death (**Fig. 4.5**).

4.4 Knockdown of *HS3ST3A1* mRNA expression by siRNA was gene-specific and dose-dependent.

Next, 3 different siRNAs corresponding to 3 different regions of *HS3ST3A1* mRNA were used to screen if any of them could knockdown *HS3ST3A1* expression under the same parameters. **Fig. 4.6** shows that the #2 (siRNA ID: 113287 in Ambion siRNA database, Amibon, Inc.) sequence of the siRNA achieved the most significant knockdown effect (suppression ~91.58%). Repeated experiments results showed that

this siRNA could obtain an average of 86.26% suppression at 48 hrs (Fig. 4.7).

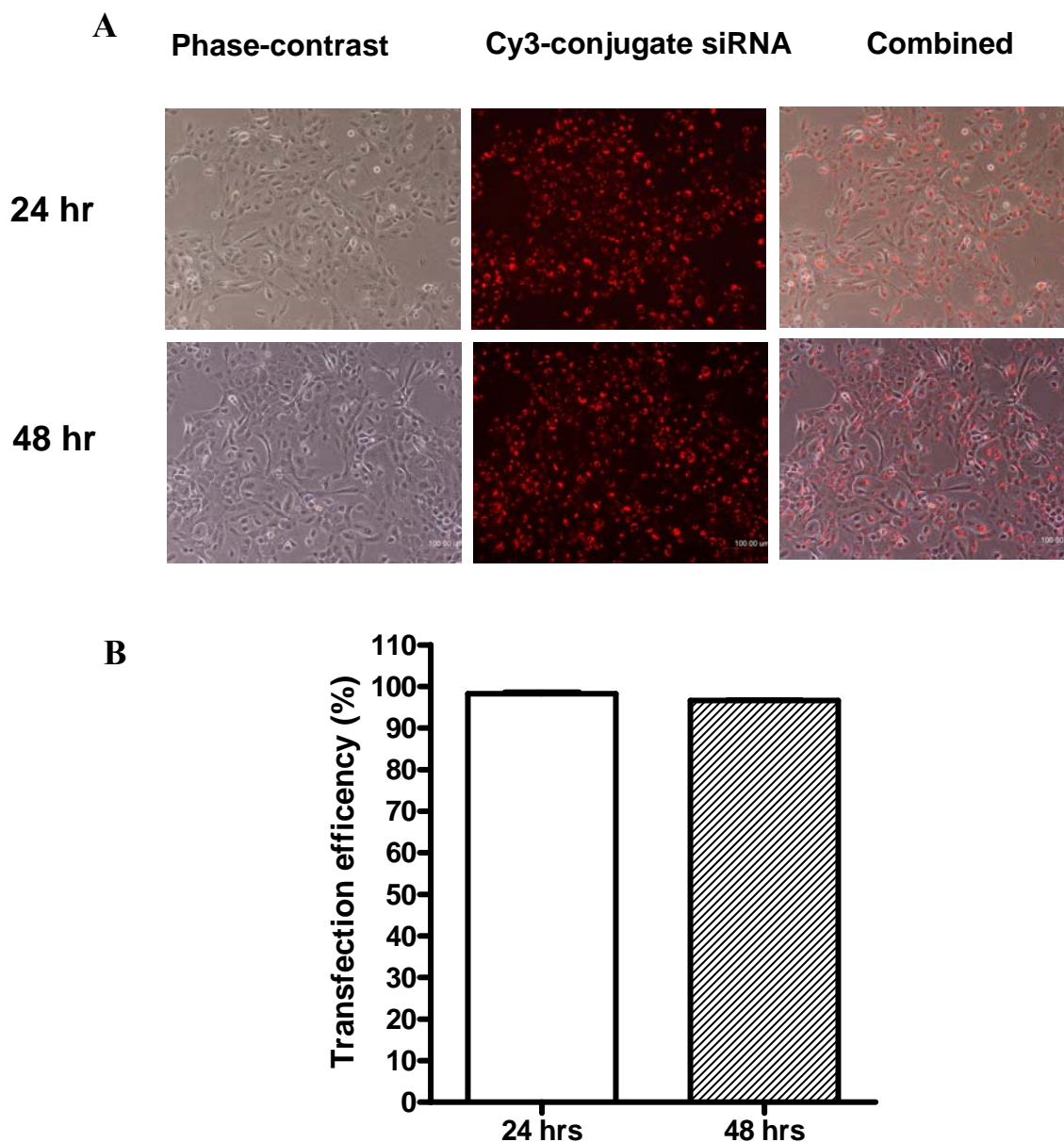


Fig. 4.3. Determination of transfection efficiency by Cy3-labelled control siRNA in the MCF-12A cells. MCF-12A human breast epithelial cells were transfected with Cy3-labelled non-targeting (control) siRNA using optimal conditions suggested by the manufacturers' protocols (Ambion, InC.) The optimized parameters in the transfection: 3.5×10^5 cell per well with $8 \mu\text{l}$ siPORT Amine and 30 nM siRNA. (A) Cy3-labeled siRNAs in transfected cells (Positive transfected cells) were visualized using a Nikon inverted fluorescence microscope. Experiments were repeated three times in duplicates and representative images are presented. (B) The data represent the mean \pm SD, $n = 5$. The optimized transfection efficiency was 97.1% at 24 hrs.

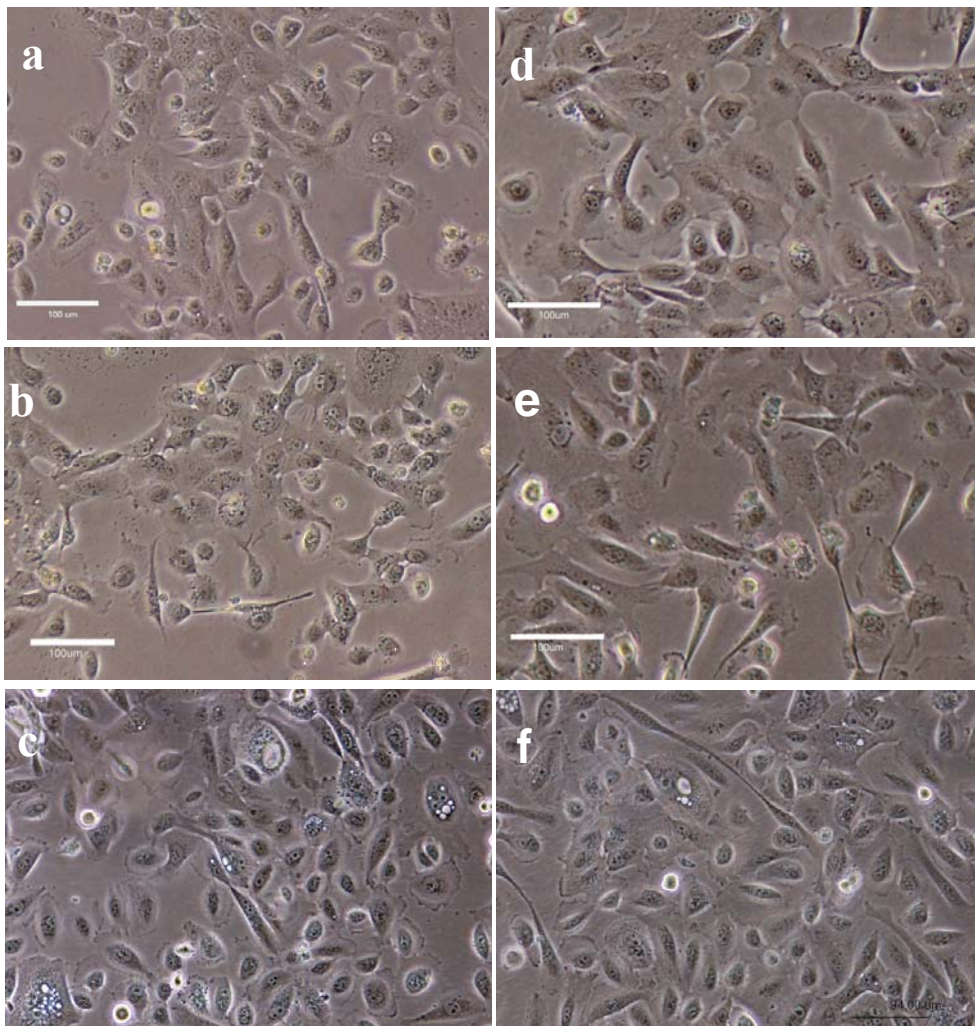


Fig. 4.4. Cell morphology after transfection. Under optimized transfection conditions siPORT Amine transfection reagent did not adversely affect MCF-12A cell morphology at 48 hrs (a, b) and 72 hrs (c, d). a and b: control non-targeting siRNA. d, e: GAPDH siRNA. c and f: normal cells under maintaining medium at 48 hrs and 72 hrs.

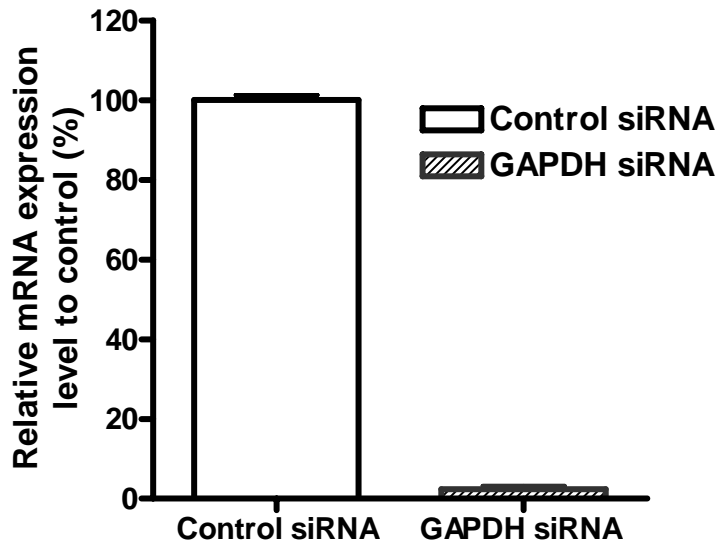
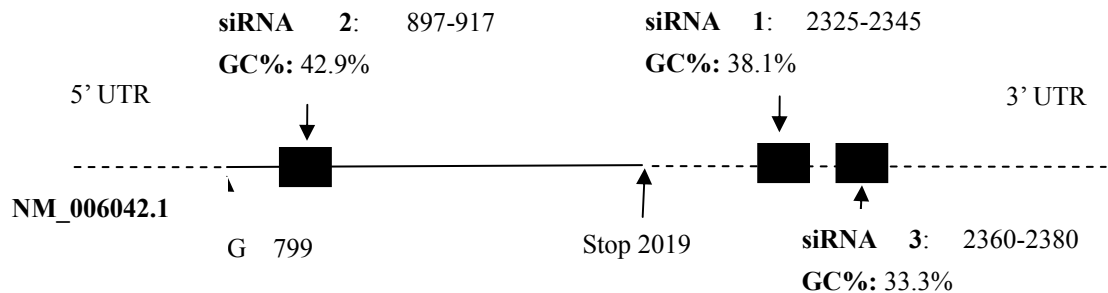


Fig. 4.5. Silencing effect of positive siRNA targeting *GAPDH* mRNA in MCF-12A cells. Under optimized parameters, *GAPDH* mRNA expression was silenced more than 95% compare that in the non-targeting siRNA transfected group. The optimized parameters in the transfection: 3.5×10^5 cell per well in 6-well plate with 8 μ l siPORT Amine and 30 nM siRNA.

A



B

HS3ST3A1 mRNA NM_006042.1

siRNA 1 Ambion ID 17338

Sense: 5'-GGUUAACAUCUCUCUCUCtt--3'

Antisense: 5'-GAGAGAGAGAUGUUUAACCtc-3'

GC% : 38.1%

siRNA 2 Ambion ID 113287 we used this siRNA

Sense: 5'-CGUCCCUUUACGUCUUCUAtt-3'

Antisense: 5'-UAGAAGACGUAAAGGGACGtg-3'

GC% :42.9%

siRNA 3 Ambion ID 17338

Sense: 5'-GGCCCUGAUAAAAUUGAUAtt-3'

Antisense: 5'-UAUCAAUUUUAUCAGGGCCtt-3'

GC% :33.3%

C

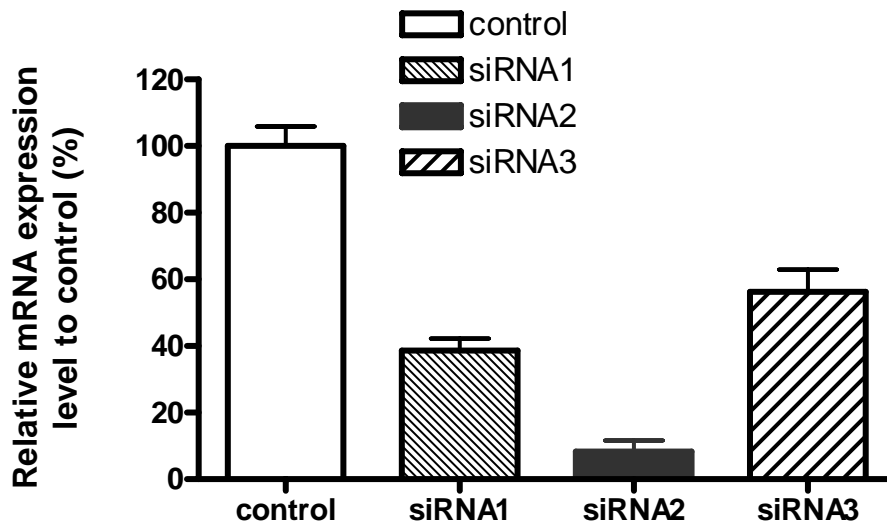


Fig. 4.6. Knockdown effect of three different siRNA sequences targeting *HS3ST3A1* mRNA in MCF-12A cells.

- (A) Design and synthesis of siRNAs against *HS3ST3A1*. Schematic representation of the primary structure of human *HS3ST3A1* mRNA (gi: NM_006042.1) and three target sites of siRNAs. The exact position of each target site was shown in the diagram and GC% was calculated
- (B) Sequences of siRNA duplexes. 3 different siRNAs were designed against *HS3ST3A1* mRNA by Ambion, Inc.
- (C) #2 siRNA achieved the most significant silencing effect. Note: From here onwards, #2 *HS3ST3A1* siRNA was used in the following experiments

As chemically synthesized siRNA degrades within a few days, silencing effects at different time points after transfection thus were examined. **Fig. 4.7** shows that the knockdown effect lasted at least 96 hrs in this study. The most significant knockdown effect was achieved at 48 hrs with more than 86% silencing (**Fig. 4.7A**). Though with time lapse, the silencing effect was reduced, there was still 77.62% reduction at 72 hrs and 61.31% reduction at 96 hrs (**Fig. 4.7A**). This knockdown effect was specific to *HS3ST3A1* as shown in **Fig. 4.7A** and **B**. There was only limited suppression on the *HS3ST3B1* mRNA expression, the closest isoform of *HS3ST3A1*. As shown in **Fig. 4.7B**, under the transfection conditions, *HS3ST3B1* mRNA was knocked down only 3.71% at 48 hrs, 18.62% at 72 hrs and 27.03% at 96 hrs, respectively. These results indicate the knockdown effect could last at least 96 hrs and was gene-specific. So #2 siRNA was chosen in the later experiments and termed as *HS3ST3A1* siRNA. The single sharp peak in melting curve and single band in the agarose gel electrophoresis analysis as shown in **Fig. 4.8** suggested specific gene amplification of *HS3ST3A1* and *HS3ST3B1* mRNA both in control and siRNA silenced cells.

As too much siRNA has been reported to have non-specific silencing effect and cytotoxicity (Sandy *et al.*, 2005), dose-dependent effect on the silencing efficiency were analyzed. Two smaller final concentration of siRNA (7.5 nM and 15 nM) were used to compare the results from 30 nM final concentration of siRNA. **Fig. 4.9A** shows that 30 nM final concentration was an ideal concentration as it achieved the greatest silencing effect while the other two concentrations could not achieve more than 80% reduction at 48 hrs. In all of the three concentrations, no significant

silencing effect was seen on *HS3ST3B1* expression (Fig. 4.9B). Eighty percent silencing was deemed as the significant level in this study to carry out the subsequent experiments.

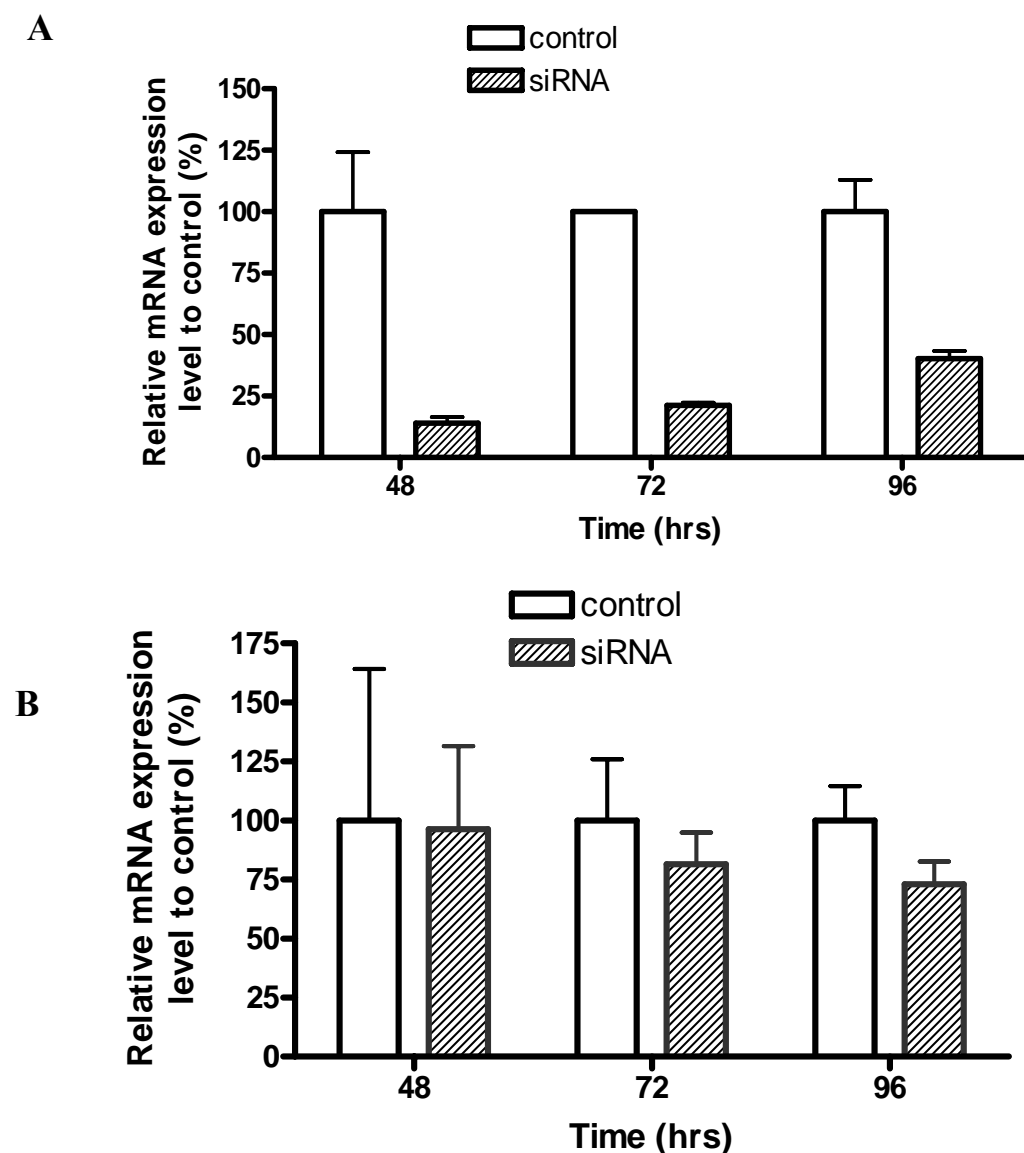


Fig. 4.7. Time-dependent knockdown effect of *HS3ST3A1* siRNA on the mRNA expression of *HS3ST3A1* and *HS3ST3B1* in MCF-12A cells. *HS3ST3A1* siRNA showed significant inhibitory effect on *HS3ST3A1* mRNA expression in MCF-12A cells at 48, 72, and 96 hrs (A), while no such significant reduction was seen in the *HS3ST3B1* mRNA expression (B). mRNA expression level was determined by quantitative real-time PCR using β -actin as the reference gene for normalization. Histograms represent the relative expression level in the cells. Data are 3 separate experiments mean \pm S.D.

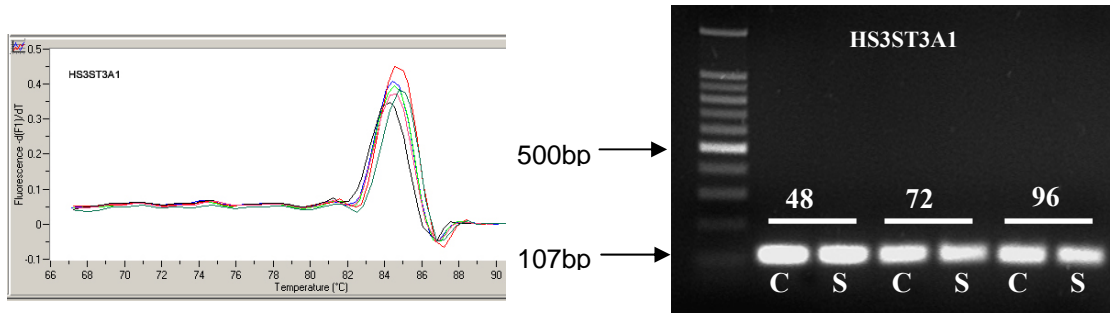
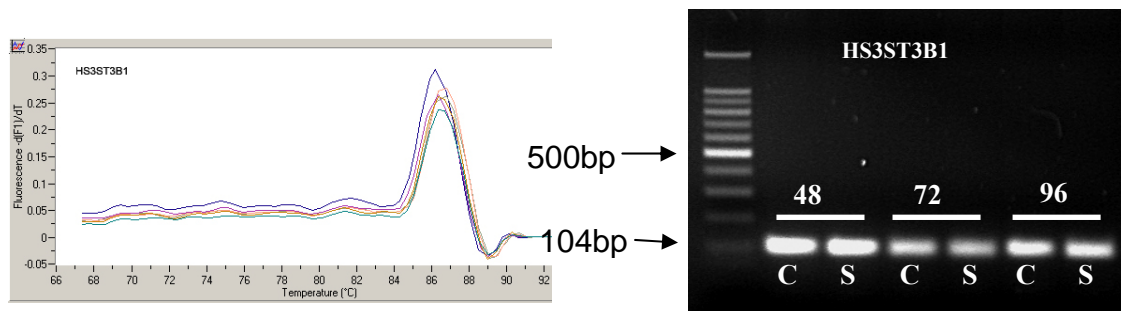
A**B**

Fig. 4.8. Real-time PCR melting curve and agarose gel electrophoresis analysis of *HS3ST3A1* and *HS3ST3B1* amplification. The melting curves are displayed as first negative derivative of the fluorescence versus the temperature. Thus, a single peak can be seen at the melting temperature. The results here show the specific amplification of *HS3ST3A1* (A) and *HS3ST3B1* (B) mRNA at 48, 72 and 96 hrs both in control and silenced groups. C, control; S, siRNA.

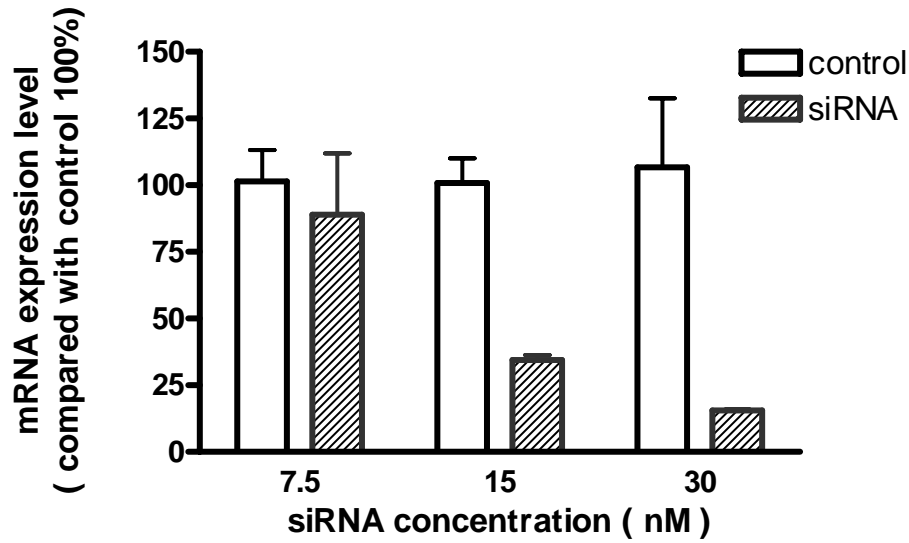
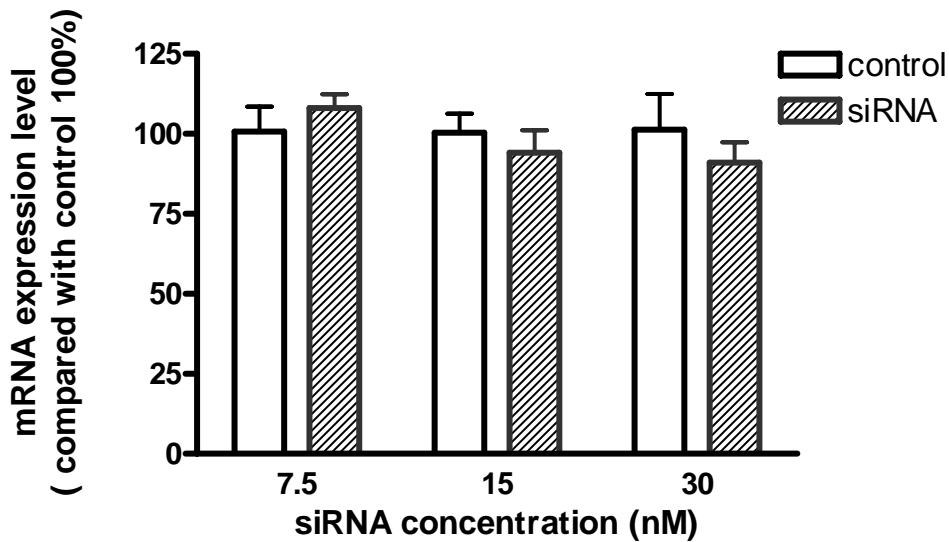
A**B**

Fig. 4.9. Silencing effect of concentration titration of *HS3ST3A1* siRNA on the mRNA expression of *HS3ST3A1* and *HS3ST3B1* in MCF-12A cells. Real-time PCR analysis showed the optimized concentration of 30 nM siRNA achieved the maximal reduction of expression of *HS3ST3A1* mRNA (A), but no significant suppression on the expression of *HS3ST3B1* mRNA (B). mRNA expression level was determined by quantitative real-time PCR using β -actin as the reference gene for normalization. Histograms representing the relative expression level in the cells. Data are 3 separate experiments mean \pm S.D.

4.5 Silencing the expression of *HS3ST3A1* impaired the synthesis of HSPG in MCF-12A cells.

To study if the HSPG synthesis was impaired after successfully silencing *HS3ST3A1* mRNA expression, immunohistochemical staining of HSPG in MCF12A cells was performed. *HS3ST3A1* enzyme transfers 3-O-sulphation group to HSPG chain. Immunohistochemical staining showed that after silencing of *HS3ST3A1* mRNA, HSPG intensity was significantly reduced compared with that in the control group (**Fig. 4.10**). This immunohistochemical staining results clearly indicated that silencing of *HS3ST3A1* mRNA suppressed the enzymatic activity of *HS3ST3A1* enzyme which resulted in the impaired synthesis of HSPG in MCF-12A cells.

4.6 Reduction of *HS3ST3A1* expression by siRNA in the MCF-12A cells inhibited cell proliferation.

The effects after silencing *HS3ST3A1* mRNA on the phenotype alterations in MCF-12A cells were further studied. Cell proliferation change was first investigated because HSPG is known to be involved in the regulation of cellular proliferation. Cell proliferation was measured by direct cell counting. MCF-12A cells were transfected in triplicate with the siRNA targeting *HS3ST3A1* mRNA or the control scrambled siRNA. Cells were trypsinized and counted three days after transfection. **Fig. 4.11** shows the effect of silencing *HS3ST3A1* mRNA expression on MCF-12A cell proliferation. Reduction of *HS3ST3A1* mRNA expression by siRNA inhibited MCF-12A cell growth by 21.64% (Student's *t*-test, $**p = 0.0043$) compared with cells transfected by scrambled siRNA (control) (**Fig. 4.11**).

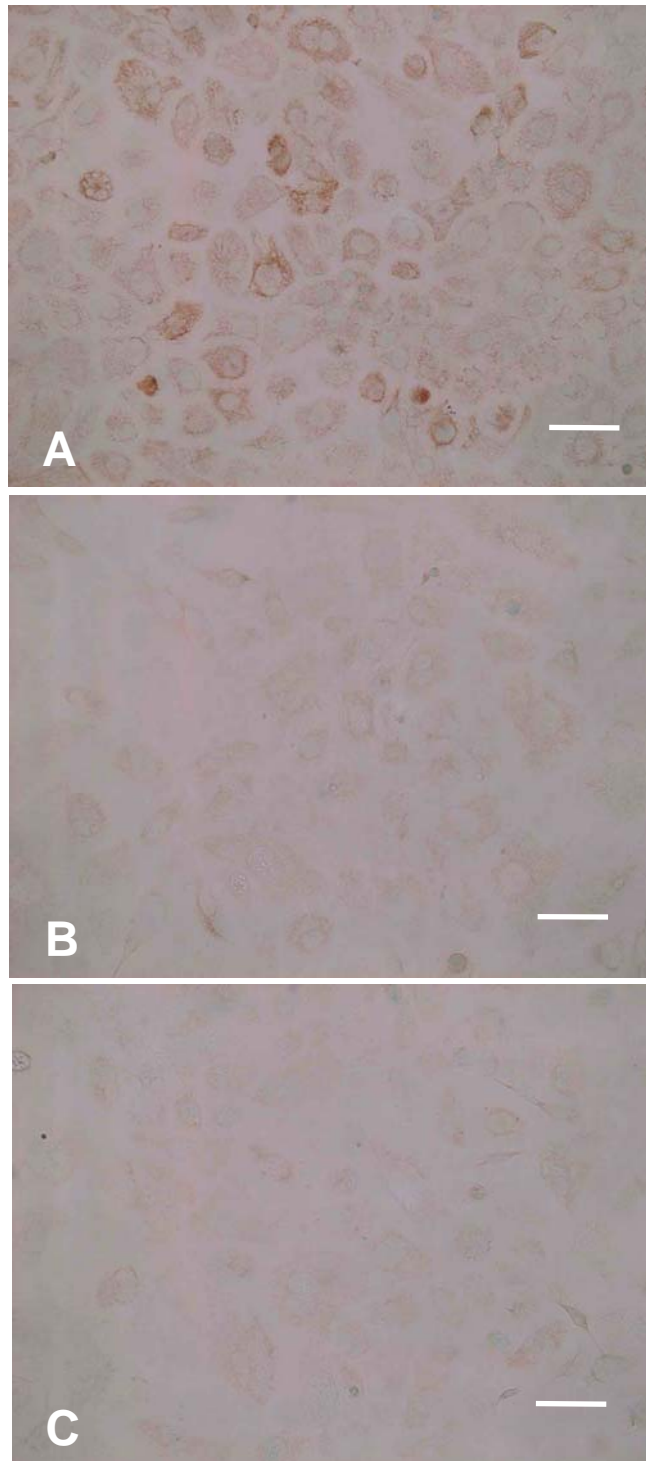


Fig. 4.10. Immunohistochemical localization of heparan sulphate proteoglycan in MCF-12A cells after silencing *HS3ST3A1*. Cells were stained by using 10E4 mAb (anti-heparan sulphate antibody) with ABC method 72 hrs post siRNA transfection.. The cell surface is characteristically stained with the antibody. The staining is significantly weaker or almost negative in the *HS3ST3A1* siRNA transfected cells.

A: Non-targeting siRNA control B: *HS3ST3A1* siRNA knockdown C: Immunohistochemical negative control (without 10E4 antibody)

Scale bar = 50 μ m

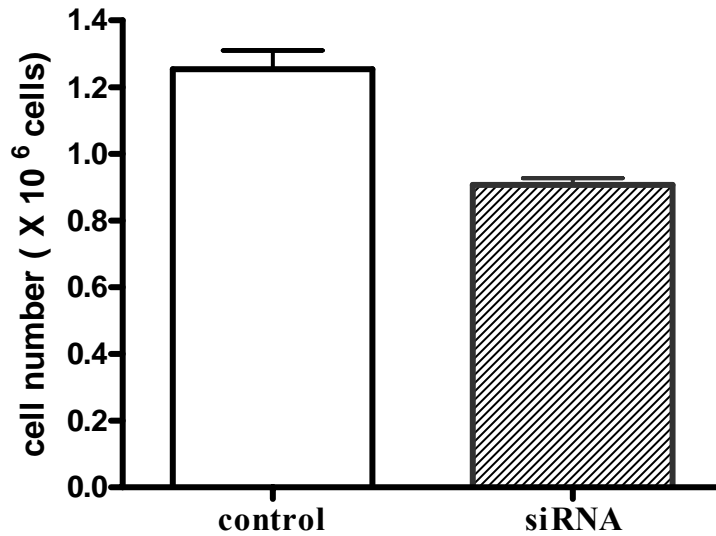


Fig. 4.11. Reduction of *HS3ST3A1* expression inhibited MCF-12A cell proliferation. Direct counting cells 72 hrs post silencing *HS3ST3A1* in MCF-12 cells revealed that cell proliferation was inhibited by 21.64%. Cells were trypsinized and counted at 72 hrs after transfection using a hemacytometer. Experiments were performed in triplicate and in three independent experiments. Results are expressed as mean \pm SD. Student's *t*-test, $**p = 0.0043$

4.7 Reduction of *HS3ST3A1* expression by siRNA in the MCF-12A cells inhibited cell cycle S/G₂ transition.

Cell cycle progress reflects cell proliferation. To confirm the proliferation inhibition in MCF-12A cells and to study which phase of the cell cycle was affected by the suppression of *HS3ST3A1* mRNA expression, cell cycle distribution was examined in MCF-12A cells transfected with siRNA targeting *HS3ST3A1* and scrambled siRNA (control) (Fig. 4.12 and Table 4.2).

After 72 hrs post transfection, the S-phase fraction of the control cells was 28.01% whereas in the siRNA transfected cells S-phase was 38.21%. These mean the cells in S phase increased by 36.42% (Student's *t*-test, $**p < 0.001$). This was accompanied by a decrease of the G₂-M phase cells from 17.68% to 11.47%, about

down 35.13% in G₂-M phase (Student's *t*-test, ***p* < 0.001, **Table 4.2**). These results suggest that the impaired cell proliferation by reduced HSPG synthesis may be due to the delay in the transition from S phase to G₂ phase in cell cycle progression.

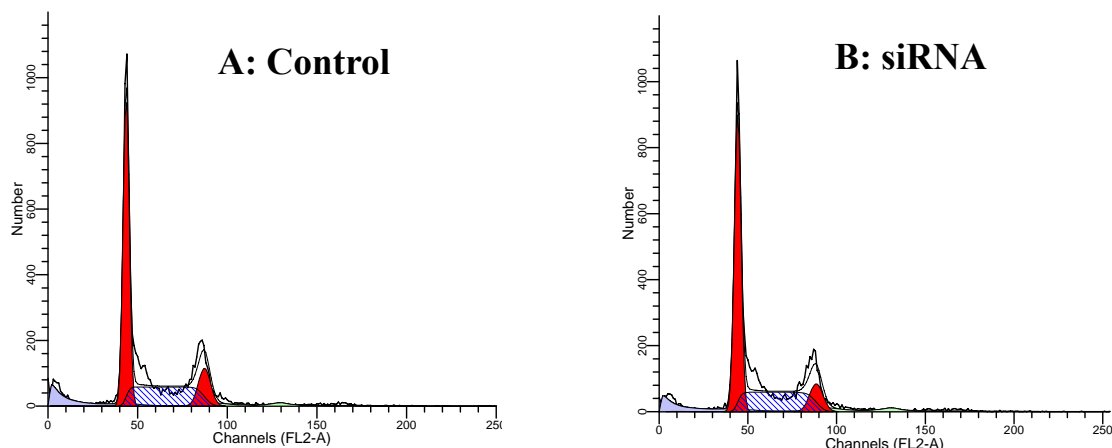


Fig. 4.12 Representative histograms of MCF-12A cell cycle analyzed by ModFit software. A: control cells, B: siRNA silenced cells.

	G ₁	S phase	G ₂
control	54.31 ± 0.83	28.01 ± 1.50	17.68 ± 1.29
siRNA	50.39 ± 1.93	38.21 ± 2.14**	11.47 ± 1.14**

Table 4.3 Reduction of *HS3ST3A1* expression inhibited MCF-12A cell cycle progression. MCF-12A cells were transfected with the siRNA targeting *HS3ST3A1* gene or the control scrambled siRNA. Compared with control, siRNA transfected group increased the percentage at S phase and correspondingly decreased the percentage of cells at G₂/M phase. MCF-12A cells were trypsinized 72 hrs after transfection and stained with propidium iodide in Vindelov's cocktail for 1 hr at 4°C in the dark. The stained cells were analyzed using FACS caliber flow cytometer (Becton Dickinson) with excitation wave-length of 488 nm to determine the percentage of cells in G₁/S and G₂/M. The resulting histograms were analyzed by program MODFIT (Becton Dickinson) for cell distribution in cell cycle phases. Data were expressed as mean ± SEM. N = 6. Student's *t*-test, ** *p* < 0.01

4.8 Knockdown of *HS3ST3A1* expression in MCF-12A cells inhibited cell adhesion to fibronectin and collagen I

Sulphation pattern of proteoglycans is widely known to be involved in cell adhesion to fibronectin, collagen, lamin and vitronectin in the extracellular matrix. To investigate the effect of suppression of *HS3ST3A1* expression on MCF-12A cell adhesion to fibronectin and collagen I, MCF-12A cells were transfected with the siRNA targeting *HS3ST3A1* gene or the control scrambled siRNA for 72 hrs and the cells were re-seeded into fibronectin- and collagen I-coated wells of 96-well plates. The cells were allowed to attach for 30 mins. It was found that the adhesion ability of the siRNA-knockdown cells was significantly impaired on both substrates. **Fig. 4.13** shows that MCF-12A cell adhesion to fibronectin and collagen I was reduced by 21.76% (Student's *t*-test, $**p < 0.01$) and by 16.21% (Student's *t*-test, $**p < 0.01$), respectively. These results demonstrate that the impairment of HSPG synthesis after silencing of *HS3ST3A1* inhibits the adhesion of MCF-12A cells to extracellular matrix substrates.

4.9 Suppression of *HS3ST3A1* expression in MCF-12A cells promoted cell migration *in vitro*.

Acquisition of migration and invasion capacity into the ECM and basement membrane are characteristics of the normal cell developing into malignant cell. To study whether suppression of *HS3ST3A1* expression in MCF-12A cells would influence the migration ability of MCF-12A cells, transwell migration assay were performed. Experimental results revealed that suppressing *HS3ST3A1* expression in

MCF-12A cells rendered the cells migrate faster by ~76.5% compared with the control cells (Student's *t*-test, ** $p < 0.01$, Fig. 14A and B).

4.10 Suppression of *HS3ST3A1* expression increased MCF-12A cell invasive capacity through Matrigel *in vitro*.

The capability of silencing *HS3ST3A1* expression to stimulate MCF-12A cell migration predicts its role in promoting cell invasion, so invasive capacity of MCF-12A cells after reduction the *HS3ST3A1* expression was studied. The results showed that silencing *HS3ST3A1* expression also markedly enhanced MCF-12A cell invasion through Matrigel *in vitro* (Fig. 4.15A and B).

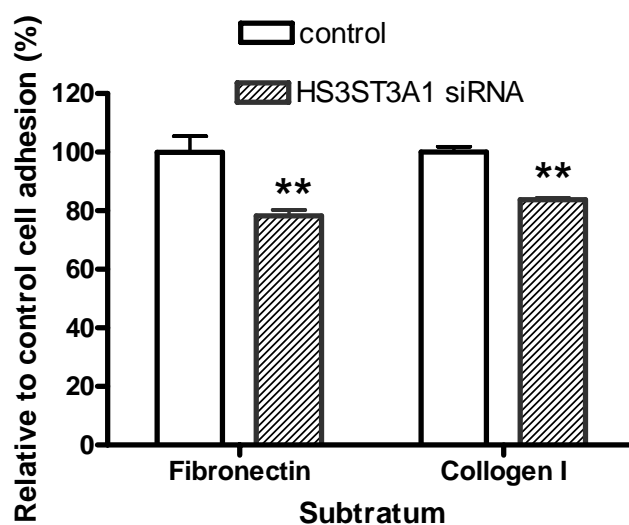
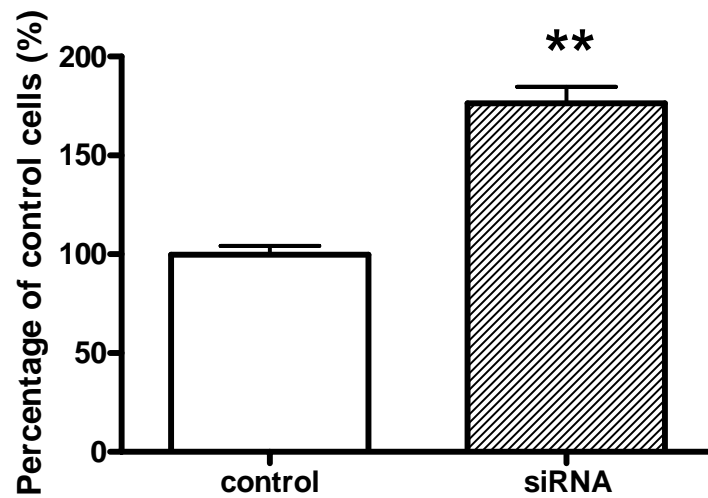


Fig. 4.13. Suppression of *HS3ST3A1* expression decreased MCF-12A cell adhesion to fibronectin and collagen I. 72 hrs post-transfection of the control scrambled-siRNA and siRNA targeting *HS3ST3A1*, MCF-12A cells were trypsinized, harvested and resuspended in DMEM/F12 medium containing 0.1%BSA. 8×10^4 cells/well were re-seeded in DMEM/ F12 medium containing 0.1%BSA in 96-well plates coated with fibronectin and collagen I and allowed to attach for 30min. MTS methods (CellTiter 96® AQueous One Solution Cell Proliferation Assay, MTS, Promega) were used to determine the attached cell number. Data are representative of 3 separate experiments mean \pm SE, N = 8. Student's *t*-test, * $p < 0.05$, ** $p < 0.01$

A



B

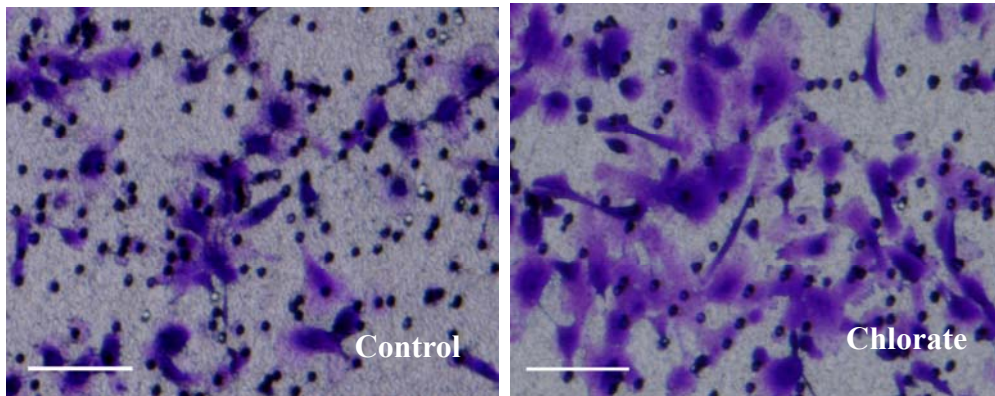
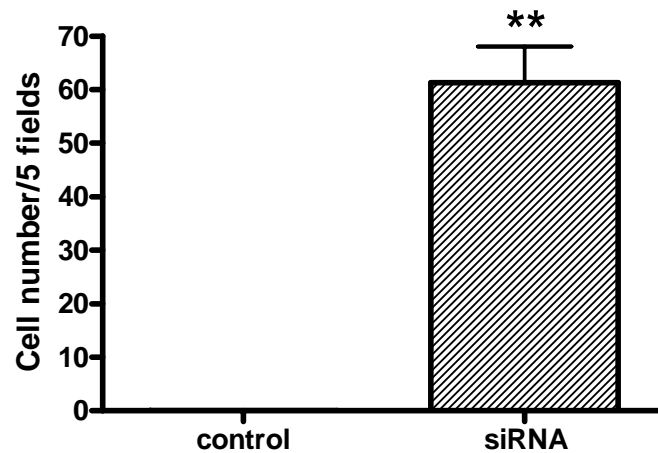


Fig. 4.14 Suppression of *HS3ST3A1* expression in MCF-12A cells promoted cell migration *in vitro*. 72 hrs post-transfection, MCF-12A cells were trypsinized and resuspended in DMEM/F12 medium. 5×10^4 cells/well were re-seeded in DMEM/F12 medium containing 0.1% BSA (Sigma-Aldrich) without FBS in the upper chamber and 15% FBS in DMEM/ F12 medium in the lower chamber was used as chemoattractant. Cells were allowed to migrate 16 hrs. Migrated cells were stained with crystal violet and counted under a microscope. at 100 x magnification (Nikon). Experiments were repeated 3 times each run 2 replicates. (A) Data represent the cell number of five randomly selected microscopic fields from a single chamber. Data are mean \pm SE, N = 5, Student's *t*-test, $**p < 0.01$. (B) Images show representative fields of crystal violet stained MCF-12A cells on the bottom of a transwell insert as captured from a Nikon microscope at 100 \times magnifications. Cell number at the bottom of the chamber was normalized against the control which was set at 100%. Scale bar = 100 μ m.

A



B

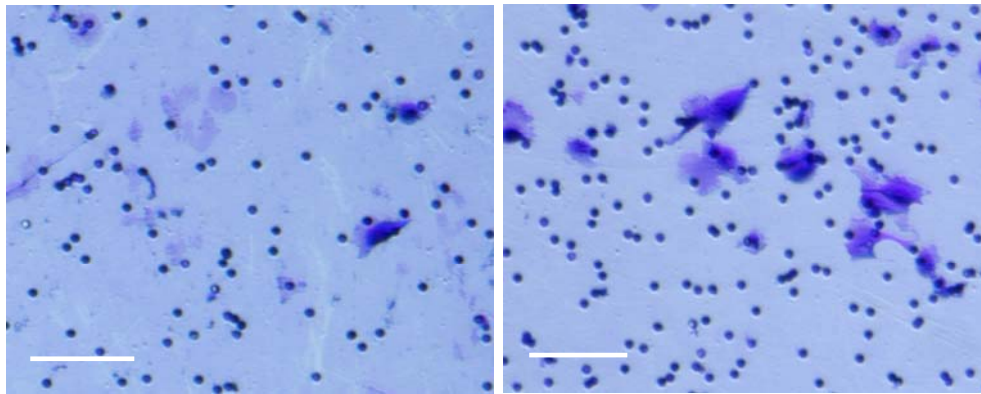


Fig. 4.15. Suppression of *HS3ST3A1* expression increased MCF-12A cell invasion *in vitro*. 72 hrs post-transfection, MCF-12A cells were trypsinized and re-suspended in DMEM/F12 medium. 1×10^5 cells/well were re-seeded in DMEM/ F12 medium containing 0.1% BSA (Sigma-Aldrich) without FBS in the upper chamber and 15% FBS in DMEM/ F12 medium in the lower chamber was used as chemoattractant. Cells were allowed to invade 24 hrs. Invaded cells were stained with crystal violet and counted under a microscope at 100 x magnification (Nikon). Experiments were repeated 3 times each run 2 replicates. (A) Data represent the cell number of five randomly selected microscopic fields from a single chamber. Cell number at the bottom of the chamber was subtracted from the control which was considered as background. Data are mean \pm SE, N = 6, Student's *t*-test, $**p < 0.01$. (B) Images show representative fields of crystal violet stained MCF-12A cells on the bottom of an invasion chamber as captured from a Nikon microscope at 100 \times magnifications. Scale bar = 100 μ m.

Discussion

The present study has shown that expression of *HS3ST3A1* was significantly down-regulated in breast cancer cell lines as well as in cancer tissues compared with their benign counterparts. Knockdown of the expression of *HS3ST3A1* by siRNA inhibited MCF-12A cell growth in culture, reduced its adhesion while increased its migration and invasive capacity *in vitro*, suggesting the possible functions of *HS3ST3A1* in breast growth and tumorigenesis.

Heparan sulphate proteoglycans (HSPGs) are widely distributed on cell surfaces and in extracellular matrix. HSPGs regulate many biological processes by interacting with a variety of proteins including cytokines, extracellular matrix proteins, enzymes, protease inhibitors, growth factors and other molecules (Bernfield *et al.*, 1999; Lander and Selleck, 2000; Iozzo, 2001; Esko and Selleck, 2002; Nakato and Kimata, 2002). The positioning of the negatively charged sulphate groups on the disaccharide units covalently attached to the core protein are important for the specificity of the interactions (Esko and Selleck, 2002; Kusche-Gullberg and Kjellen, 2003). The 3-O-sulphate groups on glucosamine units is supposed to be involved in important biological functions as 3-O sulphation occurs late in the HSPG biosynthesis and in unusual structures (Shworak *et al.*, 1999a). Indeed, one of the most studied enzyme 3-O-sulphotransferase (3-O-ST, now known as 3-O-ST-1, HS3ST1) converts non-anticoagulant heparan sulphate into the anticoagulant heparan sulphate, which is

widely used in clinic and well known as heparin (Petitou and van Boeckel, 2004; Dementiev *et al.*, 2004).

HS3ST3 are type II integral membrane glycoproteins of 406 amino acid residues. *HS3ST3* has two isoforms, *HS3ST3A1* and *HS3STB1* which are widely expressed in human tissues with multiple transcripts (Shukla *et al.*, 1999; Shworak *et al.*, 1999; Liu *et al.*, 1999b). The entire sulphotransferase domain sequence of the *HS3ST3B1* is 99.2% identical to the same region of *HS3ST3A1*, which strongly suggests that these two isoforms may have similar function in the sulphation of HSPG (Liu *et al.*, 1999b).

Recently years, many studies have explored the possible biological functions of the members of 3-O-sulphotransferase (HS3ST) family in cancers. Miyanoto *et al.* (2003) first reported low expression of *HS3ST2* in breast cancers. They observed the average expression level of *HS3ST2* in 37 breast cancers was significantly lower ($p < 0.005$) than that in the non-cancerous samples, although the expression in the non-cancerous tissues was also variable. They also pointed out that the low expression of *HS3ST2* in breast cancer may be due to hypermethylation of the 5'-region of the mRNA of *HS3ST2* as they detected 75 of 85 primary breast cancers (88%) contain hypermethylation in the 5'-region of the mRNA. The authors also found that hypermethylation of this gene also existed in a majority of colon (80%), lung (70%), and pancreas (100%) cancers.

Promoter methylation often results in low expression or silencing of the gene, which is widely believed to be indicative of the specific role of the gene in the tumorigenesis (Siegfried and Cedar, 1997; Jones, 1999; Momparler and Bovenzi,

2000; Toyota and Issa, 2000; Wajed *et al.*, 2001). The findings of promoter methylation of *HS3ST2* and low expression in cancers have raised much interest. Takahashi *et al.* (2004) found promoter hypermethylation of *HS3ST2* in gallbladder carcinoma. Actually, they found *HS3ST2* was the most frequently (72%) methylated gene in gallbladder carcinoma compared with other genes. Such a promoter-methylation-induced low expression of *HS3ST2* was also found more recently in non-small cell lung cancers (Shivapurkar *et al.*, 2007). The low expression of *HS3ST2* gene thus indicates that altered modification of HSPGs by this gene could be involved in cancer development and progression in a broad range of cancers.

Promoter methylation of other 3-OST isoforms has also been studied. Dick *et al.* (2004) reported their findings of the expression of 3-OST isoforms in 69 breast cancers. The authors found that methylation was frequent in the promoters of *HS3ST2* (51%, 40/69), *HS3ST3B* (41%, 28/69), and *HS3ST4*, (45%, 32/69), but rare in *HS3ST1* (1%, 1/69). However, they did not detect promoter methylation in *HS3ST3A*. High levels of methylation and thus a possible low expression of specific 3-O-ST isoforms suggests that HSPGs modified by these enzymes may play an important role in breast carcinogenesis and development.

Though promoter methylation of *HS3ST3A* has not been detected in breast cancer (Dick *et al.*, 2004), the possibility of low expression level of *HS3ST3A* compared with that in normal breast epithelial cells is not excluded. Thus a study on the expression level of *HS3ST3A* in breast cancer cells and normal breast epithelial cells is needed. Such an investigation may give more information on the function of *HS3ST3A* in breast

cancer. Thus expression profile of *HS3ST3* in a normal breast epithelial cell line and four breast cancer cell lines available in our lab were examined. Real-time PCR data showed that expression of one of the isoforms of *HS3ST3*, *HS3ST3A1*, was unanimously reduced, especially in the highly invasive cell line MDA-MB-231 cells compared with that in the normal breast cell line MCF-12A cells. The other isoform *HS3ST3B1* was also down regulated in the MCF-7, T47D and ZR-75-1 cell lines and only slightly up regulated in MDA-MB-231 cells. The expression profile of *HS3ST3A1* in breast cancer cell lines promoted consideration of *HS3ST3A1* expression in breast cancer patients. Thus the mRNA expression of this gene in a panel of 22 corresponding breast normal and cancer tissues was studied by using in situ hybridization. The expression results in the clinical samples were consistent with those in the cell lines.

Till today, most of the functional studies on the *HS3ST3A1* have been limited to biochemical studies, e.g. the substrate specificity. The specific binding sites for glycoprotein gD interaction for herpes simplex virus type 1 (HSV-1) still remain the only known example demonstrating the potential relationship between the formation of a biologically significant motif of HS and expression of *HS3ST3A1* isoform (Liu *et al.*, 1999a; Liu *et al.*, 1999b; Tiwari *et al.*, 2007). Although some of the biological functions of HS3STs in cancers, especially in breast cancer, were also studied and their significance in breast cancer development and progression was also suggested as mentioned above, the causal relationship between the expression of *HS3ST3A1* isoform and breast tumourigenesis is still not clear.

To answer whether this gene exerts its function in the transformation of normal breast cells into cancer cells, siRNA technology was used to knockdown the expression of *HS3ST3A1* in the normal breast epithelial MCF-12A cells to explore the phenotype changes in the cells because the expression of this gene in all of the cancer cell lines was remarkably down-regulated.

Proliferation, adhesion, migration and invasion are key features in tumour cell growth and metastases. It is widely believed that the expression of HS with defined structural properties is essential for those processes. Thus the phenotypic alterations in proliferation, adhesion, migration and invasion after down-regulation of *HS3ST3A1* expression were examined *in vitro*. The findings in this study demonstrated that after knockdown expression of *HS3ST3A1*, MCF-12A cells acquired the properties of malignant cells which include less adhesive to the ECM substrate fibronectin and collagen I as well as enhanced migration and invasion *in vitro*.

Previously Mei *et al.* (2003) reported that repeated treatments of non-cancerous human breast epithelial cells MCF-10A (a similar cell line to MCF-12A cells) with a low dose of a tobacco-specific carcinogen induced malignant transformation of these cells. The transformed cells acquired cancerous properties including increased cell motility and invasion in Matri gel *in vitro* and increased tumourigenicity *in vivo*. It has been demonstrated that increasing invasiveness of cells indicated an increased metastatic potential. Suppression of cell-substrate adhesion has been proposed to correlate with increased motility of cancerous cells (Berx *et al.*, 1995; Sun and Rotenberg, 1999b; Critchley, 2000).

However, in this study, proliferation was retarded in the *HS3ST3A1* silenced cells. It has been reported that overexpression of PKC α in MCF-10A cells results in a significant suppression of cell proliferation but endowed MCF-10A cells with properties consistent with the metastatic phenotype (Sun and Rotenberg, 1999). Similar results were found in oncogenic Ha-Ras overexpression transformed MCF-10A cells which showed a reduce cell proliferation in monolayer cell culture with two times of doubling time compared with that of the control (Zantek *et al.*, 2001), although the transformed cells had malignant phenotypes. In contrast, ectopic expression of oncogenic Ha-Ras in MCF-10A cells induces increased cell proliferation (Basolo *et al.*, 1991; Ochieng *et al.*, 1991). However, overexpression of oncogenic R-Ras2 in MCF-10A cells did not cause any detectable changes in the rate of cell proliferation (Clark *et al.*, 1996). These results taken together indicate that malignantly transformed MCF-10A cells by oncogenic proteins are not necessarily accompanied by increased rate of cell proliferation. Such notion may also be applied in the MCF-12A cells.

To further determine the mechanism by which reduction of *HS3ST3A1* inhibits breast cell growth but promotes its metastasis potential *in vitro*, a systematic analysis of the gene expression profile could be valuable and informative.

As *HS3ST3* plays a role in the notch-signaling pathway in *Drosophila* (Kamimura *et al.*, 2004) and notch-signaling pathway is a well known regulatory network in breast development and tumorigenesis (Nam *et al.*, 2002; Callahan and Egan, 2004; Shi and Harris, 2006), the study on gene expression profile after silencing *HS3ST3A1* in breast

epithelial cells could also reveal whether any pathways are dysregulated by suppression of *HS3ST3A1* in breast carcinogenesis.

In summary, the present study has shown for the first time in mammalian cells that knockdown of the expression of *HS3ST3A1* inhibited breast epithelial cell growth, reduces its adhesion while increases migration and invasive capacity *in vitro*, suggesting the possibility that *HS3ST3A1* function in malignant transformation of breast epithelial cell.

CHAPTER 5

CHAPTER 5 Gene expression profiling by Affymetrix GeneChips in MCF-12A cells after silencing *HS3ST3A1* mRNA

Microarray technology has the ability to simultaneously evaluate gene expression across tens of thousands of genes and thus has revolutionized the fields of molecular biology. To further explore the possible mechanisms for the phenotype changes induced by the transfection of *HS3ST3A1* siRNA, Affymetrix GeneChip analysis was applied in MCF-12A cells following silencing *HS3ST3A1*.

5.1. Assessment of yield, quality and integrity of total RNA obtained from MCF-12A cells.

The success of microarray analysis in determining differential gene expression of thousands of genes is dependent upon the quality and integrity of the starting RNA because the quality of the initial RNA sample is the first step to ensure successful cDNA and cRNA synthesis before microarray hybridization. The quantity and quality of total RNA were first analyzed spectrophotometrically. All the samples had ratio of absorbance at 260/280 more than 1.80. RNA was then further assessed for quality and integrity using Agilent's 2100 Bioanalyzer. Total RNA from cultured MCF-12A cells were analyzed using RNA 6000 LabChip kit. The Agilent 2100 bioanalyzer provides two visual representations of each sample, an electropherogram (**Fig. 5.1A**) and a gel-like image (**Fig. 5.1B**).

The Agilent Bioanalyzer is one of the most effective tools for characterizing

RNA integrity by capillary microelectrophoresis, in which RNA degradation is indicated by an altered 28S/18S ribosomal RNA (rRNA) signal ratio. Using an Agilent Bioanalyzer, typical indications of high quality, intact total RNA samples are electropherograms showing distinct 18S and 28S rRNA subunit spikes, with a ratio of $28S/18S > 1.80$ with flat baselines.

The Agilent Bioanalyzer also adopts RIN software algorithm RNA Integrity Number, which allows for the quality classification of total RNA, based on a numbering system from 1 to 10, with 1 being the most degraded profile and 10 being the most intact. Analysis results of the total RNA showed all the sample RNA had sharp peaks at 18S and 28S with the 28S/18S ratio around 2.0 (1.8~2.3), and RNA number 10 (**Fig. 5.1A and B**). This ratio, along with the contours of the electropherogram and the RIN value led to the conclusion that the RNA samples were undegraded and of high quality.

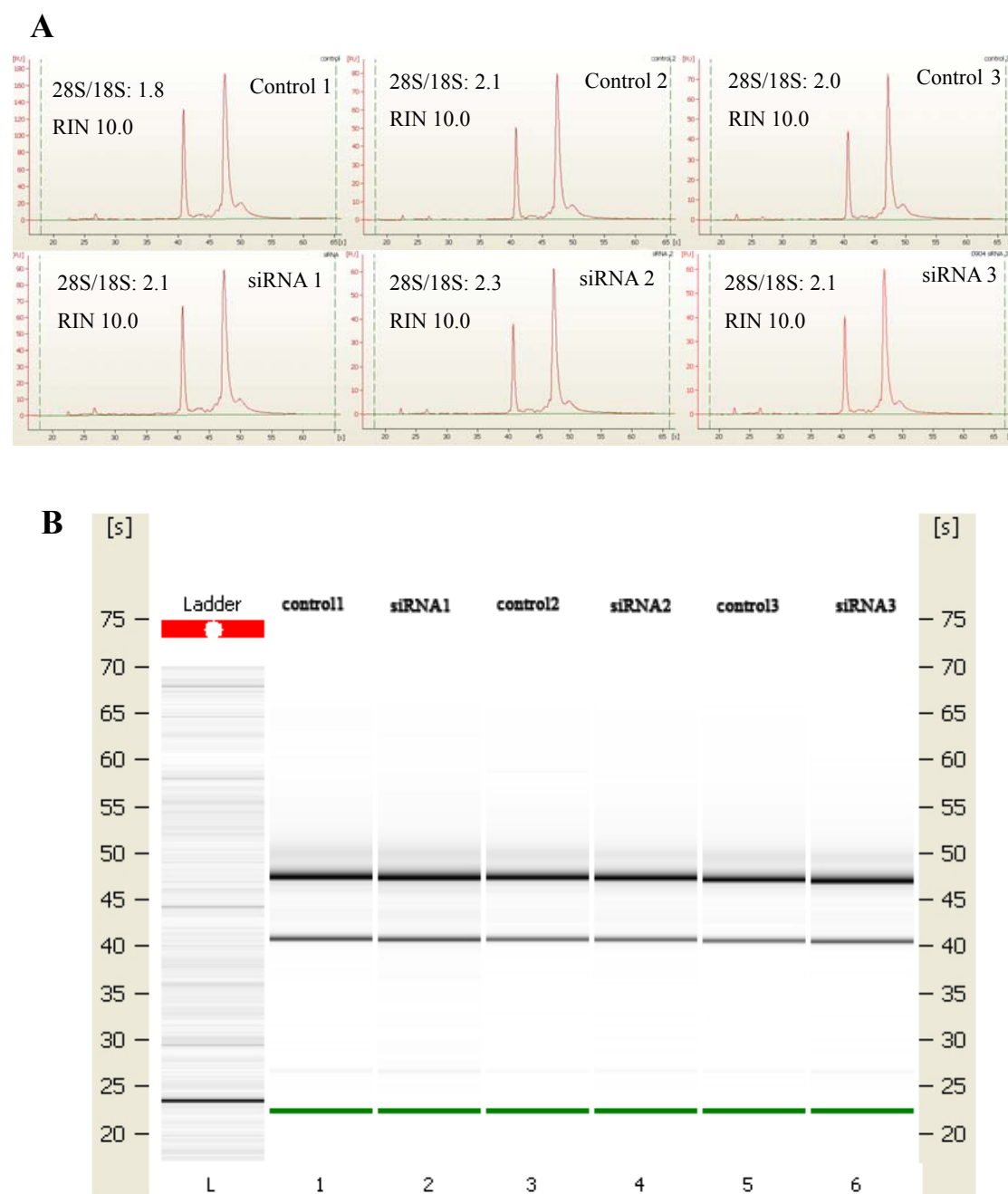


Fig. 5.1. Analysis of total RNA of MCF-12A cells after silencing *HS3ST3A1* expression by using RNA 6000 LabChip kit. The Agilent 2100 bioanalyzer provides two visual representations of each sample, an electropherogram (A) and a gel-like image (B). Prominent bands can be seen as sharp peaks at 18S and 28S indicating highly intact RNA. MCF-12A cells were transfected with the siRNA targeting *HS3ST3A1* gene or the control scrambled siRNA for 48 hrs and the total RNA was extracted by RNeasy mini kit as in Chapter 2 *Materials and Methods*.

5.2. Assessment of yield and quality / integrity of total cRNA and fragmented cRNA

The preparation of the target cRNA is a multi-step procedure that requires total RNA isolation, first strand cDNA synthesis with an oligo(dT) T7 primerr, second-strand cDNA synthesis, and a final step of *in vitro* transcription using T7 RNA polymerase and biotinylated ribonucleotides. The cRNA was further fragmented into 25~200bp oligonucleotides. These enzymatic reactions are sensitive to the quality of the starting RNA, the intermediate cDNA template, the occurrence of endogenous priming. The quality of the unfragmented cRNA and the fragmented cRNA were analyzed by using the Agilent Bioanalyzer.

Bioanalyzer analysis showed the unfragmented cRNA was quite satisfactory (**Fig.5.2A and B**) with the median size around 1500bp. The size of the resultant fragmented cRNA was about 25~200bp indicating good quality for microarray hybridization (**Fig.5.3A and B**).

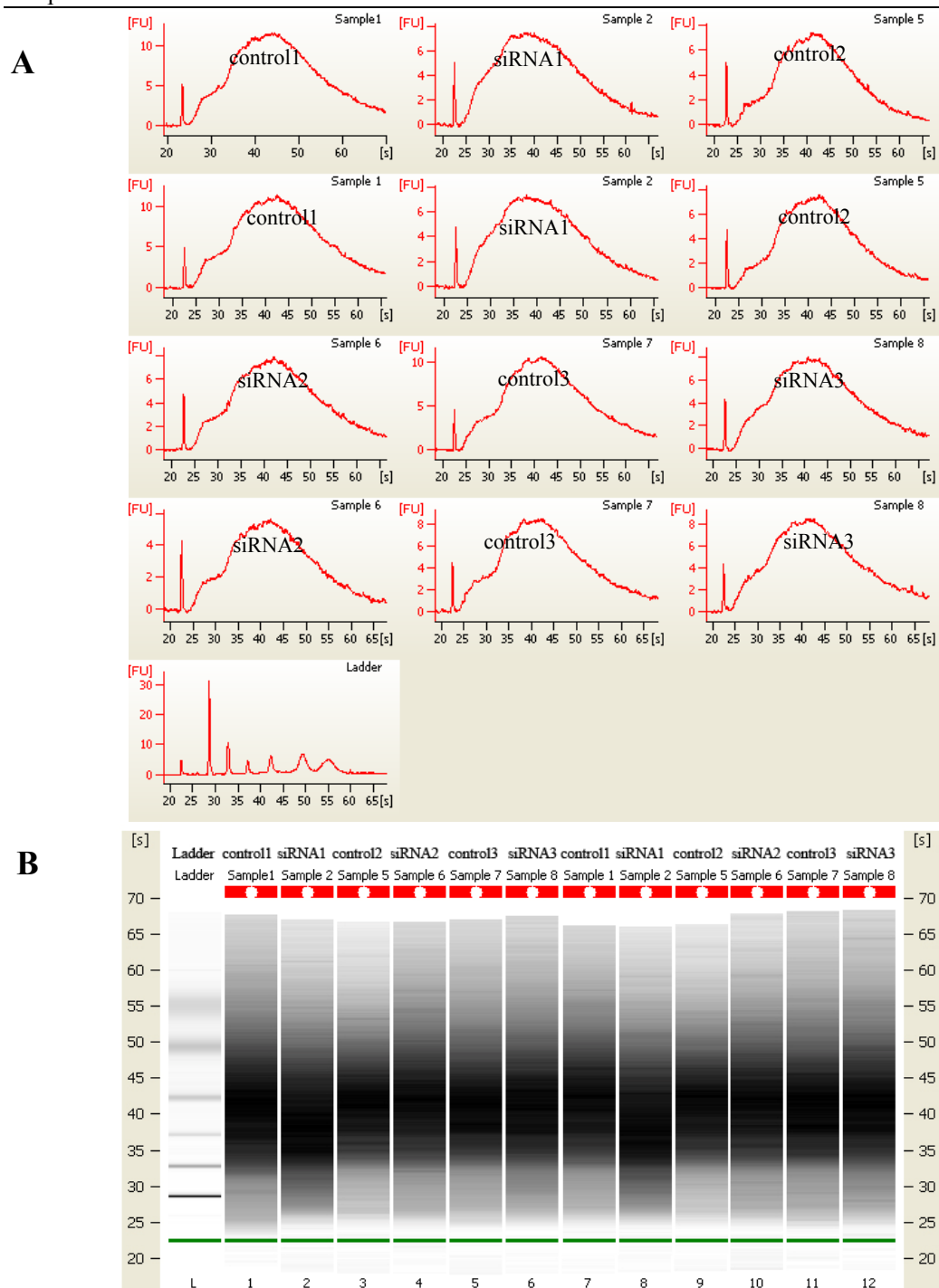


Fig. 5.2. Analysis of unfragmented cRNA quality and size distribution. 1 μ l unfragmented cRNA were analyzed using the RNA 6000 LabChip kit by Agilent 2100 Bioanalyzer. Samples run in duplicates (A). Lowest frame of the panel shows the classic output of RNA 6000 ladder (the RNA 6000 Ladder, Cat# 7152; Ambion) with six RNA peaks (50 (internal marker), 200, 500, 1,000, 2,000, 4,000, and 6,000 bp from left to right). The resulting electropherogram shows the classic output of high quality unfragmented cRNA samples with median size around 1500 bp. The median size was determined by selecting the point (nt) at which separating 50% of the area in the electropherogram against the ladder. Data is displayed as electropherograms (A) and a gel-like image (B).

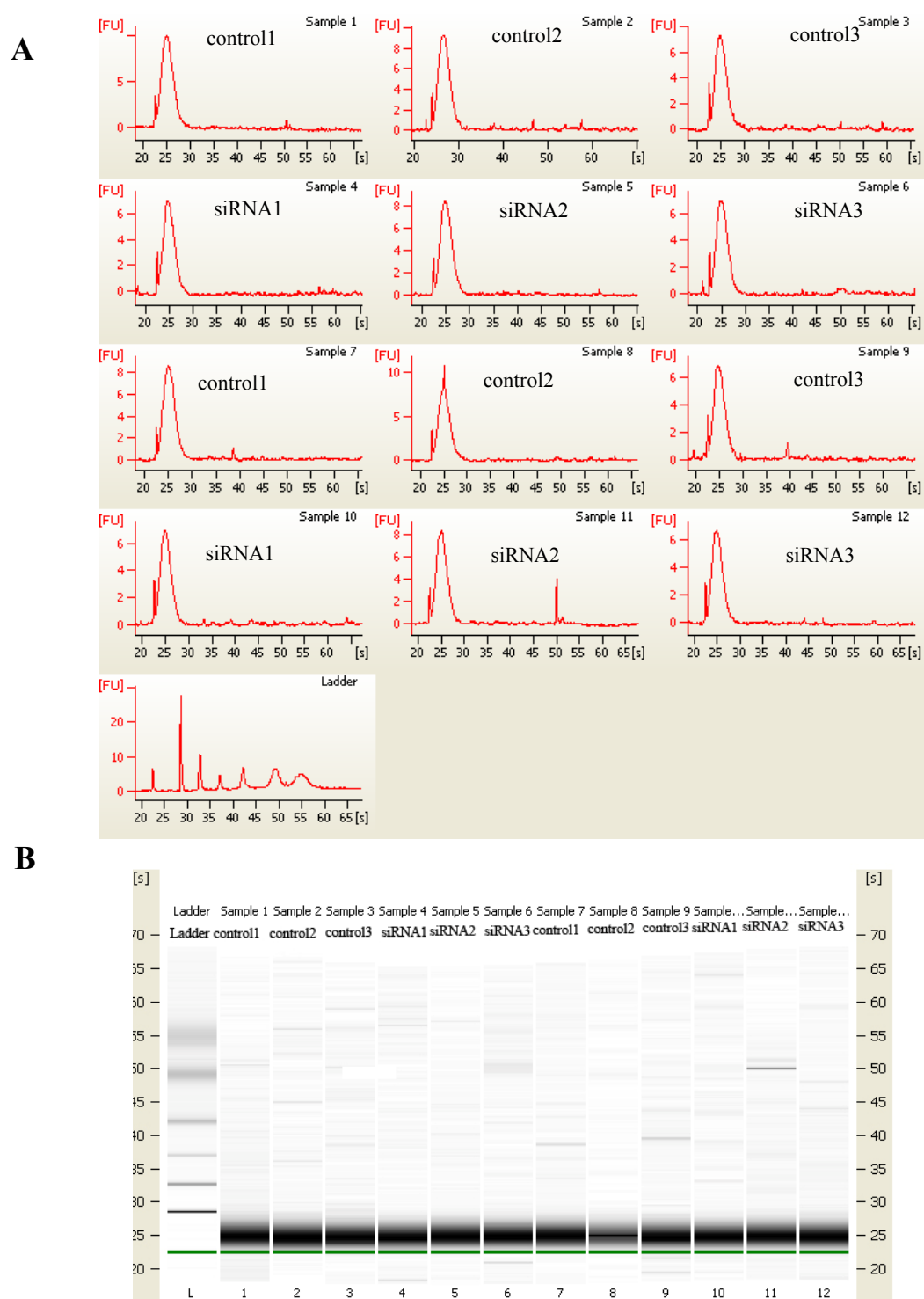


Fig.5.3. Analysis of fragmented cRNA quality and size. 1 μ l fragmented cRNA were analyzed using the RNA 6000 LabChip kit by Agilent 2100 Bioanalyzer.

Lowest frame of the panel A shows the classic output of RNA 6000 ladder (the RNA 6000 Ladder, Cat# 7152; Ambion) with six RNA peaks (50 (internal marker), 200, 500, 1,000, 2,000, 4,000, and 6,000 bp from left to right). The resulting electropherogram shows the classic output of high quality fragmented cRNA samples with size about 25~200 bp. Data is displayed as electropherograms and gel-like image.

Test array hybridization: Fragmented cRNA was hybridized to Affymetrix Test chips (Affymetrix, Santa Clara, CA, USA) to verify the quality and IVT labeling efficiency of cRNA. On these chips, a number of house keeping genes (e.g. β -actin and GAPDH) are controlled with a set of 3 probes directed toward the 5-prime, middle, and 3-prime region of the transcript. For good quality cRNA, the signal ratio between the 3'- and 5'- of these genes should not exceed 3. The 3'/5' ratio was less than 2 in this project as shown in Table 5.1. These results showed that the cRNA quality was quite satisfactory.

Table 5.1 cRNA quality verification on Test Chips

	3'/5' ratio					
	control1	control2	control3	siRNA1	siRNA2	siRNA3
β -actin	1.46	1.63	1.80	1.60	1.47	1.75
GAPDH	1.11	1.27	1.00	1.16	1.31	1.16

5.3 Analysis of microarray data

To check the quality of the data from the hybridizations, the hybridization data acquired from the Affymetrix MAS 5.0 (GCOS) were first analyzed by using two-dimensional scatterplot. A scatter-plot summary of the 6 microarray expression data (54,676 probeset) including all genes represented on the HU133 Plus 2.0 GeneChip is shown in **Fig. 5.4**. The consistent location of average expression values of the control groups and the siRNA groups along the first diagonal (the line for $x = y$ in **Fig. 5.4**) indicates that there was no systematic bias between control and siRNA experimental groups. As expected, a higher variance is seen at lower expression levels, most of them Absent-Absent call, than at higher ones, which were Present- Present call (The

absolute analysis generated by GCOS revealed Present calls were between 37.03% ~38.99% on all of the 6 arrays). **Fig. 5.4** also indicates that, although the expression levels of most genes do not differ between the control and siRNA groups, a substantial number of genes are differentially expressed between the two groups.

The data from the arrays were then extracted/normalized using four different analytical softwares (MAS5, dCHIP, RMA and Genespring). The differentially expressed probe sets (genes) list was generated by the selection criteria in each software as in Chapter 2 Materials and Methods. Only those genes that pass the selection criteria in each software were selected. The overlapped gene list was selected by comparing the 4 gene lists produced from the analysis softwares. Venn diagrams were generated to visualize gene probes that were commonly selected by these four analysis software packages. **Fig. 5.5** shows the experimental design and Venn diagram of differentially expressed genes among the four different software packages. It can be found from **Fig. 5.5**, MAS5 analysis showed 592 probes, dChip analysis showed 877 probes, RMA analysis showed 1216 probes and GeneSpring analysis showed 648 probes. The overlapped (common expressed) probe sets among the 4 software analysis was 213 probes, with 70 probes up-regulated and 143 probes down-regulated (or 186 genes with 63 up-regulated and 123 down-regulated) (**Table 5.2**).

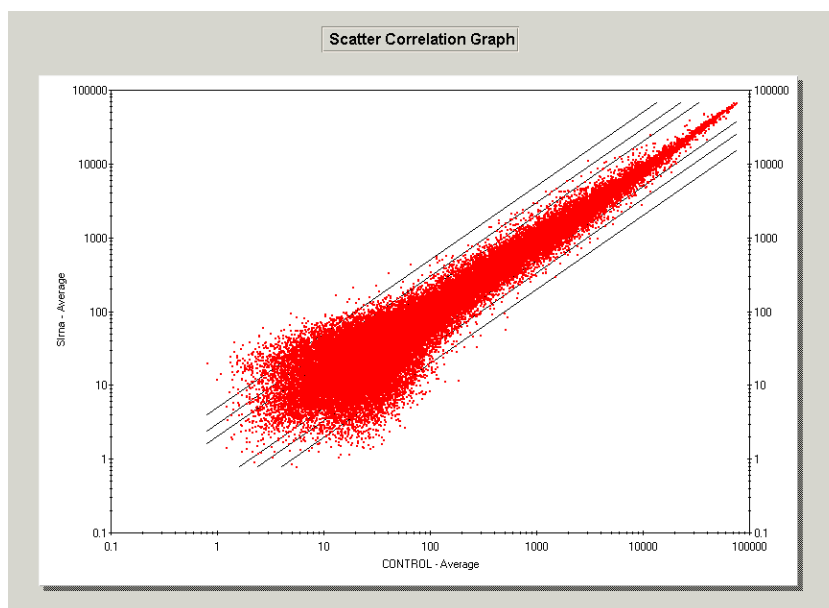


Fig. 5.4. Representative two-dimensional scatter-plot of microarray hybridization data. Linear scatter plot of normalized average gene expression intensity measured from the three control hybridizations and the average gene expression intensity from the three siRNA transfection hybridizations. Control values (x-axis) were plotted against the siRNA values (y-axis). Genes with similar average expression levels appear along the first diagonal (the line $y=x$); genes with expression levels that are different in the two groups appear above and below this line, respectively. The parallel green lines mark the limits for two-fold, three-fold and five-fold differences, respectively.

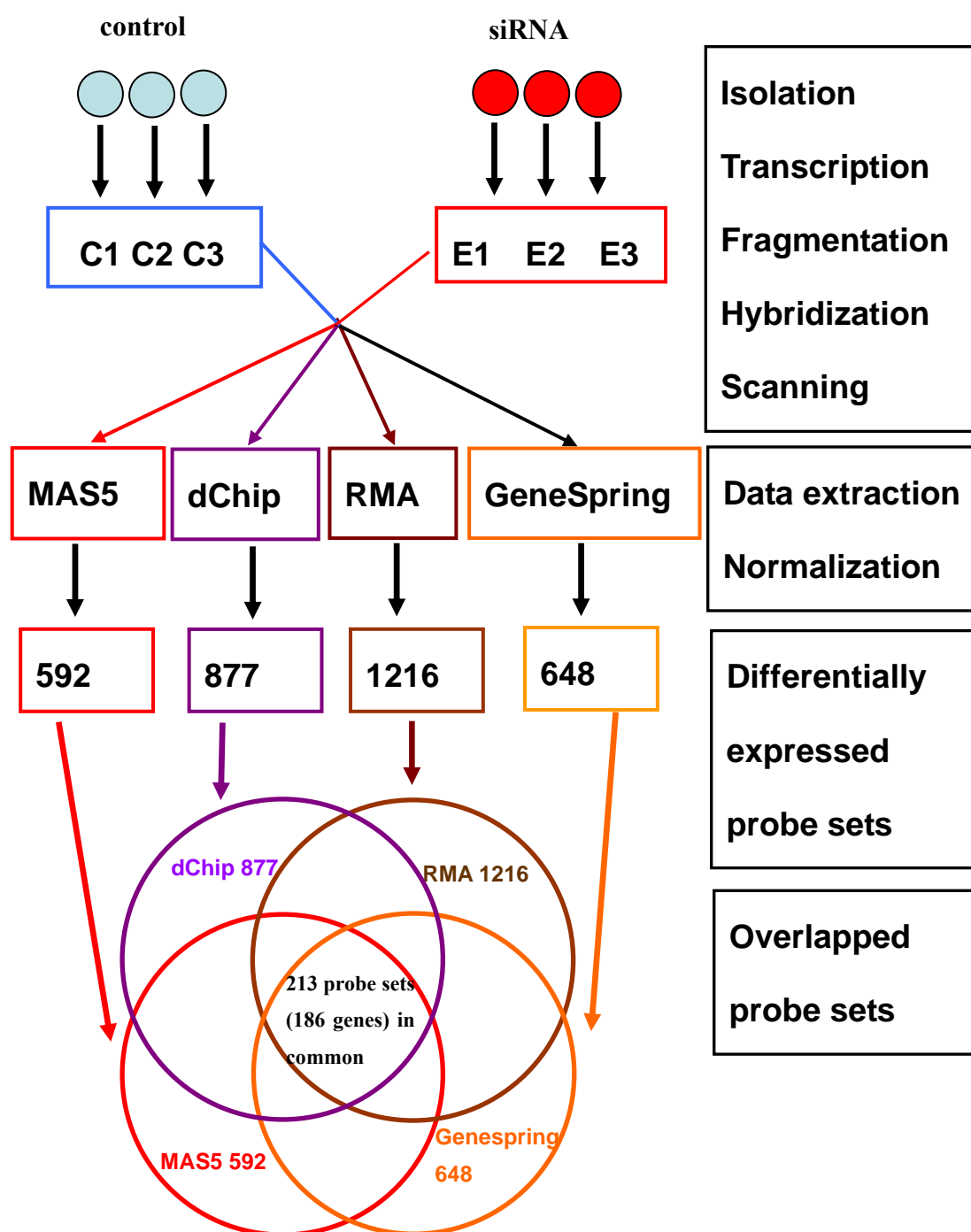


Fig. 5.5. Experimental design and comparison of the overlapped probesets among four analysis softwares. RNA samples from three controls and three siRNA silenced MCF-12A cell cultures were analyzed on Affymetrix GeneChip HU133 plus 2.0. The data from the arrays were then extracted/normalized using four different analytical softwares (MAS5, dCHIP, RMA and Genespring). The total number of differentially expressed genes revealed by each software is indicated. The overlapped genes list was selected by comparing the 4 gene lists produced in each software represented in the intersecting segments of the Venn diagram.

5.4 Validation of microarray expression data by real-time PCR

The reliability of microarray expression data was independently verified by the use of real-time PCR of the mRNAs used in the microarray experiments. Quantitative real-time RT-PCR were done for 80 genes (**Table 5.4**), among them, 57 genes (**Table 5.5**) was selected from the common expressed gene list (213 probe sets, 186 genes, see **Table 5.2 and 5.3**), and 23 genes (**Table 5.6**) were randomly selected. 55 of the 57 genes (96.5%) that were selected from the common expressed gene list were confirmed to be the same regulated direction after silencing *HS3ST3A1* in MCF-12A cells. Among the 23 randomly selected genes, 21 genes (91.3%) were validated to be the same regulated direction. The four genes that showed opposition regulation direction between the real-time PCR and the microarray data were *HIST1H1C*, *HIST1H4H*, *HIST1H2AE*, and *HIST2H2BE*. All of them were Histone isoforms. To make a statistical inference about the validation rate by real-time PCR for genes of 2-fold or expression change obtained by microarray analysis, a confidence interval was calculated according to the following formula: where $Sp = \sqrt{pq/n}$, p = percentage of genes validated, $q = 1 - p$, $\mu_{0.05} = 1.96$, n = total population size (number of 2-fold change genes identified in microarray analysis). The present microarray analysis revealed a total of 186 genes (213 probe sets) with expression changes >2-fold. RT-PCR analysis confirmed the microarray results in 76 of the 80 genes analyzed (95%). The confidence interval for all the 186 genes to be verifiable was $0.919 \leq p \leq 0.981$. Hence, statistically there was 95% confident that 91.9–98.1% of the genes with

2-fold change or above can be validated by real-time RT-PCR. Overall, quantitative real-time PCR showed quite similar regulation trends compared with the data recorded by the Affymetrix U133 plus 2.0 Genechip Arrays. Most importantly, microarray data showed that *HS3ST3A1* itself was down-regulated (MAS5 -3.98, dChip -3.25, Genespring -4.12, and RMA -6.19) which is another evidence to show the reliability of microarray results. When the calculation of fold differences by the two methods in the samples are compared, most of the cases are reminiscent but not equal (Leo *et al.*, 2005). Because of a much more precise detection of real-time PCR, it is considered that the real-time PCR results are much reliable. **Fig. 5.6** presents the fold changes in the expression of nine example genes after comparative analyses using real-time PCR and microarray expression analysis.

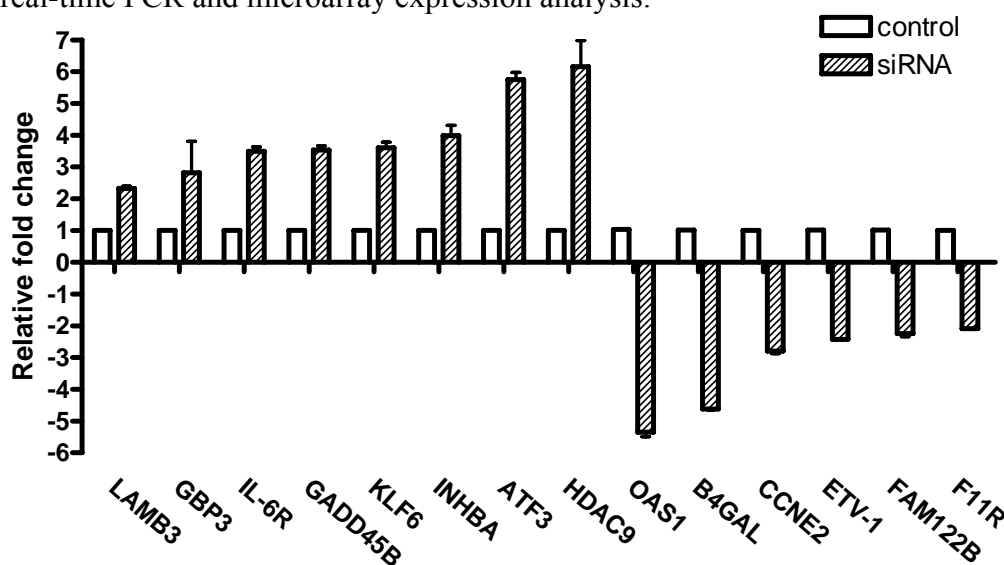


Fig. 5.6. Validation of mRNA expression of selected 14 gene examples by quantitative real-time PCR for microarray data. MCF-12A cells were transfected with control siRNA or *HS3ST3A1* siRNA for 48 hrs. RNA was re-isolated from 3 replicate experiments. mRNAs expression level was determined by semi-quantitative real-time PCR by using β -actin as the reference gene for normalization. Histograms represent the relative expression level in the cells. Data are 3 separate experiments mean \pm SD. Note: Overall the validation data showed the same trend observed in the microarray analysis (also see Table 5.5 and 5.6).

Table 5.2 63 genes significantly up-regulated by *HS3ST3A1* silencing in MCF-12A cells (threshold 2 fold change) with functional categories.

Function	Gene Symbol	Gene Name	Entrez ID
Apoptosis	PPP1R15A	protein phosphatase 1, regulatory (inhibitor) subunit 15A	U83981
	TNFRSF25	tumor necrosis factor receptor superfamily, member 25	AF026071
Cell cycle	CYLD	cylindromatosis (turban tumor syndrome)	BE046443
	HDAC9	histone deacetylase 9	NM_014707
	MDM2	Mdm2, transformed 3T3 cell double minute 2	NM_002392
	SESN2	sestrin 2	AL136551
Cell-ECM communication	ARHGAP27	Rho GTPase activating protein 27	AI769587
	C20orf161	chromosome 20 open reading frame 161	CA447177
	DGKQ	diacylglycerol kinase, theta 110kDa	N45308
	DUSP2	dual specificity phosphatase 2	NM_004418
	FLJ20186	hypothetical protein FLJ20186	BE676248
	FSD1L	fibronectin type III and SPRY domain containing 1-like	AI970348
	GEM	GTP binding protein overexpressed in skeletal muscle	NM_005261
	GPSM1	G-protein signalling modulator 1 (AGS3-like, <i>C. elegans</i>)	AI242661
	HSPG2	heparan sulfate proteoglycan 2 (perlecan)	M85289
	IL6R	interleukin 6 receptor	NM_000565
	LAMB3	laminin, beta 3	L25541
	PILRB	paired immunoglobulin-like type 2 receptor beta	NM_013440
	PVT1	Pvt1 oncogene homolog, MYC activator (mouse)	BG200951
	Transcription	ATF3	activating transcription factor 3
ETS1		v-ets erythroblastosis virus E26 oncogene homolog 1 (avian)	BC017314
EZH1		enhancer of zeste homolog 1 (<i>Drosophila</i>)	AB002386
HABP4		hyaluronan binding protein 4	AK025144
HIC2		hypermethylated in cancer 2	AL043112
JMJD2B		jumonji domain containing 2B	AW237172
KLF6		Kruppel-like factor 6	AB017493
ZNF282		zinc finger protein 282	AW130128
Metabolism			
Protein metabolism	DNAJB2	DnaJ (Hsp40) homolog, subfamily B, member 2	NM_006736
	PTPN21	protein tyrosine phosphatase, non-receptor type 21	X79510
	STK40	serine/threonine kinase 40	BC005169
	USP35	ubiquitin specific peptidase 35	AB037793
	YOD1	YOD1 OTU deubiquinating enzyme 1 homolog (<i>S. cerevisiae</i>)	AF090896

Table 5.2 63 genes significantly up-regulated by *HS3ST3A1* silencing in MCF-12A cells (threshold 2 fold change) with functional categories.

Function	Gene Symbol	Gene Name	Entrez ID
Lipid metabolism			
	PRKAB2	protein kinase, AMP-activated, beta 2 non-catalytic subunit	AL552001
Nucleotide metabolism			
	C20orf194	chromosome 20 open reading frame 194	AI498144
	HIST1H1C	histone 1, H1c	BC002649
	HIST1H2AC	histone 1, H2ac	AL353759
	HIST1H2BC	histone 1, H2bc	NM_003526
	HIST1H4H	histone 1, H4h	NM_003543
	POLG	polymerase (DNA directed), gamma	NM_002693
	PSPC1	paraspeckle component 1	NM_018282
	PTBP2	polypyrimidine tract binding protein 2	NM_021190
	SFRS7	splicing factor, arginine/serine-rich 7, 35kDa	AA524053
	STX1A	syntaxin 1A (brain)	NM_004603
	ZXDC	ZXD family zinc finger C	NM_025112
Others			
Stress			
	OR5AU1	ribonuclease, RNase A family, 7	AK023343
	RNASE7	ribonuclease, RNase A family, 7	AJ131212
	SQSTM1	sequestosome 1	N30649
Iron binding			
	ZDHHC11	zinc finger, DHHC-type containing 11	AF267859
Unknown			
	C1orf54	chromosome 1 open reading frame 54	NM_024579
	C6orf141	chromosome 6 open reading frame 141	NM_153344
	C8orf58	chromosome 8 open reading frame 58	AL519427
	C14orf78	chromosome 14 open reading frame 78	AI935123
	DKFZp451A211	DKFZp451A211 protein	BC036906
	FAM46B	family with sequence similarity 46, member B	AA531023
	FAM54B	family with sequence similarity 54, member B	AL512766
	FLJ10404	hypothetical protein FLJ10404	NM_019057
	GRSF1	Transcribed locus	AI075999
	JOSD3	Josephin domain containing 3	AF275800
	LOC388796	hypothetical LOC388796	AA827892
	LOC440248	hect domain and RLD 2 pseudogene 2	AB002391
	SETD4	SET domain containing 4	NM_017438
	SH3TC1	SH3 domain and tetratricopeptide repeats 1	NM_018986
	TMEM40	transmembrane protein 40	NM_018306

Table 5.3 123 genes significantly down-regulated by *HS3ST3A1* silencing in MCF-12A cells (threshold 2 fold change) with functional categories.

Function	Gene Symbol	Gene Name	Entrez ID
Apoptosis			
	BCL2L12	BCL2-like 12 (proline rich)	AF289220
	SNCA	synuclein, alpha (non A4 component of amyloid precursor)	BG260394
Cell growth			
	EMP2	epithelial membrane protein 2	AV686514
	TMEM97	transmembrane protein 97	BF038366
	VANGL1	vang-like 1 (van gogh, Drosophila)	NM_024062
Cell cycle			
	BARD1	BRCA1 associated RING domain 1	NM_000465
	BRCA1	breast cancer 1, early onset	NM_007295
	BRRN1	barren homolog 1 (Drosophila)	D38553
	CCNE2	cyclin E2	NM_004702
	CDC2	cell division cycle 2, G1 to S and G2 to M	NM_001786
	CDC6	CDC6 cell division cycle 6 homolog (S. cerevisiae)	U77949
	CDCA3	cell division cycle associated 3	NM_031299
	DCC1	defective in sister chromatid cohesion homolog 1	NM_024094
	E2F5	E2F transcription factor 5, p130-binding	U15642
	MCM10	MCM10 minichromosome maintenance deficient 10 (S. cerevisiae)	NM_018518
	MND1	meiotic nuclear divisions 1 homolog (S. cerevisiae)	AY028916
	NBL1	neuroblastoma, suppression of tumorigenicity 1	NM_005380
	PLK4	polo-like kinase 4 (Drosophila)	NM_014264
	PRC1	protein regulator of cytokinesis 1	NM_003981
	SPBC24	spindle pole body component 24 homolog (S. cerevisiae)	AI469788
	WEE1	WEE1 homolog (S. pombe)	X62048
Cell-ECM communication			
	ARHGAP18	Rho GTPase activating protein 18	BE644830
	ASAM	adipocyte-specific adhesion molecule	BF056275
	CLDND1	claudin domain containing 1	BC013610
	DST	dystonin	AL096710
	EVA1	epithelial V-like antigen 1	BF437750
	F11R	F11 receptor	AF191495
	FZD2	frizzled homolog 2 (Drosophila)	L37882
	IFNAR1	interferon (alpha, beta and omega) receptor 1	AA811138
	IGSF3	immunoglobulin superfamily, member 3	AB007935
	IL1B	interleukin 1, beta	NM_000576
	KLHL5	kelch-like 5 (Drosophila)	AK002174
	NMU	neuromedin U	NM_006681
	OIP5	Opa interacting protein 5	BE045993
	RAB22A	RAB22A, member RAS oncogene family	N95443
	RAB38	RAB38, member RAS oncogene family	NM_022337
	RAB7L1	RAB7, member RAS oncogene family-like 1	BC002585
	SNTB2	CDNA clone IMAGE:5263917	AI695684
	SSX2IP	synovial sarcoma, X breakpoint 2 interacting protein	R52678

Table 5.3 123 genes significantly down-regulated by *HS3ST3A1* silencing in MCF-12A cells (threshold 2 fold change) with functional categories.

Function	Gene Symbol	Gene Name	Entrez ID
Transcription			
	ETV1	ets variant gene 1	BE881590
	GPR177	G protein-coupled receptor 177	AA775681
	LHX6	LIM homeobox 6	NM_014368
	MYST2	MYST histone acetyltransferase 2	NM_007067
	PIR	pirin (iron-binding nuclear protein)	NM_003662
	SIX4	sine oculis homeobox homolog 4 (Drosophila)	AI554514
	SURB7	SRB7 suppressor of RNA polymerase B homolog (yeast)	AI688580
	TMPO	thymopoietin	AW272611
	TWIST2	twist homolog 2 (Drosophila)	AI086614
	WDHD1	WD repeat and HMG-box DNA binding protein 1	AW772140
Metabolism			
Protein metabolism			
	ABHD7	abhydrolase domain containing 7	AI807532
	ASPH	aspartate beta-hydroxylase	AF306765
	LACTB2	lactamase, beta 2	BC000878
	RNF20	ring finger protein 20	AK022532
Carbohydrate metabolism			
	B4GALT6	UDP-Gal:betaGlcNAc beta 1,4- galactosyltransferase, polypeptide 6	BG503479
	EXTL2	exostoses (multiple)-like 2	AF000416
	FUT1	fucosyltransferase 1 (galactoside 2-alpha-L-fucosyltransferase, H blood group)	AI417362
	GNS	glucosamine (N-acetyl)-6-sulfatase (Sanfilippo disease IIID)	AW167793
	HS3ST3A1	heparan sulfate (glucosamine) 3-O-sulfotransferase 3A1	NM_006042
	SLC35D1	solute carrier family 35 (UDP-glucuronic acid/UDP-N-acetylgalactosamine dual transporter), member D1	AI769637
Lipid metabolism			
	ACSL3	acyl-CoA synthetase long-chain family member 3	NM_004457
	CPOX	coproporphyrinogen oxidase	NM_000097
	MLSTD2	male sterility domain containing 2	N63551
	PIGK	phosphatidylinositol glycan, class K	AI275605
	PTGS1	prostaglandin-endoperoxide synthase 1	NM_000962
	SGPL1	sphingosine-1-phosphate lyase 1	AB033078
Nucleotide metabolism			
	ALG9	asparagine-linked glycosylation 9 homolog	NM_024740
	ASF1B	ASF1 anti-silencing function 1 homolog B (<i>S. cerevisiae</i>)	NM_018154
	ATAD2	ATPase family, AAA domain containing 2	AI139629
	CTDSPL	CTD (carboxy-terminal domain, RNA polymerase II, polypeptide A) small phosphatase-like	NM_005808
	DHFR	dihydrofolate reductase	AI144299
	FIGNL1	figetin-like 1	NM_022116
	FLJ20273	RNA-binding protein	NM_019027
	GINS1	GINS complex subunit 1 (Psf1 homolog)	NM_021067
	GINS2	GINS complex subunit 2 (Psf2 homolog)	BC003186
	HELLS	helicase, lymphoid-specific	NM_018063
	POLE2	polymerase (DNA directed), epsilon 2 (p59 subunit)	NM_002692
	RBM18	RNA binding motif protein 18	AA167623
	SLC29A1	solute carrier family 29 (nucleoside transporters), member 1	AF079117
	SNRPD1	small nuclear ribonucleoprotein D1 polypeptide 16kDa	NM_006938
	SR140	U2-associated SR140 protein	AB002330

Table 5.3 123 genes significantly down-regulated by *HS3ST3A1* silencing in MCF-12A cells (threshold 2 fold change) with functional categories.

Function	Gene Symbol	Gene Name	Entrez ID
Transport			
	ATP10D	ATPase, Class V, type 10D	AI478147
	ATP11C	ATPase, Class VI, type 11C	BF475862
	DBNDD2	dysbindin (dystrobrevin binding protein 1) domain containing 2	NM_018478
	KCNK1	potassium channel, subfamily K, member 1	NM_002245
	PDCL	phosducin-like	AF031463
	SLC16A14	solute carrier family 16 (monocarboxylic acid transporters), member 14	R15072
	SLC16A7	solute carrier family 16 (monocarboxylic acid transporters), member 7	NM_004731
	SLC35A4	solute carrier family 35, member A4	BE618656
	XK	X-linked Kx blood group (McLeod syndrome)	NM_021083
Others			
Stress			
	BLM	Bloom syndrome	NM_000057
	SERPINA1	serpin peptidase inhibitor, clade A (alpha-1 antiproteinase, antitrypsin), member 1	NM_000295
	SQSTM1	sequestosome 1	N30649
Iron binding			
	CALU	calumenin	NM_001219
	KLHL23	kelch-like 23 (<i>Drosophila</i>)	BE326381
	TPD52	tumor protein D52	AI632972
	VSNL1	visinin-like 1	NM_003385
	ZDHHC23	zinc finger, DHHC-type containing 23	AW003367
Protein binding			
	ANKRD32	ankyrin repeat domain 32	AL136560
	ANTXR1	anthrax toxin receptor 1	AF279145
	KIAA1794	KIAA1794	BG403615
	MOBK1B	MOB1, Mps One Binder kinase activator-like 1B (yeast)	AK023321
	SLITRK5	SLIT and NTRK-like family, member 5	AW449813
Unknow			
	C11orf75	chromosome 11 open reading frame 75	NM_020179
	C16orf75	hypothetical protein MGC24665	AW138157
	C9orf40	chromosome 9 open reading frame 40	NM_017998
	CCDC99	coiled-coil domain containing 99	AF269167
	CPNE8	copine VIII	AI765180
	DKFZP761M1511	hypothetical protein DKFZP761M1511	AK026748
	DPY19L1	dpy-19-like 1 (<i>C. elegans</i>)	AB020684
	FAM111A	family with sequence similarity 111, member A	NM_022074
	FAM122B	similar to hypothetical protein MGC17347	AI348001
	FAM54A	family with sequence similarity 54, member A	AL138828
	FAM72A	family with sequence similarity 72, member A	AL135396
	FSIP1	fibrous sheath interacting protein 1	NM_152597
	KIAA0152	KIAA0152	NM_014730
	LOC201725	hypothetical protein LOC201725	BE620598
	LOC54103	hypothetical protein LOC54103	AK026747
	MTX3	metaxin 3	AI743044
	RCCD1	RCC1 domain containing 1	AW007826
	SPG20	spastic paraplegia 20, spartin (Troyer syndrome)	AI651603
	TMEM57	transmembrane protein 57	AI582192
	TMEM64	transmembrane protein 64	BF732480
	TMEM87A	transmembrane protein 87A	AL049944

Table 5.4 Primers for 80 genes selected for validation by real-time PCR

Gene	Used seq	Forward	Reverse	Product size
ACSL3	NM_004457	gactctgggaacacgtgaag	ttggttctgacccaacatc	169
ANTXR1	NM_032208	tggaacagttggctcacaat	taagtgtcctcctggcaga	160
ARHGAP27	NM_199282	caagtttccaccctgagta	cttatgccaggtgctgatgat	166
ARL14	NM_025047	gctctgactgctgaggacatc	cttgaagaacgccaagtgtc	183
ASPH	NM_004318	gatgctgatgggatggagat	tcgatattctggggttctgc	165
ATF3	NM_001674	agcccctgaagaagatgaaag	tctgagccttcagttcagcat	152
B4GALT6	NM_004775	agctgccttatatgcaggat	aggaatgagaactgccacctt	158
C11orf75	NM_020179	acacacctctagcatcctc	aaacaccacgatcaagagcac	173
C6orf141	NM_153344	ctcaggaggctgcgaatc	ctgccgttctgtcctcgt	165
CCNE2	NM_057735	caggtttggagtgggacagta	cttctccagcatagccaaat	168
CLDND1	NM_001040199	ggattgtggagacgggtatc	gagatcaatcccgtattgtg	168
CPEB2	NM_182485.1	tcgattgagctatccacatcc	agcgttctattcgtctccat	173
CPOX	NM_000097	ggcatcagctgtgtactcaa	ataacagagctcacgccata	176
DBNDD2	NM_001048222	cgaggacatttacagccaga	aagaacacatctgctgcatcc	171
DGKQ	NM_001347	acctctgctccgacttcatct	ggcagacagcacagaacttg	192
DKFZp451A211	NM_001003399	gacgcaggcaggtgaatc	catgtctgaggctcttttct	168
DKFZP761M1511	DR002751	tacctgtctcctgctctgga	ggtagagagctgtctgcatcg	166
DST	NM_183380	ggtacaagaatgaacgggaca	gggcaaggatctcctgaaag	164
DUSP10(MKP5)	NM_144729	atctfgcccttctcttctct	ttctgcttctgctgtcagtg	173
DUSP2(PAC-1)	NM_004418	ccactccctgtacttctctg	aggtagggcaagatctccaca	175
EMP2	NM_001424	cctggtgggtagagatgagt	tggagcacgaagatgaagaag	175
ETV1	NM_004956	gcagtcaagaacagccctta	ggtcaggttccggtgatgag	180
EVA1	NM_005797	tctcttggcatacagctcac	ggacgaaaattccaggtcact	165
EXTL2	NM_001439	cgtctgttttccccattg	gggaaaggaggagaaaagagaa	115
F11R	NM_144503	aacagctatggggagggtcaag	cccatcttgaaccagggtgta	162
FAM122B	NM_145284	agtctgacatggctcaggaga	tgtgacggctcataattgttg	180
GABARAPL1	NM_031412	ggaggaccatccctttgagta	ctggccaacagtaaggtcaga	160
GADD45B	NM_015675	gtacgagctggccaagtgtgat	cacgatgttgatgctgtgtc	151
GBP3	NM_018284	tgaacaagctagctgggaaga	tcattctggttgcacccttc	172
GEM	NM_005261	tggctctctgactccacagac	tgtatcttctcccagcacctc	168
GINS1	NM_021067	tcaacgaggatgactcagac	gcagcgtcgaatttctaacag	155
GPSM1	NM_015597	cgaggacctgaagacactgag	gagtggtttcccagggttcc	172
HABP4	NM_014282	gggaataccgacctatgaga	ctctctggtcaaaagcgtcaa	189
HDAC9(HDAC7)	NM_178423	ctctccaccttagtggaaac	gcttctctctctgccattt	154
HIC2	NM_015094	ctgctgctcacatggtgtct	gatgatgacgtcacacaggaa	161
HIST1H1C	NM_005319	gccgtatcaactgtgtctca	tggcttcttaggtttgttcc	161
HIST1H2AC	NM_003512	cgtaaaggcaactacgcagag	cagttgttgagctcctcgtc	186
HIST1H2AE	NM_021052	tcttagagctagctggcaacg	tcttctaggcagaatacgg	174
HIST1H2BG	NM_003518	catgcctgaaccagctaaatc	gtatcggggtgaacctgtttt	159
HIST1H4H	NM_003543	ttgggtaaggaggagctaa	gaatcacgttctccaggaaca	173
HIST2H2BE	NM_003528	gtgtgaaggtcatggaaatg	gcctaattgagaaccgactcc	150
HS3ST3A1	NM_006042	cagtgcctctccacctc	gccaggcagtagaagacgtaa	108

Table 5.4 Primers for 80 genes selected for validation by real-time PCR

Gene	Used seq	Forward	Reverse	Product size
HSPG2	NM_005529	gggcacctgtcttcaggta	gacttggatggaacctctgc	128
IFIT2	NM_001547	ctgcaacctgagtgagaaca	tcacattctgaaactcagtc	151
IL1B	NM_000576	agctgatggccctaaacagat	cagcatcttctcagctgttc	160
IL6R	NM_000565	agctgggactgtgcacttg	gccggactgttctgaaactt	168
IL8	NM_000584	ctgcgccaacacagaaatta	gcttgaagtctcactggcctc	179
INHBA	NM_002192	ggagaacgggtatgtggagat	gtcactgccttctctggaaat	151
IRAK2	NM_001570	ggctgaggatgaacaggaag	ggaggtgctgaagtcctttg	178
KLF6	NM_001300	tacacaaaagctcccacttg	tcagacctgaaaaaaccttg	188
KLHL5	NM_001007075	cagcttcacatccaactgt	caatttcgctgctggttaat	154
KREMEN1	NM_001039570	gcctgggtgagcacaactat	ggtgccagttagaggaggtg	176
LAMA5	NM_005560	cctggagtacaacgaggtcaa	ctcttggaggaggcaagaac	171
LAMB3	NM_000228	caagcctgagacctactgcac	ctgcagagagacagggttcac	172
LOC153222	BC041709	tcggaacaactctgatgagc	ccctcattatccaggacatctg	179
MICAL2	NM_014632	ctggacctagacctctggagc	gtcctcccaactatgagac	172
MND1	NM_032117	catgcaagcctacagaaaagc	caacttgcgcatcacagtctt	157
NMU	NM_006681	attctcagcctcaggcatcc	ggatgcacaactgacgacac	172
OAS1	NM_016816	tgtgtgtgtccaaggtggtaa	tctcttttgacaggctcca	180
OIP5	NM_007280	ccctcctagtggcattga	gcacaccattttgactctgg	162
PILRB	NM_013440	tgtatttctgccagtcgag	ttctgagtccctttgcttt	176
PPP1R15A	NM_014330	tgaggcagccggagatact	gtagcctgatgggtgctt	192
PPP2R5B	NM_006244	gaggatgagcccaatcttga	cggggatcctcactatcaaa	167
PRKAB2	NM_005399	acaagatcatggtggggagta	ggaccagagatgaagacctc	188
PTBP2	NM_021190	acggaatcgtcactgaagttg	agtacacgagaaggagcacca	178
RAB22A	NM_020673	gtattgtgtggcggtttgtg	agccgacctcgtatagtaca	179
RAB38	NM_022337	acgtgcaccagaactctcc	gcaccatagcttctcggtta	172
RAB7L1	NM_003929	caggacagctcagcaaaaca	gcagaggcatcccataata	164
RASAL2	NM_004841	caatatttctggggcgaac	tacaaattggcgaccagtea	166
RNASE7	NM_032572	tgcaaacctcaaacaccttc	acctgcagttcggatacttc	169
SERPINA1	NM_001002235	cgaagaggccaagaaacagat	gaagtctcttctcgtgttc	175
SESN2	NM_031459	atgctgtctttgtggaagac	ctggaacttctcatccagcag	171
SFRS7	NM_001031684	aaggtcaaggtcagcatctcc	tgtctgtgaaatagacctgga	160
SLC35D1	NM_015139	gcgtgctccaattacagat	agtggaaactcttctcagagt	151
TMEM57	NM_018202	gcacacagaaaggggaggtg	agccaaacccaaagtacc	167
VANGL1	NM_138959	gcttctacagcctgggacac	cattgttactggggccatct	174
VSNL1	NM_003385	tgagcatgaaactcaagcagtg	tgaactctcggaaagtcaatgg	188
XK	NM_021083	ccaggcagaaggcaactaat	caatggacaacagggatatgg	173
YOD1	NM_018566	atggggataccattctggaag	agaggcaagagttgtctgctg	180
ZDHHC23	NM_173570	cgtggcctactgtttgtgtga	gggatgatgctgatgtcact	171

Table 5.5 Validation for the expression of 57 genes selected from differentially expressed gene list

Gene Symbol	Gene Name	Microarray	Real-time PCR
Down-regulated genes			
ACSL3	acyl-CoA synthetase long-chain family member 3	↓	↓
ANTXR1	anthrax toxin receptor 1	↓	↓
ASPH	aspartate beta-hydroxylase	↓	↓
B4GALT6	UDP-Gal:betaGlcNAc beta 1,4- galactosyltransferase, polypeptide 6	↓	↓
C11orf75	chromosome 11 open reading frame 75	↓	↓
CCNE2	cyclin E2	↓	↓
CPOX	coproporphyrinogen oxidase	↓	↓
DBNDD2	dysbindin (dystrobrevin binding protein 1) domain containing 2	↓	↓
DKFZP761M1511	hypothetical protein DKFZP761M1511	↓	↓
DST	dystonin	↓	↓
EMP2	epithelial membrane protein 2	↓	↓
ETV1	ets variant gene 1	↓	↓
EVA1	epithelial V-like antigen 1	↓	↓
EXTL2	exostoses (multiple)-like 2	↓	↓
F11R	F11 receptor	↓	↓
FAM122B	similar to hypothetical protein MGC17347	↓	↓
GINS1	GINS complex subunit 1 (Psf1 homolog)	↓	↓
HS3ST3A1	heparan sulfate (glucosamine) 3-O-sulfotransferase 3A1	↓	↓
IL1B	interleukin 1, beta	↓	↓
KLHL5	kelch-like 5 (Drosophila)	↓	↓
MND1	meiotic nuclear divisions 1 homolog (S. cerevisiae)	↓	↓
NMU	neuromedin U	↓	↓
OIP5	Opa interacting protein 5	↓	↓
RAB22A	RAB22A, member RAS oncogene family	↓	↓
RAB38	RAB38, member RAS oncogene family	↓	↓
RAB7L1	RAB7, member RAS oncogene family-like 1	↓	↓
SERPINA1	serpin peptidase inhibitor, clade A (alpha-1 antiproteinase, antitrypsin), member 1	↓	↓
SLC35D1	solute carrier family 35 (UDP-glucuronic acid/UDP-N-acetylgalactosamine dual transporter), member D1	↓	↓
TMEM57	transmembrane protein 57	↓	↓
VANGL1	vang-like 1 (van gogh, Drosophila)	↓	↓
VSNL1	visinin-like 1	↓	↓
XK	X-linked Kx blood group (McLeod syndrome)	↓	↓
ZDHHC23	zinc finger, DHHC-type containing 23	↓	↓

Table 5.5 Validation for the expression of 57 genes selected from differentially expressed gene list

Gene Symbol	Gene Name	Microarray	Real-time PCR
Up-regulated genes			
ARHGAP27	Rho GTPase activating protein 27	↑	↑
ATF3	activating transcription factor 3	↑	↑
DGKQ	diacylglycerol kinase, theta 110kDa	↑	↑
DUSP2	dual specificity phosphatase 2	↑	↑
GEM	GTP binding protein overexpressed in skeletal muscle	↑	↑
GPSM1	G-protein signalling modulator 1 (AGS3-like, <i>C. elegans</i>)	↑	↑
HABP4	hyaluronan binding protein 4	↑	↑
HDAC9	histone deacetylase 9	↑	↑
HIC2	hypermethylated in cancer 2	↑	↑
HIST1H1C	histone 1, H1c	↑	↓
HIST1H2AC	histone 1, H2ac	↑	↑
HIST1H4H	histone 1, H4h	↑	↓
HSPG2	heparan sulfate proteoglycan 2 (perlecan)	↑	↑
IL6R	interleukin 6 receptor /// interleukin 6 receptor	↑	↑
KLF6	Kruppel-like factor 6	↑	↑
LAMB3	laminin, beta 3	↑	↑
PILRB	paired immunoglobulin-like type 2 receptor beta	↑	↑
PPP1R15A	protein phosphatase 1, regulatory (inhibitor) subunit 15A	↑	↑
PRKAB2	protein kinase, AMP-activated, beta 2 non-catalytic subunit	↑	↑
PTBP2	polypyrimidine tract binding protein 2	↑	↑
RNASE7	ribonuclease, RNase A family, 7	↑	↑
SESN2	sestrin 2	↑	↑
SFRS7	splicing factor, arginine/serine-rich 7, 35kDa	↑	↑
YOD1	YOD1 OTU deubiquinating enzyme 1 homolog (<i>S. cerevisiae</i>)	↑	↑

Table 5.6 Validation for the expression of 23 genes randomly selected from microarray data

Gene Symbol	Gene Name	Microarray	Real-time PCR
Down-regulated genes			
CLDND1	claudin domain containing 1	↓	↓
KREMEN1	kringle containing transmembrane protein 1	↓	↓
OAS1	oligoadenylate synthetase 1	↓	↓
Up-regulated genes			
ARL14	ADP-ribosylation factor-like 14	↑	↑
C6orf141	chromosome 6 open reading frame 141	↑	↑
CPEB2	cytoplasmic polyadenylation element binding protein 2	↑	↑
DKFZp451A211	DKFZp451A211 protein	↑	↑
DUSP10	dual specificity phosphatase 10	↑	↑
GABARAPL1	GABA(A) receptor-associated protein like 1	↑	↑
GADD45B	growth arrest and DNA-damage-inducible, beta	↑	↑
GBP3	guanylate binding protein 3	↑	↑
HIST1H2AE	histone 1, H2ae	↑	↓
HIST1H2BG	histone 1, H2bg	↑	↓
HIST2H2BE	histone 2, H2be	↑	↑
IFIT2	interferon-induced protein with tetratricopeptide repeats 2	↑	↑
IL8	interleukin 8	↑	↑
INHBA	inhibin, beta A (activin A, activin AB alpha polypeptide)	↑	↑
IRAK2	interleukin-1 receptor-associated kinase 2	↑	↑
LAMA5	laminin, alpha 5	↑	↑
LOC153222	adult retina protein	↑	↑
MICAL2	microtubule associated monooxygenase, calponin and LIM domain containing 2	↑	↑
PPP2R5B	protein phosphatase 2, regulatory subunit B (B56), beta isoform	↑	↑
RASAL2	RAS protein activator like 2	↑	↑

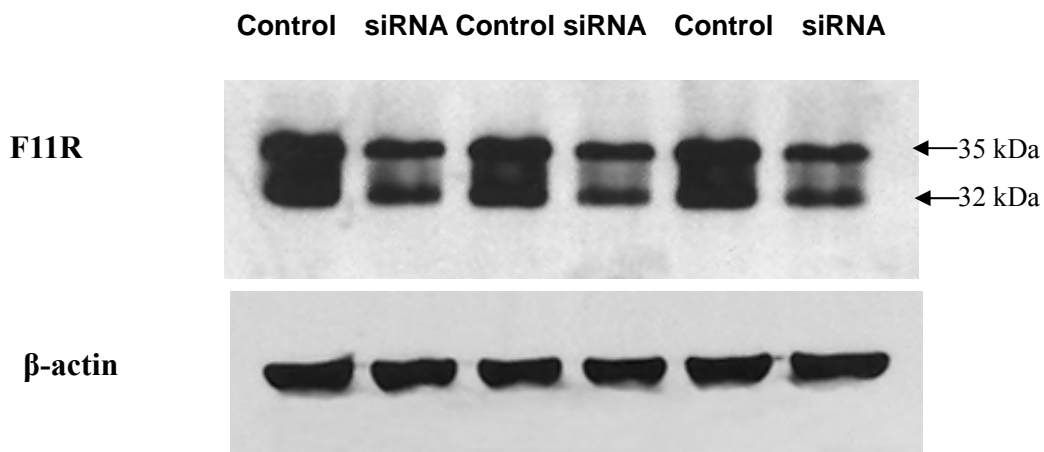
Western blot analysis and immunohistochemical staining for F11R (also known as Junction Adhesion Molecule, JAM) were performed to test if down-regulation is also reflected at the protein level. Cell lysates were extracted at 72 hrs post transfection and the level of F11R protein expression were determined by non-reducing Western blotting (**Fig. 5.7A**). Densitometric analysis of the Western blotting showed that after 72 hrs of silencing *HS3ST3A1* expression, protein level of F11R was 2.26-fold lower in the *HS3ST3A1*-silenced cells compared to that in the controls (**Fig. 5.7B**), which was consistent with the suppression at the mRNA level (-2.09 fold) (**Figs. 5.6**). The down-regulation in protein levels were also verified by immunocytochemical staining (**Fig. 5.7C**). After confirming of the microarray expression data, the gene expression pattern was further explored.

5.5 Principal component analysis (PCA) of microarray expression data

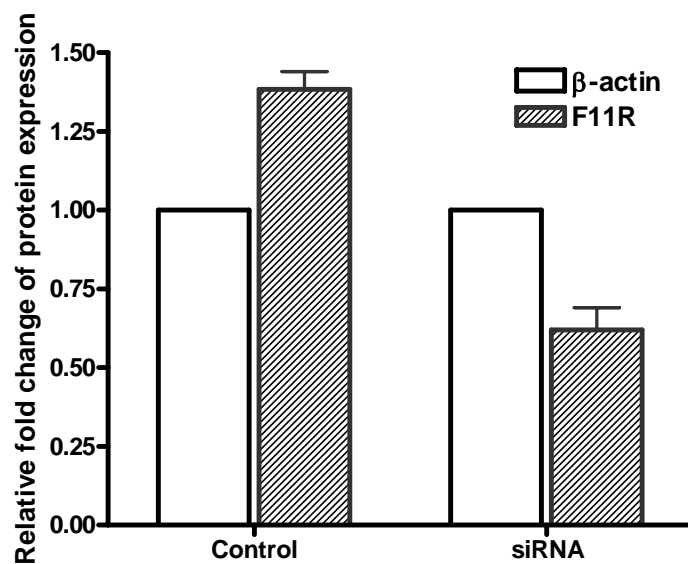
Principal Component Analysis (PCA) was applied to cluster the expression data in the control groups vs siRNA silencing groups. PCA is commonly used in microarray data analysis as a cluster analysis tool (Yeung and Ruzzo, 2001). PCA simplifies the dimensionality of the data set to a few principal components and thus identifies patterns in the microarray expression data. Using this analysis tool, microarray data in this study clearly showed that the 3 samples of the control groups (c1, c2 and c3) were separating distinctly from those of the siRNA groups (e1, e2 and e3) (**Fig. 5.8**). As shown in **Fig. 5.8**, silencing the expression of *HS3ST3A1* in

MCF-12A cells resulted in a systematic change in the gene expression.

A



B



C

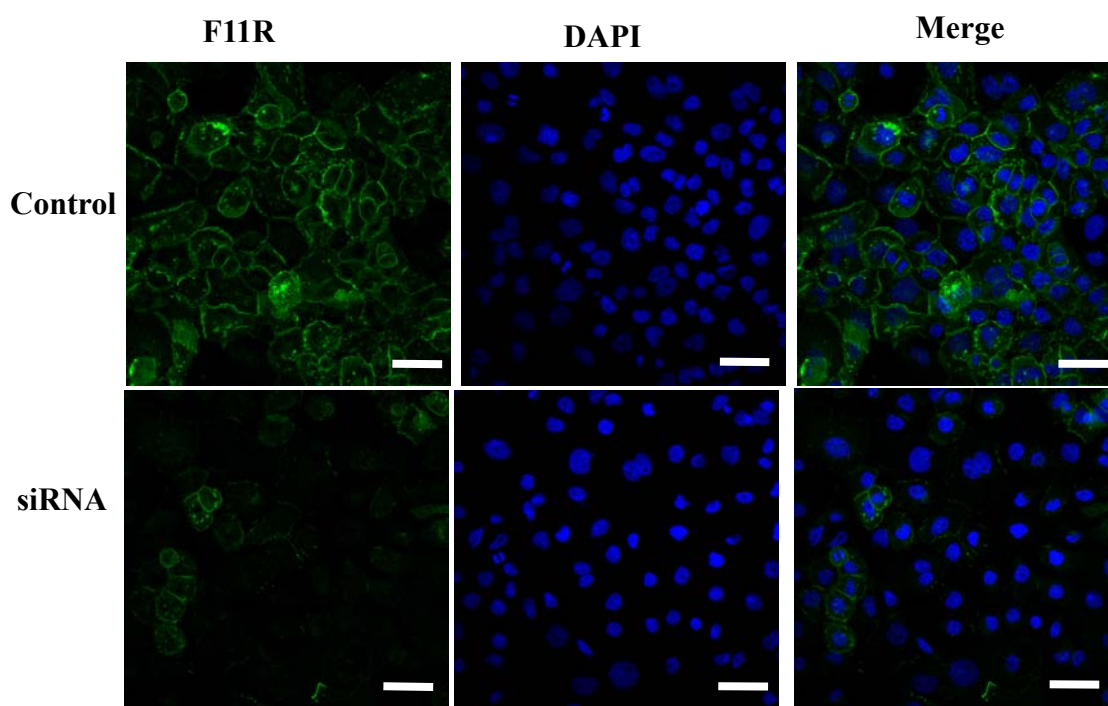


Fig. 5.7. Validation for the expression of F11R protein. (A) Western blot analysis of F11R protein expression after 72 hrs post silencing *HS3ST3A1* gene in MCF-12A cells. Western blot analysis under non-reducing conditions shows two major bands of F1R, migrating at 32 and 35 kDa, probably representing one of the glycosylated forms (Naik *et al.*, 1995). Protein was extracted and processed as in *Chapter 2 Materials and Methods*. (B) Densitometry analysis of the Western band. Both 32 kDa and 35 kDa bands were quantified by densitometry and analyzed by QuantityOne software (Bio-rad). Data are expressed as F11R normalized to β -actin and represented the Mean \pm SD. (Student *t*-test, $**p < 0.05$, $n = 3$). (C) Immunocytochemical staining of F11R protein. MCF-12A cells were cultured on coverslips. 72 hrs post silencing *HS3ST3A1* mRNA. MCF-12A cells were fixed, processed for detection of F11R expression with anti-F11R mAb (immunofluorescence) and visualized by using confocal microscopy.

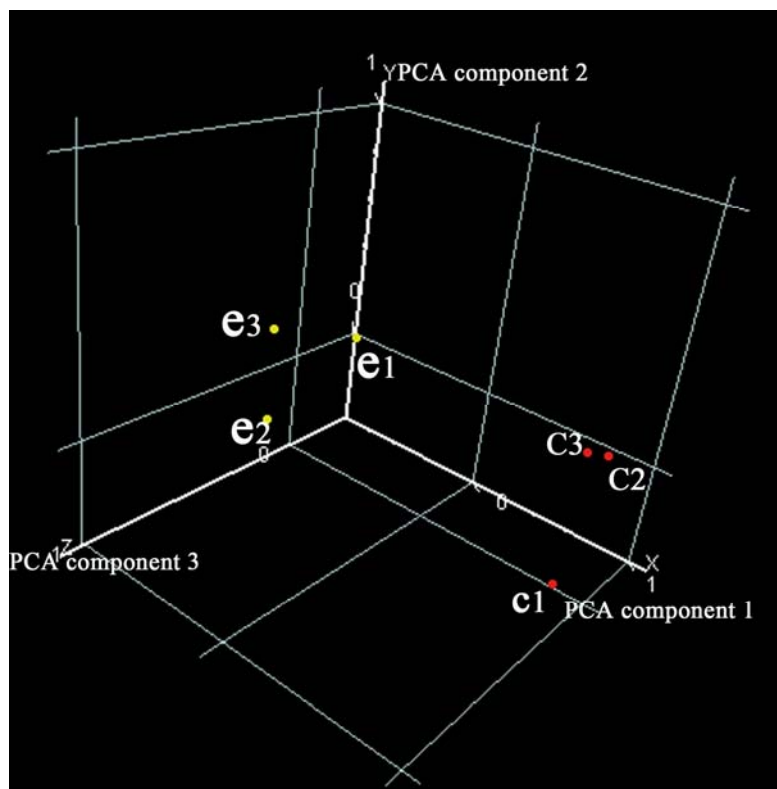


Fig. 5.8. Principal component analysis (PCA) of microarray data. Principle component analysis of gene expression was generated in a three dimensional platform and presented here as graph providing a global view on the difference and similarities among the control and siRNA groups. Note: The 3 arrays of the control group (c1, c2 and c3) were separating distinctly from those of the siRNA group (e1, e2 and e3)

5.6 Hierarchical clustering of microarray expression data

To further analyze the data for a clear visualization the expression pattern, 648 differentially expressed probes that were generated in the analysis by GeneSpring v7.0 were sent into the software for hierarchical clustering. **Fig. 5.9** depicts a dendrogram of the two-way hierarchical clustering (genes-horizontal, samples-vertical) of differentially expressed genes in the siRNA groups as compared with those in the control groups. Hierarchical cluster analysis by GeneSpring v7.0 demonstrated good concordance between the 3 biologic replicates (**Fig. 5.9**) as the control and siRNA samples clustered together perfectly. Two main vertical branches were also identified that clearly discriminated the control groups from the siRNA groups, reflecting the two groups of genes that are up- and down-regulated between the control and siRNA samples.

5.7 Functional categorization of target genes

Based mainly on the Gene Ontology (GO) Biological Function categories (Cheng *et al.*, 2004; Harris *et al.*, 2004), the list of differentially expressed genes (213 probe set, 186 genes) among the four analysis softwares could be divided into different functional categories. It was found that silencing *HS3ST3A1* in MCF-12A cells altered a variety of genes which were identified in this study covering a diverse range of biological functions. These differentially expressed genes were grouped into 7 major functional categories as is shown in Table 5.2 and 5.3, which includes cell cycle, cell-ECM adhesion and communications, carbohydrate metabolism and transcription.

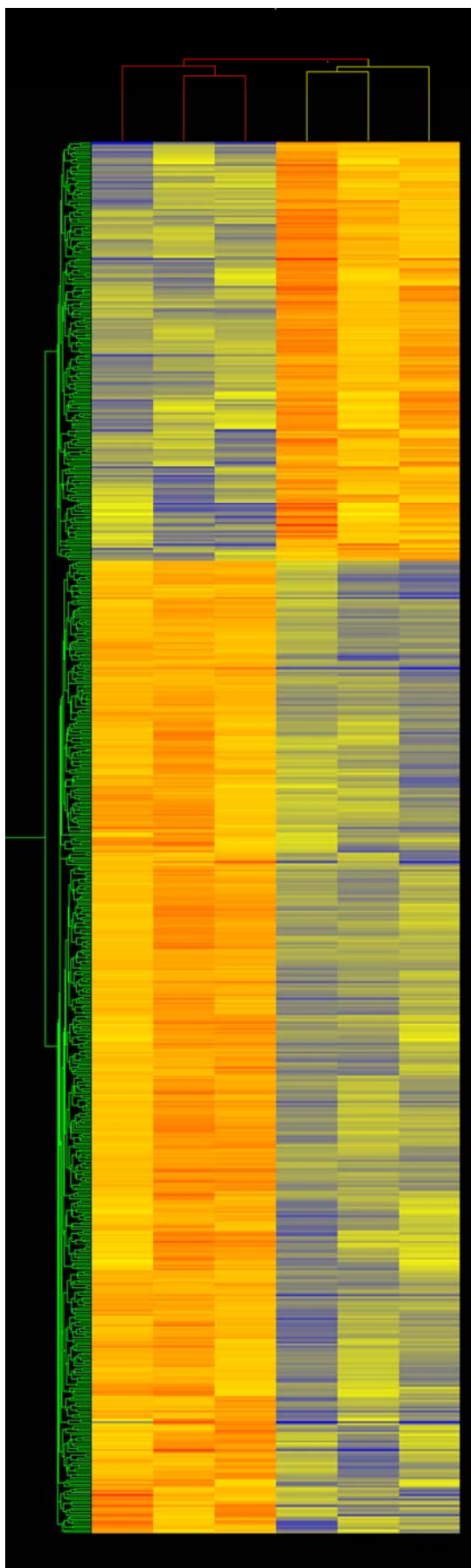


Fig. 5.9. Hierarchical clustering of differentially expressed genes in the control groups as compared with those in the siRNA groups. Two-way hierarchical clustering (genes-horizontal, samples-vertical) was performed on the log₂ normalized data using GeneSpring v7.0. Each row denotes a single gene and each column represents an individual sample. The dendrogram to the left presents the list of probe sets grouped by similarity using Pearson correlation. Yellow indicates no change from controls, red indicates probe sets with enhanced expression relative to controls, increasing in brightness with higher values, and blue indicates suppressed expression relative to controls, increasing in brightness with lower values. Note that the control and siRNA samples cluster together perfectly. Two main vertical branches were identified that clearly discriminated the control groups from the siRNA groups.

5.8 Possible pathway analysis

The relationship between the genome-wide gene expression changes with the phenotype alterations in biological function assays which were demonstrated above was further explored. As genes function together in these biological processes such as cell proliferation, adhesion, migration and invasion, PathwayStudio 4.0 (Nikitin *et al.*, 2003) was used to generate possible pathways involved in the phenotype changes after silencing *HS3ST3A1* genes expression. All the differentially genes were displayed and selected, and the "Build Pathway" command was used with the option of "Find only direct interactions between selected nodes" to create new pathways. The whole complicate gene interaction in pathways was too big to be included here. So the complicated interaction network was further narrowed down. **Fig.5.10** provides schematic representation of the models generated through this analysis, focusing on cell cycle-related genes (**Fig.5.10A**) and the pathway associated with cell-ECM and cytoskeleton related genes (**Fig.5.10B**) in MCF-12A cell phenotype alterations.

Combined together, the genomic gene expression profiling results provide strong evidence that the Affymetrix GeneChip microarray represents an ideal tool to analyze differentially expressed genes and identifies potentially important genes in the phenotype alteration after silencing *HS3ST3A1* expression in MCF-12A cells.

Fig. 5.10A

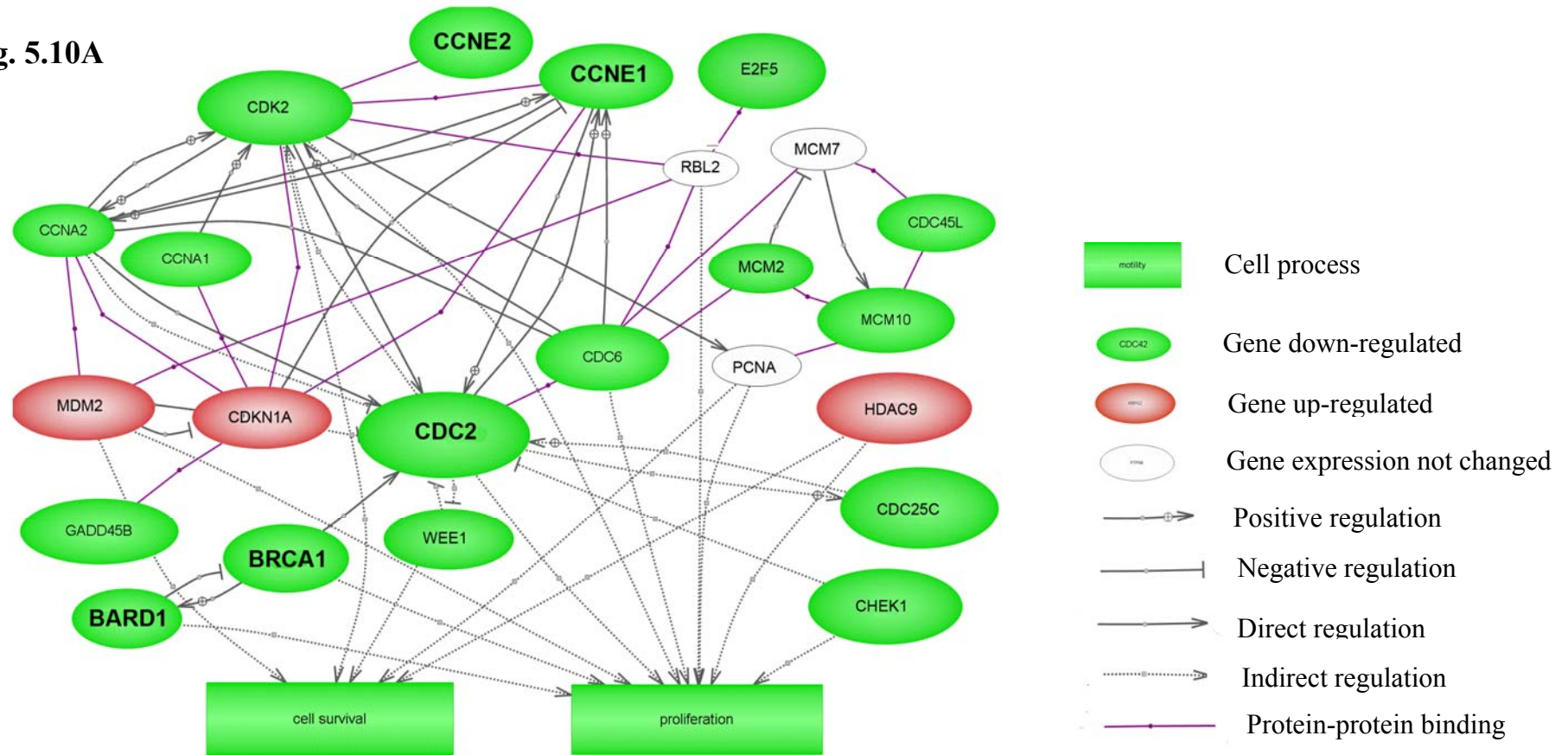
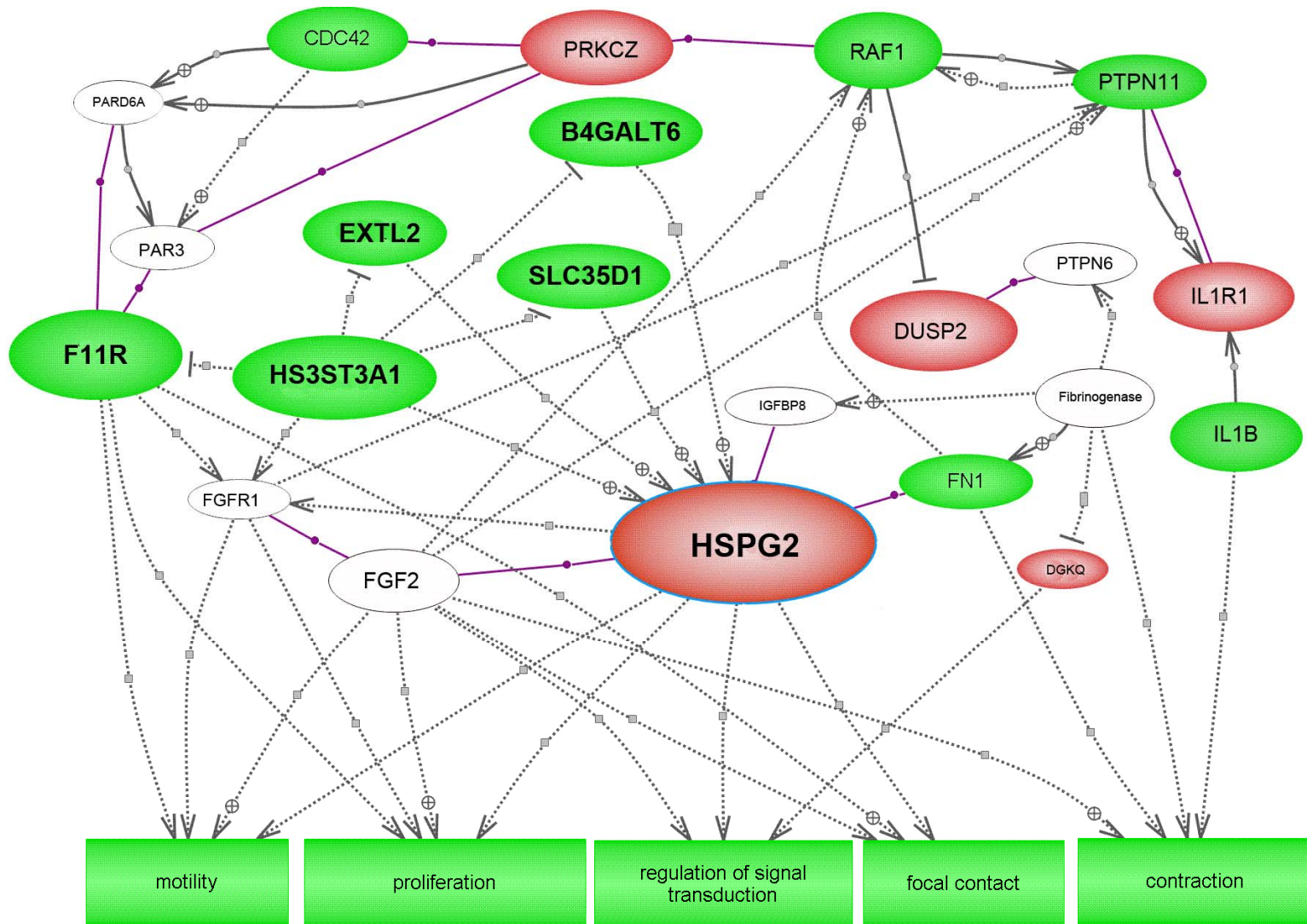


Fig. 5.10 Interactive pathway analysis in PathwayStudio 4.0 from the list of differentially expressed genes. A: cell cycle associated genes differentially regulated by *HS3ST3A1* silencing in MCF-12A cells. B: Cell-communication and cell cytoskeleton associated genes differentially regulated by *HS3ST3A1* silencing in MCF-12A cells, focusing on the function of perlecan (HSPG2) and F11R. Only selected genes that could be linked from the selected genes to other genes, functions, or categories are included in the map. Cellular processes, such as “proliferation”, “cell survival”, “focal contacts” and “mobility” are also incorporated into the map. Genes with name bolded are discussed in the text.

Fig. 5.10B



Discussion

Genome-wide gene expression profiling with microarray technique allows simultaneously analysis of tens of thousands of genes that were differentially expressed under two conditions such as treatment and without treatment, or between control and knock down samples. In this study, three controls and three siRNA silenced MCF-12A cell culture RNA samples were hybridized and analyzed on Affymetrix HU133 plus 2.0 GeneChip. The gene expression was globally analyzed using different softwares for data normalization and subsequently identification and clustering of differentially expressed genes were performed.

Analysis of microarray data is currently a dynamic field. Recent research trends have suggested the use of various normalization approaches to minimize experimental variation. Affymetrix MAS 5.0, Robust Multiarray Analysis(RMA, Irizarry *et al.*, 2003a; Irizarry *et al.*, 2003b), DNA-Chip Analyzer (D-Chip, Li and Wong, 2001a; Li and Wong, 2001b) and Genespring as well as others are widely used. In the analysis of data from this study, D-Chip, RMA and GeneSpring v7.0 in addition to MAS 5.0 were utilized to determine differentially expressed genes. Comparison of gene list from all of these methods revealed the overlapping genes among the four analysis tools, which were differentially expressed in response to *HS3ST3A1* silencing. This gene list is more conservative and thus more reliable in the likelihood that they are really differentially expressed genes.

In the present study, the main aim is focused on the identification of subgroups of genes that may account for the phenotype alterations in MCF-12A cells after silencing *HS3ST3A1* gene by siRNA. Furthermore, possible pathways that might link those differentially expressed genes with concordant functions in the phenotype changes were also explored.

Using different microarray analysis tools, a detailed comparison of the genomic expression profiles between the three controls and three knockdown samples were performed. It revealed 186 genes (2-fold as the threshold) were differentially expressed, among them 123 genes were down-regulated and 63 genes were up-regulated. The expression data from microarray were further validated by real-time PCR for 80 genes and the expression of one gene, F11R was confirmed by both immunohistochemistry and Western blot.

Based mainly on the Gene Ontology Biological Function categories (Cheng *et al.*, 2004), the list of differentially expressed genes (186 genes) could be divided into different functional categories. It was found that the silencing *HS3ST3A1* in MCF-12A cells altered a variety of genes which were identified in this study covering a diverse range of biological functions (Table 5.2 and 5.3).

Identification of molecular pathways

To reveal potential pathways affected by *HS3ST3A1* silencing-induced alterations in gene expression, PathwayStudio 4.0 software (Nikitin *et al.*, 2003) was used. PathwayStudio 4.0 software is incorporated with the “build pathway” function. Only genes that are recognized by the software and found to be part of a pathway are included. Genes that were significantly (2- fold threshold) were imported into the software. A simplified graphical summary of the pathway for genes associated with *HS3ST3A1* silencing in MCF-12A cells is shown in **Fig.5.10A and B**.

One of the pathways revealed by the PathwayStudio software was cell cycle related. There were a considerable number of genes that could be linked to cell cycle and proliferation regulation rather than apoptosis, including genes such as CDC2, CDC6, CDCA3, CCNE2, CCND3, BRCA1 and BARD1. The proliferation of breast cells and cancer cells is regulated by extracellular growth signals such as FGF-2 (Delehedde *et al.*, 1996). During this period, growth factors induced signals (either stimulatory or inhibitory) are transduced from the extracellular environment to cell cycle operating apparatus in cytoplasm and nucleus. This apparatus, composed of cyclins and their cyclin-dependent kinases, may respond by setting the cell into cell division program that carries the cells through G₁, S, G₂ and M phases or, alternatively, by causing exit from the active cell cycle into the quiescent G₀ state. The majority of genes in this group are down-regulated in *HS3ST3A1* silenced MCF-12A cells, indicating that a major negative influence on cell cycle transition.

Cyclin E

Microarray results showed a down-regulation of Cyclin E2 in the *HS3ST3A1*-silenced MCF-12A cells. E-type cyclins (both cyclin E1 and cyclin E2) (Koff *et al.*, 1991; Zariwala *et al.*, 1998; Lauper *et al.*, 1998; Gudas *et al.*, 1999) are expressed during the late G₁ phase of the cell cycle until the end of the S-phase. Cyclin E-CDK2 complex plays a critical role for mammalian cells progression of G₁/S transition (Koff *et al.*, 1992; Dulic *et al.*, 1992). Many research demonstrated that Cyclin E protein overexpression was often found in human breast cancers. For example, Payton *et al.* (2002) reported the expression and associated catalytic activity for both cyclin E1 and cyclin E2 were elevated in primary breast tumours when compared to normal breast tissue with a significantly increased expression of Cyclin E2 compared with Cyclin E1 (Payton *et al.*, 2002). Such evidence was also reported by Geng *et al.* (Geng *et al.*, 2001). They also found cyclin E2 was overexpressed in approximately 24% human mammary carcinomas.

It was clear now that overexpression of cyclin E protein was not only associated with tumour initiation, progression and proliferation, but also indicated a more malignant phenotype (Yasmeen *et al.*, 2003a; Moroy and Geisen, 2004). Furthermore its overexpression also has been associated with a poor prognosis in primary breast cancer patients (Keyomarsi *et al.*, 1994; Keyomarsi *et al.*, 2002; Keyomarsi *et al.*, 2003; Yasmeen *et al.*, 2003b). Indeed, cyclin E2 has the potential to be a breast cancer predictor in clinics. In microarray molecular prediction signature of breast cancer, Cyclin E2, but not Cyclin E1, overlapped between the 76-gene prediction signature

from Wang *et al.* (Wang *et al.*, 2005) and the 70-gene prediction signature from van't Veer *et al.* (van't Veer *et al.*, 2002) for metastasis-free survival of lymph node-negative breast cancer patients. This suggested that Cyclin E2 plays a critical role in breast cancer progression.

CDC2 (cell division cycle 2, G₁ to S and G₂ to M), also known as cyclin-dependent kinase 1, CDK1.

While cyclin E-CDK2 complex regulates the G₁/S phase transition CDC2-Cyclin B complex control the G₂/M transition (Zhan *et al.*, 1999). Progression of the cell cycle from the G₂ to the M phase is controlled by a protein kinase complex, called mitosis or maturation promoting factor (MPF) (Hoffmann *et al.*, 1993). MPF consists of two major proteins, the catalytic subunit, p34cdc2 and cyclin B1. The G₂/M DNA damage checkpoint serves to prevent the cell from entering mitosis (M-phase) if the genome is damaged. Thus the activity of the cdc2-cyclin B complex is pivotal in regulating this transition. During the G₂-phase, cdc2 is maintained in an inactive state by the kinases Wee1 and Myt1. As cells approach M-phase, the phosphatase cdc25 is activated by phosphorylation which in turn activates cdc2, establishing a feedback amplification loop that efficiently drives the cell into mitosis. It is now known that p34cdc2 is necessary for the induction of mitosis because it participates in the condensation of chromosomes, the formation of the mitotic spindle, and the breakdown of the nuclear membrane (Wiesener *et al.*, 1998). Microarray data in this study showed the CDC2 gene expression was down regulated, which was consistent with the changes in cell proliferation.

BRCA1

Of particular interest in this pathway is the down-regulation of BRCA1 and BRAD1, because of their relationship to the control of cell cycle and breast cancer development. BRCA1, a tumour suppressor gene on chromosome 17q21, was identified based on its linkage to hereditary breast and ovarian cancer syndromes (Easton *et al.*, 1993; Miki *et al.*, 1994) from which its name was derived, breast and ovarian cancer susceptibility gene-1.

BRCA1 has been found to play a important role in cell cycle control. Loss of BRCA1 results in cell cycle checkpoint dysfunction, improper DNA damage repair, and genomic instability. Xu *et al.* (1999b) found in their BRCA1 mutant mice model, tumours displayed characteristic genomic aberrations and cell cycle defects that were very similar to those seen in BRCA1-deficient mammary gland tumours (Brodie *et al.*, 2001). More research has established that the control function of BRCA1 in cell cycle was attributed to its function of maintenance of genomic integrity via participation in homologous-recombination-mediated double-strand-break repair, and centrosome amplification control (reviewed in Deng and Wang, 2003; Venkitaraman, 2002)).

BRCA1 was also one of the first genes to be associated with familial breast cancer susceptibility in humans. Carriers of mutations in BRCA1 account for a much higher risk of early onset familial breast cancer and/or breast/ovarian cancer than noncarriers (Easton *et al.*, 1993; Miki *et al.*, 1994; Ford *et al.*, 1995). Targeted deletion of BRCA1 in mammary epithelium resulted in carcinomas and adenocarcinomas of varying histology (Bowen *et al.*, 2005). Using conditional

knockout mice, Xu *et al.* (1999) have found mice with deletion of exon 11 of BRCA1 displayed variable types of mammary carcinomas, commonly ductal and lobular carcinomas as well as more rare cases of squamous carcinomas, medullary carcinomas, and anaplastic carcinomas, all of which are found in human familial breast cancers. All these studies suggest mutant BRCA1 and thus low expression of BRCA1 plays a vital role in breast tumorigenesis.

BARD1

BRCA1-associated RING domain protein (BARD1) which binds to the BRCA1 N-terminal RING domain (Wu *et al.*, 1996) was down-regulated in the present study. Wu *et al.* (1996) found that most BRCA1 molecules form heterodimers with BARD1 *in vivo*. Research evidence showed that BRCA1/BARD1 heterodimer complex plays a critical role in mitotic spindle assembly that likely contributes to its role in chromosome stability control (Joukov *et al.*, 2006) and loss of this mitotic function might contribute to tumorigenesis (Clarke and Sanderson, 2006).

The spindle assembly checkpoint modulates the timing of anaphase initiation in mitotic cells containing improperly aligned chromosomes and increases the probability of successful delivery of an euploid chromosome set to each daughter cell. Failure to properly form spindle poles can lead to chromosome segregation and postmitotic nuclear-assembly defects, abnormalities that are characteristics of both BRCA1/BARD1-deficient cells and many tumour cells (Xu *et al.*, 1999; Fant *et al.*, 2004).

Using BRCA1/BARD1-siRNA-treated cells, researchers have found the chromosome segregation defects and micronucleus formation. Mutations in the BARD1 gene and thus possibly loss of its function in primary breast and ovarian cancers have also been reported (Thai *et al.*, 1998; Ghimenti *et al.*, 2002). Studies also found that reduced BRCA1 expression level was simultaneously existed with over-expressed MDM2, one of negative regulators of p53 (Sourvinos and Spandidos, 1998). In this study, MDM2 was also up-regulated, suggesting it may function together with BRCA1 and BARD1.

To summarize above, as HS and its sulphation pattern have different functions with the interaction of a myriad of growth factors, such functions are often with opposing effects, due to the binding to pro- or anti-mitogenic effect of these growth factors. From previous study, silencing *HS3ST3A1* impaired the sulphation of HS (Fig. 4.10), it is not surprising genes that are known to inhibit or promote tumour proliferation are both dysregulated. The net effect on cell growth undoubtedly depends on the intricate interplay between these genes. The data from microarray analysis showed down-regulation of most of the cell cycle related genes, which strongly suggested that silencing *HS3ST3A1* in MCF-12A cell rendered a negative effect on the breast cell proliferation. At the same, the expression profile of this group genes from microarray analysis in present study and the results from all the researches cited above demonstrated that the phenotype changes after *HS3ST3A1* silencing in MCF-12A cells could be reconciled. One possibility is that the down-regulation those genes such as Cyclin E2 and CDC2 resulted in cell cycle arrest and thus proliferation

inhibition. But at the same time, loss of function of those genes such as BRCA1 and BARD1 rendered the *HS3ST3A1*-silenced MCF12A cell tumourigenic phenotype with features of higher mobility and invasion as the primary function of BRCA1 and BARD1 genes might not be to regulate cell cycle and proliferation during the development of breast cancers.

Another possible pathway revealed by Pathway studio 4.0 software is related to cell-ECM communication. HSPGs are widely expressed at cell surface or in the ECM of virtually every type of cells. It influences cell function by interaction with a variety of proteins in the ECM or directly influence cell shape remodeling during cell migration, adhesion or invasion.

The microarray analysis showed that **HSPG2** (Perlecan) was up-regulated with 4 others genes that are involved in HS synthesis were down-regulated. They are **EXTL2**, **β 4GALT6**, **HS3ST3A1** and **SLC35D1**. *HS3ST3A1* is the gene that was the target to be silenced. Also noted is that the remaining 4 genes in the “carbohydrate metabolism group” were all down-regulated, suggesting a possible dysregulation in heparan sulphate synthesis (Table 5.3).

EXTL2

From Chapter 1 Introduction, it is clear that chain polymerization for HS is initiated once an α -GlcNAc is transferred to the tetrasaccharide linkage (-glucuronic acid-galactose-galactose-xylose where Xyl is attached to a serine residue in the core protein) by the action of α -GlcNAc transferase I (GlcNAcT-I) (Fritz *et al.*, 1994),

whereas β -GalNAc transferase triggers CS/DS synthesis (Rohrmann *et al.*, 1985; Nadanaka *et al.*, 1999).

Elongation then proceeds by the action of glycosyltransferases (GlcNAc-TII and GlcA-TII), which add 1,4-GlcA and 1,4-GlcNAc units in alternating sequence to the nonreducing end of the growing polymer. The exostosin (EXT) family of genes encodes this α -glycosyltransferase involved in heparan sulphate biosynthesis. Five human members of this family have been cloned to date: EXT1 (Ahn *et al.*, 1995), EXT2 (Le Merrer *et al.*, 1994), EXTL1 (Wise *et al.*, 1997), EXTL2 (Wuyts *et al.*, 1997), and EXTL3 (Van *et al.*, 1998). EXT1 and EXT2 have dual enzyme activities (Kim *et al.*, 2003; Busse and Kusche-Gullberg, 2003), GlcA-TII and GlcNAc-TII. EXTL1 shows GlcNAc-TII activity (Kim *et al.*, 2001) while EXTL2 and EXTL3 have GlcNAc-TI activity (Kitagawa *et al.*, 1999; Kim *et al.*, 2001). EXTL2 protein is an α -1,4-N-acetylhexoaminyltransferase I that transfers not only α -GalNAc but also GlcNAc to the common linkage-region, segregating HS from CS/DS biosynthesis (Kitagawa *et al.*, 1999).

The human hereditary multiple exostoses (EXT) family genes are tumour suppressors. The EXT is an autosomal dominant disorder characterized by cartilage-capped skeletal excrescences (benign tumours of bony outgrowths), which has been attributed to mutations in EXT1 and EXT2 (Schmale *et al.*, 1994; Zak *et al.*, 2002). Down-regulation of EXTL2 may suggest its active role in breast tumourigenesis.

HSPG2 (Perlecan)

In this possible pathway, HSPG2 (perlecan) has been put into the centre. In the presents study, HSPG2 was up-regulated. HSPG has three types. The third types are secreted into extracellular matrix. This includes collagen type XVIII, agrin, and perlecan. Human perlecan, encoded by a single-copy HSPG2 gene, consists of 94 exons and spans more than 120 kb of genomic DNA (Iozzo and Murdoch, 1996) with a 14.35-kb mRNA (Murdoch *et al.*, 1992; Kallunki and Tryggvason, 1992). The protein core of human perlecan is about 470 kDa. It can be attached with as many as four HS chains and numerous other O-linked oligosaccharides (Dolan *et al.*, 1997; Friedrich *et al.*, 1999).

Perlecan is the most abundant ECM HSPG of epithelial cells and endothelial basement membranes (BM). As a major HSPG in BMs, perlecan plays active roles in cell proliferation, adhesion, differentiation, and growth factor binding (Knox and Whitelock, 2006). Expression of perlecan was increased in a number of tumour types, both *in vivo* and *in vitro*.

It has been also shown to promote invasive behaviours (Iozzo *et al.*, 1994). Nerlich *et al.* (1997 and 1998) reported that high expression levels of perlecan mRNA were detected in both human breast tumour and stromal cells which was consistent with the findings that human breast cancer stroma has been detected with abundant deposits of perlecan proteins (Iozzo *et al.*, 1994). Sabit *et al.* (2001) showed strong expression of perlecan core protein was detected in tumour stroma in human intrahepatic cholangiocarcinoma (ICC), and liver carcinoma metastasized from the

colon, whereas only small amounts of perlecan were detected in normal livers. Similar findings were revealed in human metastatic melanomas. Perlecan mRNA level was markedly increased compared to normal tissue. Perlecan core protein was over-expressed in the ECM, which seemed to be related to the invasiveness of the melanoma cells (Cohen *et al.*, 1994).

The upregulation of perlecan was also observed *in vitro*. The tumourigenic mouse epidermal cell line RT101 synthesized more perlecan at both mRNA and protein levels than its normal counterpart (Tapanadechopone *et al.*, 2001). Studies also found that down-regulation of perlecan expression inhibited tumour growth and angiogenesis *in vivo* (Sharma *et al.*, 1998) and suppressed the proliferation of melanoma cells *in vitro* (Adatia *et al.*, 1997).

More evidence was accumulated in recent years. Ghiselli *et al.* (2001) demonstrated that by using targeted homologous recombination method, they found the perlecan-deficient human colon carcinoma cells grew much more slowly both *in vitro* and *in vivo*, did not respond to FGF7 and were less tumourigenic than control cells. Jiang *et al.* (2004) showed that antisense targeting of perlecan inhibited tumour cell growth *in vitro* and *in vivo*, while exogenous recombinant perlecan restored the growth of antisense perlecan-expressing cells of mouse RT101 epithelial tumours. Zhou *et al.* (2004) showed very similar findings in proteoglycan-mutated mice which exhibited significantly retarded FGF-2-induced tumour growth, and defective angiogenesis. Using a ribozyme approach to knockdown the expression of perlecan both at mRNA and protein levels in prostate cells, Savoe *et al.* (2005) showed that

knockdown perlecan reduced cell adhesion *in vitro* and tumour growth *in vivo* with smaller tumour size and less vascularization.

Though a lot of experiments showed a positive effect of perlecan in tumourigenesis, growth, invasion and metastasis, there were also evidence showing the different effect of perlecan in tumours. Mathiak *et al.* (1997) reported that in human fibrosarcoma cells, antisense suppression of perlecan expression resulted in stimulation of tumour cell growth, both *in vitro* and *in vivo*, and increased invasion of ECM. Later in human Kaposi's sarcoma cells, Marchisone *et al.* (2000) demonstrated that antisense reduction of perlecan reduced cell migration and proliferation *in vitro* but increased tumour growth *in vivo*.

To reconcile the discrepancy, Knox and collaborators (Knox and Whitelock, 2006) suggested that the local context of the extracellular microenvironment defines the function and downstream effects of perlecan. Many researches have confirmed that perlecan exerted its function together with the binding of many growth factors such as FGF2, VEGF and FGF7. Perlecan may modulate the activities of those growth factors by either sequestering them in the BMs and ECM or presenting them to their cell surface receptors (Jiang and Couchman, 2003; Fjeldstad and Kolset, 2005), such that in the positive relationship of perlecan with tumour growth, perlecan may favour the diffusion and presentation of growth factors, leading to enhanced tumour growth.

This can also be the explanation in the present findings up-regulation of HSPG2 and down-regulation of EXTL2 render the *HS3ST3A1* silenced MCF-12A cell

malignant phenotype which showed increased migration and invasion while decreased cell adhesion *in vitro*.

Although many genes found in the present study have not been directly linked each other in the PathwayStudio software, they may also function in the phenotype alterations in the MCF-12A cells after silencing *HS3ST3A1*.

Results in Chapter 4 have shown that silencing *HS3ST3A1* in MCF-12A cells made the cell less adhesive to substrate and enhanced migration. Altered-expression of genes encoding cell adhesion/cytoskeleton-associated molecules is thus a reflection of the phenotype alterations. It may be relevant that expressions of some epithelial adhesion molecules which are known to be associated with the breast cancer growth and proliferation and even invasion or metastasis are changed.

One such gene is F11R. F11R which is also known as Junctional adhesion molecule-A (JAM-A), JAM, JAM-1, belongs to the immunoglobulin (Ig) superfamily of cell adhesion molecules and contains two Ig-like domains in its 236-amino-acid long extracellular region (Bazzoni, 2003). It was first identified in human platelets as a 32/36 kDa protein. Later it was also found widely expressed at cell–cell contacts in endothelial and epithelial cell monolayers and predominantly localized to the tight junctions of these cells (Martin-Padura *et al.*, 1998; Liu *et al.*, 2000).

Its down-regulation at mRNA level in MCF-12A cells after silencing *HS3ST3A1* was confirmed by using real-time PCR (**Fig. 5.6**). Down-regulation at protein level was validated by Western blot and immunocytochemical staining (**Fig.5.7**).

Structurally F11R is a transmembrane protein, with the Ig-like extracellular domain, the transmembrane domain and a PDZ-domain-binding cytoplasmic domain. On the basis of this localization and structure of this protein, accumulating evidence showed that F11R in these cells was believed to be involved in the formation of tight junctions (TJs) and the regulation of their integrity (Liang *et al.*, 2000; Bazzoni *et al.*, 2000; Bazzoni *et al.*, 2000b; Liu *et al.*, 2000; Ostermann *et al.*, 2002)..

Tight junctions is a cell-cell adhesion complex in epithelial and endothelial cell monolayers, forming continuous seals around cells and serving as a physical barrier to prevent solutes and water from passing freely through the paracellular space. TJ structure is composed of three regions: (1) the transmembrane region incorporates three families of proteins, occludins, JAMs (JAM-1, 2, 3) and claudins; (2) the peripheral region (comprising the zonula occludens (ZO- 1, 2, 3 and other MAGUK proteins such as MAGI-1); (3) associated proteins (such as AF-6, PAR3cingulin, afadin and α -catenin) (Ebnet *et al.*, 2000; Bazzoni *et al.*, 2000; Bazzoni *et al.*, 2000b; Ebnet *et al.*, 2003; Ebnet *et al.*, 2004). F11R, through its PDZ-domain-binding cytoplasmic domain is involved in the recruitment of ZO-1, AF-6 and Par-3 which are also PDZ-domain-containing proteins.

Growing evidence indicates that F11R proteins contribute to the regulation of TJ integrity. Researches have indicated that in mammalian cells, the recruitment of F11R to the cellular borders to form homodimer appears to be a vital step (Hamazaki *et al.*, 2002), as it allows Par3 to interact with the cytoplasmic domain of F11R. This binding triggers the junctional recruitment of the Par3/Par6/aPKC complex. The latter

step regulates late stages of tight junction assembly that allows the maturation of TJs (Matter and Balda, 2003; Ebnet *et al.*, 2003).

One of the crucial changes detected upon decrease of cell adhesion and enhanced migration is the loss or alteration of intercellular cell–cell contacts and junctions. It was therefore presumed that overexpression of F11R would enhance tight junction formation and inhibit cell migration by enhancing cell-cell contacts. Consistent with this notion, it has recently been shown that loss of F11R enhanced the spontaneous and random motility of F11R-null mouse endothelial cells (Bazzoni *et al.*, 2005). In turn, the enhanced motility of F11R defective cells was abolished after transfection of full-length F11R cDNA (Bazzoni *et al.*, 2005). Moreover, if tested under the presence of shear stress, F11R absence increased protrusion extension in the direction of flow (Huang *et al.*, 2006). Knockdown of endogenous F11R reduced adhesion to vitronectin (Naik *et al.*, 2003b; Naik and Naik, 2006), suggesting that surface expression of F11R regulated the adhesive function. Previous studies have confirmed that F11R also plays a critical role in leukocyte adhesion and migration by heterophilic interactions with FA-L1 integrins (Martin-Padura *et al.*, 1998; Del Maschio *et al.*, 1999; Ostermann *et al.*, 2002; Cera *et al.*, 2004; Corada *et al.*, 2005).

Research findings pointed out that when treating breast cancer MCF-7 and MDA-MB-231 cells with hepatocyte growth factor (HGF), F11R mRNA was reduced (Martin *et al.*, 2004; Martin *et al.*, 2004b). Previously Liu *et al.* (2000) demonstrated that F11R-specific monoclonal antibodies markedly inhibited the function of tight junctions. As studies have been pointed out that HGF promotes both migration and

invasion of breast cancer cell lines (Jiang *et al.*, 2001; Martin and Jiang, 2001; Jiang *et al.*, 2003), these results suggested that the loss of function of F11R may enhance breast cancer migration and invasion. Indeed Martin *et al.* (2007) published a recent paper that revealed strengthening the function of TJs significantly reduced *in vitro* invasion of MDA-MB-231 cells through an endothelial cell barrier and reduced 17-beta-estradiol induced breast cancer cell motility.

Naik *et al.* (2003a) has also showed that F11R was important in the regulation of basic fibroblast growth factor (bFGF)-induced endothelial cell proliferation and angiogenesis. Inhibition of F11R signaling blocks bFGF-induced endothelial cell proliferation, tube formation and *in vivo* angiogenesis.

Taken together, the functional assay results in Chapter 4 are consistent with the above F11R-related experimental data that the proliferation and adhesion were inhibited while the migration and invasion were enhanced.

To summarize above, this study on the gene expression profile after silencing of *HS3ST3A1* gene results in a pattern of transcriptional alterations that represent a unique molecular pathogenesis in the MCF-12A cells. Even this is not yet a full picture of the malignant transformation of breast epithelial cells, the evidence of its function on the phenotype changes and the gene expression signature are pretty informative that *HS3ST3A1* gene is indeed involved in the malignant transformation of breast epithelial cells. The gene expression signature and the possible pathways are consistent with the observation of the phenotypic changes in the MCF-12 cells after silencing *HS3ST3A1* gene. An extensive understanding of the molecular mechanisms

by *HS3ST3A1* mediated through 3-O sulphation in heparan sulphate can not only provide an explanation for the phenotype changes but also suggest novel therapeutic targets for breast cancer.

CHAPTER 6

CONCLUSIONS

AND

FUTURE STUDIES

In the first part of this study, the functions of sulphation status of heparan sulphate in breast cancers were studied and the differentially regulatory effects of exogenous heparan sulphate from different species on the breast cancer behaviours were investigated. The main findings were that undersulphation of heparan sulphate induced by sodium chlorate, a competitive analogue of PAPS in heparan sulphate synthesis, significantly inhibited breast cancer cell growth, decreased breast cancer migration and invasion, possibly through increasing the cell adhesion to ECM components. These data verified that sulphation group in the glycosaminoglycan was involved in cell proliferation of breast cancer. The other main findings were that sulphated heparan sulphate from porcine intestine mucosa (HS-PM) rescued completely the inhibitory effect of sodium chlorate on MCF-7 cell growth. It also showed a rescuing effect, to a less extent on cell growth in MDA-MB-231 cells treated with sodium chlorate. But sulphated heparan sulphate from bovine kidney showed no rescuing effect on the growth impairment induced by sodium chlorate in both breast cancer cell lines. Such diametrically opposite effects were also demonstrated between these two heparan sulphate species on breast cancer cell migration. However, there was a different scenario regarding the function of these two exogenous heparan sulphate in breast cancer cell adhesion.

The study results showed sulphated HS-BK completely abolished the enhancing effect of chlorate on MCF-7 cell adhesion to fibronectin and drastically blocked the increment of cell adhesion to collagen I. But HS-PM showed only a partial blockage of the enhancing effect induced by sodium chlorate on cell adhesion to fibronectin.

However, HS-PM also showed a complete blockage of enhancement induced by sodium chlorate in cell adhesion to collagen I. Such different blockage effects of these two heparan sulphate species were also found in MDA-MB-231 breast cancer cells. As heparan sulphate from porcine intestine mucosa possesses a higher degree of sulphation compared to that obtained from bovine kidney (Toida *et al.*, 1997; Tsuda *et al.*, 1996), conclusion was made that HS-PM and HS-BK may thus be differentially effective in blocking the effect of sodium chlorate on cell adhesion to fibronectin and collagen I.

These results are reminiscent of the Janus-faced functions of heparan sulphate in cancer growth and progression. HSPG functions were not only depended on its sequence and sulphation pattern, but also relied on the growth factors, cytokines, signaling molecules and ECM proteins that were within the proximal microenvironment where heparan sulphate presents and performs its influence.

In the second part of this study, the use of knockdown model to define the functional relationships between HS biosynthetic enzyme *HS3ST3A1* and its biological impact was investigated *in vitro* and the gene interaction networks regulated by 3-O-sulphation of HS was examined by microarray analysis. The results shown in Chapter 4 were that the expression levels of *HS3ST3A1* in four breast cancer cell lines were significantly down-regulated or were not detected compared with that in normal breast epithelial MCF-12A cells. *In situ* hybridization results also showed lower expression levels of *HS3ST3A1* in breast cancer tissues. The results obtained in this study indicated the expression level of *HS3STA1* may play a vital role in breast

tumourigenesis as many researches have revealed that abnormally high or low expression of one gene in normal and/or malignant cells suggests its important function in the transition of the cell phenotype.

Using *HS3ST3A1* siRNA, the expression of *HS3ST3A1* was successfully reduced more than 80%. Thus *in vitro* functional assays were carried out. The results obtained from functional experiments showed that after silencing *HS3ST3A1*, MCF-12A cells were less adhesive to extracellular matrix surface and became more migratory in chemoattractant model and invasive in Matri-gel *in vitro*, two main behaviours of malignant cells. One of the reasons is that the poorer adhesiveness of the cell permits the cells to detach from the cell mass and to shed into their environment, which is the first step for a malignant tumour to metastasize. To metastasize, the cells must further acquire the migratory ability to penetrate epithelial layer of blood vessels and invade into the basal layer of the vessel. Another reason is that silencing the expression *HS3ST3A1* modulates the synthesis of HSPG, which in turn modulates the growth factors sequestered inside, and thus regulating cell signaling. These results also indicate that silencing the expression of *HS3ST3A1* renders in breast epithelial cells a malignant phenotype.

This study also found that MCF-12A cells became less proliferative and cell cycle progression was delayed at the S-G₂ phase transition after the expression of *HS3ST3A1* was silenced. These results in this study are unexpected because they are not consistent with the malignant cell behaviours. However, less proliferation is also often found in other malignant transformation models. For a cell to become more

malignant, it must acquire the ability to grow faster than the normal cells *in vivo* and obtain the dominant status in the cell mass and form a tumour core. One possible explanation for the unexpected results is that HSPG has promoting or inhibitory function on cell growth depending on the sulphation domain of HSPG as well as on its interacting proteins, such as growth factors. Reduction in 3-O-sulphation domain along the HS chains by the siRNA of *HS3ST3A1* possibly changes the interaction of HSPG with growth factors, such as FGF-7 (Ye *et al.*, 2001). Other possible explanation is that cells cultured in 2-D culture *in vitro* are different from the behaviours *in vivo*.

The possible mechanisms underlying the phenotype alterations after silencing *HS3ST3A1* gene expression were studied by genomic gene expression profiling analysis. In Chapter 5, the differential expressed genes were revealed by Affymetrix microarray and a variety of genes that accounted for the alterations in the phenotype of MCF-12A cells after silencing *HS3ST3A1* were identified. Two possible pathways were found, one was cell-cycle related, accounting for less proliferation, and another one was cell-extracellular matrix communication related, accounting for malignant transformation. Taken together the present microarray analysis of the alteration in gene expression reveals a broad panel of genes that help define the signaling pathways used by MCF-12A cell to response to the impaired 3-O sulphation of HS.

The present findings are an excellent pilot work that has begun to delineate gene expression profiles in the transformation of breast epithelial cell to tumour cells after *HS3ST3A1* silencing. The knockdown system also increased understanding of the

novel aspects of HS function in regulatory networks responsible for phenotype alterations. This study has shown for the first time the gene expression alteration at genomic level after silencing *HS3ST3A1* expression in mammalian cells. The gene expression signature revealed by microarray analysis following *HS3ST3A1* silencing provides a complex and interesting base for future studies.

Future studies

Base on the findings in the present study, not only the sulphation degree of heparan sulphate but also the sulphation position plays a role in different function exerted by heparan sulphate in breast cancer behaviours. As commercially available exogenous heparan sulphate are quite heterogeneous in their sulphation degree, other studies using heparan sulphate with defined length or even short oligosaccharides with consistent sulphation pattern should reveal more defined function of sulphation. Experiment using specific enzymatic modified heparan sulphate should give valuable information of the biological function of a particular sulphation position on heparan sulphate.

The results of the function of *HS3ST3A1* gene in this study have important implications for further studies on the involvement of 3-O sulphation of HS as modulators of human breast cancer growth and tumour development. The knockdown effect in MCF-12A cells should be examined using vector-based siRNA and the transfected MCF-12A cells should be further developed into stable siRNA expression cell line. Stable transfected breast epithelial MCF-12A cell lines may represent a useful tool in *in vivo* studies, which could achieve reproducibility and to avoid the

variability of epithelial cell characteristics usually observed in cell cultures conditions. The proliferation and invasion assays should be studied *in vivo* by transplanting this stable cell line into SCID or nude mouse. Stable transfected breast epithelial MCF-12A cell lines should be useful in angiogenesis research *in vivo* as angiogenesis is an important step in tumour progression which requires the tumour size of about 1 mm³.

The regulatory networks revealed in this study should be further investigated by over-expressing down-regulated gene(s) or knocking down up-regulated gene(s) in the stably cell line. By such a method, specific pathways in the downstream of silencing *HS3ST3A1* can be elucidated. The ligands of 3-O sulphated HS should be identified to examine the functions of this class of enzyme in the breast tumourigenesis. Ligand binding study should reveal new insights into the function of *HS3ST3A1* gene in the development of breast cancer.

REFERENCES

Adatia,R., Albini,A., Carlone,S., Giunciuglio,D., Benelli,R., Santi,L., and Noonan,D.M. (1997). Suppression of invasive behavior of melanoma cells by stable expression of anti-sense perlecancDNA. *Ann Oncol* 8, 1257-1261.

Affymetrix (2001). *Microarray Suite User Guide version 5.0*, Affymetrix, Santa Clara, CA.

Affymetrix Inc (2002). *Statistical algorithms description document*.

[www.affymetrix.com/support/technical/whitepapers/sadd whitepaper.pdf](http://www.affymetrix.com/support/technical/whitepapers/sadd%20whitepaper.pdf).

Ahn,J., Ludecke,H.J., Lindow,S., Horton,W.A., Lee,B., Wagner,M.J., Horsthemke,B., and Wells,D.E. (1995). Cloning of the putative tumour suppressor gene for hereditary multiple exostoses (EXT1). *Nat. Genet.* 11, 137-143.

Aikawa,J.i., Grobe,K., Tsujimoto,M., and Esko,J.D. (2001). Multiple Isozymes of Heparan Sulfate/Heparin GlcNAc N-Deacetylase/GlcN N-Sulfotransferase. Structure and activity of the forth member, NDST4. *J. Biol. Chem.* 276, 5876-5882.

American Cancer Society. (2007). *Cancer Facts and Figures 2007*.Atlanta, GA. <http://www.cancer.org/downloads/STT/CAFF2007PWSecured.pdf>.

Andrieu,N., Goldgar,D.E., Easton,D.F., Rookus,M., Brohet,R., Antoniou,A.C., Peock,S., Evans,G., Eccles,D., Douglas,F., Nogues,C., Gauthier-Villars,M., Chompret,A., Van Leeuwen,F.E., Kluijdt,I., Benitez,J., Arver,B., Olah,E., and Chang-Claude,J. (2006). Pregnancies, breast-feeding, and breast cancer risk in the International BRCA1/2 Carrier Cohort Study (IBCCS). *J Natl. Cancer Inst.* 98, 535-544.

Anfosso,F., Bardin,N., Frances,V., Vivier,E., Camoin-Jau,L., Sampol,J., and Dignat-George,F. (1998). Activation of Human Endothelial Cells via S-Endo-1 Antigen (CD146) Stimulates the Tyrosine Phosphorylation of Focal Adhesion Kinase p125FAK. *J. Biol. Chem.* 273, 26852-26856.

Averbeck,M., Gebhardt,C., Anderegg,U., Termeer,C., Sleeman,J.P., and Simon,J.C. (2007). Switch in syndecan-1 and syndecan-4 expression controls maturation associated dendritic cell motility. *Exp. Dermatol.* 16, 580-589.

Aviezer,D., Levy,E., Safran,M., Svahn,C., Buddecke,E., Schmidt,A., David,G, Vlodaysky,I., and Yayon,A. (1994). Differential structural requirements of heparin and heparan sulfate proteoglycans that promote binding of basic fibroblast growth factor to its receptor. *J Biol. Chem.* 269, 114-121.

Bai,X., and Esko,J.D. (1996). An animal cell mutant defective in heparan sulfate hexuronic acid 2-O-sulfation. *J Biol Chem* 271, 17711-17717.

Bai,X., Wei,G., Sinha,A., and Esko,J.D. (1999). Chinese Hamster Ovary Cell Mutants Defective in Glycosaminoglycan Assembly and Glucuronosyltransferase I. *Journal of Biological Chemistry* 274, 13017-13024.

Balmain,A., Gray,J., and Ponder,B. (2003). The genetics and genomics of cancer. *Nat Genet* 33 *Suppl*, 238-244.

Bame,K.J., and Esko,J.D. (1989). Undersulfated heparan sulfate in a Chinese hamster ovary cell mutant defective in heparan sulfate N-sulfotransferase. *Journal of Biological Chemistry* 264, 8059-8065.

Barton,M.B., Harris,R., and Fletcher,S.W. (1999). The rational clinical examination. Does this patient have breast cancer? The screening clinical breast examination: should it be done? How? *JAMA* 282, 1270-1280.

Basolo,F., Elliott,J., Tait,L., Chen,X.Q., Maloney,T., Russo,I.H., Pauley,R., Momiki,S., Caamano,J., Klein-Szanto,A.J., and . (1991). Transformation of human breast epithelial cells by c-Ha-ras oncogene. *Mol Carcinog.* 4, 25-35.

Bazzoni,G. (2003). The JAM family of junctional adhesion molecules. *Curr. Opin. Cell Biol.* 15, 525-530.

Bazzoni,G., Tonetti,P., Manzi,L., Cera,M.R., Balconi,G., and Dejana,E. (2005). Expression of junctional adhesion molecule-A prevents spontaneous and random motility. *J Cell Sci.* 118, 623-632.

Bazzoni,G., Martinez-Estrada,O.M., Mueller,F., Nelboeck,P., Schmid,G., Bartfai,T., Dejana,E., and Brockhaus,M. (2000a). Homophilic Interaction of Junctional Adhesion Molecule. *J. Biol. Chem.* 275, 30970-30976.

Bazzoni,G., Martinez-Estrada,O.M., Orsenigo,F., Cordenosi,M., Citi,S., and Dejana,E. (2000b). Interaction of Junctional Adhesion Molecule with the Tight Junction Components ZO-1, Cingulin, and Occludin. *J. Biol. Chem.* 275, 20520-20526.

Beauvais,D.M., Burbach,B.J., and Rapraeger,A.C. (2004). The syndecan-1 ectodomain regulates alphavbeta3 integrin activity in human mammary carcinoma cells. *J Cell Biol.* 167, 171-181.

Beauvais,D.M., and Rapraeger,A.C. (2003). Syndecan-1-mediated cell spreading requires signaling by [alpha]v[beta]3 integrins in human breast carcinoma cells. *Experimental Cell Research* 286, 219-232.

Benson,S.R., Blue,J., Judd,K., and Harman,J.E. (2004). Ultrasound is now better than mammography for the detection of invasive breast cancer. *Am J Surg.* 188, 381-385.

Berg,W.A., Gutierrez,L., NessAiver,M.S., Carter,W.B., Bhargavan,M., Lewis,R.S., and Ioffe,O.B. (2004). Diagnostic accuracy of mammography, clinical examination, US, and MR imaging in preoperative assessment of breast cancer. *Radiology* 233, 830-849.

Bernfield,M., Gotte,M., Park,P.W., Reizes,O., Fitzgerald,M.L., Lincecum,J., and Zako,M. (1999). Functions of cell surface heparan sulfate proteoglycans. *Annu. Rev. Biochem* 68, 729-777.

- Bernstein,E., Caudy,A.A., Hammond,S.M., and Hannon,G.J. (2001). Role for a bidentate ribonuclease in the initiation step of RNA interference. *Nature* 409, 363-366.
- Berx,G., Cleton-Jansen,A.M., Nollet,F., de Leeuw,W.J., van,d., V, Cornelisse,C., and van,R.F. (1995). E-cadherin is a tumour/invasion suppressor gene mutated in human lobular breast cancers. *EMBO J* 14, 6107-6115.
- Bianchini,P., Liverani,L., Mascellani,G., and Parma,B. (1997). Heterogeneity of unfractionated heparins studied in connection with species, source, and production processes. *Semin. Thromb Hemost.* 23, 3-10.
- Bogenrieder,T., and Herlyn,M. (2003). Axis of evil: molecular mechanisms of cancer metastasis. *Oncogene* 22, 6524-6536.
- Bowen,T.J., Yakushiji,H., Montagna,C., Jain,S., Ried,T., and Wynshaw-Boris,A. (2005). Atm heterozygosity cooperates with loss of Brca1 to increase the severity of mammary gland cancer and reduce ductal branching. *Cancer Res* 65, 8736-8746.
- Boyd,D.D., and Nakajima,M. (2004). Involvement of heparanase in tumor metastases: a new target in cancer therapy? *J. Natl. Cancer Inst.* 96, 1194-1195.
- Brodie,S.G., Xu,X., Qiao,W., Li,W.M., Cao,L., and Deng,C.X. (2001). Multiple genetic changes are associated with mammary tumorigenesis in Brca1 conditional knockout mice. *Oncogene* 20, 7514-7523.
- Brunner,G., Reibold,K., Meissauer,A., Schirmacher,V., and Erkell,L.J. (1998). Sulfated glycosaminoglycans enhance tumor cell invasion in vitro by stimulating plasminogen activation. *Exp. Cell Res* 239, 301-310.
- Burbach,B.J., Ji,Y., and Rapraeger,A.C. (2004). Syndecan-1 ectodomain regulates matrix-dependent signaling in human breast carcinoma cells. *Experimental Cell Research* 300, 234-247.
- Busse,M., and Kusche-Gullberg,M. (2003). In Vitro Polymerization of Heparan Sulfate Backbone by the EXT Proteins. *J. Biol. Chem.* 278, 41333-41337.
- Callahan,R., and Egan,S.E. (2004). Notch signaling in mammary development and oncogenesis. *J Mammary. Gland. Biol. Neoplasia.* 9, 145-163.
- Carlson,R.W., Hudis,C.A., and Pritchard,K.I. (2006). Adjuvant endocrine therapy in hormone receptor-positive postmenopausal breast cancer: evolution of NCCN, ASCO, and St Gallen recommendations. *J Natl. Compr. Canc. Netw.* 4, 971-979.
- Carmichael,A.R. (2006). Obesity as a risk factor for development and poor prognosis of breast cancer. *BJOG.* 113, 1160-1166.

Cary,L.A., and Guan,J.L. (1999). Focal adhesion kinase in integrin-mediated signaling. *Front Biosci.* *4*, D102-D113.

Cera,M.R., Del,P.A., Vecchi,A., Corada,M., Martin-Padura,I., Motoike,T., Tonetti,P., Bazzoni,G., Vermi,W., Gentili,F., Bernasconi,S., Sato,T.N., Mantovani,A., and Dejana,E. (2004). Increased DC trafficking to lymph nodes and contact hypersensitivity in junctional adhesion molecule-A-deficient mice. *J Clin Invest* *114*, 729-738.

Chaiwun,B., and Thorner,P. (2007). Fine needle aspiration for evaluation of breast masses. *Curr. Opin. Obstet. Gynecol.* *19*, 48-55.

Chambers,A.F., Groom,A.C., and MacDonald,I.C. (2002). Dissemination and growth of cancer cells in metastatic sites. *Nat Rev. Cancer* *2*, 563-572.

Chang,H. (2007). RNAi-mediated knockdown of target genes: a promising strategy for pancreatic cancer research. *Cancer Gene Ther* *14*, 677-685.

Charnaux,N., Brule,S., Hamon,M., Chaigneau,T., Saffar,L., Prost,C., Lievre,N., and Gattegno,L. (2005). Syndecan-4 is a signaling molecule for stromal cell-derived factor-1 (SDF-1)/ CXCL12. *FEBS J* *272*, 1937-1951.

Chen,J., Duncan,M.B., Carrick,K., Pope,R.M., and Liu,J. (2003). Biosynthesis of 3-O-sulfated heparan sulfate: unique substrate specificity of heparan sulfate 3-O-sulfotransferase isoform 5. *Glycobiology* *13*, 785-794.

Chen,J., and Liu,J. (2005). Characterization of the structure of antithrombin-binding heparan sulfate generated by heparan sulfate 3-O-sulfotransferase 5. *Biochim. Biophys. Acta* *1725*, 190-200.

Chen,L., Klass,C., and Woods,A. (2004). Syndecan-2 regulates transforming growth factor- β signaling. *Journal of Biological Chemistry* *279*, 15715-15718.

Cheng,J., Sun,S., Tracy,A., Hubbell,E., Morris,J., Valmeekam,V., Kimbrough,A., Cline,M.S., Liu,G., Shigeta,R., Kulp,D., and Siani-Rose,M.A. (2004). NetAffx Gene Ontology Mining Tool: a visual approach for microarray data analysis. *Bioinformatics.* *20*, 1462-1463.

Chew,I., Tan,Y., and Tan,P.H. (2006). Cytology is useful in breast screening: results and long-term follow-up of the Singapore Breast Screening Pilot Project. *Cytopathology* *17*, 227-232.

Chia,K.S., Reilly,M., Tan,C.S., Lee,J., Pawitan,Y., Adami,H.O., Hall,P., and Mow,B. (2005). Profound changes in breast cancer incidence may reflect changes into a Westernized lifestyle: a comparative population-based study in Singapore and Sweden. *Int. J Cancer* *113*, 302-306.

Chu,L., Scharf,E., and Kondo,T. (2001). GeneSpringTM: Tools for Analyzing Microarray Expression Data. *Genome Informatics* *12*, 227-229.

- Chua,C.C., Rahimi,N., Forsten-Williams,K., and Nugent,M.A. (2004). Heparan sulfate proteoglycans function as receptors for fibroblast growth factor-2 activation of extracellular signal-regulated kinases 1 and 2. *Circ. Res* 94, 316-323.
- Clark,G.J., Kinch,M.S., Gilmer,T.M., Burridge,K., and Der,C.J. (1996). Overexpression of the Ras-related TC21/R-Ras2 protein may contribute to the development of human breast cancers. *Oncogene* 12, 169-176.
- Clarke,P.R., and Sanderson,H.S. (2006). A mitotic role for BRCA1/BARD1 in tumor suppression? *Cell* 127, 453-455.
- Clemons,M., and Goss,P. (2001). Estrogen and the risk of breast cancer. *N. Engl. J Med.* 344, 276-285.
- Cohen,I., Pappo,O., Elkin,M., San,T., Bar-Shavit,R., Hazan,R., Peretz,T., Vlodaysky,I., and Abramovitch,R. (2006). Heparanase promotes growth, angiogenesis and survival of primary breast tumors. *Int. J Cancer* 118, 1609-1617.
- Cohen,I.R., Murdoch,A.D., Naso,M.F., Marchetti,D., Berd,D., and Iozzo,R.V. (1994). Abnormal Expression of Perlecan Proteoglycan in Metastatic Melanomas. *Cancer Res* 54, 5771-5774.
- Collaborative Group on Hormonal Factors in Breast Cancer. (2001). Familial breast cancer: collaborative reanalysis of individual data from 52 epidemiological studies including 58,209 women with breast cancer and 101,986 women without the disease. *Lancet* 358, 1389-1399.
- Collins,F.S., Green,E.D., Guttmacher,A.E., and Guyer,M.S. (2003). A vision for the future of genomics research. *Nature* 422, 835-847.
- Coltrini,D., Rusnati,M., Zoppetti,G., Oreste,P., Grazioli,G., Naggi,A., and Presta,M. (1994). Different effects of mucosal, bovine lung and chemically modified heparin on selected biological properties of basic fibroblast growth factor. *Biochem J* 303 (Pt 2), 583-590.
- Contreras,H.R., Fabre,M., Granes,F., Casaroli-Marano,R., Rocamora,N., Herreros,A.G., Reina,M., and Vilaro,S. (2001). Syndecan-2 Expression in Colorectal Cancer-Derived HT-29 M6 Epithelial Cells Induces a Migratory Phenotype. *Biochemical and Biophysical Research Communications* 286, 742-751.
- Cool,S.M., and Nurcombe,V. (2006). Heparan sulfate regulation of progenitor cell fate. *J. Cell Biochem.* 99, 1040-1051.
- Coombe,D.R., and Kett,W.C. (2005b). Heparan sulfate-protein interactions: therapeutic potential through structure-function insights. *Cell Mol. Life Sci.* 62, 410-424.
- Coombe,D.R., and Kett,W.C. (2005a). Heparan sulfate-protein interactions: therapeutic potential through structure-function insights. *Cell Mol Life Sci.* 62, 410-424.

Coombs,N.J., Taylor,R., Wilcken,N., and Boyages,J. (2005). Hormone replacement therapy and breast cancer: estimate of risk. *BMJ* 331, 347-349.

Corada,M., Chimenti,S., Cera,M.R., Vinci,M., Salio,M., Fiordaliso,F., De,A.N., Villa,A., Bossi,M., Staszewsky,L.I., Vecchi,A., Parazzoli,D., Motoike,T., Latini,R., and Dejana,E. (2005). Junctional adhesion molecule-A-deficient polymorphonuclear cells show reduced diapedesis in peritonitis and heart ischemia-reperfusion injury. *Proc. Natl. Acad. Sci U. S. A* 102, 10634-10639.

Couch,F.J., Cerhan,J.R., Vierkant,R.A., Grabrick,D.M., Therneau,T.M., Pankratz,V.S., Hartmann,L.C., Olson,J.E., Vachon,C.M., and Sellers,T.A. (2001). Cigarette Smoking Increases Risk for Breast Cancer in High-Risk Breast Cancer Families. *Cancer Epidemiol Biomarkers Prev* 10, 327-332.

Couldrey,C., and Green,J.E. (2000). Metastases: the glycan connection. *Breast Cancer Res* 2, 321-323.

Critchley,D.R. (2000). Focal adhesions - the cytoskeletal connection. *Curr. Opin. Cell Biol* 12, 133-139.

Datta,M.W., Hernandez,A.M., Schlicht,M.J., Kahler,A.J., DeGueme,A.M., Dhir,R., Shah,R.B., Farach-Carson,C., Barrett,A., and Datta,S. (2006). Perlecan, a candidate gene for the CAPB locus, regulates prostate cancer cell growth via the Sonic Hedgehog pathway. *Mol Cancer* 5, 9.

David,G., Bai,X.M., Van der Schueren,B., Cassiman,J.J., and Van den Berghe,H. (1992). Developmental changes in heparan sulfate expression: in situ detection with mAbs. *J. Cell Biol.* 119, 961-975.

Dejima,K., Seko,A., Yamashita,K., Gengyo-Ando,K., Mitani,S., Izumikawa,T., Kitagawa,H., Sugahara,K., Mizuguchi,S., and Nomura,K. (2006). Essential roles of 3'-phosphoadenosine 5'-phosphosulfate (PAPS) synthase in embryonic and larval development of the nematode *Caenorhabditis elegans*. *Journal of Biological Chemistry* M601509200.

Del Maschio,A., De Luigi,A., Martin-Padura,I., Brockhaus,M., Bartfai,T., Fruscella,P., Adorini,L., Martino,G., Furlan,R., De Simoni,M.G., and Dejana,E. (1999). Leukocyte Recruitment in the Cerebrospinal Fluid of Mice with Experimental Meningitis Is Inhibited by an Antibody to Junctional Adhesion Molecule (JAM). *J. Exp. Med.* 190, 1351-1356.

Delehedde,M., Deudon,E., Boilly,B., and Hondermarck,H. (1996a). Heparan sulfate proteoglycans play a dual role in regulating fibroblast growth factor-2 mitogenic activity in human breast cancer cells. *Exp. Cell Res* 229, 398-406.

Delehedde,M., Deudon,E., Boilly,B., and Hondermarck,H. (1996b). [Involvement of sulfated proteoglycans in the control of proliferation of MCF-7 breast cancer cells]. *Bull. Cancer* 83, 129-134.

Delehedde,M., Lyon,M., Sergeant,N., Rahmoune,H., and Fernig,D.G. (2001). Proteoglycans: pericellular and cell surface multireceptors that integrate external stimuli in the mammary gland. *J*

Mammary. Gland. Biol Neoplasia. 6, 253-273.

Dementiev,A., Petitou,M., Herbert,J.M., and Gettins,P.G. (2004). The ternary complex of antithrombin-anhydrothrombin-heparin reveals the basis of inhibitor specificity. *Nat. Struct. Mol. Biol.* 11, 863-867.

Deng,C.X., and Wang,R.H. (2003). Roles of BRCA1 in DNA damage repair: a link between development and cancer. *Hum. Mol Genet* 12 *Spec No 1*, R113-R123.

Derksen,P.W., Keehnen,R.M., Evers,L.M., van Oers,M.H., Spaargaren,M., and Pals,S.T. (2002). Cell surface proteoglycan syndecan-1 mediates hepatocyte growth factor binding and promotes Met signaling in multiple myeloma. *Blood* 99, 1405-1410.

Desbordes,S.C., and Sanson,B. (2003). The glypican Dally-like is required for Hedgehog signalling in the embryonic epidermis of *Drosophila*. *Development* 130, 6245-6255.

Devi,G.R. (2006). siRNA-based approaches in cancer therapy. *Cancer Gene Ther.* 13, 819-829.

Dhoot,G.K., Gustafsson,M.K., Ai,X., Sun,W., Standiford,D.M., and Emerson,C.P., Jr. (2001). Regulation of Wnt signaling and embryo patterning by an extracellular sulfatase. *Science* 293, 1663-1666.

Dick,C.P.C., Going,J.J., and Brock,G.J.R. (2004). Promoter methylation in five members of the 3-OST gene family in breast cancer. *Journal of Pathology* 204, 3A.

Dillon,M.F., Hill,A.D., Quinn,C.M., O'Doherty,A., McDermott,E.W., and O'Higgins,N. (2005). The accuracy of ultrasound, stereotactic, and clinical core biopsies in the diagnosis of breast cancer, with an analysis of false-negative cases. *Ann Surg.* 242, 701-707.

Dolan,M., Horchar,T., Rigatti,B., and Hassell,J.R. (1997). Identification of sites in domain I of perlecan that regulate heparan sulfate synthesis. *J Biol. Chem.* 272, 4316-4322.

Duffy,M.J. (1999). CA 15-3 and related mucins as circulating markers in breast cancer. *Ann Clin Biochem.* 36 (Pt 5), 579-586.

Duggan,D.J., Bittner,M., Chen,Y., Meltzer,P., and Trent,J.M. (1999). Expression profiling using cDNA microarrays. *Nat. Genet.* 21, 10-14.

Dulic,V., Lees,E., and Reed,S.I. (1992). Association of human cyclin E with a periodic G1-S phase protein kinase. *Science* 257, 1958-1961.

Dumur,C.I., Nasim,S., Best,A.M., Archer,K.J., Ladd,A.C., Mas,V.R., Wilkinson,D.S., Garrett,C.T., and Ferreira-Gonzalez,A. (2004). Evaluation of quality-control criteria for microarray gene expression analysis. *Clin Chem* 50, 1994-2002.

Duncan,M.B., Chen,J., Krise,J.P., and Liu,J. (2004). The biosynthesis of anticoagulant heparan sulfate by the heparan sulfate 3-O-sulfotransferase isoform 5. *Biochim. Biophys. Acta* 1671, 34-43.

Dupont,W.D., and Page,D.L. (1985). Risk factors for breast cancer in women with proliferative breast disease. *N Engl J Med* 312, 146-151.

Early Breast Cancer Trialists' Collaborative Group (1998). Tamoxifen for early breast cancer: an overview of the randomised trials. *Lancet* 351, 1451-1467.

Easton,D.F., Bishop,D.T., Ford,D., and Crockford,G.P. (1993b). Genetic linkage analysis in familial breast and ovarian cancer: results from 214 families. The Breast Cancer Linkage Consortium. *Am J Hum. Genet.* 52, 678-701.

Easton,D.F., Bishop,D.T., Ford,D., and Crockford,G.P. (1993a). Genetic linkage analysis in familial breast and ovarian cancer: results from 214 families. The Breast Cancer Linkage Consortium. *Am J Hum. Genet* 52, 678-701.

Ebnet,K., Suzuki,A., Ohno,S., Vestweber,D., Cera,M.R., Del,P.A., Vecchi,A., Corada,M., Martin-Padura,I., Motoike,T., et al. (2004). Junctional adhesion molecules (JAMs): more molecules with dual functions? *J Cell Sci* 117, 19-29.

Ebnet,K., Schulz,C.U., Meyer zu Brickwedde,M.-K., Pendl,G.G., and Vestweber,D. (2000). Junctional Adhesion Molecule Interacts with the PDZ Domain-containing Proteins AF-6 and ZO-1. *J. Biol. Chem.* 275, 27979-27988.

Ebnet,K., urrand-Lions,M., Kuhn,A., Kiefer,F., Butz,S., Zander,K., Brickwedde,M.-K.M.z., Suzuki,A., Imhof,B.A., and Vestweber,D. (2003). The junctional adhesion molecule (JAM) family members JAM-2 and JAM-3 associate with the cell polarity protein PAR-3: a possible role for JAMs in endothelial cell polarity. *J Cell Sci* 116, 3879-3891.

Eccles,S.A. (1999). Heparanase: breaking down barriers in tumors. *Nat. Med.* 5, 735-736.

Edovitsky,E., Elkin,M., Zcharia,E., Peretz,T., and Vlodavsky,I. (2004a). Heparanase gene silencing, tumor invasiveness, angiogenesis, and metastasis. *J Natl. Cancer Inst.* 96, 1219-1230.

Eiermann,W., Paepke,S., Appfelstaedt,J., Llombart-Cussac,A., Eremin,J., Vinholes,J., Mauriac,L., Ellis,M., Lassus,M., Chaudri-Ross,H.A., Dugan,M., and Borgs,M. (2001). Preoperative treatment of postmenopausal breast cancer patients with letrozole: A randomized double-blind multicenter study. *Ann Oncol* 12, 1527-1532.

Elbashir,S.M., Lendeckel,W., and Tuschl,T. (2001). RNA interference is mediated by 21- and 22-nucleotide RNAs. *Genes Dev.* 15, 188-200.

Elkin,M., Cohen,I., Zcharia,E., Orgel,A., Guatta-Rangini,Z., Peretz,T., Vlodavsky,I., and Kleinman,H.K. (2003). Regulation of heparanase gene expression by estrogen in breast cancer 18. *Cancer Res* 63, 8821-8826.

Elkin,M., Ilan,N., Ishai-Michaeli,R., Friedmann,Y., Papo,O., Pecker,I., and Vlodavsky,I. (2001). Heparanase as mediator of angiogenesis: mode of action. *FASEB J* 15, 1661-1663.

- Esko,J.D., Elgavish,A., Prasthofer,T., Taylor,W.H., and Weinke,J.L. (1986). Sulfate transport-deficient mutants of Chinese hamster ovary cells. Sulfation of glycosaminoglycans dependent on cysteine. *J Biol Chem* 261, 15725-15733.
- Esko,J.D., and Selleck,S.B. (2002). Order out of chaos: assembly of ligand binding sites in heparan sulfate. *Annu. Rev. Biochem* 71, 435-471.
- Fant,X., Merdes,A., and Haren,L. (2004). Cell and molecular biology of spindle poles and NuMA. *Int. Rev. Cytol.* 238, 1-57.
- Farach-Carson,M.C., Hecht,J.T., and Carson,D.D. (2005). Heparan sulfate proteoglycans: key players in cartilage biology. *Crit Rev. Eukaryot. Gene Expr.* 15, 29-48.
- Farndale,R.W., Buttle,D.J., and Barrett,A.J. (1986). Improved quantitation and discrimination of sulphated glycosaminoglycans by use of dimethylmethylene blue. *Biochim. Biophys. Acta* 883, 173-177.
- Fears,C.Y., Gladson,C.L., and Woods,A. (2006). Syndecan-2 is expressed in the microvasculature of gliomas and regulates angiogenic processes in microvascular endothelial cells. *J Biol Chem* 281, 14533-14536.
- Fears,C.Y., and Woods,A. (2006). The role of syndecans in disease and wound healing. *Matrix Biology* 25, 443-456.
- Ferrara,N. (1996). Vascular endothelial growth factor. *Eur. J Cancer* 32A, 2413-2422.
- Ferrara,N., and Gerber,H.P. (2001). The role of vascular endothelial growth factor in angiogenesis. *Acta Haematol.* 106, 148-156.
- Ferretti,G, Felici,A., Papaldo,P., Fabi,A., and Cognetti,F. (2007). HER2/neu role in breast cancer: from a prognostic foe to a predictive friend. *Curr. Opin. Obstet. Gynecol.* 19, 56-62.
- Feyerabend,T.B., Li,J.P., Lindahl,U., and Rodewald,H.R. (2006). Heparan sulfate C5-epimerase is essential for heparin biosynthesis in mast cells. *Nat Chem Biol* 2, 195-196.
- Filmus,J. (2001). Glypicans in growth control and cancer. *Glycobiology* 11, 19R-23R.
- Filmus,J., and Selleck,S.B. (2001). Glypicans: proteoglycans with a surprise. *J Clin Invest* 108, 497-501.
- Fire,A., Xu,S., Montgomery,M.K., Kostas,S.A., Driver,S.E., and Mello,C.C. (1998). Potent and specific genetic interference by double-stranded RNA in *Caenorhabditis elegans*. *Nature* 391, 806-811.
- Fjeldstad,K., and Kolset,S.O. (2005). Decreasing the Metastatic Potential in Cancers - Targeting the Heparan Sulfate Proteoglycans. *Current Drug Targets* 6, 665-682.

Floris,S., van den,B.J., van der Pol,S.M., Dijkstra,C.D., and De Vries,H.E. (2003). Heparan sulfate proteoglycans modulate monocyte migration across cerebral endothelium. *J Neuropathol. Exp. Neurol.* 62, 780-790.

Fodor,S.P., Rava,R.P., Huang,X.C., Pease,A.C., Holmes,C.P., and Adams,C.L. (1993). Multiplexed biochemical assays with biological chips. *Nature* 364, 555-556.

Fodor,S.P., Read,J.L., Pirrung,M.C., Stryer,L., Lu,A.T., and Solas,D. (1991). Light-directed, spatially addressable parallel chemical synthesis. *Science* 251, 767-773.

Ford,D., Easton,D.F., and Peto,J. (1995). Estimates of the gene frequency of BRCA1 and its contribution to breast and ovarian cancer incidence. *Am J Hum. Genet* 57, 1457-1462.

Forsberg,E., and Kjellen,L. (2001a). Heparan sulfate: lessons from knockout mice. *J. Clin. Invest* 108, 175-180.

Forsten,K.E., Courant,N.A., and Nugent,M.A. (1997). Endothelial proteoglycans inhibit bFGF binding and mitogenesis. *J Cell Physiol* 172, 209-220.

Fournier,A., Berrino,F., Riboli,E., Avenel,V., and Clavel-Chapelon,F. (2005). Breast cancer risk in relation to different types of hormone replacement therapy in the E3N-EPIC cohort. *Int. J Cancer* 114, 448-454.

Fraser,J.R., Laurent,T.C., and Laurent,U.B. (1997). Hyaluronan: its nature, distribution, functions and turnover. *J Intern. Med* 242, 27-33.

Friedrich,M.V., Gohring,W., Morgelin,M., Brancaccio,A., David,G., and Timpl,R. (1999). Structural basis of glycosaminoglycan modification and of heterotypic interactions of perlecan domain V. *J Mol Biol.* 294, 259-270.

Fritz,A., Percy,C., Jack,A., Shanmugaratnam,K., Sobin,L., Parkin,D.M., and Whelan,S. (2000). *International Classification of Diseases for Oncology. 3rd Edition.* Geneva: World Health Organization.

Fritz,T.A., Gabb,M.M., Wei,G., and Esko,J.D. (1994). Two N-acetylglucosaminyltransferases catalyze the biosynthesis of heparan sulfate. *J Biol. Chem.* 269, 28809-28814.

Fuchs,U., and Borkhardt,A. (2007). The application of siRNA technology to cancer biology discovery. *Adv. Cancer Res* 96, 75-102.

Fujiwara,Y., and Kaji,T. (1999). Possible mechanism for lead inhibition of vascular endothelial cell proliferation: a lower response to basic fibroblast growth factor through inhibition of heparan sulfate synthesis. *Toxicology* 133, 147-157.

Funderburgh,J.L. (2000). Keratan sulfate: structure, biosynthesis, and function. *Glycobiology* 10, 951-958.

Gago-Dominguez,M., Yuan,J.M., Sun,C.L., Lee,H.P., and Yu,M.C. (2003). Opposing effects of dietary n-3 and n-6 fatty acids on mammary carcinogenesis: The Singapore Chinese Health Study. *Br. J Cancer* 89, 1686-1692.

Gaither,A., and Iourgenko,V. (2007). RNA interference technologies and their use in cancer research. *Curr. Opin. Oncol.* 19, 50-54.

Gartel,A.L., and Kandel,E.S. (2006). RNA interference in cancer. *Biomol. Eng* 23, 17-34.

Gebiski,V., Lagleva,M., Keech,A., Simes,J., and Langlands,A.O. (2006). Survival Effects of Postmastectomy Adjuvant Radiation Therapy Using Biologically Equivalent Doses: A Clinical Perspective. *J. Natl. Cancer Inst.* 98, 26-38.

Geng,Y., Yu,Q., Whoriskey,W., Dick,F., Tsai,K.Y., Ford,H.L., Biswas,D.K., Pardee,A.B., Amati,B., Jacks,T., Richardson,A., Dyson,N., and Sicinski,P. (2001). Expression of cyclins E1 and E2 during mouse development and in neoplasia. *Proc. Natl. Acad. Sci. U. S. A* 98, 13138-13143.

Ghimenti,C., Sensi,E., Presciuttini,S., Brunetti,I.M., Conte,P., Bevilacqua,G., and Caligo,M.A. (2002). Germline mutations of the BRCA1-associated ring domain (BARD1) gene in breast and breast/ovarian families negative for BRCA1 and BRCA2 alterations. *Genes Chromosomes. Cancer* 33, 235-242.

Ghiselli,G., Eichstetter,I., and Iozzo,R.V. (2001). A role for the perlecan protein core in the activation of the keratinocyte growth factor receptor. *Biochem. J* 359, 153-163.

Gingis-Velitski,S., Zetser,A., Flugelman,M.Y., Vlodavsky,I., and Ilan,N. (2004a). Heparanase induces endothelial cell migration via protein kinase B/Akt activation. *J Biol Chem.* 279, 23536-23541.

Gingis-Velitski,S., Zetser,A., Kaplan,V., Ben Zaken,O., Cohen,E., Levy-Adam,F., Bashenko,Y., Flugelman,M.Y., Vlodavsky,I., and Ilan,N. (2004b). Heparanase uptake is mediated by cell membrane heparan sulfate proteoglycans. *J. Biol. Chem.* 279, 44084-44092.

Giroux,J.L., Matou,S., Bros,A., Tapon-Brethaudiere,J., Letourneur,D., and Fischer,A.M. (1998). Modulation of human endothelial cell proliferation and migration by fucoidan and heparin. *Eur. J Cell Biol* 77, 352-359.

Goldhirsch,A., Coates,A.S., Gelber,R.D., Glick,J.H., Thurlimann,B., and Senn,H.J. (2006). First--select the target: better choice of adjuvant treatments for breast cancer patients. *Ann Oncol* 17, 1772-1776.

Goldhirsch,A., Glick,J.H., Gelber,R.D., Coates,A.S., Thurlimann,B., and Senn,H.J. (2005). Meeting highlights: international expert consensus on the primary therapy of early breast cancer 2005. *Ann Oncol* 16, 1569-1583.

Gonzalez,A.D., Kaya,M., Shi,W., Song,H., Testa,J.R., Penn,L.Z., and Filmus,J. (1998). OCI-5/GPC3, a glypican encoded by a gene that is mutated in the Simpson-Golabi-Behmel

overgrowth syndrome, induces apoptosis in a cell line-specific manner. *J Cell Biol* *141*, 1407-1414.

Gotte,M., and Yip,G.W. (2006). Heparanase, hyaluronan, and CD44 in cancers: a breast carcinoma perspective. *Cancer Res* *66*, 10233-10237.

Greve,H., Cully,Z., Blumberg,P., and Kresse,H. (1988). Influence of chlorate on proteoglycan biosynthesis by cultured human fibroblasts. *J Biol Chem.* *263*, 12886-12892.

Grobe,K., Ledin,J., Ringvall,M., Holmborn,K., Forsberg,E., Esko,J.D., and Kjellen,L. (2002). Heparan sulfate and development: differential roles of the N-acetylglucosamine N-deacetylase/N-sulfotransferase isozymes. *Biochim. Biophys. Acta* *1573*, 209-215.

Gudas,J.M., Payton,M., Thukral,S., Chen,E., Bass,M., Robinson,M.O., and Coats,S. (1999). Cyclin E2, a novel G1 cyclin that binds Cdk2 and is aberrantly expressed in human cancers. *Mol Cell Biol.* *19*, 612-622.

Guimond,S., Maccarana,M., Olwin,B.B., Lindahl,U., and Rapraeger,A.C. (1993). Activating and inhibitory heparin sequences for FGF-2 (basic FGF). Distinct requirements for FGF-1, FGF-2, and FGF-4. *J Biol Chem.* *268*, 23906-23914.

Guo,C.H., Koo,C.Y., Bay,B.H., Tan,P.H., and Yip,G.W. (2007). Comparison of the effects of differentially sulphated bovine kidney- and porcine intestine-derived heparan sulphate on breast carcinoma cellular behaviour. *Int. J Oncol* *31*, 1415-1423.

Guo,S., Sato,T., Shirane,K., and Furukawa,K. (2001). Galactosylation of N-linked oligosaccharides by human {beta}-1,4-galactosyltransferases I, II, III, IV, V, and VI expressed in Sf-9 cells. *Glycobiology* *11*, 813-820.

Gupta,G.P., and Massague,J. (2006). Cancer metastasis: building a framework. *Cell* *127*, 679-695.

Habuchi,H., Habuchi,O., and Kimata,K. (2004). Sulfation pattern in glycosaminoglycan: does it have a code? *Glycoconj. J* *21*, 47-52.

Habuchi,O. (2000). Diversity and functions of glycosaminoglycan sulfotransferases. *Biochimica et Biophysica Acta (BBA) - General Subjects* *1474*, 115-127.

Hacker,U., Nybakken,K., and Perrimon,N. (2005). Heparan sulphate proteoglycans: the sweet side of development. *Nat. Rev. Mol. Cell Biol.* *6*, 530-541.

Hakomori,S.i. (1996). Tumor Malignancy Defined by Aberrant Glycosylation and Sphingo(glyco)lipid Metabolism. *Cancer Res* *56*, 5309-5318.

Hamazaki,Y., Itoh,M., Sasaki,H., Furuse,M., and Tsukita,S. (2002). Multi-PDZ domain protein 1 (MUPP1) is concentrated at tight junctions through its possible interaction with claudin-1 and junctional adhesion molecule. *J Biol. Chem.* *277*, 455-461.

Hanahan,D., and Weinberg,R.A. (2000). The hallmarks of cancer. *Cell* *100*, 57-70.

- Hanks,S.K., Ryzhova,L., Shin,N.Y., and Brabek,J. (2003). Focal adhesion kinase signaling activities and their implications in the control of cell survival and motility. *Front Biosci.* 8, d982-d996.
- Harmer,N.J. (2006). Insights into the role of heparan sulphate in fibroblast growth factor signalling. *Biochem. Soc. Trans.* 34, 442-445.
- Harris,M.A., Clark,J., Ireland,A., Lomax,J., Ashburner,M., Foulger,R., Eilbeck,K., Lewis,S., Marshall,B., Mungall,C. et al. (2004). The Gene Ontology (GO) database and informatics resource. *Nucleic Acids Res* 32, D258-D261.
- Hartmann,L.C., Sellers,T.A., Frost,M.H., Lingle,W.L., Degnim,A.C., Ghosh,K., Vierkant,R.A., Maloney,S.D., Pankratz,V.S., Hillman,D.W., Suman,V.J., Johnson,J., Blake,C., Tlsty,T., Vachon,C.M., Melton,L.J., III, and Visscher,D.W. (2005). Benign breast disease and the risk of breast cancer. *N Engl J Med* 353, 229-237.
- Hoffmann,I., Clarke,P.R., Marcote,M.J., Karsenti,E., and Draetta,G (1993). Phosphorylation and activation of human cdc25-C by cdc2--cyclin B and its involvement in the self-amplification of MPF at mitosis. *EMBO J* 12, 53-63.
- Huang,H., Cruz,F., and Bazzoni,G (2006). Junctional adhesion molecule-A regulates cell migration and resistance to shear stress. *J Cell Physiol* 209, 122-130.
- Humphries,D.E., and Silbert,J.E. (1988). Chlorate: a reversible inhibitor of proteoglycan sulfation. *Biochem Biophys. Res Commun.* 154, 365-371.
- Humphries,D.E., Wong,G.W., Friend,D.S., Gurish,M.F., Qiu,W.T., Huang,C., Sharpe,A.H., and Stevens,R.L. (1999). Heparin is essential for the storage of specific granule proteases in mast cells. *Nature* 400, 769-772.
- Ibrahimi,O.A., Zhang,F., Hrstka,S.C., Mohammadi,M., and Linhardt,R.J. (2004). Kinetic model for FGF, FGFR, and proteoglycan signal transduction complex assembly. *Biochemistry* 43, 4724-4730.
- Ilan,N., Elkin,M., and Vlodaysky,I. (2006). Regulation, function and clinical significance of heparanase in cancer metastasis and angiogenesis. *Int. J Biochem. Cell Biol.* 38, 2018-2039.
- Imada,T., Matsuoka,J., Nobuhisa,T., Okawa,T., Murata,T., Tabuchi,Y., Shirakawa,Y., Ohara,N., Gunduz,M., Nagatsuka,H., Umeoka,T., Yamamoto,Y., Nakajima,M., Tanaka,N., and Naomoto,Y. (2006). COX-2 induction by heparanase in the progression of breast cancer. *Int. J Mol Med* 17, 221-228.
- Iozzo,R.V. (2005). Basement membrane proteoglycans: from cellar to ceiling. *Nat. Rev. Mol. Cell Biol.* 6, 646-656.
- Iozzo,R.V., Cohen,I.R., Grassel,S., and Murdoch,A.D. (1994). The biology of perlecan: the multifaceted heparan sulphate proteoglycan of basement membranes and pericellular matrices.

Biochem. J 302 (Pt 3), 625-639.

Iozzo,R.V., and Murdoch,A.D. (1996). Proteoglycans of the extracellular environment: clues from the gene and protein side offer novel perspectives in molecular diversity and function. *FASEB J. 10*, 598-614.

Iozzo,R.V. (2001). Series Introduction: Heparan sulfate proteoglycans: intricate molecules with intriguing functions. *J. Clin. Invest. 108*, 165-167.

Irizarry,R.A., Bolstad,B.M., Collin,F., Cope,L.M., Hobbs,B., and Speed,T.P. (2003a). Summaries of Affymetrix GeneChip probe level data. *Nucleic Acids Res 31*, e15.

Irizarry,R.A., Hobbs,B., Collin,F., Beazer-Barclay,Y.D., Antonellis,K.J., Scherf,U., and Speed,T.P. (2003b). Exploration, normalization, and summaries of high density oligonucleotide array probe level data. *Biostatistics. 4*, 249-264.

Isabel,Z., Shlomo,B., Zamir,H., Sharon,M., Avner,Y., and Moshe,P. (2001). Soluble and matrix-associated heparan sulfate proteoglycans increase expression of erb-B2 and erb-B3 in colon cancer cell lines. *International. Journal of Cancer 91*, 316-321.

Ishihara,M., Takano,R., Kanda,T., Hayashi,K., Hara,S., Kikuchi,H., and Yoshida,K. (1995). Importance of 6-O-Sulfate Groups of Glucosamine Residues in Heparin for Activation of FGF-1 and FGF-2. *J Biochem (Tokyo) 118*, 1255-1260.

Jaye,M., Schlessinger,J., and Dionne,C.A. (1992). Fibroblast growth factor receptor tyrosine kinases: molecular analysis and signal transduction. *Biochimica et Biophysica Acta (BBA) - Molecular Cell Research 1135*, 185-199.

Jazag,A., Ijichi,H., Kanai,F., Imamura,T., Guleng,B., Ohta,M., Imamura,J., Tanaka,Y., Tateishi,K., Ikenoue,T., Kawakami,T., Arakawa,Y., Miyagishi,M., Taira,K., Kawabe,T., and Omata,M. (2005). Smad4 silencing in pancreatic cancer cell lines using stable RNA interference and gene expression profiles induced by transforming growth factor-beta. *Oncogene 24*, 662-671.

Jemth,P., Kreuger,J., Kusche-Gullberg,M., Sturiale,L., Gimenez-Gallego,G., and Lindahl,U. (2002). Biosynthetic oligosaccharide libraries for identification of protein-binding heparan sulfate motifs. Exploring the structural diversity by screening for fibroblast growth factor (FGF)1 and FGF2 binding. *J Biol Chem 277*, 30567-30573.

Jenniskens,G.J., Veerkamp,J.H., and van Kuppevelt,T.H. (2006). Heparan sulfates in skeletal muscle development and physiology. *J. Cell Physiol 206*, 283-294.

Jiang,W.G., Grimshaw,D., Lane,J., Martin,T.A., Abounader,R., Lathera,J., and Mansel,R.E. (2001). A hammerhead ribozyme suppresses expression of hepatocyte growth factor/scatter factor receptor c-MET and reduces migration and invasiveness of breast cancer cells. *Clin Cancer Res 7*, 2555-2562.

Jiang,W.G., Grimshaw,D., Martin,T.A., Davies,G., Parr,C., Watkins,G., Lane,J., Abounader,R., Laterra,J., and Mansel,R.E. (2003). Reduction of stromal fibroblast-induced mammary tumor growth, by retroviral ribozyme transgenes to hepatocyte growth factor/scatter factor and its receptor, c-MET. *Clin Cancer Res* 9, 4274-4281.

Jiang,X., and Couchman,J.R. (2003a). Perlecan and tumor angiogenesis. *J Histochem. Cytochem.* 51, 1393-1410.

Jiang,X., Mulhaupt,H., Chan,E., Schaefer,L., Schaefer,R.M., and Couchman,J.R. (2004). Essential contribution of tumor-derived perlecan to epidermal tumor growth and angiogenesis. *J Histochem. Cytochem.* 52, 1575-1590.

Jiang,X., and Couchman,J.R. (2003b). Perlecan and Tumor Angiogenesis. *J. Histochem. Cytochem.* 51, 1393-1410.

Jones,L.P., Tilli,M.T., Assefnia,S., Torre,K., Halama,E.D., Parrish,A., Rosen,E.M., and Furth,P.A. (2007). Activation of estrogen signaling pathways collaborates with loss of Brcal to promote development of ERalpha-negative and ERalpha-positive mammary preneoplasia and cancer. *Oncogene*.

Jones,P.A. (1999). The DNA methylation paradox. *Trends Genet* 15, 34-37.

Joukov,V., Groen,A.C., Prokhorova,T., Gerson,R., White,E., Rodriguez,A., Walter,J.C., and Livingston,D.M. (2006). The BRCA1/BARD1 heterodimer modulates ran-dependent mitotic spindle assembly. *Cell* 127, 539-552.

Kallunki,P., and Tryggvason,K. (1992). Human basement membrane heparan sulfate proteoglycan core protein: a 467-kD protein containing multiple domains resembling elements of the low density lipoprotein receptor, laminin, neural cell adhesion molecules, and epidermal growth factor. *J. Cell Biol.* 116, 559-571.

Kamimura,K., Fujise,M., Villa,F., Izumi,S., Habuchi,H., Kimata,K., and Nakato,H. (2001). Drosophila heparan sulfate 6-O-sulfotransferase (dHS6ST) gene. Structure, expression, and function in the formation of the tracheal system. *J Biol. Chem.* 276, 17014-17021.

Kamimura,K., Rhodes,J.M., Ueda,R., McNeely,M., Shukla,D., Kimata,K., Spear,P.G., Shworak,N.W., and Nakato,H. (2004). Regulation of Notch signaling by Drosophila heparan sulfate 3-O sulfotransferase. *J Cell Biol.* 166, 1069-1079.

Kaneider,N.C., Dunzendorfer,S., and Wiedermann,C.J. (2004). Heparan sulfate proteoglycans are involved in opiate receptor-mediated cell migration. *Biochemistry* 43, 237-244.

Karesen,R., Jensen,H.H., Sauer,T., Schlichting,E., Skaane,P., and Wang,H. (2002). Logistics of referral, diagnostic assessment and treatment of patients with breast symptoms and signs. *Scand. J Surg.* 91, 232-238.

Karey,K.P., and Sirbasku,D.A. (1988). Differential Responsiveness of Human Breast Cancer Cell Lines MCF-7 and T47D to Growth Factors and 17{beta}-Estradiol. *Cancer Research* 48, 4083-4092.

Kato,I., Tominaga,S., and Suzuki,T. (1988). Factors related to late menopause and early menarche as risk factors for breast cancer. *Jpn. J Cancer Res* 79, 165-172.

Keller,K.M., Brauer,P.R., and Keller,J.M. (1989). Modulation of cell surface heparan sulfate structure by growth of cells in the presence of chlorate. *Biochemistry* 28, 8100-8107.

Kerlikowske,K., Grady,D., Barclay,J., Sickles,E.A., Eaton,A., and Ernster,V. (1993). Positive predictive value of screening mammography by age and family history of breast cancer. *JAMA* 270, 2444-2450.

Kerlikowske,K., Grady,D., Rubin,S.M., Sandrock,C., and Ernster,V.L. (1995). Efficacy of screening mammography. A meta-analysis. *JAMA* 273, 149-154.

Keum,E., Kim,Y., Kim,J., Kwon,S., Lim,Y., Han,I., and Oh,E.S. (2004). Syndecan-4 regulates localization, activity and stability of protein kinase C-alpha. *Biochem. J* 378, 1007-1014.

Keyomarsi,K., O'Leary,N., Molnar,G., Lees,E., Fingert,H.J., and Pardee,A.B. (1994). Cyclin E, a potential prognostic marker for breast cancer. *Cancer Res* 54, 380-385.

Keyomarsi,K., Tucker,S.L., and Bedrosian,I. (2003). Cyclin E is a more powerful predictor of breast cancer outcome than proliferation. *Nat Med.* 9, 152.

Keyomarsi,K., Tucker,S.L., Buchholz,T.A., Callister,M., Ding,Y., Hortobagyi,G.N., Bedrosian,I., Knickerbocker,C., Toyofuku,W., Lowe,M., Herliczek,T.W., and Bacus,S.S. (2002). Cyclin E and Survival in Patients with Breast Cancer. *N Engl J Med* 347, 1566-1575.

Kim,B.T., Kitagawa,H., Tamura,J.i., Saito,T., Kusche-Gullberg,M., Lindahl,U., and Sugahara,K. (2001). Human tumor suppressor EXT gene family members EXTL1 and EXTL3 encode alpha 1,4- N-acetylglucosaminyltransferases that likely are involved in heparan sulfate/ heparin biosynthesis. *Proceedings of the National Academy of Sciences* 98, 7176-7181.

Kim,B.T., Kitagawa,H., Tanaka,J., Tamura,J.i., and Sugahara,K. (2003). In Vitro Heparan Sulfate Polymerization: Crucial roles of core protein moieties of primer substrates in addition of the EXT1-EXT2 interaction. *J. Biol. Chem.* 278, 41618-41623.

Kinnunen,T., Huang,Z., Townsend,J., Gatdula,M.M., Brown,J.R., Esko,J.D., and Turnbull,J.E. (2005a). Heparan 2-O-sulfotransferase, hst-2, is essential for normal cell migration in *Caenorhabditis elegans*. *Proc. Natl. Acad. Sci. U. S. A* 102, 1507-1512.

Kinnunen,T., Huang,Z., Townsend,J., Gatdula,M.M., Brown,J.R., Esko,J.D., and Turnbull,J.E. (2005b). Heparan 2-O-sulfotransferase, hst-2, is essential for normal cell migration in *Caenorhabditis elegans*. *Proc Natl Acad Sci U. S. A* 102, 1507-1512.

- Kitagawa,H., Shimakawa,H., and Sugahara,K. (1999). The tumor suppressor EXT-like gene EXTL2 encodes an alpha1, 4-N-acetylhexosaminyltransferase that transfers N-acetylgalactosamine and N-acetylglucosamine to the common glycosaminoglycan-protein linkage region. The key enzyme for the chain initiation of heparan sulfate. *J Biol. Chem.* *274*, 13933-13937.
- Kjellen,L., and Lindahl,U. (1991). Proteoglycans: structures and interactions. *Annu. Rev Biochem* *60*, 443-475.
- Kleeff,J., Ishiwata,T., Kumbasar,A., Friess,H., Buchler,M.W., Lander,A.D., and Korc,M. (1998). The cell-surface heparan sulfate proteoglycan glypican-1 regulates growth factor action in pancreatic carcinoma cells and is overexpressed in human pancreatic cancer. *J Clin Invest* *102*, 1662-1673.
- Kleeff,J., Wildi,S., Kumbasar,A., Friess,H., Lander,A.D., and Korc,M. (1999). Stable transfection of a glypican-1 antisense construct decreases tumorigenicity in PANC-1 pancreatic carcinoma cells. *Pancreas* *19*, 281-288.
- Klein,C.A. (2003). The systemic progression of human cancer: a focus on the individual disseminated cancer cell--the unit of selection. *Adv. Cancer Res* *89*, 35-67.
- Knox,S., and Whitelock,J. (2006). Perlecan: how does one molecule do so many things? *Cellular and Molecular Life Sciences (CMLS)* *63*, 2435-2445.
- Koff,A., Giordano,A., Desai,D., Yamashita,K., Harper,J.W., Elledge,S., Nishimoto,T., Morgan,D.O., Franza,B.R., and Roberts,J.M. (1992). Formation and activation of a cyclin E-cdk2 complex during the G1 phase of the human cell cycle. *Science* *257*, 1689-1694.
- Koff,A., Cross,F., Fisher,A., Schumacher,J., Leguellec,K., Philippe,M., and Roberts,J.M. (1991). Human cyclin E, a new cyclin that interacts with two members of the CDC2 gene family. *Cell* *66*, 1217-1228.
- Koo,C.Y., Bay,B.H., Lui,P.C., Tse,G.M., Tan,P.H., and Yip,G.W. (2006). Immunohistochemical expression of heparan sulfate correlates with stromal cell proliferation in breast phyllodes tumors. *Mod. Pathol* *19*, 1344-1350.
- Kouhara,H., Hadari,Y.R., Spivak-Kroizman,T., Schilling,J., Bar-Sagi,D., Lax,I., and Schlessinger,J. (1997). A Lipid-Anchored Grb2-Binding Protein That Links FGF-Receptor Activation to the Ras/MAPK Signaling Pathway. *Cell* *89*, 693-702.
- Kreuger,J., Spillmann,D., Li,J.P., and Lindahl,U. (2006). Interactions between heparan sulfate and proteins: the concept of specificity. *J. Cell Biol.* *174*, 323-327.
- Kuhl,H. (2005). Breast cancer risk in the WHI study: the problem of obesity. *Maturitas* *51*, 83-97.
- Kusche-Gullberg,M., and Kjellen,L. (2003). Sulfotransferases in glycosaminoglycan biosynthesis. *Curr. Opin. Struct. Biol* *13*, 605-611.

Laflamme,M., and Robichaud,G.A. (2007). Gene suppression technologies in high-throughput analysis: front- and back-side applications. *OMICS*. *11*, 129-142.

LaFlamme,S.E., and Auer,K.L. (1996). Integrin signaling. *Semin. Cancer Biol* *7*, 111-118.

Lai,J., Chien,J., Staub,J., Avula,R., Greene,E.L., Matthews,T.A., Smith,D.I., Kaufmann,S.H., Roberts,L.R., and Shridhar,V. (2003). Loss of HSulf-1 up-regulates heparin-binding growth factor signaling in cancer. *J Biol. Chem.* *278*, 23107-23117.

Lai,J.P., Chien,J., Strome,S.E., Staub,J., Montoya,D.P., Greene,E.L., Smith,D.I., Roberts,L.R., and Shridhar,V. (2004). HSulf-1 modulates HGF-mediated tumor cell invasion and signaling in head and neck squamous carcinoma. *Oncogene* *23*, 1439-1447.

Lamanna,W.C., Kalus,I., Padva,M., Baldwin,R.J., Merry,C.L., and Dierks,T. (2007). The heparanome--the enigma of encoding and decoding heparan sulfate sulfation. *J Biotechnol.* *129*, 290-307.

Lander,A.D., and Selleck,S.B. (2000). The Elusive Functions of Proteoglycans: In Vivo Veritas. *J. Cell Biol.* *148*, 227-232.

Lander,E.S., Linton,L.M., Birren,B., Nusbaum,C., Zody,M.C., Baldwin,J., Devon,K., Dewar,K., Doyle,M., FitzHugh,W. et al (2001). Initial sequencing and analysis of the human genome. *Nature* *409*, 860-921.

Lark,M.W., Latterra,J., and Culp,L.A. (1985). Close and focal contact adhesions of fibroblasts to a fibronectin-containing matrix. *Fed. Proc.* *44*, 394-403.

Lauper,N., Beck,A.R., Cariou,S., Richman,L., Hofmann,K., Reith,W., Slingerland,J.M., and Amati,B. (1998). Cyclin E2: a novel CDK2 partner in the late G1 and S phases of the mammalian cell cycle. *Oncogene* *17*, 2637-2643.

Le Merrer,M., Legeai-Mallet,L., Jeannin,P.M., Horsthemke,B., Schlunzel,A., Plauchu,H., Toutain,A., Achard,F., Munnich,A., and Maroteaux,P. (1994). A gene for hereditary multiple exostoses maps to chromosome 19p. *Hum. Mol. Genet.* *3*, 717-722.

LeBaron,R.G., Esko,J.D., Woods,A., Johansson,S., and Hook,M. (1988). Adhesion of glycosaminoglycan-deficient chinese hamster ovary cell mutants to fibronectin substrata. *J Cell Biol* *106*, 945-952.

Leo,J.C., Wang,S.M., Guo,C.H., Aw,S.E., Zhao,Y., Li,J.M., Hui,K.M., and Lin,V.C. (2005). Gene regulation profile reveals consistent anticancer properties of progesterone in hormone-independent breast cancer cells transfected with progesterone receptor. *Int. J Cancer* *117*, 561-568.

Leppa,S., Harkonen,P., and Jalkanen,M. (1991). Steroid-induced epithelial-fibroblastic conversion associated with syndecan suppression in S115 mouse mammary tumor cells. *Cell Regul.* *2*, 1-11.

- Leppa,S., Mali,M., Miettinen,H.M., and Jalkanen,M. (1992). Syndecan expression regulates cell morphology and growth of mouse mammary epithelial tumor cells. *Proc Natl Acad Sci U. S. A* 89, 932-936.
- Leung,G.M., Thach,T.Q., Lam,T.H., Hedley,A.J., Foo,W., Fielding,R., Yip,P.S., Lau,E.M., and Wong,C.M. (2002). Trends in breast cancer incidence in Hong Kong between 1973 and 1999: an age-period-cohort analysis. *Br. J Cancer* 87, 982-988.
- Li,C., and Wong,W.H. (2001a). Model-based analysis of oligonucleotide arrays: expression index computation and outlier detection. *Proc. Natl. Acad. Sci U. S. A* 98, 31-36.
- Li,C., and Wong,W.H. (2001b). Model-based analysis of oligonucleotide arrays: model validation, design issues and standard error application. *Genome Biol* 2, RESEARCH0032.
- Li,J., Kleeff,J., Abiatari,I., Kayed,H., Giese,N.A., Felix,K., Giese,T., Buchler,M.W., and Friess,H. (2005). Enhanced levels of Hsulf-1 interfere with heparin-binding growth factor signaling in pancreatic cancer. *Mol Cancer* 4, 14.
- Li,J.P., Gong,F., Hagner-McWhirter,A., Forsberg,E., Abrink,M., Kisilevsky,R., Zhang,X., and Lindahl,U. (2003). Targeted Disruption of a Murine Glucuronyl C5-epimerase Gene Results in Heparan Sulfate Lacking L-Iduronic Acid and in Neonatal Lethality. *Journal of Biological Chemistry* 278, 28363-28366.
- Li,W., Xiao,C., Vonderhaar,B.K., and Deng,C.X. (2007). A role of estrogen/ERalpha signaling in BRCA1-associated tissue-specific tumor formation. *Oncogene*.
- Li,X., Herz,J., and Monard,D. (2006). Activation of ERK signaling upon alternative protease nexin-1 internalization mediated by syndecan-1. *J Cell Biochem.* 99, 936-951.
- Liang,T.W., DeMarco,R.A., Mrsny,R.J., Gurney,A., Gray,A., Hooley,J., Aaron,H.L., Huang,A., Klassen,T., Tumas,D.B., and Fong,S. (2000). Characterization of huJAM: evidence for involvement in cell-cell contact and tight junction regulation. *Am J Physiol Cell Physiol* 279, C1733-C1743.
- Lim,S.T., Longley,R.L., Couchman,J.R., and Woods,A. (2003). Direct binding of syndecan-4 cytoplasmic domain to the catalytic domain of protein kinase C alpha (PKC alpha) increases focal adhesion localization of PKC alpha. *J Biol Chem.* 278, 13795-13802.
- Lin,V.C., Ng,E.H., Aw,S.E., Tan,M.G., Ng,E.H., and Bay,B.H. (2000). Progesterone induces focal adhesion in breast cancer cells MDA-MB-231 transfected with progesterone receptor complementary DNA. *Mol Endocrinol.* 14, 348-358.
- Lin,X. (2004). Functions of heparan sulfate proteoglycans in cell signaling during development. *Development* 131, 6009-6021.
- Lin,Y.L., Lei,Y.T., Hong,C.J., and Hsueh,Y.P. (2007). Syndecan-2 induces filopodia and dendritic spine formation via the neurofibromin-PKA-Ena/VASP pathway. *J Cell Biol.* 177, 829-841.

- Lindahl,U., Kusche-Gullberg,M., and Kjellen,L. (1998). Regulated diversity of heparan sulfate 2. *J. Biol. Chem.* *273*, 24979-24982.
- Lipshutz,R.J., Fodor,S.P., Gingeras,T.R., and Lockhart,D.J. (1999). High density synthetic oligonucleotide arrays. *Nat. Genet.* *21*, 20-24.
- Liu,D., Shriver,Z., Qi,Y., Venkataraman,G., and Sasisekharan,R. (2002a). Dynamic regulation of tumor growth and metastasis by heparan sulfate glycosaminoglycans. *Semin. Thromb Hemost.* *28*, 67-78.
- Liu,D., Shriver,Z., Venkataraman,G., El Shabrawi,Y., and Sasisekharan,R. (2002b). Tumor cell surface heparan sulfate as cryptic promoters or inhibitors of tumor growth and metastasis. *Proc. Natl. Acad. Sci. U. S. A* *99*, 568-573.
- Liu,J., and Pedersen,L.C. (2006). Anticoagulant heparan sulfate: structural specificity and biosynthesis. *Appl. Microbiol. Biotechnol.*
- Liu,J., Shriver,Z., Blaiklock,P., Yoshida,K., Sasisekharan,R., and Rosenberg,R.D. (1999a). Heparan sulfate D-glucosaminyl 3-O-sulfotransferase-3A sulfates N-unsubstituted glucosamine residues. *J. Biol. Chem.* *274*, 38155-38162.
- Liu,J., Shworak,N.W., Fritze,L.M., Edelberg,J.M., and Rosenberg,R.D. (1996). Purification of heparan sulfate D-glucosaminyl 3-O-sulfotransferase. *J. Biol. Chem.* *271*, 27072-27082.
- Liu,J., Shworak,N.W., Sinay,P., Schwartz,J.J., Zhang,L., Fritze,L.M., and Rosenberg,R.D. (1999b). Expression of heparan sulfate D-glucosaminyl 3-O-sulfotransferase isoforms reveals novel substrate specificities. *J. Biol. Chem.* *274*, 5185-5192.
- Liu,W., Litwack,E.D., Stanley,M.J., Langford,J.K., Lander,A.D., and Sanderson,R.D. (1998). Heparan sulfate proteoglycans as adhesive and anti-invasive molecules. Syndecans and glypican have distinct functions. *J Biol Chem* *273*, 22825-22832.
- Liu,Y., Nusrat,A., Schnell,F.J., Reaves,T.A., Walsh,S., Pochet,M., and Parkos,C.A. (2000). Human junction adhesion molecule regulates tight junction resealing in epithelia. *J Cell Sci* *113*, 2363-2374.
- Livak,K.J., and Schmittgen,T.D. (2001). Analysis of relative gene expression data using real-time quantitative PCR and the 2(-Delta Delta C(T)) Method. *Methods* *25*, 402-408.
- Lo,N.W., Shaper,J.H., Pevsner,J., and Shaper,N.L. (1998). The expanding beta 4-galactosyltransferase gene family: messages from the databanks. *Glycobiology* *8*, 517-526.
- Lockhart,D.J., Dong,H., Byrne,M.C., Follettie,M.T., Gallo,M.V., Chee,M.S., Mittmann,M., Wang,C., Kobayashi,M., Horton,H., and Brown,E.L. (1996). Expression monitoring by hybridization to high-density oligonucleotide arrays. *Nat. Biotechnol.* *14*, 1675-1680.

Longley,R.L., Woods,A., Fleetwood,A., Cowling,G.J., Gallagher,J.T., and Couchman,J.R. (1999b). Control of morphology, cytoskeleton and migration by syndecan-4. *Journal of Cell Science* *112*, 3421-3431.

Longley,R.L., Woods,A., Fleetwood,A., Cowling,G.J., Gallagher,J.T., and Couchman,J.R. (1999a). Control of morphology, cytoskeleton and migration by syndecan-4. *J Cell Sci* *112* (Pt 20), 3421-3431.

Lu,X., and Kang,Y. (2007). Organotropism of breast cancer metastasis. *J. Mammary. Gland. Biol. Neoplasia.* *12*, 153-162.

Lundmark,K., Tran,P.K., Kinsella,M.G, Clowes,A.W., Wight,T.N., and Hedin,U. (2001). Perlecan inhibits smooth muscle cell adhesion to fibronectin: role of heparan sulfate. *J Cell Physiol* *188*, 67-74.

Maccarana,M., Casu,B., and Lindahl,U. (1993). Minimal sequence in heparin/heparan sulfate required for binding of basic fibroblast growth factor. *J Biol Chem.* *268*, 23898-23905.

Maccarana,M., Sakura,Y., Tawada,A., Yoshida,K., and Lindahl,U. (1996). Domain Structure of Heparan Sulfates from Bovine Organs. *J. Biol. Chem.* *271*, 17804-17810.

Maeda,T., Alexander,C.M., and Friedl,A. (2004). Induction of syndecan-1 expression in stromal fibroblasts promotes proliferation of human breast cancer cells. *Cancer Res* *64*, 612-621.

Maeda,T., Desouky,J., and Friedl,A. (2006). Syndecan-1 expression by stromal fibroblasts promotes breast carcinoma growth in vivo and stimulates tumor angiogenesis. *Oncogene* *25*, 1408-1412.

Mahalingam,Y., Gallagher,J.T., and Couchman,J.R. (2007). Cellular Adhesion Responses to the Heparin-binding (HepII) Domain of Fibronectin Require Heparan Sulfate with Specific Properties. *Journal of Biological Chemistry* *282*, 3221-3230.

Mahtouk,K., Hose,D., Raynaud,P., Hundemer,M., Jourdan,M., Jourdan,E., Pantesco,V., Baudard,M., De,V.J., Larroque,M., Moehler,T., Rossi,J.F., Reme,T., Goldschmidt,H., and Klein,B. (2007). Heparanase influences expression and shedding of syndecan-1, and its expression by the bone marrow environment is a bad prognostic factor in multiple myeloma. *Blood* *109*, 4914-4923.

Majack,R.A., and Clowes,A.W. (1984). Inhibition of vascular smooth muscle cell migration by heparin-like glycosaminoglycans. *J Cell Physiol* *118*, 253-256.

Marchisone,C., Del,G.F., Masiello,L., Prat,M., Santi,L., and Noonan,D.M. (2000). Phenotypic alterations in Kaposi's sarcoma cells by antisense reduction of perlecan. *Pathol Oncol Res* *6*, 10-17.

Marker,P.C. (2007). Perlecan, a candidate gene for the CAPB locus, regulates prostate cancer cell growth via the Sonic Hedgehog pathway Datta MW, Hernandez AM, Schlicht MJ, Kahler AJ,

DeGueme AM, Dhir R, Shah RB, Farach-Carson C, Barrett A, Datta S, Department of Pathology, Emory University, Atlanta, GA. *Urol. Oncol.* 25, 280.

Martin,T.A., Das,T., Mansel,R.E., and Jiang,W.G. (2007). Enhanced tight junction function in human breast cancer cells by antioxidant, selenium and polyunsaturated lipid. *J Cell Biochem.* 101, 155-166.

Martin,T.A., and Jiang,W.G. (2001). Tight junctions and their role in cancer metastasis. *Histol. Histopathol.* 16, 1183-1195.

Martin,T.A., Watkins,G., Mansel,R.E., and Jiang,W.G. (2004a). Hepatocyte growth factor disrupts tight junctions in human breast cancer cells. *Cell Biol. Int.* 28, 361-371.

Martin,T.A., Watkins,G., Mansel,R.E., and Jiang,W.G. (2004b). Loss of tight junction plaque molecules in breast cancer tissues is associated with a poor prognosis in patients with breast cancer. *Eur. J Cancer* 40, 2717-2725.

Martin-Padura,I., Lostaglio,S., Schneemann,M., Williams,L., Romano,M., Fruscella,P., Panzeri,C., Stoppacciaro,A., Roco,L., Villa,A., Simmons,D., and Dejana,E. (1998). Junctional Adhesion Molecule, a Novel Member of the Immunoglobulin Superfamily That Distributes at Intercellular Junctions and Modulates Monocyte Transmigration. *J. Cell Biol.* 142, 117-127.

Mathiak,M., Yenisey,C., Grant,D.S., Sharma,B., and Iozzo,R.V. (1997). A role for perlecan in the suppression of growth and invasion in fibrosarcoma cells. *Cancer Res* 57, 2130-2136.

Matsuda,K., Maruyama,H., Guo,F., Kleeff,J., Itakura,J., Matsumoto,Y., Lander,A.D., and Korc,M. (2001). Glypican-1 is overexpressed in human breast cancer and modulates the mitogenic effects of multiple heparin-binding growth factors in breast cancer cells. *Cancer Res* 61, 5562-5569.

Matter,K., and Balda,M.S. (2003). Signalling to and from tight junctions. *Nat Rev. Mol Cell Biol.* 4, 225-236.

Maxhimer,J.B., Quiros,R.M., Stewart,R., Dowlatsahi,K., Gattuso,P., Fan,M., Prinz,R.A., and Xu,X. (2002). Heparanase-1 expression is associated with the metastatic potential of breast cancer. *Surgery* 132, 326-333.

McQuade,K.J., Beauvais,D.M., Burbach,B.J., and Rapraeger,A.C. (2006). Syndecan-1 regulates alphavbeta5 integrin activity in B82L fibroblasts. *J Cell Sci.* 119, 2445-2456.

Mei,J., Hu,H., McEntee,M., Plummer III,H., Song,P., and Wang,H.C. (2003). Transformation of Non-Cancerous Human Breast Epithelial Cell Line MCF10A by the Tobacco-Specific Carcinogen NNK. *Breast Cancer Research and Treatment* 79, 95-105.

Meisel,M., Weise,J., Schwesinger,G., and Straube,W. (1998). Cancer associated serum antigen (CASA) levels in patients with breast carcinoma and in 3 control groups without breast cancer. *Arch. Gynecol. Obstet.* 261, 159-162.

Mendes de Aguiar,C.B., Garcez,R.C., Alvarez-Silva,M., and Trentin,A.G. (2002). Undersulfation of proteoglycans and proteins alter C6 glioma cells proliferation, adhesion and extracellular matrix organization. *Int. J Dev. Neurosci.* 20, 563-571.

Menes,T.S., Ozao,J., and Kim,U. (2007). Breast cancer and ethnicity: strong association between reproductive risk factors and estrogen receptor status in Asian patients - a retrospective study. *Breast J* 13, 352-358.

Merry,C.L.R., Bullock,S.L., Swan,D.C., Backen,A.C., Lyon,M., Beddington,R.S.P., Wilson,V.A., and Gallagher,J.T. (2001). The Molecular Phenotype of Heparan Sulfate in the Hs2st^{-/-} Mutant Mouse. *Journal of Biological Chemistry* 276, 35429-35434.

Miki,Y., Swensen,J., Shattuck-Eidens,D., Futreal,P.A., Harshman,K., Tavtigian,S., Liu,Q., Cochran,C., Bennett,L.M., Ding,W., and . (1994). A strong candidate for the breast and ovarian cancer susceptibility gene BRCA1. *Science* 266, 66-71.

Minn,A.J., Kang,Y., Serganova,I., Gupta,G.P., Giri,D.D., Doubrovin,M., Ponomarev,V., Gerald,W.L., Blasberg,R., and Massague,J. (2005). Distinct organ-specific metastatic potential of individual breast cancer cells and primary tumors. *J Clin Invest* 115, 44-55.

Mitra,S.K., Hanson,D.A., and Schlaepfer,D.D. (2005). Focal adhesion kinase: in command and control of cell motility. *Nat Rev. Mol Cell Biol* 6, 56-68.

Miyamoto,K., Asada,K., Fukutomi,T., Okochi,E., Yagi,Y., Hasegawa,T., Asahara,T., Sugimura,T., and Ushijima,T. (2003). Methylation-associated silencing of heparan sulfate D-glucosaminyl 3-O-sulfotransferase-2 (3-OST-2) in human breast, colon, lung and pancreatic cancers. *Oncogene* 22, 274-280.

Mochizuki,H., Yoshida,K., Gotoh,M., Sugioka,S., Kikuchi,N., Kwon,Y.D., Tawada,A., Maeyama,K., Inaba,N., Hiruma,T., Kimata,K., and Narimatsu,H. (2003). Characterization of a heparan sulfate 3-O-sulfotransferase-5, an enzyme synthesizing a tetrasulfated disaccharide. *J. Biol. Chem.* 278, 26780-26787.

Momparler,R.L., and Bovenzi,V. (2000). DNA methylation and cancer. *J Cell Physiol* 183, 145-154.

Moon,A.F., Edavetta,S.C., Krahn,J.M., Munoz,E.M., Negishi,M., Linhardt,R.J., Liu,J., and Pedersen,L.C. (2004). Structural analysis of the sulfotransferase (3-o-sulfotransferase isoform 3) involved in the biosynthesis of an entry receptor for herpes simplex virus 1. *J. Biol. Chem.* 279, 45185-45193.

Moon,J.J., Matsumoto,M., Patel,S., Lee,L., Guan,J.L., and Li,S. (2005). Role of cell surface heparan sulfate proteoglycans in endothelial cell migration and mechanotransduction. *J Cell Physiol* 203, 166-176.

Morimoto-Tomita,M., Uchimura,K., Werb,Z., Hemmerich,S., and Rosen,S.D. (2002). Cloning and characterization of two extracellular heparin-degrading endosulfatases in mice and humans. *J Biol.*

Chem. 277, 49175-49185.

Moroy,T., and Geisen,C. (2004). Cyclin E. *Int. J Biochem. Cell Biol.* 36, 1424-1439.

Mostafavi-Pour,Z., Askari,J.A., Parkinson,S.J., Parker,P.J., Ng,T.T., and Humphries,M.J. (2003). Integrin-specific signaling pathways controlling focal adhesion formation and cell migration. *J Cell Biol* 161, 155-167.

Mulloy,B., and Rider,C.C. (2006). Cytokines and proteoglycans: an introductory overview. *Biochem. Soc. Trans.* 34, 409-413.

Murakami,M., Horowitz,A., Tang,S., Ware,J.A., and Simons,M. (2002). Protein kinase C (PKC) delta regulates PKCalpha activity in a Syndecan-4-dependent manner. *J Biol Chem.* 277, 20367-20371.

Murdoch,A.D., Dodge,G.R., Cohen,I., Tuan,R.S., and Iozzo,R.V. (1992). Primary structure of the human heparan sulfate proteoglycan from basement membrane (HSPG2/perlecan). A chimeric molecule with multiple domains homologous to the low density lipoprotein receptor, laminin, neural cell adhesion molecules, and epidermal growth factor. *J. Biol. Chem.* 267, 8544-8557.

Nadanaka,S., Kitagawa,H., Goto,F., Tamura,J., Neumann,K.W., Ogawa,T., and Sugahara,K. (1999). Involvement of the core protein in the first beta-N-acetylgalactosamine transfer to the glycosaminoglycan-protein linkage-region tetrasaccharide and in the subsequent polymerization: the critical determining step for chondroitin sulphate biosynthesis. *Biochem. J* 340 (Pt 2), 353-357.

Naik,M.U., and Naik,U.P. (2006). Junctional adhesion molecule-A-induced endothelial cell migration on vitronectin is integrin alpha v beta 3 specific. *J Cell Sci* 119, 490-499.

Naik,M.U., Mousa,S.A., Parkos,C.A., and Naik,U.P. (2003a). Signaling through JAM-1 and {alpha}v{beta}3 is required for the angiogenic action of bFGF: dissociation of the JAM-1 and {alpha}v{beta}3 complex. *Blood* 102, 2108-2114.

Naik,M.U., Vuppalanchi,D., and Naik,U.P. (2003b). Essential Role of Junctional Adhesion Molecule-1 in Basic Fibroblast Growth Factor-Induced Endothelial Cell Migration. *Arterioscler Thromb Vasc Biol* 23, 2165-2171.

Naik,U.P., Ehrlich,Y.H., and Kornecki,E. (1995). Mechanisms of platelet activation by a stimulatory antibody: cross-linking of a novel platelet receptor for monoclonal antibody F11 with the Fc gamma RII receptor. *Biochem. J* 310 (Pt 1), 155-162.

Nakamura,Y., Haines,N., Chen,J., Okajima,T., Furukawa,K., Urano,T., Stanley,P., Irvine,K.D., and Furukawa,K. (2002). Identification of a Drosophila gene encoding xylosylprotein beta4-galactosyltransferase that is essential for the synthesis of glycosaminoglycans and for morphogenesis. *J Biol. Chem.* 277, 46280-46288.

Nakato,H., and Kimata,K. (2002). Heparan sulfate fine structure and specificity of proteoglycan functions. *Biochim. Biophys. Acta 1573*, 312-318.

Nam,Y., Aster,J.C., and Blacklow,S.C. (2002). Notch signaling as a therapeutic target. *Curr. Opin. Chem. Biol.* 6, 501-509.

Napoli,C., Lemieux,C., and Jorgensen,R. (1990). Introduction of a Chimeric Chalcone Synthase Gene into Petunia Results in Reversible Co-Suppression of Homologous Genes in trans. *Plant Cell* 2, 279-289.

Narita,K., Chien,J., Mullany,S.A., Staub,J., Qian,X., Lingle,W.L., and Shridhar,V. (2007). Loss of HSulf-1 expression enhances autocrine signaling mediated by amphiregulin in breast cancer. *J Biol. Chem.* 282, 14413-14420.

Narita,K., Staub,J., Chien,J., Meyer,K., Bauer,M., Friedl,A., Ramakrishnan,S., and Shridhar,V. (2006). HSulf-1 inhibits angiogenesis and tumorigenesis in vivo. *Cancer Res* 66, 6025-6032.

Nerlich,A.G., Lebeau,A., Hagedorn,H.G., Sauer,U., and Schleicher,E.D. (1998). Morphological aspects of altered basement membrane metabolism in invasive carcinomas of the breast and the larynx. *Anticancer Res* 18, 3515-3520.

Nerlich,A.G., Wiest,I., Wagner,E., Sauer,U., and Schleicher,E.D. (1997). Gene expression and protein deposition of major basement membrane components and TGF-beta 1 in human breast cancer. *Anticancer Res* 17, 4443-4449.

Ng,E.H., Gao,F., Ji,C.Y., Ho,G.H., and Soo,K.C. (1997). Risk factors for breast carcinoma in Singaporean Chinese women: the role of central obesity. *Cancer* 80, 725-731.

Nikitin,A., Egorov,S., Daraselina,N., and Mazo,I. (2003). Pathway studio--the analysis and navigation of molecular networks. *Bioinformatics.* 19, 2155-2157.

Nomura,T., Takizawa,M., Aoki,J., Arai,H., Inoue,K., Wakisaka,E., Yoshizuka,N., Imokawa,G., Dohmae,N., Takio,K., Hattori,M., and Matsuo,N. (1998). Purification, cDNA cloning, and expression of UDP-Gal: glucosylceramide beta-1,4-galactosyltransferase from rat brain. *J Biol. Chem.* 273, 13570-13577.

Nurcombe,V., Smart,C.E., Chipperfield,H., Cool,S.M., Boilly,B., and Hondermarck,H. (2000). The proliferative and migratory activities of breast cancer cells can be differentially regulated by heparan sulfates. *J Biol Chem* 275, 30009-30018.

O'connell,M.P., Billings,P.C., Fiori,J.L., Deirmengian,G., Roach,H.I., Shore,E.M., and Kaplan,F.S. (2007). HSPG modulation of BMP signaling in fibrodysplasia ossificans progressiva cells. *J Cell Biochem.*

Ochieng,J., Basolo,F., Albin,A., Melchiori,A., Watanabe,H., Elliott,J., Raz,A., Parodi,S., and Russo,J. (1991). Increased invasive, chemotactic and locomotive abilities of c-Ha-ras-transformed human breast epithelial cells. *Invasion Metastasis* 11, 38-47.

- Ogawa,T., Tsubota,Y., Hashimoto,J., Kariya,Y., and Miyazaki,K. (2007). The short arm of laminin gamma2 chain of laminin-5 (laminin-332) binds syndecan-1 and regulates cellular adhesion and migration by suppressing phosphorylation of integrin beta4 chain. *Mol Biol. Cell* 18, 1621-1633.
- Ohto,T., Uchida,H., Yamazaki,H., Keino-Masu,K., Matsui,A., and Masu,M. (2002). Identification of a novel nonlysosomal sulphatase expressed in the floor plate, choroid plexus and cartilage. *Genes Cells* 7, 173-185.
- Olson,S.T., and Bjork,I. (1994). Regulation of thrombin activity by antithrombin and heparin. *Semin. Thromb. Hemost.* 20, 373-409.
- Ono,K., Hattori,H., Takeshita,S., Kurita,A., and Ishihara,M. (1999). Structural features in heparin that interact with VEGF165 and modulate its biological activity. *Glycobiology* 9, 705-711.
- Orosco,A., Fromigue,O., Bazille,C., Entz-Werle,N., Levillain,P., Marie,P.J., and Modrowski,D. (2007). Syndecan-2 affects the basal and chemotherapy-induced apoptosis in osteosarcoma. *Cancer Res* 67, 3708-3715.
- Ostermann,G., Weber,K.S.C., Zerneck,A., Schroder,A., and Weber,C. (2002). JAM-1 is a ligand of the [beta]2 integrin LFA-1 involved in transendothelial migration of leukocytes. *Nat Immunol* 3, 151-158.
- Paine,T.M., Soule,H.D., Pauley,R.J., and Dawson,P.J. (1992). Characterization of epithelial phenotypes in mortal and immortal human breast cells. *Int. J. Cancer* 50, 463-473.
- Pakula,R., Melchior,A., Denys,A., Vanpouille,C., Mazurier,J., and Allain,F. (2007). Syndecan-1/CD147 association is essential for cyclophilin B-induced activation of p44/42 mitogen-activated protein kinases and promotion of cell adhesion and chemotaxis. *Glycobiology* 17, 492-503.
- Park,H., Han,I., Kwon,H.J., and Oh,E.S. (2005). Focal adhesion kinase regulates syndecan-2-mediated tumorigenic activity of HT1080 fibrosarcoma cells. *Cancer Res* 65, 9899-9905.
- Payton,M., Scully,S., Chung,G., and Coats,S. (2002). Deregulation of cyclin E2 expression and associated kinase activity in primary breast tumors. *Oncogene* 21, 8529-8534.
- Petitou,M., and van Boeckel,C.A. (2004). A synthetic antithrombin III binding pentasaccharide is now a drug! What comes next? *Angew. Chem. Int. Ed Engl.* 43, 3118-3133.
- Peyrat,J.P., Hondermark,H., Louchez,M.M., and Boilly,B. (1991). Demonstration of basic fibroblast growth factor high and low affinity binding sites in human breast cancer cell lines. *Cancer Commun.* 3, 323-329.
- Piccart-Gebhart,M.J., Procter,M., Leyland-Jones,B., Goldhirsch,A., Untch,M., Smith,I., Gianni,L., Baselga,J., Bell,R., Jackisch,C., et al. (2005). Trastuzumab after adjuvant chemotherapy in HER2-positive breast cancer. *N Engl J Med* 353, 1659-1672.

Pikas,D.S., Li,J.P., Vlodaysky,I., and Lindahl,U. (1998). Substrate specificity of heparanases from human hepatoma and platelets.. *J. Biol. Chem.* *273*, 18770-18777.

Poole,R., and Paridaens,R. (2007). The use of third-generation aromatase inhibitors and tamoxifen in the adjuvant treatment of postmenopausal patients with hormone-dependent breast cancer: evidence based review. *Curr. Opin. Oncol* *19*, 564-572.

Pratt,T., Conway,C.D., Tian,N.M.M., Price,D.J., and Mason,J.O. (2006). Heparan Sulphation Patterns Generated by Specific Heparan Sulfotransferase Enzymes Direct Distinct Aspects of Retinal Axon Guidance at the Optic Chiasm. *Journal of Neuroscience* *26*, 6911-6923.

Punglia,R.S., Morrow,M., Winer,E.P., and Harris,J.R. (2007). Local Therapy and Survival in Breast Cancer. *N Engl J Med* *356*, 2399-2405.

Pye,D.A., Vives,R.R., Turnbull,J.E., Hyde,P., and Gallagher,J.T. (1998). Heparan sulfate oligosaccharides require 6-O-sulfation for promotion of basic fibroblast growth factor mitogenic activity. *J Biol. Chem.* *273*, 22936-22942.

Pytela,R., Pierschbacher,M.D., and Ruoslahti,E. (1985). Identification and isolation of a 140 kd cell surface glycoprotein with properties expected of a fibronectin receptor. *Cell* *40*, 191-198.

Rauch,B.H., Millette,E., Kenagy,R.D., Daum,G, Fischer,J.W., and Clowes,A.W. (2005). Syndecan-4 is required for thrombin-induced migration and proliferation in human vascular smooth muscle cells. *J Biol. Chem.* *280*, 17507-17511.

Reiland,J., Sanderson,R.D., Waguespack,M., Barker,S.A., Long,R., Carson,D.D., and Marchetti,D. (2004). Heparanase degrades syndecan-1 and perlecan heparan sulfate: functional implications for tumor cell invasion. *J. Biol. Chem.* *279*, 8047-8055.

Ries,L.A.G, Melbert,D., Krapcho,M., Mariotto,A., Miller BA, Feuer EJ, Clegg L, Horner MJ, Howlander N, Eisner MP, Reichman M, and Edwards BK (2007). SEER Cancer Statistics Review, 1975-2004. National Cancer Institute. Bethesda, MD. http://seer.cancer.gov/csr/1975_2004/, based on November 2006 SEER data submission, posted to the SEER web site.

Robinson,C.J., Mulloy,B., Gallagher,J.T., and Stringer,S.E. (2006). VEGF165-binding sites within heparan sulfate encompass two highly sulfated domains and can be liberated by K5 lyase. *J Biol Chem* *281*, 1731-1740.

Rohrmann,K., Niemann,R., and Buddecke,E. (1985). Two N-acetylgalactosaminyltransferase are involved in the biosynthesis of chondroitin sulfate. *Eur. J Biochem.* *148*, 463-469.

Romond,E.H., Perez,E.A., Bryant,J., Suman,V.J., Geyer,C.E., Jr., Davidson,N.E., Tan-Chiu,E., Martino,S., Paik,S., Kaufman,P.A., Swain,S.M., Pisansky,T.M., Fehrenbacher,L., Kutteh,L.A., Vogel,V.G., Visscher,D.W., Yothers,G., Jenkins,R.B., Brown,A.M., Dakhil,S.R., Mamounas,E.P., Lingle,W.L., Klein,P.M., Ingle,J.N., and Wolmark,N. (2005). Trastuzumab plus adjuvant chemotherapy for operable HER2-positive breast cancer. *N Engl J Med* *353*, 1673-1684.

- Sabit,H., Tsuneyama,K., Shimonishi,T., Harada,K., Cheng,J., Ida,H., Saku,T., Saito,K., and Nakanuma,Y. (2001). Enhanced expression of basement-membrane-type heparan sulfate proteoglycan in tumor fibro-myxoid stroma of intrahepatic cholangiocarcinoma. *Pathol Int.* 51, 248-256.
- Sachse,C., Krausz,E., Kronke,A., Hannus,M., Walsh,A., Grabner,A., Ovcharenko,D., Dorris,D., Trudel,C., Sonnichsen,B., and Echeverri,C.J. (2005). High-throughput RNA interference strategies for target discovery and validation by using synthetic short interfering RNAs: functional genomics investigations of biological pathways. *Methods Enzymol.* 392, 242-277.
- Safaiyan,F., Lindahl,U., and Salmivirta,M. (1998). Selective reduction of 6-O-sulfation in heparan sulfate from transformed mammary epithelial cells. *Eur. J. Biochem.* 252, 576-582.
- Safaiyan,F., Kolset,S.O., Prydz,K., Gottfridsson,E., Lindahl,U., and Salmivirta,M. (1999). Selective Effects of Sodium Chlorate Treatment on the Sulfation of Heparan Sulfate. *J. Biol. Chem.* 274, 36267-36273.
- Sala-Newby,G.B., George,S.J., Bond,M., Dhoot,G.K., and Newby,A.C. (2005). Regulation of vascular smooth muscle cell proliferation, migration and death by heparan sulfate 6-O-endosulfatase1. *FEBS Letters* 579, 6493-6498.
- Sanderson,R.D., Yang,Y., Suva,L.J., and Kelly,T. (2004). Heparan sulfate proteoglycans and heparanase--partners in osteolytic tumor growth and metastasis. *Matrix Biol.* 23, 341-352.
- Sandy,P., Ventura,A., and Jacks,T. (2005). Mammalian RNAi: a practical guide. *Biotechniques* 39, 215-224.
- Saoncella,S., Echtermeyer,F., Denhez,F., Nowlen,J.K., Mosher,D.F., Robinson,S.D., Hynes,R.O., and Goetinck,P.F. (1999). Syndecan-4 signals cooperatively with integrins in a Rhoddependent manner in the assembly of focal adhesions and actin stress fibers. *Proceedings of the National Academy of Sciences* 96, 2805-2810.
- Sasisekharan,R., Raman,R., and Prabhakar,V. (2006). Glycomics approach to structure-function relationships of glycosaminoglycans. *Annu. Rev. Biomed. Eng.* 8, 181-231.
- Saslow,D., Boetes,C., Burke,W., Harms,S., Leach,M.O., Lehman,C.D., Morris,E., Pisano,E., Schnall,M., Sener,S., Smith,R.A., Warner,E., Yaffe,M., Andrews,K.S., and Russell,C.A. (2007). American Cancer Society guidelines for breast screening with MRI as an adjunct to mammography. *CA Cancer J Clin* 57, 75-89.
- Sato,T., Furukawa,K., Bakker,H., Van den Eijnden,D.H., and Van,D., I (1998). Molecular cloning of a human cDNA encoding beta-1,4-galactosyltransferase with 37% identity to mammalian UDP-Gal:GlcNAc beta-1,4-galactosyltransferase. *Proc. Natl. Acad. Sci. U. S. A* 95, 472-477.
- Sato,T., Shirane,K., Kido,M., and Furukawa,K. (2000). Correlated gene expression between beta-1,4-galactosyltransferase V and N-acetylglucosaminyltransferase V in human cancer cell lines. *Biochem. Biophys. Res Commun.* 276, 1019-1023.

Saunders,S., and Bernfield,M. (1988). Cell surface proteoglycan binds mouse mammary epithelial cells to fibronectin and behaves as a receptor for interstitial matrix. *J Cell Biol* 106, 423-430.

Savore,C., Zhang,C., Muir,C., Liu,R., Wyrwa,J., Shu,J., Zhau,H.E., Chung,L.W., Carson,D.D., and Farach-Carson,M.C. (2005). Perlecan knockdown in metastatic prostate cancer cells reduces heparin-binding growth factor responses in vitro and tumor growth in vivo. *Clin Exp. Metastasis* 22, 377-390.

Schaller,M.D. (2004). FAK and paxillin: regulators of N-cadherin adhesion and inhibitors of cell migration? *J Cell Biol* 166, 157-159.

Schena,M., Shalon,D., Davis,R.W., and Brown,P.O. (1995). Quantitative monitoring of gene expression patterns with a complementary DNA microarray. *Science* 270, 467-470.

Schmale,G.A., Conrad,E.U., III, and Raskind,W.H. (1994). The natural history of hereditary multiple exostoses. *J Bone Joint Surg. Am* 76, 986-992.

Segev,A., Nili,N., and Strauss,B.H. (2004). The role of perlecan in arterial injury and angiogenesis. *Cardiovasc. Res* 63, 603-610.

Seidel,C., Borset,M., Hjertner,O., Cao,D., Abildgaard,N., Hjorth-Hansen,H., Sanderson,R.D., Waage,A., and Sundan,A. (2000). High levels of soluble syndecan-1 in myeloma-derived bone marrow: modulation of hepatocyte growth factor activity. *Blood* 96, 3139-3146.

Seow,A., Koh,W.P., Chia,K.S., Shi,L.M., Lee,H.P., and K Shanmugaratnam (2004). Trends in cancer incidence in Singapore 1968-2002. Singapore Cancer Registry. http://www.hpb.gov.sg/data/hpb.home/files/edu/Report_1968_2002.pdf.

Sharma,B., Handler,M., Eichstetter,I., Whitelock,J.M., Nugent,M.A., and Iozzo,R.V. (1998). Antisense Targeting of Perlecan Blocks Tumor Growth and Angiogenesis In Vivo. *J. Clin. Invest.* 102, 1599-1608.

Shen,Y.C., Chang,C.J., Hsu,C., Cheng,C.C., Chiu,C.F., and Cheng,A.L. (2005). Significant difference in the trends of female breast cancer incidence between Taiwanese and Caucasian Americans: implications from age-period-cohort analysis. *Cancer Epidemiol. Biomarkers Prev.* 14, 1986-1990.

Shi,W., and Harris,A.L. (2006). Notch signaling in breast cancer and tumor angiogenesis: cross-talk and therapeutic potentials. *J Mammary. Gland. Biol. Neoplasia.* 11, 41-52.

Shirane,K., Sato,T., Segawa,K., and Furukawa,K. (1999). Involvement of beta-1,4-galactosyltransferase V in malignant transformation-associated changes in glycosylation. *Biochem. Biophys. Res Commun.* 265, 434-438.

Shivapurkar,N., Stastny,V., Suzuki,M., Wistuba,I.I., Li,L., Zheng,Y., Feng,Z., Hol,B., Prinsen,C., Thunnissen,F.B., and Gazdar,A.F. (2007). Application of a methylation gene panel by quantitative PCR for lung cancers. *Cancer Lett.* 247, 56-71.

- Shriver,Z., Liu,D., and Sasisekharan,R. (2002). Emerging views of heparan sulfate glycosaminoglycan structure/activity relationships modulating dynamic biological functions. *Trends Cardiovasc. Med.* *12*, 71-77.
- Shukla,D., Liu,J., Blaiklock,P., Shworak,N.W., Bai,X., Esko,J.D., Cohen,G.H., Eisenberg,R.J., Rosenberg,R.D., and Spear,P.G. (1999). A novel role for 3-O-sulfated heparan sulfate in herpes simplex virus 1 entry. *Cell* *99*, 13-22.
- Shworak,N.W., Liu,J., Petros,L.M., Zhang,L., Kobayashi,M., Copeland,N.G., Jenkins,N.A., and Rosenberg,R.D. (1999). Multiple isoforms of heparan sulfate D-glucosaminyl 3-O-sulfotransferase. Isolation, characterization, and expression of human cdnas and identification of distinct genomic loci. *J. Biol. Chem.* *274*, 5170-5184.
- Siegfried,Z., and Cedar,H. (1997). DNA methylation: a molecular lock. *Curr. Biol* *7*, R305-R307.
- Sim,X., Ali,R.A., Wedren,S., Goh,D.L., Tan,C.S., Reilly,M., Hall,P., and Chia,K.S. (2006). Ethnic differences in the time trend of female breast cancer incidence: Singapore, 1968-2002. *BMC Cancer* *6*, 261.
- Singletary,S.E., and Connolly,J.L. (2006). Breast cancer staging: working with the sixth edition of the AJCC Cancer Staging Manual. *CA Cancer J Clin* *56*, 37-47.
- Singletary,S.E. (2003). Candidates for Minimally Invasive Therapy of Breast Cancer: Redefining the Standards. *Ann Surg Oncol* *10*, 591-592.
- Soletormos,G, Nielsen,D., Schioler,V., Mouridsen,H., and Dombernowsky,P. (2004). Monitoring different stages of breast cancer using tumour markers CA 15-3, CEA and TPA. *Eur. J Cancer* *40*, 481-486.
- Soletormos,G, Nielsen,D., Schioler,V., Skovsgaard,T., and Dombernowsky,P. (1996). Tumor markers cancer antigen 15.3, carcinoembryonic antigen, and tissue polypeptide antigen for monitoring metastatic breast cancer during first-line chemotherapy and follow-up. *Clin Chem.* *42*, 564-575.
- Sorlie,T., Tibshirani,R., Parker,J., Hastie,T., Marron,J.S., Nobel,A., Deng,S., Johnsen,H., Pesich,R., Geisler,S., Demeter,J., Perou,C.M., Lonning,P.E., Brown,P.O., Borresen-Dale,A.L., and Botstein,D. (2003). Repeated observation of breast tumor subtypes in independent gene expression data sets. *Proc. Natl. Acad. Sci. U. S. A* *100*, 8418-8423.
- Sotiriou,C., and Piccart,M.J. (2007). Taking gene-expression profiling to the clinic: when will molecular signatures become relevant to patient care? *Nat. Rev. Cancer* *7*, 545-553.
- Sourvinos,G, and Spandidos,D.A. (1998). Decreased BRCA1 expression levels may arrest the cell cycle through activation of p53 checkpoint in human sporadic breast tumors. *Biochem. Biophys. Res Commun.* *245*, 75-80.

Southern,E., Mir,K., and Shchepinov,M. (1999). Molecular interactions on microarrays. *Nat. Genet.* 21, 5-9.

Spivak-Kroizman,T., Lemmon,M.A., Dikic,I., Ladbury,J.E., Pinchasi,D., Huang,J., Jaye,M., Crumley,G., Schlessinger,J., and Lax,I. (1994). Heparin-induced oligomerization of FGF molecules is responsible for FGF receptor dimerization, activation, and cell proliferation. *Cell* 79, 1015-1024.

Staub,J., Chien,J., Pan,Y., Qian,X., Narita,K., Aletti,G., Scheerer,M., Roberts,L.R., Molina,J., and Shridhar,V. (2007). Epigenetic silencing of HSulf-1 in ovarian cancer:implications in chemoresistance. *Oncogene* 26, 4969-4978.

Stickens,D., Zak,B.M., Rougier,N., Esko,J.D., and Werb,Z. (2005). Mice deficient in Ext2 lack heparan sulfate and develop exostoses. *Development* 132, 5055-5068.

Su,G., Blaine,S.A., Qiao,D., and Friedl,A. (2007). Shedding of syndecan-1 by stromal fibroblasts stimulates human breast cancer cell proliferation via FGF2 activation. *J Biol. Chem.* 282, 14906-14915.

Sun,X.G., and Rotenberg,S.A. (1999). Overexpression of protein kinase Calpha in MCF-10A human breast cells engenders dramatic alterations in morphology, proliferation, and motility. *Cell Growth Differ.* 10, 343-352.

Takahashi,T., Shivapurkar,N., Riquelme,E., Shigematsu,H., Reddy,J., Suzuki,M., Miyajima,K., Zhou,X., Bekele,B.N., Gazdar,A.F., and Wistuba,I.I. (2004). Aberrant Promoter Hypermethylation of Multiple Genes in Gallbladder Carcinoma and Chronic Cholecystitis. *Clin Cancer Res* 10, 6126-6133.

Tapanadechopone,P., Tumova,S., Jiang,X., and Couchman,J.R. (2001). Epidermal transformation leads to increased perlecan synthesis with heparin-binding-growth-factor affinity. *Biochem. J* 355, 517-527.

Tavani,A., Braga,C., La Vecchia,C., Negri,E., and Franceschi,S. (1997). Hormone replacement treatment and breast cancer risk: an age-specific analysis. *Cancer Epidemiol Biomarkers Prev* 6, 11-14.

Terry,P.D., and Rohan,T.E. (2002). Cigarette Smoking and the Risk of Breast Cancer in Women: A Review of the Literature. *Cancer Epidemiol Biomarkers Prev* 11, 953-971.

Thai,T.H., Du,F., Tsan,J.T., Jin,Y., Phung,A., Spillman,M.A., Massa,H.F., Muller,C.Y., Ashfaq,R., Mathis,J.M., Miller,D.S., Trask,B.J., Baer,R., and Bowcock,A.M. (1998). Mutations in the BRCA1-associated RING domain (BARD1) gene in primary breast, ovarian and uterine cancers. *Hum. Mol Genet* 7, 195-202.

The Early Breast Cancer Trialists' Collaborative Group (1995). Effects of radiotherapy and surgery in early breast cancer. An overview of the randomized trials. *N Engl J Med* 333, 1444-1455.

- Timar,J., Lapis,K., Dudas,J., Sebestyen,A., Kopper,L., and Kovalszky,I. (2002). Proteoglycans and tumor progression: Janus-faced molecules with contradictory functions in cancer. *Semin. Cancer Biol* 12, 173-186.
- Tiwari,V., O'donnell,C., Copeland,R.J., Scarlett,T., Liu,J., and Shukla,D. (2007). Soluble 3-O-sulfated heparan sulfate can trigger herpes simplex virus type 1 entry into resistant Chinese hamster ovary (CHO-K1) cells. *J Gen. Virol.* 88, 1075-1079.
- Toida,T., Yoshida,H., Toyoda,H., Koshiishi,I., Imanari,T., Hileman,R.E., Fromm,J.R., and Linhardt,R.J. (1997). Structural differences and the presence of unsubstituted amino groups in heparan sulphates from different tissues and species. *Biochem. J* 322 (Pt 2), 499-506.
- Toyota,M., and Issa,J.P. (2000). The role of DNA hypermethylation in human neoplasia. *Electrophoresis* 21, 329-333.
- Trudeau,M., Charbonneau,F., Gelmon,K., Laing,K., Latreille,J., Mackey,J., McLeod,D., Pritchard,K., Provencher,L., and Verma,S. (2005). Selection of adjuvant chemotherapy for treatment of node-positive breast cancer. *Lancet Oncol* 6, 886-898.
- Tsuda,H., Yamada,S., Yamane,Y., Yoshida,K., Hopwood,J.J., and Sugahara,K. (1996). Structures of five sulfated hexasaccharides prepared from porcine intestinal heparin using bacterial heparinase. Structural variants with apparent biosynthetic precursor-product relationships for the antithrombin III-binding site. *J Biol Chem.* 271, 10495-10502.
- Tuckett,F., and Morriss-Kay,G. (1988). Alcian blue staining of glycosaminoglycans in embryonic material: effect of different fixatives. *Histochem. J* 20, 174-182.
- Tuma,R.S. (2006). Trastuzumab Faces Trials, Clinical and Otherwise. *J. Natl. Cancer Inst.* 98, 296-298.
- Turnbull,J., Powell,A., and Guimond,S. (2001). Heparan sulfate: decoding a dynamic multifunctional cell regulator. *Trends Cell Biol* 11, 75-82.
- Turner,C.E. (1998). Paxillin. *Int. J Biochem. Cell Biol* 30, 955-959.
- Turner,C.E. (2000). Paxillin interactions. *J Cell Sci* 113 Pt 23, 4139-4140.
- Ursin,G., Sun,C.L., Koh,W.P., Khoo,K.S., Gao,F., Wu,A.H., and Yu,M.C. (2006). Associations between soy, diet, reproductive factors, and mammographic density in Singapore Chinese women. *Nutr. Cancer* 56, 128-135.
- van't Veer,L.J., Dai,H., van,d., V, He,Y.D., Hart,A.A., Mao,M., Peterse,H.L., van der,K.K., Marton,M.J., Witteveen,A.T., Schreiber,G.J., Kerkhoven,R.M., Roberts,C., Linsley,P.S., Bernards,R., and Friend,S.H. (2002). Gene expression profiling predicts clinical outcome of breast cancer. *Nature* 415, 530-536.

Van,H.W., Wuyts,W., Hendrickx,J., Speleman,F., Wauters,J., De,B.K., Van,R.N., Bossuyt,P., and Willems,P.J. (1998). Identification of a third EXT-like gene (EXTL3) belonging to the EXT gene family. *Genomics* 47, 230-237.

Van,V.D., Wall,D.P., and Johnson,K.G. (2006). Heparan sulfate proteoglycans and the emergence of neuronal connectivity. *Curr. Opin. Neurobiol.* 16, 40-51.

Vanpouille,C., Deligny,A., Delehedde,M., Denys,A., Melchior,A., Lienard,X., Lyon,M., Mazurier,J., Fernig,D.G, and Allain,F. (2007). The heparin/heparan sulfate sequence that interacts with cyclophilin B contains a 3-o-sulfated N-unsubstituted glucosamine residue. *J Biol. Chem.* 282, 24416-24429.

Venkitaraman,A.R. (2002). Cancer Susceptibility and the Functions of BRCA1 and BRCA2. *Cell* 108, 171-182.

Venter,J.C., Adams,M.D., Myers,E.W., Li,P.W., Mural,R.J., Sutton,G.G., Smith,H.O., Yandell,M., Evans,C.A., Holt,R.A. et al. (2001). The sequence of the human genome. *Science* 291, 1304-1351.

Verma,S., and Clemons,M. (2007). First-line treatment options for patients with HER-2 negative metastatic breast cancer: the impact of modern adjuvant chemotherapy. *Oncologist.* 12, 785-797.

Vives,R.R., Lortat-Jacob,H., and Fender,P. (2006). Heparan sulphate proteoglycans and viral vectors : ally or foe? *Curr. Gene Ther.* 6, 35-44.

Vlodavsky,I., Friedmann,Y., Elkin,M., Aingorn,H., Atzmon,R., Ishai-Michaeli,R., Bitan,M., Pappo,O., Peretz,T., Michal,I., Spector,L., and Pecker,I. (1999). Mammalian heparanase: gene cloning, expression and function in tumor progression and metastasis. *Nat. Med.* 5, 793-802.

Waddington,R.J., and Embery,G. (2001). Proteoglycans and Orthodontic Tooth Movement. *Journal of Orthodontics* 28, 281-290.

Wahl,R.L., Cody,R.L., Hutchins,G.D., and Mudgett,E.E. (1991). Primary and metastatic breast carcinoma: initial clinical evaluation with PET with the radiolabeled glucose analogue 2-[F-18]-fluoro-2-deoxy-D-glucose. *Radiology* 179, 765-770.

Wahl,R.L., Siegel,B.A., Coleman,R.E., and Gatsonis,C.G. (2004). Prospective multicenter study of axillary nodal staging by positron emission tomography in breast cancer: a report of the staging breast cancer with PET Study Group. *J Clin Oncol* 22, 277-285.

Wajed,S.A., Laird,P.W., and DeMeester,T.R. (2001). DNA methylation: an alternative pathway to cancer. *Ann Surg* 234, 10-20.

Walsh,T., Casadei,S., Coats,K.H., Swisher,E., Stray,S.M., Higgins,J., Roach,K.C., Mandell,J., Lee,M.K., Ciernikova,S., Foretova,L., Soucek,P., and King,M.C. (2006). Spectrum of mutations in BRCA1, BRCA2, CHEK2, and TP53 in families at high risk of breast cancer. *JAMA* 295, 1379-1388.

- Walsh,T., and King,M.C. (2007). Ten genes for inherited breast cancer. *Cancer Cell* *11*, 103-105.
- Wang,S., Ai,X., Freeman,S.D., Pownall,M.E., Lu,Q., Kessler,D.S., and Emerson,C.P., Jr. (2004). QSulf1, a heparan sulfate 6-O-endosulfatase, inhibits fibroblast growth factor signaling in mesoderm induction and angiogenesis. *Proc. Natl. Acad. Sci. U. S. A* *101*, 4833-4838.
- Wang,Y., Klijn,J.G., Zhang,Y., Sieuwerts,A.M., Look,M.P., Yang,F., Talantov,D., Timmermans,M., Meijer-van Gelder,M.E., Yu,J., Jatko,T., Berns,E.M., Atkins,D., and Foekens,J.A. (2005). Gene-expression profiles to predict distant metastasis of lymph-node-negative primary breast cancer. *Lancet* *365*, 671-679.
- Warda,M., Mao,W., Toida,T., and Linhardt,R.J. (2003). Turkey intestine as a commercial source of heparin? Comparative structural studies of intestinal avian and mammalian glycosaminoglycans. *Comparative Biochemistry and Physiology Part B: Biochemistry and Molecular Biology* *134*, 189-197.
- Weigel,P.H., Hascall,V.C., and Tammi,M. (1997). Hyaluronan synthases. *J Biol. Chem.* *272*, 13997-14000.
- Whelan,T., and Levine,M. (2005). More Evidence That Locoregional Radiation Therapy Improves Survival: What Should We Do? *J. Natl. Cancer Inst.* *97*, 82-84.
- Whitelock,J.M., and Iozzo,R.V. (2005). Heparan sulfate: a complex polymer charged with biological activity. *Chem. Rev.* *105*, 2745-2764.
- Wiesener,B., Hauser-Kronberger,C.E., Zipperer,E., Dietze,O., Menzel,C., and Hacker,G.W. (1998). p34cdc2 in invasive breast cancer: relationship to DNA content, Ki67 index and c-erbB-2 expression. *Histopathology* *33*, 522-530.
- Wilcox-Adelman,S.A., Denhez,F., and Goetinck,P.F. (2002). Syndecan-4 Modulates Focal Adhesion Kinase Phosphorylation. *Journal of Biological Chemistry* *277*, 32970-32977.
- Williams,N.S., Gaynor,R.B., Scoggin,S., Verma,U., Gokaslan,T., Simmang,C., Fleming,J., Tavana,D., Frenkel,E., and Becerra,C. (2003). Identification and validation of genes involved in the pathogenesis of colorectal cancer using cDNA microarrays and RNA interference. *Clin Cancer Res* *9*, 931-946.
- Wise,C.A., Clines,G.A., Massa,H., Trask,B.J., and Lovett,M. (1997). Identification and localization of the gene for EXTL, a third member of the multiple exostoses gene family. *Genome Res* *7*, 10-16.
- Woods,A. (2001). Syndecans: transmembrane modulators of adhesion and matrix assembly. *J. Clin. Invest* *107*, 935-941.
- Woods,A., and Couchman,J.R. (1994). Syndecan 4 heparan sulfate proteoglycan is a selectively enriched and widespread focal adhesion component. *Mol Biol Cell* *5*, 183-192.

Woods,A., and Couchman,J.R. (2001a). Syndecan-4 and focal adhesion function. *Curr. Opin. Cell Biol* 13, 578-583.

Woods,A., Longley,R.L., Tumova,S., and Couchman,J.R. (2000). Syndecan-4 binding to the high affinity heparin-binding domain of fibronectin drives focal adhesion formation in fibroblasts. *Arch. Biochem. Biophys.* 374, 66-72.

Woods,A., Oh,E.S., and Couchman,J.R. (1998). Syndecan proteoglycans and cell adhesion. *Matrix Biol* 17, 477-483.

Woods,A., and Couchman,J.R. (2001b). Syndecan-4 and focal adhesion function. *Current Opinion in Cell Biology* 13, 578-583.

Wu,L.C., Wang,Z.W., Tsan,J.T., Spillman,M.A., Phung,A., Xu,X.L., Yang,M.C., Hwang,L.Y., Bowcock,A.M., and Baer,R. (1996). Identification of a RING protein that can interact in vivo with the BRCA1 gene product. *Nat Genet* 14, 430-440.

Wu,Z.L., Zhang,L., Yabe,T., Kuberan,B., Beeler,D.L., Love,A., and Rosenberg,R.D. (2003). The involvement of heparan sulfate (HS) in FGF1/HS/FGFR1 signaling complex. *J Biol Chem.* 278, 17121-17129.

Wuyts,W., Van,H.W., Hendrickx,J., Speleman,F., Wauters,J., De,B.K., Van,R.N., Van,A.T., Bossuyt,P., and Willems,P.J. (1997). Identification and characterization of a novel member of the EXT gene family, EXTL2. *Eur. J Hum. Genet.* 5, 382-389.

Xia,G., Chen,J., Tiwari,V., Ju,W., Li,J.P., Malmstrom,A., Shukla,D., and Liu,J. (2002). Heparan sulfate 3-O-sulfotransferase isoform 5 generates both an antithrombin-binding site and an entry receptor for herpes simplex virus, type 1. *J. Biol. Chem.* 277, 37912-37919.

Xiang,Y.Y., Ladeda,V., and Filmus,J. (2001). Glypican-3 expression is silenced in human breast cancer. *Oncogene* 20, 7408-7412.

Xu,D., Tiwari,V., Xia,G., Clement,C., Shukla,D., and Liu,J. (2005). Characterization of heparan sulphate 3-O-sulphotransferase isoform 6 and its role in assisting the entry of herpes simplex virus type 1. *Biochem. J.* 385, 451-459.

Xu,S., Zhu,X., Zhang,S., Yin,S., Zhou,L., Chen,C., and Gu,J. (2001). Over-expression of beta-1,4-galactosyltransferase I, II, and V in human astrocytoma. *J Cancer Res Clin Oncol* 127, 502-506.

Xu,X., Wagner,K.U., Larson,D., Weaver,Z., Li,C., Ried,T., Hennighausen,L., Wynshaw-Boris,A., and Deng,C.X. (1999a). Conditional mutation of Brca1 in mammary epithelial cells results in blunted ductal morphogenesis and tumour formation. *Nat. Genet.* 22, 37-43.

Xu,X., Weaver,Z., Linke,S.P., Li,C., Gotay,J., Wang,X.W., Harris,C.C., Ried,T., and Deng,C.X. (1999b). Centrosome amplification and a defective G2-M cell cycle checkpoint induce genetic instability in BRCA1 exon 11 isoform-deficient cells. *Mol Cell* 3, 389-395.

- Yang,X., and Lippman,M.E. (1999). BRCA1 and BRCA2 in breast cancer. *Breast Cancer Res Treat* 54, 1-10.
- Yasmeen,A., Berdel,W.E., Serve,H., and Muller-Tidow,C. (2003). E- and A-type cyclins as markers for cancer diagnosis and prognosis. *Expert. Rev. Mol Diagn.* 3, 617-633.
- Ye,S., Luo,Y., Lu,W., Jones,R.B., Linhardt,R.J., Capila,I., Toida,T., Kan,M., Pelletier,H., and McKeehan,W.L. (2001). Structural basis for interaction of FGF-1, FGF-2, and FGF-7 with different heparan sulfate motifs. *Biochemistry* 40, 14429-14439.
- Yeung,K.Y., and Ruzzo,W.L. (2001). Principal component analysis for clustering gene expression data. *Bioinformatics.* 17, 763-774.
- Yip,G.W., Ferretti,P., and Copp,A.J. (2002). Heparan sulphate proteoglycans and spinal neurulation in the mouse embryo. *Development* 129, 2109-2119.
- Yip,G.W., Smollich,M., and Gotte,M. (2006). Therapeutic value of glycosaminoglycans in cancer. *Mol Cancer Ther* 5, 2139-2148.
- Zak,B.M., Crawford,B.E., and Esko,J.D. (2002). Hereditary multiple exostoses and heparan sulfate polymerization. *Biochim. Biophys. Acta* 1573, 346-355.
- Zamore,P.D., Tuschl,T., Sharp,P.A., and Bartel,D.P. (2000). RNAi: double-stranded RNA directs the ATP-dependent cleavage of mRNA at 21 to 23 nucleotide intervals. *Cell* 101, 25-33.
- Zantek,N.D., Walker-Daniels,J., Stewart,J., Hansen,R.K., Robinson,D., Miao,H., Wang,B., Kung,H.J., Bissell,M.J., and Kinch,M.S. (2001). MCF-10A-NeoST: A New Cell System for Studying Cell-ECM and Cell-Cell Interactions in Breast Cancer. *Clin Cancer Res* 7, 3640-3648.
- Zariwala,M., Liu,J., and Xiong,Y. (1998). Cyclin E2, a novel human G1 cyclin and activating partner of CDK2 and CDK3, is induced by viral oncoproteins. *Oncogene* 17, 2787-2798.
- Zetser,A., Bashenko,Y., Edovitsky,E., Levy-Adam,F., Vlodaysky,I., and Ilan,N. (2006). Heparanase induces vascular endothelial growth factor expression: correlation with p38 phosphorylation levels and Src activation. *Cancer Res* 66, 1455-1463.
- Zhan,Q., Antinore,M.J., Wang,X.W., Carrier,F., Smith,M.L., Harris,C.C., and Fornace,A.J., Jr. (1999). Association with Cdc2 and inhibition of Cdc2/Cyclin B1 kinase activity by the p53-regulated protein Gadd45. *Oncogene* 18, 2892-2900.
- Zhang,L., Beeler,D.L., Lawrence,R., Lech,M., Liu,J., Davis,J.C., Shriver,Z., Sasisekharan,R., and Rosenberg,R.D. (2001). 6-O-sulfotransferase-1 represents a critical enzyme in the anticoagulant heparan sulfate biosynthetic pathway. *J Biol Chem.* 276, 42311-42321.
- Zhang,X., Liu,C., Nestor,K.E., McFarland,D.C., and Velleman,S.G. (2007a). The effect of glypican-1 glycosaminoglycan chains on Turkey myogenic satellite cell proliferation, differentiation, and fibroblast growth factor 2 responsiveness. *Poult. Sci.* 86, 2020-2028.

Reference

Zhang,Y., Li,L., Wang,Y., Zhang,J., Wei,G., Sun,Y., and Shen,F. (2007b). Downregulating the expression of heparanase inhibits the invasion, angiogenesis and metastasis of human hepatocellular carcinoma. *Biochem. Biophys. Res Commun.* 358, 124-129.

Zhang,Z.H., Chen,Y., Zhao,H.J., Xie,C.Y., Ding,J., and Hou1 YT (2007c). Silencing of Heparanase by siRNA Inhibits Tumor Metastasis and Angiogenesis of Human Breast Cancer In Vitro and In Vivo. *Cancer Biol. Ther.* 6.

Zhou,Z., Wang,J., Cao,R., Morita,H., Soininen,R., Chan,K.M., Liu,B., Cao,Y., and Tryggvason,K. (2004). Impaired angiogenesis, delayed wound healing and retarded tumor growth in perlecan heparan sulfate-deficient mice. *Cancer Res* 64, 4699-4702.

Comparison of the effects of differentially sulphated bovine kidney- and porcine intestine-derived heparan sulphate on breast carcinoma cellular behaviour

CHUN-HUA GUO¹, CHUAY-YENG KOO¹, BOON-HUAT BAY¹, PUAY-HOON TAN² and GEORGE W. YIP¹

¹Department of Anatomy, Yong Loo Lin School of Medicine, National University of Singapore, 4 Medical Drive, Block MD 10, Singapore 117597; ²Department of Pathology, Singapore General Hospital, Outram Road, Singapore 169608, Singapore

Received July 12, 2007; Accepted September 3, 2007

Abstract. Heparan sulphate is a sulphated glycosaminoglycan and is able to bind to and regulate the activity of many growth and signalling factors. We have previously shown that its expression is correlated with tumour grade and cell proliferation in breast phyllodes tumours. In this study, we examined the use of heparan sulphate as a biomarker of invasive ductal carcinoma and the effects of differentially sulphated heparan species on breast cancer cell behaviour. Immunohistochemistry using the 10E4 monoclonal antibody was carried out on 32 paraffin-embedded breast cancer specimens and paired non-cancerous breast tissues to compare the expression patterns of heparan sulphate. Upregulated expression of the sulphated 10E4 epitope in heparan sulphate was detected in both epithelial and stromal compartments of breast cancer compared with normal mammary tissues, with a 2.8X increase in immunoreactivity score. To determine the effects of differentially sulphated heparan sulphate molecules on breast cancer behaviour, cultured breast carcinoma cells were treated with chlorate, a competitive inhibitor of glycosaminoglycan sulphation, and two different heparan sulphate species. Inhibition of glycosaminoglycan sulphation resulted in a significant increase in cancer cell adhesion and a reduction in cell migration, together with upregulated expression of focal adhesion kinase and paxillin. Both porcine intestine- and bovine kidney-derived heparan sulphate species could block the change in cell adhesion. However, the former heparan sulphate species completely abolished, while the

latter exacerbated, the chlorate-induced decrease in cell migration. The results show that heparan sulphate is a useful biomarker of breast invasive ductal carcinoma. Different sulphation patterns of heparan sulphate residues have differential effects in regulating breast cancer cellular behaviour, and this may be exploited to develop heparan sulphate into a useful target for treatment of breast carcinoma.

Introduction

Breast carcinoma is the most widespread form of malignancy in women worldwide, and the commonest cause of cancer-related deaths (1,2). Besides clinical and histopathological staging and hormonal receptor status, cancer cell adhesion and migration are important parameters that affect patient prognosis (3,4). Thus, understanding the molecular regulators of cancer cellular behaviour and determination of their effects on tumour cell adhesion and migration are essential to a better comprehension of cancer biology, and is of fundamental importance in the development of therapeutic targets.

Heparan sulphate is an unbranched, polyanionic glycosaminoglycan composed of alternating repeats of glucosamine and glucuronic/iduronic acid residues (5,6). Heparan sulphate chains are attached to core protein backbones to form heparan sulphate proteoglycans, which can be found attached to the cell surface or within the extracellular matrix (7). The physiological function of heparan sulphate is highly dependent on the presence of sulphate groups, which modulate the ability of heparan sulphate to bind to and interact with different growth and signalling factors (7-9). The importance of differential sulphation of heparan sulphate has been highlighted by recent studies on knockout mice, in which loss of heparan 2-O-sulphation resulted in renal, ocular and skeletal defects whereas absence of N-sulphation led to pulmonary hypoplasia and respiratory distress in newborn pups (10-12).

Studies on the core proteins of heparan sulphate proteoglycans using breast cancer tissue samples have shown that these molecules may be important prognostic indicators. Several authors have reported increased expression of the core protein of syndecan-1, a transmembrane heparan

Correspondence to: Dr George W. Yip, Department of Anatomy, Yong Loo Lin School of Medicine, National University of Singapore, 4 Medical Drive, Block MD 10, Singapore 117597, Singapore
E-mail: georgeyip@nus.edu.sg

Key words: breast cancer, heparan sulphate, differential sulphation, bovine kidney, porcine intestine, cell adhesion, cell migration

sulphate proteoglycan, in women with aggressive forms of breast cancer associated with a poorer prognosis (13-15). Indeed, expression of syndecan-1 in breast ductal carcinoma *in situ* was found to be associated with the presence of angiogenic and lymphangiogenic factors, and correlated with the response of primary breast cancer to neoadjuvant chemotherapy (16,17). Upregulated expression of the core protein of glypican-1, a glycosylphosphatidylinositol-linked heparan sulphate proteoglycan, was also noted in human breast cancer and influenced the response of cancer cells to growth factors (18).

In contrast to the heparan sulphate proteoglycan core proteins, relatively less is known about the potential use of the heparan sulphate glycosaminoglycan chain as a biomarker of invasive ductal carcinoma in clinical samples, and the effects of differentially sulphated heparan sulphate species on breast cancer cellular behaviour. We have recently shown that expression of the heparan sulphate glycosaminoglycan chain is correlated with tumour grade and cell proliferation in phyllodes tumours (19). In the current study, we present evidence that sulphated heparan is upregulated in human breast invasive carcinoma tissues, and that the level of sulphation influences tumour cellular behaviour. We also show that differentially sulphated porcine intestine- and bovine kidney-derived heparan sulphate species have dissimilar effects on breast carcinoma cells.

Materials and methods

Clinical samples. A total of 32 archived, formalin-fixed paraffin-embedded breast cancer specimens and paired non-cancerous breast tissues from the corresponding patients were obtained from the Department of Pathology, Singapore General Hospital for this study. Ethics approval was obtained from the Institutional Review Board, Singapore General Hospital.

Immunohistochemistry. Immunohistochemical staining of clinical samples using the 10E4 antibody was performed as previously described (19). Briefly, 4- μ m thick tissue sections were deparaffinised and rehydrated. Antigen retrieval using 0.1 mg/ml testicular hyaluronidase (Sigma-Aldrich, St. Louis, MO) in PBS was carried out at room temperature for 2 h prior to overnight incubation with the 10E4 primary antibody (Seikagaku, Tokyo, Japan) at 4°C. After washing, colorimetric detection was achieved using the avidin-biotin-complex technique and diaminobenzidine. The sections were examined using an Olympus BX51 microscope and analysed using the Image J v1.33 software (NIH, USA). An immunoreactivity score (IRS) was determined for each specimen, calculated by multiplying the percentage of cells stained by the staining intensity.

Cell culture. MCF-7 and MDA-MB-231 human breast cancer cell lines were obtained from the American Tissue Culture Collection (Manassas, VA). Cells were cultured in Dulbecco's modified Eagle's medium (DMEM) supplemented with 7.5% foetal bovine serum (FBS), 2 mM glutamine and 40 mg/l gentamycin in a humidified 5% CO₂ incubator at 37°C. Bovine kidney- and porcine intestine-derived heparan sulphate

species, chlorate, and sulphate (all from Sigma-Aldrich) were added in various combinations to the culture medium.

Quantification of sulphated glycosaminoglycans. Cultured cells were collected with a cell scraper, and the glycosaminoglycans extracted by ethanol precipitation as previously described (20). Quantification of sulphated glycosaminoglycans was carried out using the Blyscan assay (Biocolor, Newtownabbey, Northern Ireland), a dye-binding assay that measures sulphated glycosaminoglycans without interference from non-sulphated glycosaminoglycans, according to the manufacturer's protocol. Briefly, the extracted glycosaminoglycans were allowed to bind to the Blyscan dye reagent to form a precipitate, which was then pelleted by centrifugation at 9,000 x g for 10 min. The precipitate was dissolved in the dissociation reagent, and the absorbance at 656 nm measured using a spectrophotometer.

Cell adhesion assay. Coating of 96-well culture plates with 20 μ g/ml fibronectin (BD Biosciences, San Jose, CA) in phosphate-buffered saline (PBS) was carried out overnight at 4°C (21). The wells were washed with PBS and the unbound sites blocked using 1% bovine serum albumin for 1 h at room temperature. The wells were then washed with PBS and dried.

Cells were pre-cultured for 48 h in serum-containing DMEM supplemented with PBS (control group), 30 mM chlorate or 30 mM chlorate plus 100 ng/ml heparan sulphate. The cells were then collected and seeded at a density of 1x10⁵ cells per well in the above fibronectin-coated culture plates and allowed to attach for 30 min at 37°C. The attached cells were washed with PBS, fixed for 15 min in 4% paraformaldehyde, and stained for 30 min using 0.25% crystal violet in 20% methanol. After washing, the number of attached cells was determined by releasing the crystal violet with 1% sodium dodecyl sulphate and measuring the absorbance at 595 nm.

Cell migration assay. Cancer cells were cultured in serum-containing DMEM in 6-well plates until they reached 90% confluence. A horizontal line was then scraped across the bottom of each well using a sterile 100- μ l plastic pipette tip, after which the culture was continued and the culture medium was supplemented with PBS (control group), 30 mM chlorate or 30 mM chlorate plus 100 ng/ml heparan sulphate. The average distance between the wound edges in each well was determined by measurement at five randomly selected sites along the length of the wound. The difference in the wound gap distance at 0 and 18 h after scraping was calculated to determine the distance migrated.

Cell proliferation assay. Cells were seeded in 96-well plates at a density of 4x10³ cells per well and cultured for 72 h in serum-containing DMEM supplemented with PBS (control group), 30 mM chlorate or 30 mM chlorate plus 100 ng/ml heparan sulphate. At the end of the culture period, the cells were washed with PBS, fixed in 4% paraformaldehyde for 15 min, and stained using 0.25% crystal violet in 20% methanol for 30 min. After washing, 1% sodium dodecyl sulphate was added for 1 h to release the crystal violet, and

Table I. Intron-spanning primers used in real-time RT-PCR analysis.

Gene	RefSeq No.	Primer sequence	Product (bp)
<i>ITGB1</i>	NM_002211	Forward: 5'-CTGCGAGTGTGGTGTCTGTAA-3' Reverse: 5'-GAACATTCCTGTGTGCATGTG-3'	162
<i>FAK</i>	NM_005607	Forward: 5'-TGGACGATGTATTGGAGAAGG-3' Reverse: 5'-ATGAGGATGGTCAAACCTGACG-3'	175
<i>PXN</i>	NM_002859	Forward: 5'-CCACACATAACCAGGAGATTGC-3' Reverse: 5'-GGGTTGGAGACACTGGAAGTT-3'	189
<i>RPLP0</i>	NM_001002	Forward: 5'-CTGTTGCATCAGTACCCCAT-3' Reverse: 5'-GCCTTGACCTTTTCAGCAAG-3'	103

the absorbance was then measured at 595 nm using a microplate reader.

Fluorescence immunocytochemistry. Cover slips were coated with fibronectin as described above. Cells were pre-cultured for 48 h in serum-containing DMEM supplemented with PBS (control group) or 30 mM chlorate. The cells were then trypsinised and washed in PBS. They were seeded at a density of 1×10^5 cells per coverslip and allowed to attach for 2 h to form adhesion. Unattached cells were then washed off. Attached cells were fixed in 4% paraformaldehyde for 10 min and washed with PBS containing 0.2% Triton X-100. After blocking, the cells were incubated with a 1:100 dilution of either mouse anti-paxillin IgG₁ antibody, clone 165 (BD Biosciences) or rabbit anti-FAK antibody (Santa Cruz Biotechnology, Santa Cruz, CA) at 4°C overnight as previously described (22,23). After washing, the signal was detected using an Alexa Fluor 568 goat anti-mouse secondary antibody (Invitrogen, Carlsbad, CA) or an Alexa Fluor 568 goat anti-rabbit secondary antibody respectively. To achieve double fluorescence labelling for F-actin, the cells were then incubated with Alexa Fluor 488 phalloidin (1:50 dilution) for 1 h at room temperature. The samples were examined using a FluoView FV1000 laser scanning confocal microscope (Olympus, Melville, NY).

For immunocytochemical detection of heparan sulphate, cells were fixed using Sainte-Marie's fixative as this gives better preservation of glycosaminoglycans (24). After blocking, cells were incubated with the anti-heparan sulphate antibody 10E4 at 1:100 dilution followed by an Alexa Fluor 488 goat anti-mouse IgM secondary antibody.

Real-time RT-PCR. Total RNA was extracted from cultured cells using the RNeasy Mini Kit (Qiagen, Valencia, CA) according to the manufacturer's protocol. After synthesis of cDNA using Superscript III (Invitrogen) and random hexamers, real-time PCR was carried out in a LightCycler (Roche, Indianapolis, IN) with the intron-spanning primers listed in Table I. After an initial activation step of 95°C for 15 min, 45 PCR cycles were performed as previously described: denaturation step of 94°C for 15 sec, annealing step of 60°C for 25 sec, and extension step of 72°C for 18 sec (25). Melting curve analysis was carried out to verify the specificity of the amplification, and the size of the PCR

product was confirmed by electrophoresis on a 2% agarose gel. The $2^{-\Delta\Delta Ct}$ method was used to determine the relative level of expression of gene transcripts after normalisation to *RPLP0* (also known as *36B4*), an oestradiol-independent mRNA control (26).

Western blot analysis. Cancer cells were grown in 100-mm petri dishes for 48 h and then lysed with 200 μ l cold lysis buffer consisting of 50 mM HEPES, 150 mM sodium chloride, 1% Triton X-100, 5 μ g/ml pepstatin A, 5 μ g/ml leupeptin, 2 μ g/ml aprotinin, 1 mM phenylmethylsulphonyl fluoride, 100 mM sodium fluoride and 1 mM sodium vanadate, pH 7.5. After standing for 20 min on ice, the protein supernatant was collected by centrifugation at 13,000 x g for 20 min. Twenty micrograms of protein were analysed by Western blotting with the ECL kit (Amersham, Little Chalfont, UK) using the following antibodies to probe the Western membrane after stripping: mouse anti-paxillin IgG₁ antibody clone 165, mouse anti-FAK IgG₁ antibody clone 77, and mouse anti- β 1-integrin IgG₁ antibody clone 18 (all from BD Biosciences). The relative protein expression level was determined by densitometry measurement of the band intensity and normalisation to β -actin.

Statistical analysis. All experiments consisted of at least three replicates. Statistical comparison between two groups was performed by the Student's t-test, and among three groups by one-way analysis of variance (ANOVA) with Tukey's post test using GraphPad Prism v4.03 for Windows (GraphPad Software, San Diego, CA). The Wilcoxon matched pairs test was used for comparison of clinical samples. Statistical significance was defined as a p-value of <0.05.

Results

Expression of heparan sulphate in breast cancer tissues. To determine if heparan sulphate is differentially expressed between breast carcinoma and non-cancerous breast tissues, we examined the expression of the 10E4 epitope in both epithelial and stromal compartments of 32 samples of invasive ductal carcinoma and paired non-cancerous mammary tissues from the corresponding patients. The mouse monoclonal antibody 10E4 is a well-established anti-heparan sulphate antibody, and requires the presence

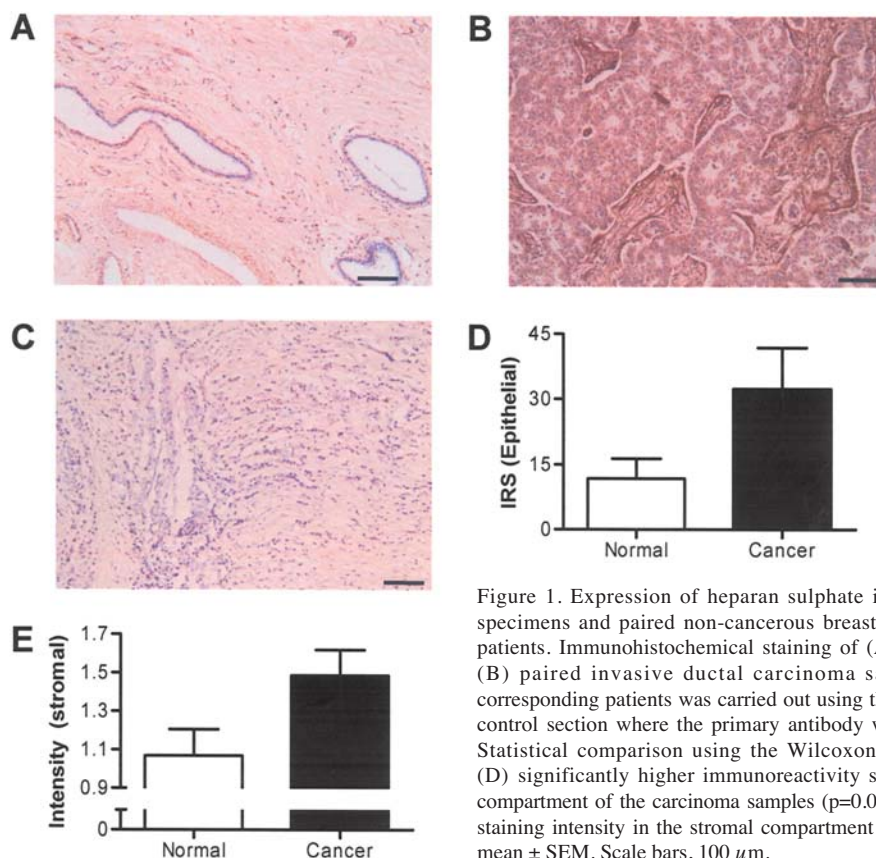


Figure 1. Expression of heparan sulphate in 32 archival breast cancer specimens and paired non-cancerous breast tissues from corresponding patients. Immunohistochemical staining of (A) normal breast tissues and (B) paired invasive ductal carcinoma samples obtained from the corresponding patients was carried out using the 10E4 antibody. A negative control section where the primary antibody was omitted is shown in (C). Statistical comparison using the Wilcoxon matched pairs test showed (D) significantly higher immunoreactivity scores (IRS) in the epithelial compartment of the carcinoma samples ($p=0.0482$), as well as (E) increased staining intensity in the stromal compartment ($p=0.0067$). Values represent mean \pm SEM. Scale bars, 100 μ m.

of the sulphate moiety on heparan sulphate for binding to its epitope (20,27,28). The mean age of the patients in the sample population was 60.4 years. As shown in Fig. 1, upregulated expression of the sulphated 10E4 epitope was detected in both the epithelial and stromal compartments of breast cancer compared with normal mammary tissues. Significantly, the mean immunoreactivity score of the cancer samples was 2.8 times higher than that of normal breast tissues, suggesting that heparan sulphate would be a useful biomarker for breast invasive ductal carcinoma.

Sulphate group in heparan sulphate is involved in regulating breast cancer cell adhesion. To determine if the sulphate group of heparan sulphate affects breast cancer cell adhesion, we cultured MCF-7 breast cancer cells in the presence of 30 mM chlorate. Chlorate is a widely used and well-known competitive inhibitor of glycosaminoglycan sulphation. It acts as a sulphate analogue in the cellular synthesis of the sulphate donor 3'-phosphoadenosine 5'-phosphosulphate, which is required for glycosaminoglycan sulphation (5,20,29-32). Previous studies involving breast cancer cell cultures and other biological systems have shown no significant effects on glycosaminoglycan chain or protein synthesis or on cell viability when chlorate was used at concentrations of up to 30 mM.

When 30 mM chlorate was added to the culture medium, MCF-7 cells showed an increase in cell adhesion, suggesting that glycosaminoglycan sulphation regulates breast cancer cell adhesion (Fig. 2A). A similar increase was also seen when MDA-MB-231 human breast cancer cells were cultured in medium containing 30 mM chlorate (Fig. 2B). Furthermore,

supplementation of chlorate-containing culture medium with exogenous sulphate blocked the increase in cell adhesion, thus confirming that the increase was indeed due to competitive inhibition of glycosaminoglycan sulphation (Fig. 2A). To further verify that glycosaminoglycan sulphation was reduced by chlorate treatment, we extracted and measured the amount of sulphated glycosaminoglycans produced by the cancer cells using the Blyscan dye-binding assay. As shown in Fig. 2C, chlorate administration resulted in 38.4% reduction in glycosaminoglycan sulphation. A decrease in sulphation of heparan sulphate was confirmed by fluorescence immunocytochemical staining of chlorate-treated cells using the 10E4 anti-heparan sulphate antibody (Fig. 2D).

Comparative effects of differentially sulphated heparan sulphate species on cancer cell adhesion. Chlorate inhibits sulphation of all glycosaminoglycans and does not act specifically on heparan sulphate. Thus, to determine if the chlorate-induced increase in cancer cell adhesion was due to a reduction in sulphation of heparan sulphate molecules, bovine kidney-derived heparan sulphate was added to MCF-7 cells grown in chlorate-containing medium. As shown in Fig. 3A, supplementation of the culture medium with adequately sulphated heparan sulphate molecules completely abolished the effect of chlorate on cell adhesion, suggesting that the sulphation status of heparan sulphate is important in regulating cancer cell adhesion. To investigate this further, we repeated the above experiment but added porcine intestine-derived heparan sulphate to the chlorate-containing culture medium instead of the bovine kidney-derived species.

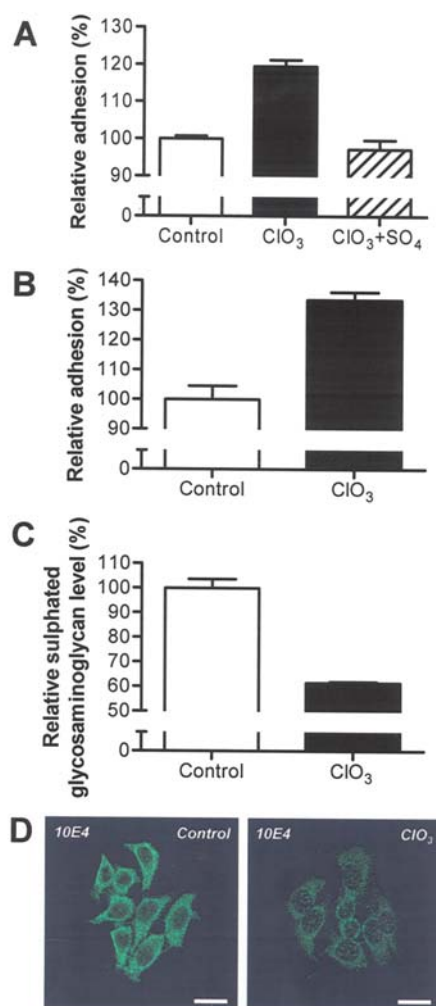


Figure 2. Effect of chlorate treatment on breast cancer cell adhesion. (A) MCF-7 cells were cultured in DMEM with 7.5% FBS in the presence of PBS (control), 30 mM chlorate (ClO_3) or 30 mM chlorate plus 10 mM sulphate (SO_4). Comparison among all three groups using one-way ANOVA showed a statistically significant difference ($p < 0.0001$), with the chlorate-alone treated group having greater cell adhesion compared to the control and the chlorate plus sulphate groups (Tukey's post test; $p < 0.001$). (B) MDA-MB-231 cells cultured in chlorate-containing medium also showed an increase in cell adhesion (Student's t-test; $p < 0.0001$). (C) Chlorate treatment resulted in a significant reduction in sulphation of glycosaminoglycans produced by MCF-7 cells (Student's t-test; $p = 0.0005$). (D) Immunofluorescence staining using the 10E4 anti-heparan sulphate antibody showed reduced staining intensity of chlorate-treated MCF-7 cells, demonstrating a decrease in sulphation of heparan sulphate molecules. Values represent mean \pm SEM of at least three replicates. Scale bars, 20 μm .

Heparan sulphate from porcine intestines possesses a lower degree of sulphation compared to that obtained from bovine kidney (33,34). We hypothesised that it may thus be less effective in blocking the effect of chlorate on cell adhesion. Indeed, as shown in Fig. 3B, addition of porcine intestine-derived heparan sulphate resulted in only a partial, instead of complete, block of the chlorate-induced increase in cell adhesion.

We also examined the effect of inhibiting glycosaminoglycan sulphation on the expression of paxillin (PAX), focal adhesion kinase (FAK) and β 1-integrin (ITGB1) in chlorate-treated MCF-7 cells. Paxillin and FAK are key regulatory components in cell adhesion and cell movement (35-37). We have previously shown that β 1-integrin (ITGB1)

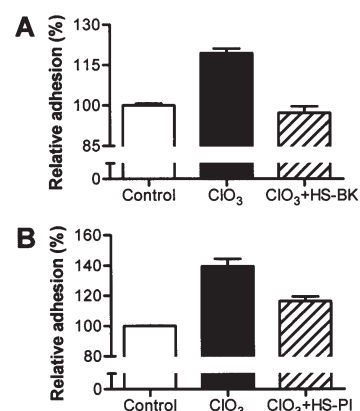


Figure 3. Sulphation status of heparan sulphate regulates breast cancer cell adhesion. MCF-7 cells were cultured in serum-containing medium supplemented with PBS (control), 30 mM chlorate (ClO_3), (A) 30 mM chlorate plus 100 ng/ml bovine kidney-derived heparan sulphate (HS-BK), or (B) 30 mM chlorate plus 100 ng/ml porcine intestine-derived heparan sulphate (HS-PI). Comparison among all three groups in each panel using one-way ANOVA showed a statistically significant difference ($p < 0.0001$), with an increase in cell adhesion in the group treated with chlorate alone compared against the control group (Tukey's post test; $p < 0.001$). Supplementation with HS-BK completely abolished the effect of chlorate on cell adhesion, with cells in this group possessing a similar degree of adhesion compared with those in the control group ($p > 0.05$). In contrast, HS-PI was only able to partially block the effect of chlorate, and cells in this group were more adherent compared against the control group ($p < 0.01$). Values represent mean \pm SEM of at least three replicates.

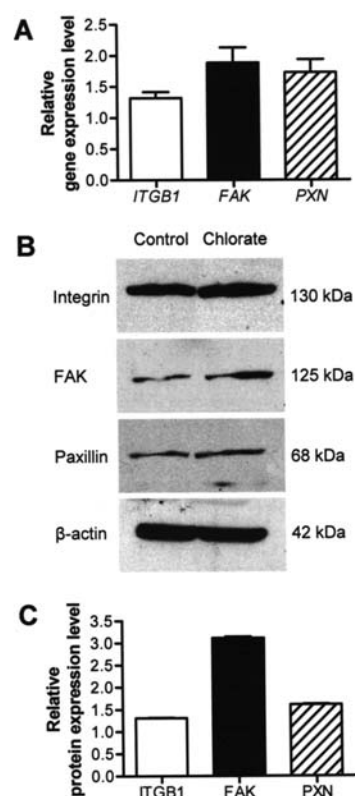


Figure 4. Effects of reduced glycosaminoglycan sulphation on ITGB1, FAK and paxillin expression. MCF-7 cells were cultured for 48 h in medium supplemented with PBS (control group) or 30 mM chlorate. (A) Gene transcript levels of *ITGB1*, *FAK* and *PXN* were measured using real-time RT-PCR. Chlorate treatment significantly upregulated the expression of *FAK* ($p = 0.0375$) and *PXN* ($p = 0.0440$). (B) Representative Western blot of three independent experiments. (C) Analysis by densitometry measurements showed increased levels of ITGB1 ($p = 0.0016$), FAK ($p = 0.0002$) and PXN ($p = 0.0003$). Values represent mean \pm SEM of three replicates.

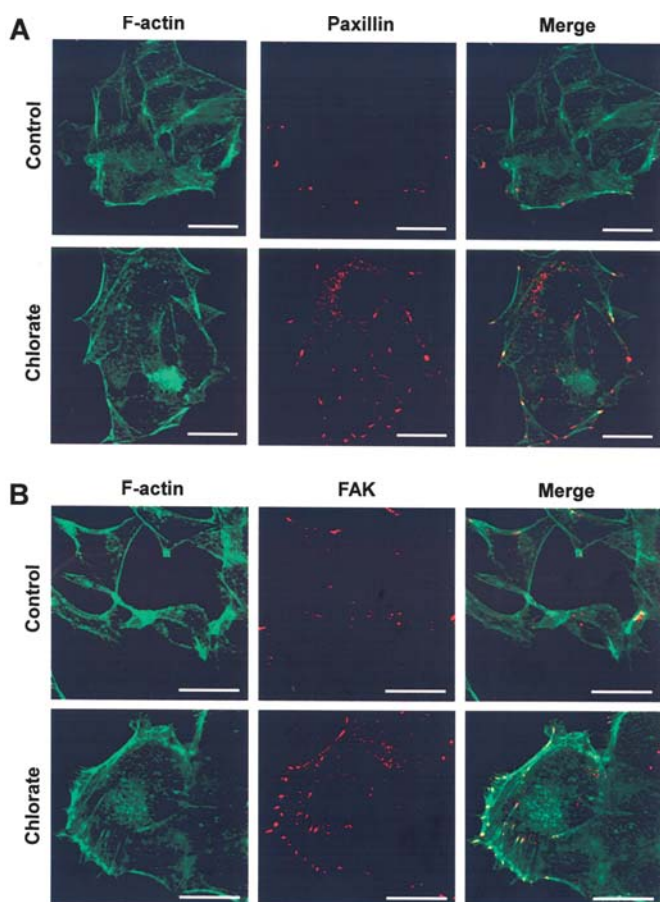


Figure 5. Fluorescence confocal microscopic analysis of focal adhesion formation. MCF-7 cells were cultured in medium supplemented with PBS (control) or 30 mM chlorate, and immunocytochemically examined for the expression of (A) paxillin (red) or (B) FAK using the respective antibodies. Actin fibres were stained using phalloidin (green). Panels shown are representative of triplicate experiments. Scale bars, 20 μ m.

influences the activity of FAK and paxillin, with resultant effects on breast cancer cell adhesion and spreading (23). Using real-time RT-PCR, reduction in glycosaminoglycan sulphation was shown to significantly increase the expression of *FAK* and *PXN* by 1.9X and 1.7X respectively (Fig. 4A). The expression of *ITGB1* was also upregulated, although this did not reach statistical significance. The changes in gene transcript levels were accompanied by similar up-regulation in protein levels, as determined by Western blotting (Fig. 4B and C). Expressions of *ITGB1*, *FAK* and *PXN* proteins in chlorate-treated cells were increased by 1.3X, 3.1X and 1.6X respectively. Using fluorescence immunocytochemistry, cells in the treatment group were found to possess an increase in focal adhesion formation together with stronger staining intensities for *PXN* and *FAK* proteins compared against those in the control group (Fig. 5).

Contrasting effects of different heparan sulphate species on cancer cell migration. To determine if the increase in cell adhesion due to reduced glycosaminoglycan sulphation would affect cancer cell migration, we cultured MCF-7 cells (Fig. 6A) and MDA-MB-231 cells (Fig. 6B) in the presence of chlorate, and measured the distance migrated by the cells across a wound gap over an 18-h period. In both cases,

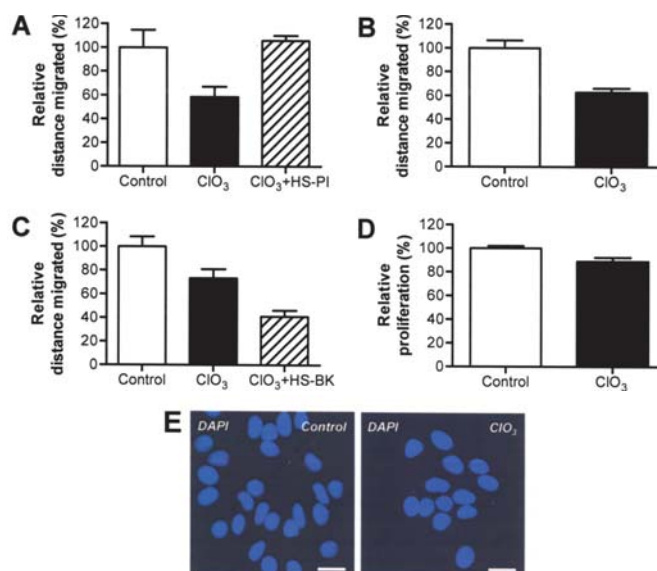


Figure 6. Effects of differentially sulphated heparan species on breast cancer cell migration. MCF-7 cells (A, C, D and E) and MDA-MB-231 cells (B) were cultured in serum-containing medium in the presence of PBS (control), 30 mM chlorate (ClO₃), or 30 mM chlorate plus (A) 100 ng/ml porcine intestine-derived heparan sulphate (HS-PI) or (C) bovine kidney-derived heparan sulphate (HS-BK). Comparison of cell migration among all three groups in (A) and (C) using one-way ANOVA showed a statistically significant difference ($p < 0.01$), with a decrease in cell migration in the group treated with chlorate alone compared against the control group (Tukey's post test; $p < 0.05$). Supplementation of the chlorate-containing culture medium with porcine intestine-derived heparan sulphate completely blocked the effect of chlorate ($p < 0.05$). In contrast, addition of bovine kidney-derived heparan sulphate resulted in a further reduction in cell migration ($p < 0.05$). (B) As in the case of MCF-7 cells, inhibition of glycosaminoglycan sulphation in MDA-MB-231 cells resulted in reduced cell migration (Student's *t*-test; $p < 0.01$). (D) Chlorate treatment decreased cell proliferation ($p < 0.05$), but did not induce cell apoptosis (E). Values represent mean \pm SEM of at least three replicates. Scale bars, 20 μ m.

inhibition of glycosaminoglycan sulphation resulted in a significant decrease in cell migration. This chlorate-induced reduction in cell migration could be completely abolished by supplementation of the culture medium with porcine intestine-derived heparan sulphate (Fig. 6A). However, in contrast to what was observed in the cell adhesion experiments (Fig. 3), addition of bovine kidney-derived heparan sulphate to the chlorate-containing culture medium led to a significant further decrease in cell migration instead of blocking the effect of chlorate (Fig. 6C). This suggests that differentially sulphated heparan sulphate species have diametrically opposite effects on breast cancer cell migration.

To examine if changes in cell proliferation as a result of chlorate treatment would confound the interpretation of the wound gap cell migration data, we cultured MCF-7 cells in medium supplemented with chlorate and measured the effect on cell growth. Despite treating the cells with chlorate for 72 h, cell proliferation was reduced by only 11% (Fig. 6D). Although this was statistically significant, the small change in cell proliferation makes it unlikely to be an important confounding factor in interpreting the 42% decrease in cell migration resulting from chlorate treatment (Fig. 6A). Chlorate-treated cells did not show any chromatin condensation, suggesting that reducing glycosaminoglycan sulphation did not result in apoptosis (Fig. 6E).

Discussion

We have investigated the use of heparan sulphate glycosaminoglycan as a biomarker of invasive breast ductal carcinoma in patient samples, and compared the effects of differentially sulphated porcine intestine- and bovine kidney-derived heparan sulphate species on cancer cell adhesion and migration. Adhesion of cancer cells to the extracellular matrix is an important determinant of local tumour invasion and distant metastasis (38-41). Changes in cell adhesion enable tumour cells to invade into surrounding tissues and spread to distant sites, contributing significantly to patient morbidity and mortality.

Studies on heparanase, an endoglucuronidase that hydrolyses heparan sulphate, suggest that degradation of heparan sulphate leads to enhanced breast cancer growth and invasion (42,43). Upregulated expression of heparanase, with a consequential reduction in heparan sulphate level, has been reported in breast cancer with a larger primary tumour size and distant metastasis (44). These studies suggest that heparan sulphate glycosaminoglycan chains are involved in breast carcinogenesis and that their presence implies a poorer prognosis for patients. Indeed, in the present study, upregulated expression of the sulphated 10E4 epitope in heparan sulphate was seen in the epithelial and stromal compartments of invasive ductal carcinoma compared with the corresponding normal breast tissues.

However, recent studies have shown that not all heparan sulphate chains are bad, and that the sulphation status of different heparan sulphate species is an important determinant of the biological effects of these molecules on cancer cells. This has been highlighted in the past few years in reports on the *SULF-1* gene, which codes for the enzyme sulfatase-1 that removes 6-O-sulphate groups from heparan sulphate (45-47). Loss of 6-O-sulphate groups was shown to inhibit growth of breast, pancreatic and hepatocellular cancers. In contrast, absence of *SULF-1* resulted in chemoresistance. Our experiments with chlorate, which competitively inhibits glycosaminoglycan sulphation and thus mimics over-expression of sulphatase-1 in the loss of 6-O-sulphate groups, showed an increase in cell adhesion and a reduction in cell proliferation. This phenomenon could be blocked by addition of adequately sulphated heparan sulphate to the culture medium, with bovine kidney-derived heparan sulphate containing a larger number of sulphate groups being more efficacious than porcine intestine-derived heparan sulphate (Fig. 3).

Interestingly, heparan sulphate regulation of breast cancer cell migration appears to be affected not only by the number of sulphate groups present but also by the position of the sulphate groups. Thus, inhibition of heparan sulphation, as well as the presence of highly sulphated bovine kidney-derived heparan sulphate, both led to a significant reduction in cell migration (Fig. 6). In contrast, optimally sulphated porcine intestine-derived heparan sulphate was able to block the effect of chlorate treatment. The results are in agreement with the recently proposed concept of a 'heparanome', in which differentially sulphated sugar sequences regulate the biological activities of different heparan sulphate species (8,48).

Heparan sulphate has been shown to affect cancer cellular behaviour through several mechanisms (9,49). It is able to bind to and interact with a multitude of growth factors and signalling proteins, resulting in stimulation of growth and metastasis of cancer cells (7). Heparan sulphate in the extracellular matrix also acts as a reservoir for aggregation of growth and angiogenic factors. Furthermore, binding of heparan sulphate to these molecules could protect them from degradation and thus prolong their effects on cancer cells. In breast cancer cells, fibroblast growth factor-2 (FGF-2) binds to heparan sulphate and stimulates cellular proliferation. Degradation of heparan sulphate by heparinase treatment abolished binding of the growth factor as well as the FGF-2-induced tumour growth (30). Down-regulation of *SULF-1* in MDA-MB-468 breast cancer cells, with the resultant persistent presence of 6-O-sulphate groups on heparan sulphate molecules, increases autocrine activation of the epidermal growth factor receptor-extracellular signal-regulated kinase (EGFR-ERK) pathway, mediated via amphiregulin and heparin-binding EGF-like growth factor (HB-EGF) (50). In addition, loss of *SULF-1* has been shown to increase cell proliferation in tumour-associated angiogenesis through FGF-2, hepatocyte growth factor, and vascular endothelial growth factor (VEGF) signalling.

Heparan sulphate is capable of binding to fibronectin and many other components of the extracellular matrix, and helps to regulate cell adhesion (7). Integrin-mediated cell adhesion leads to recruitment of the cytoplasmic protein tyrosine kinase FAK to focal adhesion sites, and the phosphorylation of both FAK and paxillin (36,51-55). The transmembrane heparan sulphate proteoglycan syndecan-4 is an essential element in the formation of focal adhesions (56-58). Expression of syndecan-4 in Chinese hamster ovary (CHO) cells resulted in increased numbers of focal adhesion complexes (56). On the other hand, CHO cell mutants deficient in glycosaminoglycans showed reduced focal adhesion formation when cultured on a fibronectin substrate (59). In our experiments, reduction in heparan sulphation in MCF-7 breast cancer cells was shown to increase cancer cell adhesion and upregulate FAK and paxillin at both gene transcript and protein levels, and this could be completely blocked by exogenous heparan sulphate.

Heparan sulphate has been shown to be a key player in a number of signalling pathways in cell migration. It has been reported to modulate transendothelial migration of monocytes by regulating G-protein-dependent signalling (60). HT1080 fibrosarcoma cells that overexpressed the heparan sulphate proteoglycan syndecan-2 showed activation of the small GTPase Rac and increased cell migration (61). Furthermore, in addition to acting as a co-receptor in FGF signalling, heparan sulphate may act as a direct receptor in the FGF-2 activation of ERK1/2, which is required for bronchial epithelial and corneal epithelial cell migration (62-64).

In conclusion, we have shown that heparan sulphate is a useful biomarker of breast invasive ductal carcinoma, and is involved in regulating cancer cell adhesion, migration and focal adhesion complex formation through different sulphation patterns on its sugar residues. A better understanding of the effects of differentially sulphated heparan sulphate species

on cancer cell behaviour is important for the development of these molecules into therapeutic targets for breast cancer.

Acknowledgements

The authors are grateful to Lang-Hiong Sii for technical assistance. The project was supported by Grants NMRC/0772/2003 and NMRC/1023/2005 from the National Medical Research Council, Singapore (G.W.Y.), and Grant MS0004 from the Singapore Cancer Syndicate (P.H.T.). C.H.G. is the recipient of a graduate research scholarship from the National University of Singapore.

References

- Key TJ, Verkasalo PK and Banks E: Epidemiology of breast cancer. *Lancet Oncol* 2: 133-140, 2001.
- Hortobagyi GN, de la Garza Salazar J, Pritchard K, *et al.*: The global breast cancer burden: variations in epidemiology and survival. *Clin Breast Cancer* 6: 391-401, 2005.
- Thor AD, Wang J and Bartow SA: The breast. In: Rubin's Pathology: Clinicopathologic Foundations of Medicine, 4th edition. Rubin E, Gorstein F, Rubin R, Schwarting R and Strayer D (eds). Lippincott Williams & Wilkins, Philadelphia, pp996-1017, 2005.
- Rosen PP: Rosen's Breast Pathology. 2nd edition. Lippincott Williams & Wilkins, Philadelphia, 2001.
- Conrad HE: Heparin-binding proteins. Academic Press, San Diego, 1998.
- Sharon N: IUPAC-IUB Joint Commission on Biochemical Nomenclature (JCBN). Nomenclature of glycoproteins, glycopeptides and peptidoglycans. Recommendations 1985. *Eur J Biochem* 159: 1-6, 1986.
- Bernfield M, Gotte M, Park PW, Reizes O, Fitzgerald ML, Lincecum J and Zako M: Functions of cell surface heparan sulfate proteoglycans. *Annu Rev Biochem* 68: 729-777, 1999.
- Turnbull J, Powell A and Guimond S: Heparan sulfate: decoding a dynamic multifunctional cell regulator. *Trends Cell Biol* 11: 75-82, 2001.
- Yip GW, Smollich M and Gotte M: Therapeutic value of glycosaminoglycans in cancer. *Mol Cancer Ther* 5: 2139-2148, 2006.
- Ringvall M, Ledin J, Holmborn K, *et al.*: Defective heparan sulfate biosynthesis and neonatal lethality in mice lacking N-deacetylase/N-sulfotransferase-1. *J Biol Chem* 275: 25926-25930, 2000.
- Bullock SL, Fletcher JM, Beddington RS and Wilson VA: Renal agenesis in mice homozygous for a gene trap mutation in the gene encoding heparan sulfate 2-sulfotransferase. *Genes Dev* 12: 1894-1906, 1998.
- Wilson VA, Gallagher JT and Merry CL: Heparan sulfate 2-O-sulfotransferase (Hs2st) and mouse development. *Glycoconj J* 19: 347-354, 2002.
- Barbareschi M, Maisonneuve P, Aldovini D, *et al.*: High syndecan-1 expression in breast carcinoma is related to an aggressive phenotype and to poorer prognosis. *Cancer* 98: 474-483, 2003.
- Leivonen M, Lundin J, Nordling S, von Boguslawski K and Haglund C: Prognostic value of syndecan-1 expression in breast cancer. *Oncology* 67: 11-18, 2004.
- Tsanou E, Ioachim E, Briasoulis E, *et al.*: Clinicopathological study of the expression of syndecan-1 in invasive breast carcinomas correlation with extracellular matrix components. *J Exp Clin Cancer Res* 23: 641-650, 2004.
- Gotte M, Kersting C, Ruggiero M, Tio J, Tulusan AH, Kiesel L and Wulping P: Predictive value of syndecan-1 expression for the response to neoadjuvant chemotherapy of primary breast cancer. *Anticancer Res* 26: 621-627, 2006.
- Gotte M, Kersting C, Radke L, Kiesel L and Wulping P: An expression signature of syndecan-1 (CD138), E-cadherin and c-met is associated with factors of angiogenesis and lymphangiogenesis in ductal breast carcinoma *in situ*. *Breast Cancer Res* 9: R8, 2007.
- Matsuda K, Maruyama H, Guo F, *et al.*: Glypican-1 is over-expressed in human breast cancer and modulates the mitogenic effects of multiple heparin-binding growth factors in breast cancer cells. *Cancer Res* 61: 5562-5569, 2001.
- Koo CY, Bay BH, Lui PC, Tse GM, Tan PH and Yip GW: Immunohistochemical expression of heparan sulfate correlates with stromal cell proliferation in breast phyllodes tumors. *Mod Pathol* 19: 1344-1350, 2006.
- Yip GW, Ferretti P and Copp AJ: Heparan sulphate proteoglycans and spinal neurulation in the mouse embryo. *Development* 129: 2109-2119, 2002.
- Kuzuya M, Asai T, Kanda S, Maeda K, Cheng XW and Iguchi A: Glycation cross-links inhibit matrix metalloproteinase-2 activation in vascular smooth muscle cells cultured on collagen lattice. *Diabetologia* 44: 433-436, 2001.
- Lin VC, Woon CT, Aw SE and Guo C: Distinct molecular pathways mediate progesterone-induced growth inhibition and focal adhesion. *Endocrinology* 144: 5650-5657, 2003.
- Lin VC, Ng EH, Aw SE, Tan MG, Ng EH and Bay BH: Progesterone induces focal adhesion in breast cancer cells MDA-MB-231 transfected with progesterone receptor complementary DNA. *Mol Endocrinol* 14: 348-358, 2000.
- Tuckett F and Morriss-Kay G: Alcian blue staining of glycosaminoglycans in embryonic material: effect of different fixatives. *Histochem J* 20: 174-182, 1988.
- Lim D, Phan TT, Yip GW and Bay BH: Up-regulation of metallothionein isoforms in keloid keratinocytes. *Int J Mol Med* 17: 385-389, 2006.
- Laborda J: 36B4 cDNA used as an estradiol-independent mRNA control is the cDNA for human acidic ribosomal phosphoprotein PO. *Nucleic Acids Res* 19: 3998, 1991.
- van den Born J, Salmivirta K, Henttinen T, *et al.*: Novel heparan sulfate structures revealed by monoclonal antibodies. *J Biol Chem* 280: 20516-20523, 2005.
- David G, Bai XM, van der Schueren B, Cassiman JJ and van den Berghe H: Developmental changes in heparan sulfate expression: *in situ* detection with mAbs. *J Cell Biol* 119: 961-975, 1992.
- Greve H, Cully Z, Blumberg P and Kresse H: Influence of chlorate on proteoglycan biosynthesis by cultured human fibroblasts. *J Biol Chem* 263: 12886-12892, 1988.
- Delehedde M, Deudon E, Boilly B and Hondermarck H: Heparan sulfate proteoglycans play a dual role in regulating fibroblast growth factor-2 mitogenic activity in human breast cancer cells. *Exp Cell Res* 229: 398-406, 1996.
- Safaiyan F, Lindahl U and Salmivirta M: Selective reduction of 6-O-sulfation in heparan sulfate from transformed mammary epithelial cells. *Eur J Biochem* 252: 576-582, 1998.
- Safaiyan F, Kolset SO, Prydz K, Gottfridsson E, Lindahl U and Salmivirta M: Selective effects of sodium chlorate treatment on the sulfation of heparan sulfate. *J Biol Chem* 274: 36267-36273, 1999.
- Wei Z, Lyon M and Gallagher JT: Distinct substrate specificities of bacterial heparinases against N-unsubstituted glucosamine residues in heparan sulfate. *J Biol Chem* 280: 15742-15748, 2005.
- Toida T, Yoshida H, Toyoda H, *et al.*: Structural differences and the presence of unsubstituted amino groups in heparan sulphates from different tissues and species. *Biochem J* 322: 499-506, 1997.
- Vicente-Manzanares M, Webb DJ and Horwitz AR: Cell migration at a glance. *J Cell Sci* 118: 4917-4919, 2005.
- Turner CE: Paxillin. *Int J Biochem Cell Biol* 30: 955-959, 1998.
- Turner CE: Paxillin and focal adhesion signalling. *Nat Cell Biol* 2: E231-E236, 2000.
- Okegawa T, Li Y, Pong RC and Hsieh JT: Cell adhesion proteins as tumor suppressors. *J Urol* 167: 1836-1843, 2002.
- Pupa SM, Menard S, Forti S and Tagliabue E: New insights into the role of extracellular matrix during tumor onset and progression. *J Cell Physiol* 192: 259-267, 2002.
- Boudreau N and Bissell MJ: Extracellular matrix signaling: integration of form and function in normal and malignant cells. *Curr Opin Cell Biol* 10: 640-646, 1998.
- Liotta LA and Kohn EC: The microenvironment of the tumour-host interface. *Nature* 411: 375-379, 2001.
- Vlodavsky I, Friedmann Y, Elkin M, *et al.*: Mammalian heparanase: gene cloning, expression and function in tumor progression and metastasis. *Nat Med* 5: 793-802, 1999.
- Cohen I, Pappo O, Elkin M, *et al.*: Heparanase promotes growth, angiogenesis and survival of primary breast tumors. *Int J Cancer* 118: 1609-1617, 2006.
- Maxhimer JB, Quiros RM, Stewart R, *et al.*: Heparanase-1 expression is associated with the metastatic potential of breast cancer. *Surgery* 132: 326-333, 2002.

45. Lai JP, Chien JR, Moser DR, *et al*: hSulf1 sulfatase promotes apoptosis of hepatocellular cancer cells by decreasing heparin-binding growth factor signaling. *Gastroenterology* 126: 231-248, 2004.
46. Abiatari I, Kleeff J, Li J, Felix K, Buchler MW and Friess H: HSulf-1 regulates growth and invasion of pancreatic cancer cells. *J Clin Pathol* 59: 1052-1058, 2006.
47. Narita K, Staub J, Chien J, *et al*: HSulf-1 Inhibits angiogenesis and tumorigenesis *in vivo*. *Cancer Res* 66: 6025-6032, 2006.
48. Lamanna WC, Kalus I, Padva M, Baldwin RJ, Merry CL and Dierks T: The heparanome-the enigma of encoding and decoding heparan sulfate sulfation. *J Biotechnol* 129: 290-307, 2007.
49. Gotte M and Yip GW: Heparanase, hyaluronan, and CD44 in cancers: a breast carcinoma perspective. *Cancer Res* 66: 10233-10237, 2006.
50. Narita K, Chien J, Mullany SA, Staub J, Qian X, Lingle WL and Shridhar V: Loss of HSulf-1 expression enhances autocrine signaling mediated by amphiregulin in breast cancer. *J Biol Chem* 282: 14413-14420, 2007.
51. LaFlamme SE and Auer KL: Integrin signaling. *Semin Cancer Biol* 7: 111-118, 1996.
52. Schaller MD: Biochemical signals and biological responses elicited by the focal adhesion kinase. *Biochim Biophys Acta* 1540: 1-21, 2001.
53. Liu S, Thomas SM, Woodside DG, Rose DM, Kiosses WB, Pfaff M and Ginsberg MH: Binding of paxillin to alpha4 integrins modifies integrin-dependent biological responses. *Nature* 402: 676-681, 1999.
54. Schaller MD, Otey CA, Hildebrand JD and Parsons JT: Focal adhesion kinase and paxillin bind to peptides mimicking beta integrin cytoplasmic domains. *J Cell Biol* 130: 1181-1187, 1995.
55. Burridge K, Turner CE and Romer LH: Tyrosine phosphorylation of paxillin and pp125FAK accompanies cell adhesion to extracellular matrix: a role in cytoskeletal assembly. *J Cell Biol* 119: 893-903, 1992.
56. Longley RL, Woods A, Fleetwood A, Cowling GJ, Gallagher JT and Couchman JR: Control of morphology, cytoskeleton and migration by syndecan-4. *J Cell Sci* 112: 3421-3431, 1999.
57. Woods A and Couchman JR: Integrin modulation by lateral association. *J Biol Chem* 275: 24233-24236, 2000.
58. Couchman JR and Woods A: Syndecan-4 and integrins: combinatorial signaling in cell adhesion. *J Cell Sci* 112: 3415-3420, 1999.
59. LeBaron RG, Esko JD, Woods A, Johansson S and Hook M: Adhesion of glycosaminoglycan-deficient Chinese hamster ovary cell mutants to fibronectin substrata. *J Cell Biol* 106: 945-952, 1988.
60. Floris S, van den Born J, van der Pol SM, Dijkstra CD and de Vries HE: Heparan sulfate proteoglycans modulate monocyte migration across cerebral endothelium. *J Neuropathol Exp Neurol* 62: 780-790, 2003.
61. Park H, Han I, Kwon HJ and Oh ES: Focal adhesion kinase regulates syndecan-2-mediated tumorigenic activity of HT1080 fibrosarcoma cells. *Cancer Res* 65: 9899-9905, 2005.
62. Graness A, Chwieralski CE, Reinhold D, Thim L and Hoffmann W: Protein kinase C and ERK activation are required for TFF-peptide-stimulated bronchial epithelial cell migration and tumor necrosis factor-alpha-induced interleukin-6 (IL-6) and IL-8 secretion. *J Biol Chem* 277: 18440-18446, 2002.
63. Sharma GD, He J and Bazan HE: p38 and ERK1/2 coordinate cellular migration and proliferation in epithelial wound healing: evidence of cross-talk activation between MAP kinase cascades. *J Biol Chem* 278: 21989-21997, 2003.
64. Chua CC, Rahimi N, Forsten-Williams K and Nugent MA: Heparan sulfate proteoglycans function as receptors for fibroblast growth factor-2 activation of extracellular signal-regulated kinases 1 and 2. *Circ Res* 94: 316-323, 2004.